Investigation on the Interaction of Dipeptidyl Peptidase IV with the Transactivator of Transcription Protein of Human Immunodeficiency Virus Type-1

Dissertation to achieve the academic degree of
Doctor of Natural Sciences (Dr. rer. nat.)

Submitted to the
Department of Biology, Chemistry and Pharmacy
of the
Freie-Universität Berlin

Presented by

Felista Lemnyui Tansi

from Cameroon

2010

Charité-Universitätsmedizin Berlin

Campus Benjamin Franklin

Institute of Biochemistry and Molecular biology

Arnimallee 22

14195, Berlin-Dahlem

This work was performed under the supervision of Priv. Doz. Dr. Hua Fan

The experimental work was performed from April 2005 to December 2009 in the Institute of Biochemistry and Molecular biology (AG Reutter / Fan) in Berlin

Part of the work has already been published:

Felista L. Tansi, Véronique Blanchard, Markus Berger, Rudolf Tauber, Werner Reutter and Hua Fan (2010): Interaction of human dipeptidyl peptidase IV and human immunodeficiency virus type-1 transcription transactivator in *Sf9* cells.

Virology J 7, 267

First Reviewer: Priv. Doz. Dr. Hua Fan

Second Reviewer: Prof. Dr. Rupert Mutzel

Disputation: 11-11-2010

Declaration

I hereby declare that this thesis is the result of my original work carried out at the Institute of Biochemistry and Molecular biology of the Charité-Universitätsmedizin in Berlin-Dahlem, Germany. The research was an independent study under the supervision of Priv. Doz. Dr. Hua Fan. This thesis has never been submitted in part or in whole for a degree at any institution. References to other sources or people's work have been duly cited and acknowledged.

Signed by author:

Felista Lemnyui Tansi…….

“Dignity consists not in possessing honours, but in the consciousness that we deserve them“

Aristotle

Dedicated

to

my parents, Juliana and Henry
Thanks for not only giving me life, but also making me realise the sense of being alive!

and to

my late aunt Angeline and her two daughters, my cousins Emma and Apolonia
who all died suddenly within 6 weeks.
The shock of learning you left this world together, took my breath away.
Thanks to your love and encouragements while alive, I could pick up from where you left me and become strong enough to complete the work you so much wanted me to.
May your souls find perfect peace!

Table of Contents

List of Figures

1 Introduction

All living cells are surrounded by membranes which are two dimensional solutions of oriented lipids and globular proteins (Singer & Nicolson, 1972). The membrane lipids form permeability barriers that shield functional compartments and the cells from their immediate environment, whereas proteins that span the membrane mediate nearly all other membrane functions such as communication with the environment. Thus, plasma membranes with the help of numerous proteins serve as selective gates which control the movement of molecules into and out of the cell, thereby acting as communication units between the cells and their environments. Proteins spanning the plasma membranes are involved in several biosynthetic processes and signal transduction. Numerous pathogenic reactions occur at the cell surface. As a whole, the plasma membrane, the proteins spanning the membranes and the glycans linked to the proteins play vital roles in these pathogenic reactions.

Due to the tight defence mechanism offered by plasma membranes, intracellular parasites which cannot disseminate their genetic information independently have evolved distinct strategies to utilize the host machinery. These strategies involve utility of host membrane proteins and manipulation of the host signal transduction pathways. The infection of T cells by the human immunodeficiency virus for example, involves the interplay between cell surface proteins such as CD4, chemokine receptors and several other proteins involved in the activation of T cells, such as the archetypal member of the prolyl oligopeptidase family, namely Dipeptidyl Peptidase IV. Studying the interaction of membrane proteins with proteins of parasites and the mechanisms underlying this interaction will shed light on understanding the exact roles played by specific proteins on the cell surface in various diseases. Thus, research on these host-pathogen interactions is indispensable for drug design and the fight against diseases.

1.1 The Prolyl Oligo-Peptidase family

The prolyl oligo-peptidase family (POP; EC 3.4.21.26) comprises a family of aminopeptidases and endopeptidases which are involved in several biological processes, owing on one part to their locations on the cell membrane and on the other hand, to their ability to hydrolyse the post-prolyl bond of polypeptides. The Dipeptidyl Peptidase (DPP) gene family is distinguished from other members of the POP family by a pair of glutamate residues that are distant from the catalytic serine in the primary structure (Ajami *et al.*, 2003), but within the catalytic pocket in the tertiary structure (Rasmussen *et al.*, 2003). These glutamate residues on position 205 and 206 in DPPIV are essential for dipeptidyl peptidase activity (Abbott *et al.*, 1999). The DPP gene family has six members,

including FAP (fibroblast activation protein), DPPIV, DPP8, DPP9 and the two non-enzymatic DPP-Like proteins, DPPL-1 and DPPL-2.

Dipeptidyl peptidase IV, (DPPIV) is the archetypal member of the six-member gene family. Only four of the six members of the DPP family, DPPIV (Dipeptidyl peptidase IV), FAPα, DPP8 and DPP9 constitute the subset of proteinases capable of cleaving the prolyl bond two positions from the N-terminus (Leiting *et al.*, 2003).

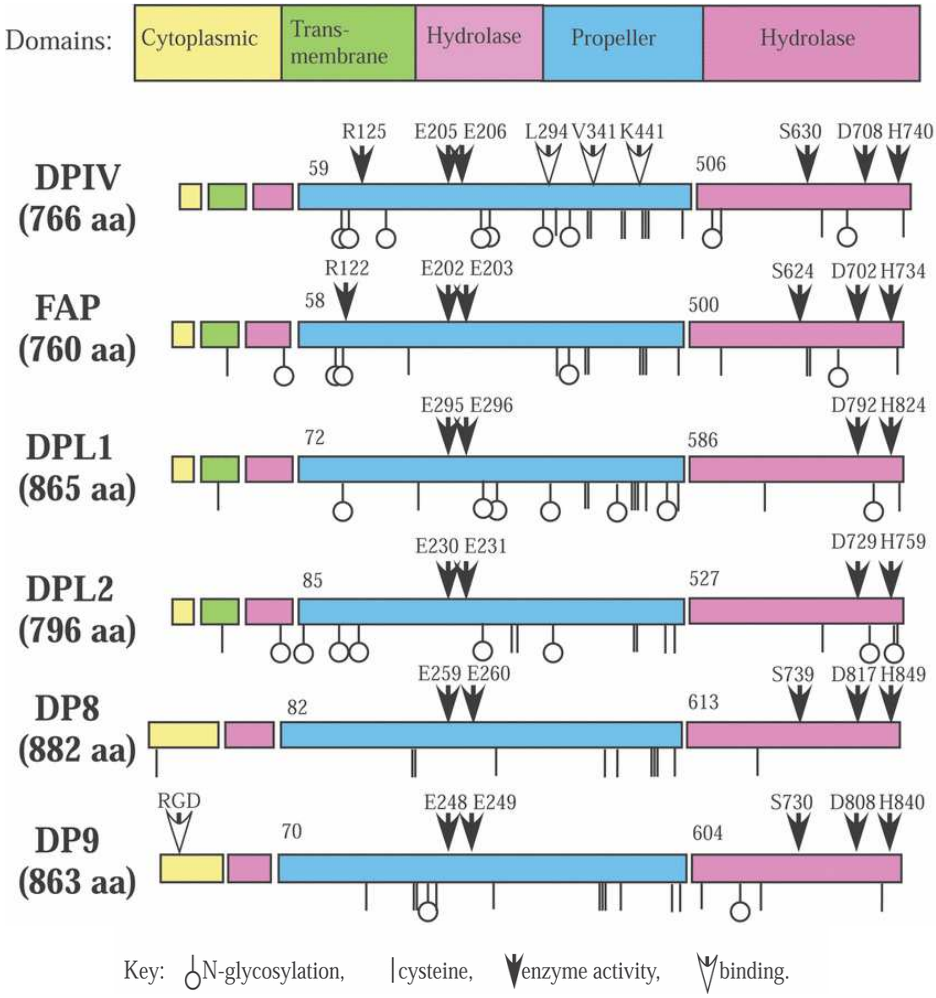

Figure 1.1: Schematic presentation of the proteins of the DPP gene family

The arrangements of structural domains as well as the approximate positions of N-glycosylation, cysteine residues and some residues required for enzyme activity and ADA or antibody binding are depicted. The diagram is not to scale. The Diagram is modified from (Gorrell, 2005).

DPPIV (EC 3.4.14.5) was the first identified member of the heterogeneous gene family. Before the discovery of other members of the gene family, DPPIV was considered the only membrane-bound enzyme specific for the cleavage of polypeptides with N-terminal proline at the penultimate position. Later on a 68% homology in primary structure of fibroblast-activation-protein-alpha (FAP-α) to human-DPPIV was reported (Scanlan *et al.*, 1994). FAP-α also shares a membrane bound feature with DPPIV but shows an additional gelatinase activity. Although FAP-α is

structurally very similar to DPPIV, its expression is largely confined to diseased and damaged tissue. Re-expression of DPPIV rescues the expression of FAP-α in melanoma cells (Wesley *et al.*, 1999), suggesting their co-action and/or functional substitution. The family members DPP8 and DPP9 are cytosolic proteins which have been pinpointed *in silico* to the two human chromosome loci 15q22 and 19p13.3 respectively (Abbott *et al.*, 2000; Olsen & Wagtmann, 2002). Both are widely distributed and indirectly implicated in immune function. Only full-length expression of the paralogous genes of DPP8 and DPP9 produce enzymatically active proteins and the mature proteins are able to cleave naturally occurring peptides of the incretin and pancreatic hormone families (Bjelke *et al.*, 2006). The two DPP-like glycoproteins, DPPL1 and DPPL2 lack peptidase activity and serve as brain-specific potassium channel modulators. Further molecules that share structural, activity and also membrane bound features with DPPIV include N-acetylated α-linked acidic dipeptidase (NAALADase) (Pangalos *et al.*, 1999), and attractin (Durinx *et al.*, 2000).

1.2 Dipeptidyl Peptidase IV (DPPIV)

Dipeptidyl peptidase IV (DPPIV) is a Type II transmembrane glycoprotein which was first described in 1966 by Hopsu-Havu and Glenner as a glycyl-prolyl-naphthylamidase (Hopsu-Havu & Glenner, 1966). Some years later it was demonstrated that the protein possessed an exopeptidase activity and thus cleaves N-terminal dipeptides from polypeptides with proline or alanine in their penultimate positions. The protein was then named Dipeptidyl-peptidase IV or Dipeptidyl-aminopeptidase IV (Callahan *et al.*, 1972; Kenny *et al.*, 1976). In 1990 the T cell activation marker CD26 was identified as DPPIV (Hegen *et al.*, 1990) and investigations on the primary structure proved that the DPPIV enzyme found in animals was identical with the human T cell activation marker CD26 (Misumi *et al.*, 1992; Tanaka *et al.*, 1992).

1.2.1 Occurrence and distribution of DPPIV

The first successful isolation of integral DPPIV was from rat liver and kidney (Hartel-Schenk *et al.*, 1990) and later on from a diverse number of tissues where it is either constitutively expressed or strictly regulated. DPPIV is ubiquitously expressed and widely distributed in mammalian tissues. Remarkably high expressions are found on epithelial and endothelial cell surfaces, fibroblasts as well as activated lymphocytes. In humans, DPPIV is constitutively expressed on epithelial cells of liver, intestine, kidney and in a soluble form in serum. In the liver, it is found mostly on the epithelial cells lining the lumen of the bile duct, whereas expression in the lungs is limited to the alveolar macrophages and interstitial cells (Hartel *et al.*, 1988). In pancreas DPPIV is found in the A-cells in secretory granules (Grondin *et al.*, 1999).

Similar to other ectopeptidases, DPPIV is involved in several immunologically relevant functions. Due to this, its expression undergoes strict onto-genetical control during T cell maturation (Fox *et al.*, 1984; Micouin & Bauvois, 1997). The expression of DPPIV on hematopoietic cells is strictly regulated depending on the activation status of the cells. On lymphocytes, DPPIV expression is found mostly on the T cell population. On a fraction of resting lymphocytes low levels of DPPIV is expressed which is strongly up-regulated after T cell activation (Mentlein *et al.*, 1986; Fleischer, 1994). In resting peripheral blood mononuclear cells (PBMC), a small subpopulation of T cells express high levels of surface DPPIV ($CD26^{brighT\ cells}$), which belong to the $CD45RO^{+}$ population of memory T cells (Vanham *et al.*, 1993). The number of $CD26^{bright}$ cells and CD26 antigen density is higher during the active phase of autoimmune diseases, such as rheumatoid arthritis (Gerli *et al.*, 1996), multiple sclerosis, Grave's disease, Hashimoto's thyroiditis and sarcoidosis (De Meester *et al.*, 1999), and decreased during immune suppression, as is the case in AIDS (Blazquez *et al.*, 1992; Vanham *et al.*, 1993), Down's syndrome (Bertotto *et al.*, 1994) and common variable hypo-gammaglobulinemia (De Meester *et al.*, 1999). A more detailed analysis of the T cell populations revealed a correlation of DPPIV expression with the T-helper subsets. The Th1 and Th0 cells display higher expressions than Th2 cells (Willheim *et al.*, 1997). Amongst human and murine thymocytes, CD26 is differentially expressed and becomes up-regulated as thymocytes mature (Ruiz *et al.*, 1998). In the ovary, the expression of DPPIV is periodically regulated (Fujiwara *et al.*, 1992), so that very high levels are expressed in placenta which decrease with the onset of pregnancy in humans (Nausch *et al.*, 1990).

Besides the integral membrane form, a soluble form of DPPIV deficient of the intracellular tail and transmembrane regions, was characterized based on its enzyme activity, immuno-reactivity and binding to ADA (Duke-Cohan *et al.*, 1995; Durinx *et al.*, 2000). This soluble DPPIV is thought to result from membrane bound DPPIV by proteolytic cleavage. It is highly active and is responsible for the inactivation of several bioactive peptides. High concentrations are found in seminal plasma (Wilson *et al.*, 1998), whereas moderate and low levels are detected in plasma, cerebrospinal fluid and urine respectively (Iwaki-Egawa *et al.*, 1998). The concentration of soluble DPPIV in serum is altered in several diseases (Hanski *et al.*, 1986; van West *et al.*, 2000). Interestingly, CD26 has the ability to enter into an endocytosis / exocytosis cycle, which involves re-entry into the Golgi apparatus and results to glycosylation changes and the production of heterogenic forms of DPPIV (Kahne *et al.*, 1996).

1.2.2 Structure of DPPIV

The human-DPPIV gene is located on the long arm of chromosome 2 (2q24.3) and spans 70 kb approximately. The protein is encoded by 26 exons ranging in size from 45 bp to 1.4 kb (Abbott *et*

al., 1994). In human and mouse, specific exons encode identical functional domains (Bernard *et al.,* 1994). Based on the presence of a single unique DPPIV mRNA, DPPIV can be considered a housekeeping protein (Hong *et al.,* 1989). The 5' flanking region of the gene contains no TATA box nor a CAAT box like the ones commonly found in housekeeping genes, but rather a 300 bp sequence that is rich in C and G and possesses potential binding sites for NF-κB, AP2 or Sp1 (Bohm *et al.,* 1995).

Rat-DPPIV consists of 767 amino acid residues, whereas human and mouse-DPPIV constitute 766 and 760 amino acid residues respectively (Ogata *et al.,* 1989; Marguet *et al.,* 1992; Misumi *et al.,* 1992). There is a 92% homology between the rat and mouse and about 85% homology between rat and human DPPIV cDNA sequence. The N-terminus contains a short cytoplasmic domain of only 6 amino acid residues, and a 22 amino acid-long hydrophobic transmembrane domain. Both domains serve as a signal peptide and a membrane anchor (Ogata *et al.,* 1989). The extracellular region of DPPIV consists of 732 (mouse) – 738/739 (human and rat) amino acid residues and can be divided into 3 distinct regions of approximately same size, with reference to specific characteristics. The primary amino acid sequence of DPPIV contains 8- (rat) or 9- (human) of the specific N-glycosylation consensus sequence - Asn-Xaa-Ser/Thr… (Tanaka *et al.,* 1992). Directly next to the membrane anchor is a large glycan-rich region which contains 5 of the total N-glycosylation sites in both species. These N-glycans are partly responsible for the biological stability and processing of the protein (Fan *et al.,* 1997). Sialylation of DPPIV also takes place on the glycan-rich region and increases significantly with age, whereas extreme hypersialylation is found in HIV-infected individuals (Smith *et al.,* 1998). A cysteine rich domain comprising 10 of the 12 cysteine residues found in DPPIV separates the glycan-rich and the C-terminal region. The cysteine residues build disulfide bridges which are responsible for the formation of the functional conformation of DPPIV (Lambeir *et al.,* 1997; Dobers *et al.,* 2000). Homodimerization induced by this domain is critical for enzyme activity of the protein (Puschel *et al.,* 1982; Walborg *et al.,* 1985).

The C-terminal region of DPPIV contains the residues which make up the catalytic centre. In human, the active site serine-630 of DPPIV is surrounded by Gly-Trp-Ser630-Tyr-Gly-Gly-Tyr-Val, which corresponds to the motif Gly-X-Ser-X-Gly proposed for serine-type peptidases. The catalytic triad of human-DPPIV is composed of the residues Ser630, Asp708, and His740, which are located within the last 140 residues of the C-terminal region (Ogata *et al.,* 1992). The catalytic triad composes of Ser631, Asp709 and His741 in rat (Ogata *et al.,* 1989) and Ser624, Asp702 and His734 in mouse (David *et al.,* 1993) respectively.

At physiological conditions DPPIV is found on the cell surface as a non-covalently linked homodimer composed of two identical subunits (Kreisel *et al.,* 1982). The unglycosylated monomeric protein backbone has a molecular weight of 84 kDa (Petell *et al.,* 1987). The molecular

weight of DPPIV homodimer depends on organ- and species in question and ranges between 210 and 280 kDa (Kenny *et al.*, 1976) due to different levels in glycosylation (Puschel *et al.*, 1982).

The crystal structure of DPPIV from various mammals including human-DPPIV was solved (Engel *et al.*, 2003; Hiramatsu *et al.*, 2003; Rasmussen *et al.*, 2003; Aertgeerts *et al.*, 2004). The crystal structures revealed a homodimer in human and tetramer in porcine-DPPIV. Each monomer is composed of two domains: an N-terminal 8-bladed β-propeller domain (residues 61–495) and a C-terminal α/β-hydrolase domain (residues 39–55 and 497–766). The cysteine- and N-glycan-rich domains are packed within the β-propeller domain. The catalytic triad (S630, D708, and H740) is at the interface of the two domains. Two openings, one in the β-propeller domain and a side opening formed at the interface of the β-propeller and hydrolase domains provide access to substrates (Aertgeerts *et al.*, 2004). The propeller opening is formed by the β-propeller domain, which is composed of an unusual eightfold repeat of blades. Each blade comprises four-strands of antiparallel β-sheets. The β-propeller domain defines a funnel shaped, solvent-filled tunnel that extends from the lower face of the β-propeller to the active site. The lower face of the funnel, distal to the hydrolase domain, has a diameter of approximately 15 Å. The size of the distal and side openings reveals why the substrates and inhibitors of DPPIV must possess a limited chain length of about 80 amino acid residues.

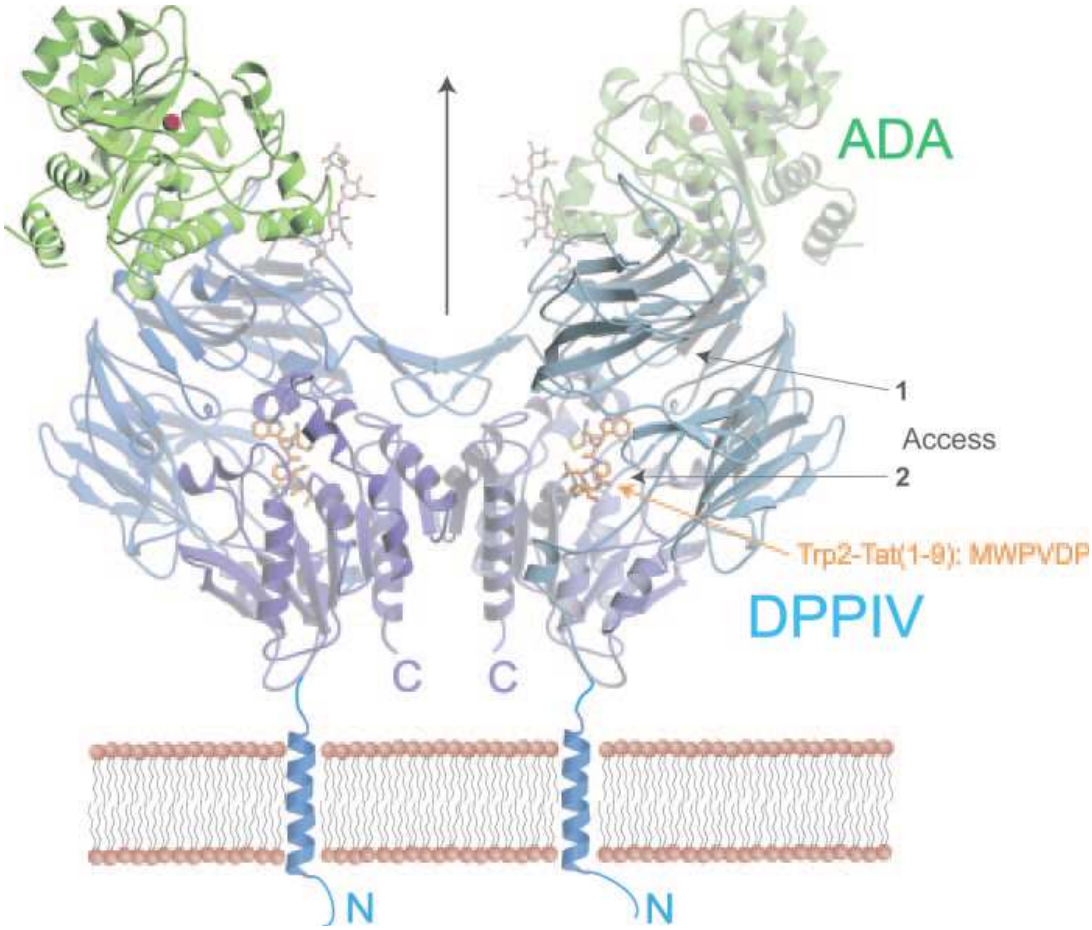

Figure 1.2: Crystal structure of human-DPPIV in complex with bovine adenosine deaminase (ADA) and two Trp2-TAT-(1–9) peptides (Weihofen *et al.*, 2005).

The membrane and membrane anchor (not seen in the electron density) are drawn schematically. The view is normal to the pseudo-2-fold axis (vertical arrow) that relates the two hDPPIVbADA in []2. The domains of hDPPIV are colored dark blue and light blue for the /-hydrolase and -propeller domains, respectively, and two tetrasaccharides (stick modeled) covalently attached to hDPPIV bind to bADA (green, with Zn2+ (red sphere) in the active site) bound to the outer ring of the –propeller domain of each hDPPIV. Six residues of the nonapeptide Trp2-Tat-(1–9) in orange bind to the active site of each hDPPIV. On the right, the upper part (N terminus) of the peptide is located in the active site between the /-hydrolase and -propeller domains of hDPPIV, and the lower part is located in the side opening that points toward the viewer. On the left, the peptide enters the active site from the back.

1.2.3 Biological functions of DPPIV

1.2.3.1 DPPIV as a serine protease

Almost all biochemical reactions in biological systems are catalyzed by enzymes. These are capable of increasing the reaction speed to 10^6 -10^{20} times faster compared to non-catalyzed reactions. The catalytic activity of many enzymes can be regulated by many different factors. DPPIV as a model example of a biological enzyme is involved in many biochemical reactions. DPPIV is highly specific to a broad range of substrates as well as the reaction in question. As an exopeptidase, DPPIV selectively cleaves dipeptides from the N-terminus of specific peptides with a proline or alanine in the penultimate position, thereby modifying their functions (Callahan *et al.*, 1972; Kenny *et al.*, 1976). Although a wide range of polypeptides with the sequence Xaa-Pro… are substrates of DPPIV, it must be noted that not all polypeptides with this sequence are substrates for DPPIV. Examples of such exceptions are intact Interleukin-2 and G-CSF (Hoffmann *et al.*, 1993). The peptide-length plays a great role in the selectivity of substrates by DPPIV. Peptides up to 80 residues in length fall in the range of substrates for DPPIV, whereas such peptides longer than 80 residues are unlikely to be proteolytically processed by DPPIV (Nausch *et al.*, 1990). Furthermore, the rate of DPPIV catalyzed proteolysis is inversely related to the chain length of the substrate (Lambeir *et al.*, 2001). The crystal structure of DPPIV revealed two openings leading to the active centre (referenced under section 1.2.2). A closer consideration of the side openings revealed that the β-propeller domain defines a funnel shaped, solvent-filled tunnel that extends from the lower face of the β-propeller to the active site. The nature of these openings seems to determine the length and nature of substrates that can reach the active site, explaining the high selectivity of DPPIV to substrates with a maximum of 80 residues of length (Aertgeerts *et al.*, 2004).

Evolutionally, the possession of proline residues provides unique structural properties to peptide chains because it is the only cyclic amino acid which affects the susceptibility/resistance of peptide bonds to cleavage (Yaron & Naider, 1993; Vanhoof *et al.*, 1995). This unique proline residue serves as a regulatory element in proteolytic processing and is quite conserved in a wide range of biologically active peptides. The ability of DPPIV and other molecules of the DPP gene family to cleave such peptides make them important modulators of biological processes. With effect to this, natural substrates of DPPIV include Neuropeptides, Peptide hormones, cytokines and chemokines (Yaron & Naider, 1993; De Meester *et al.*, 1999; Mentlein, 1999; Lambeir *et al.*, 2003). A long list of possible substrates of DPPIV has been put together, based on the sequence of peptides as well as both *in vitro* and *in vivo* catalytic assays. However, in accordance with *in vivo*- catalysis not all of the substrates can be considered physiologic substrates of DPPIV. The peptide hormones glucose dependent insulinotropic polypeptide (GIP), glucagon-like peptide 1 and 2 (GLP1 and GLP-2) and peptide-histidine-methionine (PHM) (Mentlein *et al.*, 1993; Lambeir *et al.*, 2002), growth hormone releasing hormone (GRH) (Frohman *et al.*, 1989; Bongers *et al.*, 1992), and enterostatin (Bouras *et al.*, 1995) are physiological substrates of DPPIV. GIP and GLP1 are the most important insulin-stimulating hormones (Efendic & Portwood, 2004). Both peptides are released from the gastrointestinal tract in response to ingestion of carbohydrate rich meals and stimulate glucose-dependent insulin secretion from the pancreas, thereby regulating the overall glucose homeostasis. The actions of GIP and GLP1 depend on glucose concentration in serum, and their function ceases when serum glucose level is less than 55 mg/dL (Drucker *et al.*, 1987). Cleavage by DPPIV inactivates GIP and GLP1 and abolishes their insulinotropic activity. Patients with diabetes mellitus type-2 exhibit an attenuated insulinotropic action of GIP but not GLP1 and a significant reduction in meal-stimulated levels of GLP1 (Nauck *et al.*, 1993; Toft-Nielsen *et al.*, 2001).

Further peptides involved in neurological and psychomodulatory processes such as Peptide YY and Neuropeptide Y (Mentlein *et al.*, 1993), Substance P (Heymann & Mentlein, 1978), and Endomorphin 2 (Shane *et al.*, 1999) are physiologic substrates of DPPIV. Whereas cleavage of GLP1 by DPPIV causes inactivation, cleavage of PYY_{1-36} yields the long C-terminal fragment $PYY_{3–36}$, with modified PYY receptor specificity (Grandt *et al.*, 1993). Specifically, cleavage by DPPIV converts the non-subtype-selective agonist PYY_{1-36} into a selective agonist PYY_{3-36} at Y2 and Y5 receptors (Michel *et al.*, 1998). Substance P is a short substrate that, by a stepwise release of Arg-Pro and Lys-Pro, is cleaved into the active heptapeptide substance $P_{5–11}$ which modulates T cell function (Covas *et al.*, 1997).

Peptides involved in signal transduction and immune functions also make up a subset of natural occurring substrates for DPPIV. These include chemokines such as regulated on activation, normal T cell expressed and secreted, (RANTES) (Oravecz *et al.*, 1997), stromal cell-derived factor 1

(SDF-1α) (Proost *et al.*, 1998; Shioda *et al.*, 1998), macrophage-derived chemokine (MDC), (Struyf *et al.*, 1998), LD78β (Proost *et al.*, 2000), macrophage inflammatory protein-1β (MIP-1β), monocyte chemotactic protein-2 (MCP-2) and interferon-inducible protein-10 (IP-10) amongst others (De Meester *et al.*, 1999; Lambeir *et al.*, 2001). Whereas cleavage of the chemokines Eotaxin, MDC and SDF-1α by DPPIV lead to their inactivation, cleavage of RANTES by DPPIV leads to receptor selectivity, whereby the signalling through CCR1 and CCR3 are reduced and binding to CCR5 is improved thereby contributing to its anti-HIV activity.

Due to the possession of a proline or alanine in the second position of their amino termini, many peptides can be considered substrates of DPPIV. Nevertheless, most of them such as the interleukins IL-1α, IL-1β, IL-2, IL-6, the tumor necrosis factors TNF-α, TNF-β and the chemokines CXCL2, CCL2 and CCL7 and G-CSF are not hydrolyzed by DPPIV *in vivo* (Hoffmann *et al.*, 1993; Oravecz *et al.*, 1997). In **Table 1.1** a summary of the physiologic substrates of DPPIV based on *in vitro* and *in vivo* proteolysis by DPPIV is presented.

Table 1.1: Natural Peptides with known physiological activity that serve as substrates of DPPIV

Substrate families and Peptides	**Peptide length**	**Catalytic efficiency ($M^{-1}.Sec^{-1}$)**	**Biological effect**	**Species (in vitro/in vivo)**
Incretins and gastrointestinal hormones				
GLP1	30	0.43×10^6	Inactivation Possible cardiovascular role of the product	Human (in vivo) Dog (in vivo)
GLP-2	34		Inactivation	Human (in vivo)
GIP	42	0.22×10^6	Inactivation	Human (in vivo)
GRH (1-44)	44	2.0×10^6	Inactivation	
GRH (1-29)	29	2.0×10^6	Inactivation	Human (in vitro)
PHM	27	0.19×10^6	*Inactivation*	Human (in vitro)
GRP	27		Not known	Human (in vitro) Product in dogs
Peptide YY[a]	36		Change in receptor preference	Human (in vivo), Rat (in vivo, vasoactive action)
Vasoactive peptides				
VIP	28		*Inactivation*	Human (in vitro)
BNP[a]	32		Change in receptor preference or Inactivation	Human (in vitro) Product in dogs
Neuropeptides				
NPY[b]	36	12.0×10^6	Change in receptor preference	Human (in vivo, indirectly) Rat (in vivo)
β-casomorphin	7	3.1×10^{-6}	Inactivation	Human (in vivo, indirectly) Rat (in vivo)
Endomorphin-2	4		Change in receptor preference	Rat (in vivo) Mouse (in vivo)
Substance P	11	0.91×10^6	Inactivation	Rat (in vivo) Pig (in vivo) Human (in vitro)
Chemokines				

CCL3 (MIP-1a, LD78β)	70	0.003± 0.002 x 10^6	Enhanced activity Change in receptor preference	Human (in vivo, indirectly)
CCL4 (MIP-1β)	69		Change in receptor preference	Human (in vivo, indirectly)
CCL5 (RANTES)	68	0.04 ± 0.01 x 10^6	Change in receptor preference	Human (in vitro, indirectly)
CCL11 (Eotaxin)	74	0.08± 0.01 x 10^6	Inactivation	Human (in vitro), Rat (in vivo)
CCL22 (MDC)	69	4± 1 x 10^6	Change in receptor preference	Human (in vitro)
MDC67	67	0.5± 0.1 x 10^6	Change in receptor preference	Human (in vitro)
CXCL6 (GCP-2)	73		No changes	Human (in vitro)
CXCL9 (MIG)	125	Low	Inactivation	Human (in vitro)
CXCL10 (IP-10)	77	0.5± 1 x 10^6	Inactivation, CXCR3 antagonist	Human (in vivo, indirectly)
CXCL11 (I-TAC)	73		Inactivation, CXCR3 antagonist	Human (in vivo, indirectly)
CXCL12 (SDF-1α)	68	5± 2 x 10^6	Inactivation, CXCR4 antagonist	Human (in vivo)

The information contained in this table is modified according to Mentlein *et al.*, 1993, Mentlein, 1999. De Meester *et al.*, 1999; Hildebrandt *et al.*, 2000; Boonacker and Van Noorden 2002.

Biological effect in italics refers to hypothesis. Species (in vivo/in vitro) refers to: In vivo, the existence of studies in humans or other species with inhibitors as well as the existence of the product and well-known biological effects of peptides; *indirectly* refers to the lack of in vivo studies with inhibitors. [a] Peptides belong also to the neuropeptide group, [b] Peptides belong also to the vasoactive group. **Abbreviations: VIP**, vasoactive intestinal polypeptide; **BNP**, brain natriuretic peptide; **GCP-2**, granulocyte chemotactic protein 2; **MCP**, monocyte chemotactic protein; **GIP**, glucose-dependent insulinotropic polypeptide; **GLP1**, glucagon-like peptide 1; **GRF**, growth hormone-releasing factor; **GRH**, growth hormone-releasing hormone, **IP-10**, interferon-inducible protein 10; **MDC**, macrophage-derived chemokine; **PHM**, peptide histidine methionine; **SDF-1**, stromal cell-derived factor 1. **RANTES**, regulated on activation normal T cell expressed and secreted; **MIP**, macrophage inflammatory protein; **GRP**, gastrin-releasing peptide.

1.2.3.2 DPPIV in the immune system

Repeated evidence associate DPPIV with the function of T cells (Morimoto & Schlossman, 1998; Augustyns *et al.*, 1999). DPPIV is highly expressed on activated T- and B-lymphocytes and at lower concentrations on macrophages as well. Approximately 56% of activated $CD4^+$ and 35% of $CD8^+$-T-lymphocytes express the enzyme, respectively (Fox *et al.*, 1984), whereas resting T cells show very low expression (Schon *et al.*, 1986; Dang *et al.*, 1990). A detailed analysis of lymphocytes revealed that only the T-Helper subpopulation expressing CD4, CD45RO and CD29 also express DPPIV (that is $CD4^+CD45RO^+CD29^+$ cells) (Morimoto & Schlossman, 1998). The high expression of DPPIV on particular T cell subsets and its association as well as binding with further important molecules of the immune system such as CD45, ADA and components of the extra-cellular-matrix (ECM), reveal the co-stimulatory role of DPPIV in T cell activation.

Furthermore, the proteolytic processing of several chemokines makes DPPIV a regulator of chemokine function.

1.2.3.2.1 DPPIV as a co-stimulator in T cell activation

The stimulation of the CD3/T cell receptor (TCR) complex by specific peptide-MHC contacts provide one signal and play a central role in T cell activation and function. However, this alone is not sufficient to fully induce the activation of T cells. A second signal often provided by co-stimulatory surface molecules such as CD28 and DPPIV is indispensable.

The primary structure of DPPIV reveals a very short cytoplasmic region consisting of only 6 amino-acid residues. Therefore, signal transduction function of DPPIV by this cytoplasmic tail seems unlikely. It is evident that DPPIV interacts with CD45, a protein tyrosine phosphatase and adenosine deaminase (De Meester *et al.*, 1994; Dong *et al.*, 1997), which are involved in signal transduction processes associated with T cell activation. It has been established that T cell activation involves lipid rafts. DPPIV engagement promotes aggregation of lipid rafts and facilitates co-localization of CD45 to TCR and its signalling molecules $p56^{LCK}$ and ZAP-70, thereby enhancing protein tyrosine-phosphorylation of various signalling molecules (Ishii *et al.*, 2001). Recently the signalling, caveolae structural protein Caveolin-1, (Cav-1) was identified as the ligand of DPPIV in T cell signalling (Ohnuma *et al.*, 2004). Precisely, the interaction of CD26 with caveolin-1 on antigen-loaded monocytes resulted in CD86 up-regulation, thereby enhancing the subsequent interaction of CD86 and CD28 on T cells, thus inducing antigen-specific T cell proliferation and activation (Ohnuma *et al.*, 2007). The cytoplasmic tail of DPPIV seems to be involved in this signalling in T cells, through an interaction with CARMA1. Ligation of Cav1 recruits a complex of DPPIV, CARMA1, Bcl-10 and IKKβ to lipid rafts.

It was established earlier, that only $CD4^+$ cells that express DPPIV are able to provide helper functions in the activation of cytotoxic T cells (Dang *et al.*, 1990) and induction of immunoglobulin synthesis by B-cells (Gruber *et al.*, 1988). Furthermore, anti-CD26 monoclonal antibodies have co-stimulatory activities in anti-CD3-driven activation of purified T cell subsets (De Meester *et al.*, 1995; Hegen *et al.*, 1997; von Bonin *et al.*, 1998). Cross-linking of CD26 by antibody causes tyrosine-phosphorylation of several intracellular proteins involved in TCR/CD3-mediated signal transduction, including the tyrosine kinase $p56^{lck,}$ $p59^{fyn}$, ZAP-70, mitogen-activated protein kinase (MAPK), c-Cb1 and phospholipase C, (Hegen *et al.*, 1997). Effective CD26 signalling on the other hand depends on the surface expression of the TCR/CD3 complex (Fleischer, 1994). Whether the enzymatic activity of DPPIV is important in its function in T cell activation still remains to be clarified. Whereas one research work demonstrated a higher IL-2 production in Jurkat cells expressing wild type CD26 than in those expressing enzymatically inactive mutants upon CD26-

mediated co-stimulation (Morimoto & Schlossman, 1998), another work demonstrated by using a mouse TCR^+ T cell hybridoma, that DPPIV enzyme activity is not required for its co-stimulatory function (von Bonin *et al.*, 1998). Furthermore, inhibiting the enzyme activity of DPPIV by specific inhibitors suppress T cell proliferation in vitro (Reinhold *et al.*, 1993) and leads to a decrease in antibody production in mice immunized with bovine serum albumin (Kubota *et al.*, 1992). Several other studies demonstrate alterations in various signalling pathways upon use of DPPIV inhibitors (Arndt *et al.*, 2000; Vetter *et al.*, 2000). The inhibition of the enzymatic activity of DPPIV also abrogates acute rejection, resulting in prolonged allograft survival in a rat cardiac transplantation model (Korom *et al.*, 1997). Using a series of related competitive inhibitors in pokeweed mitogen stimulated T cells, significant suppression of IL-2, IL-10, IL-12 and IFN-γ production and an increase of TGF-β (transforming growth factor-beta) were demonstrated (Reinhold *et al.*, 1997).

Taken together, the co-stimulatory role of DPPIV in T cell activation is quite evident, yet the exact role of its enzymatic activity in T cell activation is still unclear. Nevertheless, a discrepancy between these researches maybe just a result of the diversity of DPPIV action under healthy and diseased conditions. The injection of the DPPIV inhibitor Ala-boroPro and Pro-boroPro significantly reduced antibody production in BSA- immunized mice (Kubota *et al.*, 1992), and the inhibitors TMC-2a und TSL-225 showed anti-inflammatory effects on an arthritis-model (Tanaka *et al.*, 1997).

These results suggest that the enzymatic activity of DPPIV might contribute to, but is not a prerequisite for signal transduction or T cell activation.

1.2.3.2.2 DPPIV as a regulator of chemokine function

Haematopoiesis is the process by which pluripotent hematopoietic stem cells differentiate and move from the bone marrow to become mature cell components of blood. This is a tightly regulated process which on a large part is controlled by interactions between specific cytokines/chemokines (produced and released from accessory cells), and their receptors which are found on hematopoietic stem (HSC) and -progenitor cells (HPC) as well as accessory cells (Broxmeyer & Carow, 1993). These ligand- receptor interactions trigger intracellular signalling effects that mediate proliferation, self-renewal, survival, and migration of HSC and HPC. Although single cytokines or chemokines can influence functions of HSC and HPC, combinations of cytokines are likely more influential in enhancing or suppressing them.

Chemotactic cytokines, (chemokines) constitute a group of secreted bioactive peptides (8–10 kDa) which are expressed constitutively (homeostatic chemokines) and also in an inducible manner (inflammatory chemokines) (Cyster, 1999; Cyster *et al.*, 1999). Their main functions are to attract leukocytes to sites of infection and inflammation and to contribute to the homeostatic circulation of

leukocytes through tissue (Luster, 1998). They also have the capacity to directly activate leukocytes, e.g., to release granular contents and produce cytokines. Recruitment and activation of leukocytes are important for elimination of microbes, including viruses, from infected areas. All chemokines except lymphotactin possess two disulfide bridges and the super family has been divided into several subfamilies, depending on structural, functional and genetic differences. For example the classes CC, CXC and CX3C, are classified depending upon the separation between the first two cysteine residues (Baggiolini, 2001). While the subfamily of CXC chemokines predominantly target neutrophils and also lymphocytes to a lesser degree, the CC chemokines mainly attract monocytes, but also lymphocytes, basophils, eosinophils, dendritic cells and NK cells. The N-terminal domain of chemokines together with an exposed loop between their second and third cysteine, is involved in receptor binding. Proteolytic cleavage by DPPIV removes a dipeptide from the N-terminus and either activates or inactivates the chemokines. This leads to important alterations in chemokine activities and receptor specificity, thereby contributing to the regulation of target cells and consequently to a differential cell recruitment (Oravecz *et al.*, 1997).

The chemokines, CCL3 (macrophage inflammatory protein-1 isoform LD78β), MIP1, RANTES, eotaxin, MDC, CXCL9 (MlG: monokine induced by IFN-γ), IP-10, CXCL11 (I-TAC: IFN-inducible T cell chemo attractant) and SDF-1α and 1β are natural substrates of DPPIV (see details under 1.2.3.1). Amongst them, LD78, RANTES, CCL11, MDC and SDF1 exhibit altered chemotactic activities following DPPIV-mediated truncation, whereas neither CXCL6 nor IP-10 exhibit any alterations in chemotactic function. A double truncation of macrophage-derived chemokine (MDC) was observed (Proost *et al.*, 1999). MDC loses not only Gly1-Pro2 but also Tyr3-Gly4, suggesting that the substrate specificity of DPPIV might be less restricted than is generally accepted. Compared with the intact chemokine, $MDC_{5–69}$ has a reduced chemotactic activity for lymphocytes and monocyte-derived dendritic cells, but remains as chemotactic as intact $MDC_{1–69}$ for monocytes.

SDF-1α is an unusual chemokine with only 20-25% sequence identity to the CXC- and CC-chemokine family members (Crump *et al.*, 1997). SDF-1α has chemo-attractant activity for lymphocytes and monocytes, plays an important role in trafficking, export and homing of bone marrow cells, inhibits infection by T-tropic strains of HIV-1, and is involved in the spread of leukaemia to multiple marrow sites and in regulating metastasis of a number of solid tumours, including sarcomas and prostate cancer (Juarez & Bendall, 2004; Kucia *et al.*, 2004). Following proteolytic processing by DPPIV, SDF-1α becomes inactive and loses its binding and signalling activity at the CXCR4 receptor. This enhances infection of T cells by T-tropic viral strains which use CXCR4 as co-receptor. However, processed $SDF\text{-}1\alpha_{3\text{-}68}$ can still desensitize $SDF\text{-}1\alpha_{1–68}$-induced Ca^{2+} responses through CXCR4.

RANTES, a CC chemokine with chemo-attractant activities for monocytes, macrophages and eosinophils becomes active following cleavage by DPPIV. The processed $RANTES_{3–68}$ has a more than ten times lower chemotactic potency for monocytes and eosinophils and impaired binding and signalling properties through CCR1 and CCR3, but remains fully active on CCR5, which serves as co-receptor for M-tropic viruses. Thus, truncation of RANTES by DPPIV regulates its receptor selectivity (Oravecz *et al.*, 1997; Proost *et al.*, 1998) and inhibits the infection of macrophages by M-tropic viral strains.

Another CC chemokine, eotaxin, attracts eosinophils to sites of parasitic infection and allergic inflammation. Its chemotactic potency for blood eosinophils and signalling capacity through CCR3 are reduced 30 times upon truncation by DPPIV (Struyf *et al.*, 1999).

Taken together the signalling effects of DPPIV-processed chemokines are poorly studied and deserve a lot of attention. Notwithstanding, the reports available show that truncation by CD26/DPP IV often has drastic effects on the biological activity of individual chemokines and confirm the importance of their N-terminal residues for receptor activation and also expose the potential role of DPPIV in the modulation of T cell and monocyte extravagation and migration *in vivo*.

1.2.4 DPPIV interaction and binding partners

Besides its enzymatic activity the signalling activity of DPPIV seem to be more dependent on its association with other proteins of the host cells as well as proteins of many pathogens such as microbes and viruses. Through these interactions and binding, DPPIV is involved in a wide range of biologically relevant processes in the host organisms. Its association with adenosine deaminase, CD45, caveolin-1 and CARMA-1 is involved in the activation of T cells, whereas its association with fibronectin, collagen, plasminogen-2 and mannose-binding protein may play roles in cancer biology.

1.2.4.1 Adenosine deaminase (ADA)

Adenosine deaminase (ADA, EC. 3.5.4.4) is a cytosolic enzyme also found on the cell surface. In peripheral nucleated blood cells for example, ADA is found as an ectoenzyme in the majority of monocytes and B cells and in some T cells (Aran *et al.*, 1991). The main role for ecto-ADA is the degradation of extracellular adenosine and 2´-deoxyadenosine which are toxic to lymphocytes, to inosine and 2´-deoxyinosine (Dong *et al.*, 1996). Through this degradation the concentration of extracellular adenosine is tightly regulated. Hereditary ADA-deficiency in human causes impairment of T and B cell function which leads to severe combined immune-deficiency disease (SCID) (Magnuson & Perryman, 1986; Blaese *et al.*, 1995). The presence of ADA on the cell surface is facilitated by its direct binding to cell surface proteins such as DPPIV and A_1-adenosine

receptors (A_1R) (Franco *et al.*, 1998). A direct association of ADA with DPPIV was demonstrated, which revealed that DPPIV is identical to ADA-binding protein (Kameoka *et al.*, 1993). This co-association only occurs on the cell surface (Dong *et al.*, 1997), and is found in human, cattle and rabbits, but not in rats and mice (Gorrell *et al.*, 2001).

The crystal structure of DPPIV in complex with ADA revealed that each β-propeller domain of the DPPIV dimer binds one ADA, and two hydrophobic loops protruding from the β-propeller domain of DPPIV interact with two hydrophilic and heavily charged α-helices of ADA at the binding interface (see Figure 1.2). Furthermore, four glycosides linked to Asn229 of DPPIV bind to ADA (Weihofen *et al.*, 2004). The tetramer formation observed in the crystal structure of porcine-DPPIV was suggested to mediate epithelial and lymphocyte cell-cell adhesion. ADA binding to DPPIV probably regulates this adhesion, since it would abolish tetramerization (Engel *et al.*, 2003).

Through its binding to cell surface DPPIV, ADA is thought to have a co-stimulatory effect in TCR-mediated T cell activation, which results in an increased proliferation and IL-2 production in Jurkat cells upon stimulation. In the presence of extracellular adenosine, transfectants with binding site mutated DPPIV are much more sensitive to the inhibitory effect of adenosine and produce less IL-2 than transfectants with wild type DPPIV. Furthermore, similar amounts of IL-2 production are found in the absence of extracellular adenosine in transfectants with mutated and wild type DPPIV. Moreover, adenosine is known to induce DNA-fragmentation in T cells and selectively deplete the $CD4^+CD8^+$ double-positive immature thymocytes subpopulation expressing a higher level of $CD3^+$ TCR (Szondy, 1994). This suggests that the CD26-ADA complex may be involved in thymus differentiation and maturation and prevention of apoptosis (Morimoto & Schlossman, 1998). However, ADA from a healthy adult who expressed only the enzyme with a R142Q mutation showed markedly reduced binding to CD26 (Santisteban *et al.*, 1995), suggesting that like in mice, binding of ADA to CD26 is not essential for immune function in humans since it is compensable by other unknown pathways.

1.2.4.2 Collagen and Fibronectin

Collagen and fibronectin are components of the extracellular matrix. Due to the ability of DPPIV to bind via the cysteine-rich region to collagen (Loster *et al.*, 1995) and fibronectin, (Hanski *et al.*, 1985; Piazza *et al.*, 1989), DPPIV probably plays a role in cell adhesion, differentiation and migration. Consistent with this, anti-DPPIV specific antibodies inhibit hepatocyte spreading on native collagen (Hanski *et al.*, 1988). It was established that various collagen types have varying affinities to DPPIV. Whereas collagen I and III have the strongest binding ability, collagen II, IV and V have only weak binding affinities and collagen VI binds DPPIV with the lowest affinity (Loster *et al.*, 1995). The strong binding of DPPIV to collagen I is mediated by the α1 (i)-chain of

collagen I. Binding of collagen to DPPIV is independent of the enzyme activity of DPPIV. This is evident in the fact that neither substrates nor inhibitors of DPPIV can affect the binding of soluble DPPIV to collagen I in vitro (Hanski *et al.*, 1985; Hanski *et al.*, 1988). However, the regulation of collagen metabolism seems to be partly mediated by DPPIV enzyme activity. As a result, the use of DPPIV specific inhibitors in rats led to the accumulation of amyloid peptides of collagen origin (Jost *et al.*, 2009).

A direct interaction of rat-DPPIV with fibronectin was reported and the clinical relevance of this interaction in lung capillaries of breast cancer patients was postulated (Cheng *et al.*, 1998). In support of this, administration of soluble DPPIV resulted to about 80% decrease in adhesion of metastatic breast-cancer cells on lung endothelial DPPIV in rats. Binding of DPPIV to fibronectin is mediated by the consensus sequence T (I/L)TGLX(P/R)G(T/V)X (Cheng *et al.*, 2003).

Taken together the interaction of DPPIV to fibronectin makes DPPIV a cell-adhesion protein for circulating metastasing tumor cells (Cheng *et al.*, 2003; Kajiyama *et al.*, 2003).

1.2.4.3 Plasminogen type-2

Following injury of a tissue, coagulation takes place as one of the steps involved in repairs. The thrombus (clot) is rich in fibrin which needs to be removed once haemostasis is restored and the tissue repaired. The removal of the clot is achieved by the fibrinolytic pathway. Fibrinolysis involves the lyses of fibrin by the enzyme plasmin. Plasmin is able to degrade fibronectin, laminin, vitronectin and proteoglycans and activate latent collagenases (Dano *et al.*, 1985). Furthermore, plasmin mediates the increased availability of active basic fibroblast growth factor (bFGF), as a result of extracellular matrix (ECM) degradation and directly activates the latent transforming growth factor-β (TGF-β) (Rifkin *et al.*, 1997; Rifkin *et al.*, 1999).

Plasmin is converted from its inactive form, plasminogen by plasminogen activators through the so called plasminogen activation system. The plasminogen activation system is an enzymatic cascade involved in the control of fibrin degradation and in matrix turnover and cell invasion. For example, the development of an aggressive phenotype, commonly associated with the invasive behaviour of many tumours, involves the increased expression of enzymes such as urinary plasminogen activator (uPA), tissue plasminogen activator (tPA) and a variety of matrix-degrading metalloproteinases (MMPs), such as MMP-2 and MMP-9 (DeClerck & Laug, 1996), that can digest components of the ECM, thus permitting passage of malignant cells through basement membranes and stromal barriers (Nagase *et al.*, 1996). Plasminogen activation is catalyzed by the earlier mentioned enzymes uPA and tPA. Whereas uPA is regarded as the critical trigger for plasmin generation during cell migration and invasion under physiological and pathological conditions (e.g. cancer metastasis), tPA plays an important role in the control of intravascular fibrin degradation. The regulation of both

enzymes is tightly time- and space dependent (Mazzieri *et al.*, 1997; Ramos-DeSimone *et al.*, 1999).

Human-plasminogen is a 791 amino acid long, inactive zymogene which can be activated to plasmin by a single proteolytic cleavage of the Arg560Val562 peptide bond. Plasminogen type-2 (Pg2) has six glycoforms that vary in the sialic acid contents (Pirie-Shepherd *et al.*, 1995) which control their activation and regulate their function (Davidson & Castellino, 1993; Mori *et al.*, 1995).

DPPIV has been demonstrated as one of the membrane receptors for Pg2 in the highly invasive human prostate tumour cell line 1-LN. Similar to observations in human rheumatoid synovial fibroblasts, binding of Pg2 to DPPIV and uPA induced a significant rise in the cytosolic concentration of free Ca^{2+} (Gonzalez-Gronow *et al.*, 1993), which resulted in the expression of matrix metalloproteinases and enhanced invasiveness of the cells (Gonzalez-Gronow *et al.*, 1994). Amongst the six glycoforms of Pg2, DPPIV binds only to the highly sialylated glycoforms Pg2γ, Pg2δ and Pg2ε (Gonzalez-Gronow *et al.*, 2001). This binding was inhibited by increasing concentrations of L-lactose, suggesting the importance of sialic acid components of Pg2 in the mediation of its binding to DPPIV. Both DPPIV and ADA associate with Pg2 in a complex that enhances Pg2 activation (Gonzalez-Gronow *et al.*, 2004). Furthermore, it has been demonstrated in the cell line 1-LN that DPPIV in association with Pg2ε alone can regulate the expression of pro-matrix-degrading metalloproteinase 9 (proMMP-9) (Gonzalez-Gronow *et al.*, 2001). Taken together, these findings strengthen the role of DPPIV in cell migration of metastasing cancer cells, as was earlier postulated (Cheng *et al.*, 2003; Kajiyama *et al.*, 2003). This process is likely co-regulated by DPPIV and Fabα, since they play opposing roles in plasminogen activation. Whereas the DPPIV-plasminogen binding mediates plasminogen activation, Fabα associates with and converts the PA-inhibitor, a2-antiplasmin into a more active form which inhibits fibrinolysis and cell migration (Lee *et al.*, 2004).

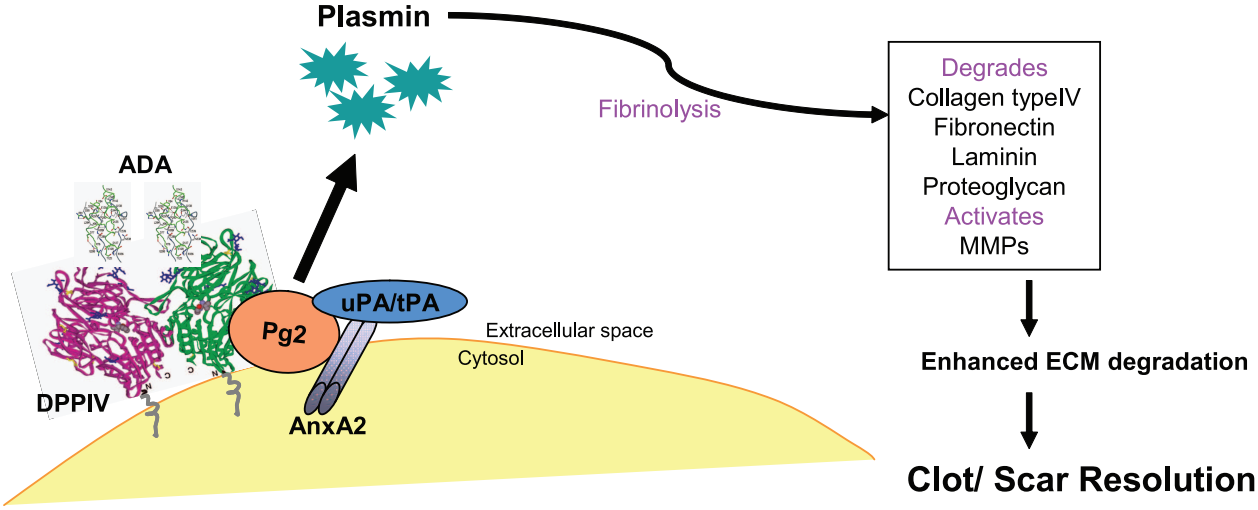

Figure 1.3: Model of the role of DPPIV in fibrinolysis

As a result of binding of DPPIV and ADA to plasminogen 2 in a complex involving the plasminogen receptor annexin 2 (AnxA2) and the plasminogen activators uPA and tPA (tissue plasminogen activator), plasminogen-2 (Pg2) activation to plasmin increases. The figure was modified according to (Gorrell, 2005).

1.2.4.4 Kidney Na^+/H^+ ion exchanger 3 (NHE3)

Reabsorption of water and filtration of sodium chloride (NaCl) and sodium bicarbonate ($NaHCO_3$) in the kidney are indispensable processes for correct elimination of waste products via excretion. The majority of NaCl, $NaHCO_3$ and water filtered by the kidney is reabsorbed in the proximal tubule. Absorption of Na^+ and secretion of H^+ across the apical membrane of proximal tubule cells occurs predominantly by Na^+-H^+ exchange (Alpern, 1990). It has been demonstrated repeatedly, that NHE3 is the Na^+-H^+ exchanger isoform responsible for most, if not all, apical membrane Na^+-H^+ exchange activity in the proximal tubule of the nephron (Biemesderfer *et al.,* 1993; Amemiya *et al.,* 1995; Schultheis *et al.,* 1998; Wang *et al.,* 1999). The NHE3 isoform, whose activity is regulated in response to a wide variety of acute and chronic physiologic stimuli, plays an important role in the maintenance of fluid and electrolyte balance (Paillard, 1997; Weinman *et al.,* 2000). The expression and regulation of transporters such as NHE3 often involves interactions with other proteins. Several studies in non-epithelial cells transfected to over express NHE3 revealed the interaction and binding of NHE3 to numerous proteins such as calmodulin (Wakabayashi *et al.,* 1995), the NHE regulatory factor (NHERF) (Weinman *et al.,* 2000) and its homologue, exchanger-3-kinase-A regulatory protein (Yun *et al.,* 2002) and the calcineurin B homologous protein (Pang *et al.,* 2002).

In a study with microvillus membranes isolated from rabbit renal cortex, Girardi and colleagues demonstrated the association of DPPIV with the NHE3 and showed evidence for the primary location of the NHE3-DPPIV complex in the microvillar micro domain of the kidney brush border (Girardi *et al.,* 2004). From these findings they suggested that the surface expression and activity of NHE3 may be affected by DPPIV. However, the role played by the NHE3-DPPIV association remains unclear.

1.2.4.5 The C-X-C Chemokine Receptor 4 (CXCR4)

CXCR4 is a 42-kDa seven-transmembrane (7-TM) G protein-coupled receptor. It serves the only receptor for SDF-1α (Bleul *et al.,* 1996). The disruption of the *cxcr4 gene* led to hematopoietic, cardiovascular and cerebellar defects as well as embryonic lethality (Nagasawa *et al.,* 1996). Almost identical phenotypes are associated with the disruption of the *sdf1α* gene suggesting that CXCR4 is the only receptor for SDF1α.

In addition to its main role as a chemokine receptor, CXCR4 is one of the principal co-receptors for the infection of human cells by T-tropic HIV strains (Feng *et al.*, 1996; Doranz *et al.*, 1999).
Binding of SDF-1α to CXCR4 induces chemotaxis and anti-viral activity in Th2 cells but not Th1 subsets, and mediates migration and activation of leukocytes during immune and inflammatory responses (Baggiolini, 1998). Long periods of treatment with SDF-1α lead to a homogeneous distribution of CXCR4 underneath the plasma membrane, and a clustered localization of DPPIV in intracellular vesicles. Interestingly, internalization of CXCR4 and DPPIV require phosphorylation of serine residues (Orsini *et al.*, 2000) and glycosylated residues (Ikushima *et al.*, 2000) respectively.
DPPIV associated directly and was co-internalized with CXCR4 in the T cell line Jurkat J32 and the B-cell line SKW6.4 (Herrera *et al.*, 2001). These results suggest that CXCR4 and DPPIV may function together. However, spontaneous, ligand-independent internalization of CXCR4 has been reported (Tarasova *et al.*, 1998), and the internalization of defective CXCR4 was hampered upon binding by SDF-1α, but did not affect the SDF-1α-mediated internalization of DPPIV in same cells. This indicates that the internalization routes for CXCR4 and DPPIV are different. As mentioned earlier, cleavage of SDF-1α by DPPIV leads to its inactivation and abolishes its binding to CXCR4, which results to the exposure of cells to infection by X4 HIV variants. Taken together, the co-association of DPPIV and the regulation of SDF-1α function by DPPIV suggest that the CXCR4-DPPIV complex is part of a functional unit which directly modulates SDF1α-induced chemotaxis and antiviral activity of lymphocytes. Thus, their manipulation by viral particles strengthens their joint role in the infection of humans by HIV.

1.2.4.6 CD45

The leukocyte common antigen, CD45 is a transmembrane glycoprotein expressed on most hematopoietic cells including all stages of B lymphocytes from pro-B to plasma cells (Charbonneau & Tonks, 1992). CD45 is involved in the regulation of src-family kinases. Dephosphorylation of the carboxyl-terminal tyrosine residue of src-family protein-tyrosine kinases (PTKs) by CD45 PTPase (protein-tyrosine phosphatase) is the triggering mechanism of their activation (Mustelin *et al.*, 1989; Ostergaard *et al.*, 1989; Trowbridge & Thomas, 1994). Activated src-family PTKs mediate the downstream signals of several extracellular stimuli, such as growth factors, cytokines and antigen stimulation, leading to diversification and amplification of the initial signals (Corey & Anderson, 1999).
Due to its PTPase activity, CD45 is required for the development and activation of T lymphocytes (Cahir McFarland *et al.*, 1993) and also for the tolerance induction and activation of B lymphocytes via antigen receptors (Justement, 2001). Interestingly, CD45 can regulate both positive and negative

cellular signals. For example, it positively regulates T cell activation through the dephosphorylation of the negative regulatory C-terminal tyrosine-phosphorylation sites of the src-kinase molecules $p56^{lck}$ and $p59^{fyn}$ (Weil & Veillette, 1996; Seavitt *et al.*, 1999). As a negative regulator, CD45 dephosphorylates components of the TCR complex (Gervais & Veillette, 1997; D'Oro & Ashwell, 1999) and inhibits the function of integrins (Roach *et al.*, 1997; Shenoi *et al.*, 1999).

Co-association of CD45 with DPPIV was demonstrated (Torimoto *et al.*, 1991). The interaction of DPPIV and CD45 promotes aggregation of lipid rafts and facilitates co-localization of CD45 to TCR and its signalling molecules $p56^{lck}$ and ZAP-70 (Zeta associated protein tyrosine kinase of 70,000 Da Mw), thereby enhancing protein tyrosine-phosphorylation of various signalling molecules which mediate cell proliferation (Ishii *et al.*, 2001). The association and recruitment of CD45 by DPPIV explains the role of DPPIV in signalling pathways which induce phosphorylation although DPPIV does not possess kinase activity.

1.2.4.7 Mannose-6-phosphate / insulin-like growth factor II receptor

The mannose-6-phosphate/insulin-like growth factor II receptor (M6P/IGF-IIR) is a multifunctional transmembrane glycoprotein whose major function is to bind and transport mannose-6-phosphate (M6P)-bearing glycoproteins from the trans-Golgi network to the surface of lysosomes (Scott & Firth, 2004). The receptor gene is considered a « candidate » tumour suppressor gene. Loss of function mutations in M6P/IGF-IIR gene could contribute to multi-step carcinogenesis (Hebert, 2006).

Binding of DPPIV to M6P/IGFIIR through residues on its carbohydrate moiety has been demonstrated, an interaction which seems relevant for DPPIV mediated T cell activation and migration (Ikushima *et al.*, 2000; Ikushima *et al.*, 2002). The enhanced migration in endothelial cells expressing M6P/IGFIIR was dependent on the enzymatic activity of DPPIV. Although DPPIV has no known motif for endocytosis, mannose-6-phosphorylation of DPPIV increases upon T cell activation, leading to increased binding to the M6P/IGFIIR which in turn results to internalization of DPPIV. Treatment of DPPIV with glycosidase or phosphatase completely abolished its binding to M6P/IGFIIR, implying that both glycosylation and phosphorylation of DPPIV are required for binding with M6P/IGFIIR (Ikushima *et al.*, 2000). The CD26–M6P/IGFIIR interaction and internalization is mediated by M6P residues on the DPPIV carbohydrate moiety and is likely a recycling or regulation pathway for the oligosaccharide chains on DPPIV. In hepatocytes and intestinal epithelial cells, this recycling seem to function in the repair of the oligosaccharide chains attached to glycoproteins, or in the regulation of terminal glycosylation e.g. in response to external stimuli (Kreisel *et al.*, 1993). Internalization and reprocessing is a property of all molecules associated with T cell activation such as the TCR/CD3 complex, DPPIV (Hwang *et al.*, 2000; Hwang & Sprent, 2001; Dietrich *et al.*, 2002; Menne *et al.*, 2002). The DPPIV-M6P/IGFIIR

interaction can therefore be considered a functional unit of the DPPIV-mediated, T cell co-stimulation cascade involved in the regulation and recycling of DPPIV.

1.2.4.8 Mannose-binding protein (MBP)

The mannose-binding protein (MBP) also called mannan-binding protein or mannan-binding lectin, (MBL) is a Ca^{2+}-dependent (C-type) serum lectin specific for mannose, N-acetylmannosamine, and fucose residues (Kawasaki, 1999; Dommett *et al.*, 2006; Taylor & Drickamer, 2007). MBP is an important serum component associated with innate immunity (Super *et al.*, 1989; Hoffmann *et al.*, 1999; Dommett *et al.*, 2006). Through the lectin pathway (Malhotra *et al.*, 1994) it activates complement system by binding to oligosaccharide ligands on the surface of microorganisms (Ikeda *et al.*, 1987). The lectin-pathway represents a host defence system, by which the host can distinguish between host cells and microorganisms based on the nature of their cell surface carbohydrates. Most mammalian cells possess complex cell surface oligosaccharides with sialic acids at their non-reducing termini, which prevents the binding of MBP to the cells. Opposed to mammalian cells many microorganisms have common oligosaccharide structures like mannose and N-acetylmannosamine, (ManNAc) on their surfaces which are recognized and bound by MBP. Interestingly, it was demonstrated that MBP binds to some human tumour cell lines, suggesting that MBP also functions as a defence factor against abnormal cells produced in host animals (Ma *et al.*, 1999; Muto *et al.*, 2001). Typical MBP-oligosaccharides from aberrant cell lines have the Le^b-Le^a structure or tandem repeats of the Le^a structure at their non-reducing termini (Terada *et al.*, 2005).
Human-MBP is a homo-oligomer which is assembled from a single polypeptide chain, consisting of a short N-terminal cysteine-rich domain, a collagen-like domain comprising 19 repeating Gly-X-Y triplets with an interruption at the 8 triplet, a 34-residue hydrophobic stretch, and a C-terminal C-type lectin domain. Three polypeptide chains form a homotrimeric structural unit, and functional MBP normally consists of two to six structural units joined by disulfide bonds at the N-termini. The molecular mass of the resulting MBP ranges between 200–1,300 kDa (Turner, 1996; Teillet *et al.*, 2005).
Recently DPPIV was identified as one of the ligand glycoprotein for MBP in the human colorectal carcinoma cell line SW1116 (Kawasaki *et al.*, 2009). DPPIV is a highly glycosylated and sialylated protein and as such not a good binding partner for MBP. Binding of MBP and DPPIV in the colorectal tumour cell line SW1116 correlated with an altered glycosylation pattern of DPPIV in these cells. Analysis of the glycosylation pattern of DPPIV revealed highly fucosylated structures. The DPPIV fraction that bound to MBP contained complex-type glycans with more than four type 1 and 2 Galβ1-4GlcNAc units which are responsible for the MBP binding. The exact role and mechanism underlying the DPPIV-MBP binding is not yet known. However, the alteration of

DPPIV expression, glycosylation and sialylation pattern seen in other diseases such as HIV/AIDS (Smith *et al.*, 1998), suggests a role for DPPIV as a defence marker of abnormal cells produced in host animals. Its recognition by MBP therefore may mark the cells for destruction.

1.2.4.9 Caveolin-1

Caveolins are a family of proteins that are involved in receptor independent endocytosis. In vertebrates the caveolin gene family has three members: CAV1, CAV2, and CAV3, coding for the proteins caveolin-1, caveolin-2 and caveolin-3, respectively. Caveolin-1, a 22 kDa protein, was the first family member discovered, and is the structural component and marker for caveolae and trans-Golgi derived transport vesicles (Glenney, 1989; Rothberg *et al.*, 1992). Caveolin-2 and Caveolin-3 were identified later, both showing structural and functional similarities to caveolin-1 (Smart *et al.*, 1999).

Caveolin-1 is expressed in a wide variety of cell types, amongst which terminally differentiated cells such as endothelial cells, adipocytes, alveolar type 1 pneumocytes, macrophages, synoviocytes and smooth muscle cells have especially high expressions (Chang *et al.*, 1994; Scherer *et al.*, 1997; Matveev *et al.*, 1999; Frank & Lisanti, 2004). In the absence of caveolin-1, caveolin-2 becomes degraded through the proteasomal pathway (Razani & Lisanti, 2001). Caveolin-3 is not dependent on the other family members and is muscle-specific. Apart from their structural function within caveolae, caveolins have the capacity to bind cholesterol as well as a variety of proteins such as receptors, src-like kinases, G-proteins, H-Ras, and nitric oxide synthases (NOS) (Feron & Kelly, 2001). It has been established that caveolin-1 is involved in the regulation of cellular cholesterol homeostasis and promotes cellular cholesterol efflux (Frank *et al.*, 2001).

Caveolin-1, a major substrate for src in v-src transformed cell lines is also a substrate for non-receptor tyrosine kinases, including src (Glenney & Zokas, 1989). When phosphorylated on Tyr-14 (pY14-Cav1) it can inhibit src, through the recruitment of C-terminal src kinase- Csk; (Radel & Rizzo, 2005).

Caveolin-1 also plays a role in cell motility via its control and polarization of signalling molecules (Shaul & Anderson, 1998). This is supported by the fact that Caveolin-1 is linked to the cytoskeleton through Filamin (Stahlhut & van Deurs, 2000) and is associated with a certain subset of integrins (Wary *et al.*, 1998; Wei *et al.*, 1999). However, other studies indicated that caveolin-1 could be a negative regulator (Galbiati *et al.*, 2001). Recently, it was demonstrated that caveolin-1 is required in fibroblasts for persistency of migration in the absence of an external chemotactic cue and for directional migration in the presence of an external stimulus, whereas it slightly slows down the velocity of random migration (Grande-Garcia *et al.*, 2007).

Interestingly, caveolin-1 has been reported to interact with or bind to several cellular molecules especially protein and receptors associated with lipid rafts. Amongst these proteins, DPPIV co-localizes and binds to Caveolin-1 on antigen presenting cells (APC) (Ohnuma *et al.*, 2004). Residues 201–211 of CD26 along with the catalytic site Ser-630 are responsible for the binding to the caveolin-1 scaffolding domain. This region in CD26 contains the typical caveolin-binding domain (CBD) **(ω*X*ω*XXXX*ω*XX*ω; ω** and *X* depict aromatic residue and any amino acid, respectively), specifically WVYEEEVFSAY in CD26 (Couet *et al.*, 1997). Recently Ohnuma *et al.* reported that caveolin-1 in association with CARMA1 triggers T cell activation via DPPIV (Ohnuma *et al.*, 2007). This strengthens the role of Caveolin-1 as one of the DPPIV-ligands in T cell activation and immune response.

1.2.4.10 CARMA1

CARMA1 is a lymphocyte-specific member of a subfamily of Caspase Recruitment Domain (CARD) and Membrane-Associated Guanylate Kinase domain (MAGUK)-containing scaffold proteins. CARMAs, also called CARD-MAGUKS (Gaide *et al.*, 2001), Bcl-10-interacting MAGUK proteins (Bimps), (McAllister-Lucas *et al.*, 2001) or CARDS (Bertin *et al.*, 2001) bind to Bcl-10 through a CARD-dependent interaction and thereby play essential roles in NF-κB activation, induced by the co-stimulation of T cell receptor (TCR) and CD28 as well as other co-stimulatory molecules. NF-κB, whose activation plays important roles for the proliferation, differentiation, and survival of T cells, is induced by different receptor-generated signals that converge by phosphorylating and activating the IκB-kinase (IKK) complex (Rothwarf & Karin, 1999).

One of the receptor generated pathways for NF-κB activation is the CD3-CD28 co-stimulation pathway. T cell activation and proliferation is induced by major histo-compatibility complex molecules of antigen-presenting cells (APC) which present antigen peptides to T cell receptors (TCR) on the surface of T cells. This together with a co-stimulatory signal generated through interaction of B7 molecules on antigen-presenting cells and CD28 receptors on T cells lead to a complete T cell activation. This CD3-CD28 co-stimulation induces a series of signal transduction pathways leading to activation of cytosolic tyrosine kinases, various adaptor proteins, small GTPases, serine/threonine kinases and phospholipases. These signalling pathways in turn, activate several transcription factors, including NF-κB, AP-1 (activator protein 1) and NF-AT (nuclear factor of activated T cells), which then control the production of various cytokines, leading to T cell activation and proliferation. Stimulation of T cells induces the formation of a large multi-component complex at the contact area between the T cell and the antigen-presenting cell, the so-called supramolecular activation complex (SMAC) or immunological synapse (IS) (Gerondakis *et al.*, 1998), which is highly enriched with cholesterol and glycosphingolipids, hence termed lipid

rafts. Whereas several molecules are expressed constitutively in these lipid rafts, others are recruited following co-stimulation. CARMA1 along with Bcl-10 (B-cell lymphoma/leukaemia 10) are signalling molecules associated with lipid rafts and have been shown recently to link the TCR and protein kinase C (PKCθ) to the activation of IKK complex (Gaide *et al.*, 2002; Jun & Goodnow, 2003). Upon TCR engagement, CARMA1 is associated with TCR, allowing the recruitment of Bcl-10 to the membrane. This together with PKCθ activation, leads to activation of the IKK complex and subsequent phosphorylation and degradation of the NF-κB inhibitor IκBα which results in NF-κB activation (Tanner *et al.*, 2007).

Coupled with the TCR/CD3-CD28 stimulation, CD26-dependent co-stimulation involves the action of caveolin-1 and CARMA1 (Ohnuma *et al.*, 2004; Ohnuma *et al.*, 2007). In this pathway CARMA1 interacts directly with the short cytoplasmic tail of CD26/DPPIV which results to signal transductions that induce NF-κB activation. Ligation of CD26/DPPIV and caveolin-1 recruits a complex of CARMA1, Bcl-10 and IKKβ to lipid rafts. A PDZ domain in CARMA1 is necessary for binding to the N-terminal cytosolic tail of DPPIV (Ohnuma *et al.*, 2007).

A model of the role of DPPIV in caveolin-1 and CARMA1 associated T cell activation and immune response is given in a model below (**Figure 1.4**)

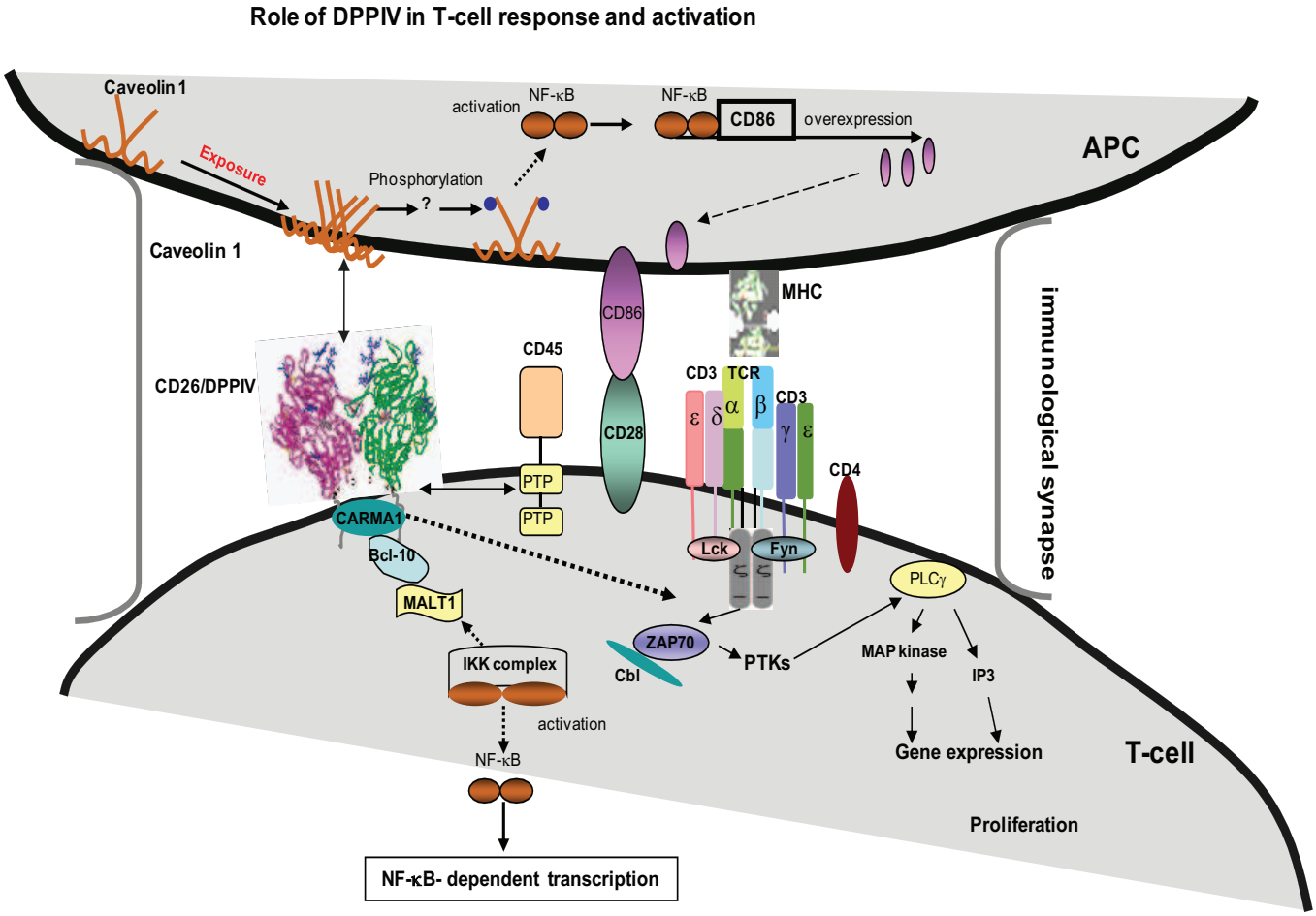

Figure 1.4: Model of the role of DPPIV in T cell activation and response

Caveolin-1 in monocytes (antigen-presenting cells; *APC*) is anchored at the inner membrane. Upon antigen engagement and presentation of MHCs on the surface of these APCs, Caveolin-1 is exposed to the outer cell surface and together with other factors induces the migration of $CD26^+$ T cells to the areas of antigen-loaded APCs. Contact between APCs and T cells results to binding of Caveolin-1 to DPPIV. This association results in signalling cascades in the APCs as well as the $CD26^+$ T cell. Phosphorylation of the caveolin-1 on APC takes place which switches on a signal cascade leading to activation of NF-κB. NF-κB-dependent up regulation of CD86 amongst other molecules that aid APC function is the result. Meanwhile, ligation of DPPIV on the surface of $CD26^+$ T cells to caveolin-1 on APCs causes the recruitment of CARMA1 by the T cells to lipid rafts. CARMA1 binds to the N-terminal cytosolic tail of DPPIV and also recruits the CARMA1-Bcl-10-IKKs complex, leading to activation of the IKK complex and finally activation of NF-κB. NF-κB-dependent transcription of further signalling molecules follows. Interaction of CD45 and DPPIV in the lipid rafts leads to internalization of DPPIV which triggers a further CD3-zeta-chain-dependent signal transduction pathway. This pathway includes phosphorylation of the PTKs $p56^{Lck}$, $p59^{Fyn}$ and zeta-associated PTK of 70 000 kDa (ZAP-70), and of MAP-kinase, Cbl, and phospholipase Cγ. Binding of TCR/CD3 complex to MHCs on APC and also binding of CD28 on T cells to CD86 and B7 molecules on APCs results to activation of the T cells and their proliferation. *TCR*: T cell receptor; *MHC*: major histocompatibility complex. The diagrams and models of molecules are not to scale. (Model modified with reference to information from (Gorrell *et al.*, 2001; Ohnuma *et al.*, 2004; Ohnuma *et al.*, 2007).

1.2.5 DPPIV and Diseases

Several physiological processes and the pathology of many diseases have been associated with altered levels of serum-DPPIV, expression on the cell surface as well as alteration in the glycosylation patterns. Some of these diseases are related with the enzymatic activities of DPPIV, whereas some seem to be based on enzyme activity -independent disorders of the protein. A list of characterized diseases with altered DPPIV expression and distribution is given in **Table 1.2**. The following section will focus on 2 of these diseases, namely Diabetes mellitus type-2 and HIV/AIDS since they seem to portray disorders caused by both enzymatic activity and co-stimulatory roles of the protein.

Table 1.2: Expression of DPPIV in physiological and pathophysiologic processes and in diseases

Disease or effect	Cell surface DPPIV	Serum DPPIV
Abstinence in alcoholics		↓
Ageing		↓
Smoking		↓
Rheumatoid arthritis (Human, Mouse)	↑ T cells	↓
Multiple sclerosis(Human)	↑	
Graves' disease	↑	↑
Hashimoto Thyroiditis	↑	
Sarcoidosis	↑	

Psychological Stress	↑	
Diabetes mellitus	↑	↓
Granulomatosis	↑	
Hepatic dysfunction , hepatitis C	↑	↑
Liver cirrhosis	↑	↑
Transplantion rejection	↑ lymphocyte	↑
Lymphotic leukemia, Hodgkin Lymphoma		↑
Hepatom (Human, Rat)	↓	↑
Kidney transplant rejection (rat)		↑
Encephalitis (Mouse)		↑
Osteoporosis (Human)		↑
Bulimia (bulimia nervosa, Anorexia nervosa)	↓ lymphocyte	↑
Oral squamous cellcarcinoma (Human)		↓
Depression/ anxiety (Human)		↓
Pregnancy		↓
Miscarriage (human)	↑ T-helper 1-cells	↓
HIV/AIDS (Human)	↓ lymphocyte	↓
Inflammatory bowel disease	↑ T cells	↓
Immunosuppression (Rat)		↓
Down Syndrome	↓ lymphocyte	
Melanoma	↓	↓
Systemic lupus erythematosus		↓ hypersialylated
Acute lymphoblastic T cell-Leukaemia		↓
Schizophrenia		↓
Autoimmune disease	↑	
Atopic dermatitis	↑	
Biliary atresia	↑	
Cancer of bile duct or pancreas	↑	↑
Colorectal carcinoma		↓
Crohn’s disease		↓
SLE (Human, NZB mouse)		↓
Psoriasis		↓
Fibromyalgia		↓
Gastro intestinal cancer		↓
hypertension		↓
Women versus men		↓
Neonates versus adults		↓
Myelocytic leukemia (human)	no change	no change

The table contains information from (De Meester *et al.*, 1999; Hildebrandt *et al.*, 2000; Gorrell *et al.*, 2001; Bauvois, 2004). HIV: Human immunodeficiency virus, AIDS: Acquired immune deficiency syndrome.

1.2.5.1 DPPIV in Diabetes Mellitus Type-2

Diabetes mellitus type-2 or adult-onset diabetes is a chronic metabolic disorder. It is characterized by two major pathophysiologic defects: (1) insulin resistance, which results in increased hepatic

glucose production and decreased peripheral glucose disposal, and (2) impaired β-cell secretory function (Kahn, 2003; Bloomgarden, 2007). Besides these, elevated fasting plasma glucagon concentrations which fail to decrease appropriately, or paradoxically may even increase after oral glucose or carbohydrate ingestion also characterize the disease (Muller *et al.*, 1970; Reaven *et al.*, 1987). Type-2 diabetes is therefore a complex disease, and optimal treatment requires a combinational approach. Existing therapies have a number of shortcomings, including safety, tolerability issues (e.g., hypoglycaemia, weight gain and gastrointestinal intolerance) and typically, treatment modalities become less effective over time as a result of progressive loss of beta-cell function (UK Prospective Diabetes Study Group (UKPDS 33) 1998). As a result many patients remain inadequately treated. This raises the need for new therapeutic strategies which can target hyperglycaemia, but yet successfully prevent the progression of the associated complications of type-2 diabetes mellitus.

Under normal physiologic conditions, incretin hormones are released from the gastrointestinal tract in response to the presence of carbohydrates and lipids following nutrient ingestion and enhance glucose-dependent insulin secretion from the pancreas. These hormones elicit their actions through direct activation of distinct G-protein-coupled receptors that are expressed on islet beta cells (Hansotia & Drucker, 2005). The two principal incretin hormones are GLP1 and GIP. GLP1 and GIP are small peptides of 30 and 42 amino acids respectively. Following an increase in blood glucose, GLP1 binds to its receptors and induces subsequent activation of adenylate cyclase. This results in accumulation of cAMP within the cell, activation of protein kinase A, elevation of intracellular calcium concentrations and mobilisation of insulin containing granules (Gromada *et al.*, 1998). This occurs however, only when glucose concentrations are higher than 55 mg/dL (Efendic & Portwood, 2004). GLP1 receptors are widely distributed in the stomach, kidney, heart, intestine, lung, and in the peripheral and central nervous systems (Estall & Drucker, 2006). Besides stimulating insulin secretion in a glucose-dependent manner, GLP1 shows other functions in control subjects and patients with type-2 diabetes. These include: (1) glucose-dependent suppression of glucagon (Nauck *et al.*, 1993), (2) reduction of appetite, food intake and body weight (Flint *et al.*, 1998), (3) deceleration of gastric emptying (Willms *et al.*, 1996) and (4) cardiac protective effects (Nikolaidis *et al.*, 2004). GLP1 and GIP have also been shown in preclinical studies to exert significant cytoprotective and proliferative effects on the islets of Langerhans (Drucker, 2003).

In patients with type-2 diabetes, a continuous deterioration of beta-cell function is seen (Brubaker & Drucker, 2004). Both GLP1 and GIP stimulate insulin secretion and contribute to physiological glucose homeostasis and the use of exogenous GLP1 and GIP was considered a good therapy to treat type-2 diabetes. However, their use is limited due to rapid degradation *in vivo* by DPPIV (Mentlein *et al.*, 1993; Marguet *et al.*, 2000).

A strategy to circumvent the limitations caused by degradation, in order to improve the pharmacokinetics of GLP1 and GIP in type-2-diabetes was the development of stable peptide analogues that are resistant to degrading enzymes such as DPPIV. Some resistant synthetic analogues of GLP1 or GIP demonstrated to be biologically active, stimulate insulin secretion and subsequently normalize blood glucose levels. They showed prolonged metabolic stability *in vivo* (Gallwitz *et al.*, 2000; Hinke *et al.*, 2002). Exenatide (commercial name: Byetta), a GLP1-receptor analogue which is resistant to DPPIV degradation was the first incretin mimetic approved by the US "Food and Drug Administration" (FDA) in April 2005 and by the European commission in November 2006. However, GLP1 analogues require injection which makes self-administration by the patients inconvenient. Moreover side effects such as nausea, vomiting and diarrhoea at the early phase of therapy and acute pancreatitis have been associated with the use of the mimetic (FDA ALERT 10/2007).

Following the elucidation of its crystal structure, DPPIV has been considered a good target in the treatment of type-2 diabetes mellitus. DPPIV inhibitors as drugs, would act by inhibiting the breakdown of GLP1 and thereby, selectively enhance insulin release under conditions when it is physiologically required. Amongst the first tested DPPIV inhibitors, diprotin A, Ile-thiazolidide, valine-pyrrolidide, NVP-DP728 were demonstrated to effectively inhibit the truncation of GLP1 and GIP by DPPIV and improve glucose tolerance in animal models (Deacon *et al.*, 1998; Pospisilik *et al.*, 2003) and in human studies (Ahren *et al.*, 2002). However, these drugs were only partially selective for DPPIV. Moreover, DPPIV has a broad range of substrates other than GLP1 and also structural homologues of its gene family which share some similar substrates. Opposed to the inactivation of GLP1 by DPPIV, cleavage of PYY converts the non-subtype-selective agonist $PYY_{1–36}$ into the selective agonist $PYY_{3–36}$, at Y2 and Y5 receptors (Michel *et al.*, 1998). $PYY_{1–36}$ is known to stimulate food intake, whereas peripherally administered PYY_{3-36} inhibits food intake in rats (Batterham *et al.*, 2002). Considering that obesity is a problem in type-2 diabetes, precluding the formation of such an endogenous food intake inhibitor by use of DPPIV inhibitors is undesirable. However, many other studies on rodents did not confirm inhibition of food intake by $PYY_{3–36}$ (Boggiano *et al.*, 2005). Recent studies in non-rodents such as pigs and humans revealed reduced food intake upon peripheral administration of relatively high concentrations of $PYY_{3–36}$ (Sloth *et al.*, 2007). On the other hand, $PYY_{3–36}$ was also reported to promote fat oxidation and improve insulin resistance in mice even under conditions of chronic administration where it did not reduce food intake (van den Hoek *et al.*, 2007). Furthermore, $PYY_{3–36}$ also lowers plasma glucose levels even in the absence of alterations in circulating insulin levels (Bischoff & Michel, 1998). Selective inhibition of GLP1-inactivation is an insulinotropic principle which is unlikely to cause hypoglycaemia between meals if DPPIV inhibitors are administered with or after meals. The lower

risk for hypoglycaemic events as compared with other insulinotropic or anti-glycaemia agents therefore makes DPPIV-inhibitors promising candidates for a more physiological treatment of type-2 diabetes (Combettes & Kargar, 2007). The need for highly selective inhibitors of DPPIV remains indispensable in the treatment of type-2 diabetes.

Recently, a series of selective inhibitors of DPPIV have been evaluated in clinical trials (Hermansen & Mortensen, 2007; Utzschneider *et al.*, 2008) and some of them have proven promising in the treatment of type-2 diabetes (**Table 1.3**).

Table 1.3: DPPIV inhibitors presently available and in development

Research Name	Commercial name	Company	Availability status
Sitagliptin	Januvia®	Merck Sharp and Dohme	Available
Vildagliptin	Galvus®	Novartis	Available
Saxagliptin	Onglyza	Bristol Myers Squibb and AstraZeneca	Available
SYR-322		Takeda	Phase II
R1438		Roche	Phase II
PSN9301		Prosidion	Phase II
TS-021		Lilly	Phase I
R1499		Roche	Phase I
PSN357		Prosidion	Phase I
ALS 2-0426		Alantos	Phase I

The table contains information from (Vilsboll and Knop 2007: http://dvd.sagepub.com/cgi/content/refs/7/2/69) modified and updated according to press releases of the United States FDA and the European Commission**.**

Sitagliptin was approved by the US FDA on October 17, 2006 as Januvia and on April 2, 2007 in combination with metformin as Janumet. Vildagliptin was approved in September 2007 and commercialized under the name Galvus. Most recently a third member of this class of drugs, Saxagliptin was approved by FDA in August 2009 and by the European Commission in October 2009 and is commercialized under the name Onglyza. Although Sitagliptin and Vildagliptin have been commercialized now for over 2 years and seem to be safe drugs which improve β-cell function (Bosi *et al.*, 2007) and reduce hyperglycaemia efficiently, the appearance of side effects with the onset of therapy cannot be completely ruled out. So far, common side effects such as headaches (Richter *et al.*, 2008) and hypoglycaemia and rare side effects such as inflammation of the liver (hepatitis) (US FDA-ALERT) have been reported in diabetic patients using Vildagliptin and Sitagliptin. Compared to other available anti-diabetic drugs, the frequency of these side-effects is relatively low, making them comparably safe. Reports show that depending on the benefit-risk ratio, DPPIV inhibitors might be a treatment strategy of priority in the early stages of type-2 diabetes in future, particularly in combination with metformin. Notwithstanding, long term safety and efficacy of the drugs still remain to be proven, e.g. the effects on cardiovascular disease (Montori *et al.*,

2007). Furthermore, DPPIV is considered a moonlighting protein and has many other roles in different pathways (Boonacker & Van Noorden, 2003) such as in immune response and collagen metabolism. Recent research with Vildagliptin on rats revealed alterations in collagen metabolism (Jost *et al.*, 2009). However, the pleiotropic effects of DPPIV raise the possibility of potential use of its inhibitors in diseases other than type-2 diabetes. These include inflammatory diseases and probably certain types of cancers (Thielitz *et al.*, 2007; Thompson *et al.*, 2007).

Although some effects may manifest as useful secondary actions when DPPIV inhibitors are being used for the treatment of diabetic patients, others may manifest as adverse events. Coupled to this, long term effects on the poorly studied endogenous inhibitors of DPPIV such as the Thromboxane-A2 receptor (Wrenger *et al.*, 2000) may be adverse. In the future, evaluation of alterations in human plasma samples from type-2 diabetes patients treated with DPPIV inhibitors will reveal deeper insights in drug action and correlate accumulated substrates with secondary pharmacological effects and ultimately develop predictive markers for selection of suitable inhibitors for subpopulations of patients (Jost *et al.*, 2009).

1.2.5.2 DPPIV in HIV infection and AIDS

Human immunodeficiency virus type-1 (HIV1) is the key agent causing AIDS. HIV infection is a massive global health problem with more than 33 million infected worldwide (UNAIDS 2007). Although the identification and isolation of the virus lies 26 years back, vaccines against HIV-infection or drugs for a complete eradication of AIDS are not available yet. One of the reasons for this is the multifaceted nature of the virus and the strategies it evolved in order to manipulate the host immune response machinery and successfully disseminate its genetic material. This manipulation begins from the point of infection via use of cell surface receptors (Sattentau, 1998), right on to integration into the host chromosome. HIV infection is mediated by interaction of the HIV envelope glycoprotein, gp120 with the primary receptor CD4 on host cells (Dalgleish *et al.*, 1984). This leads to conformational changes in gp120, resulting to its association with either CXCR4 (Feng *et al.*, 1996) or CCR5 (Sodroski *et al.*, 1996) depending on the viral strain and cell type. In the case of T-tropic (X4) viral strains, a tri-molecular complex is formed between gp120, CD4, and CXCR4 (Lapham *et al.*, 1996). These interactions are critical for subsequent conformational changes that take place in the gp120/gp41 complex, leading to the exposure of gp41 fusion peptide and the initiation of virus fusion with the host cell membrane (Broder & Collman, 1997; Berger *et al.*, 1999).

There is evidence for the involvement of DPPIV in HIV infection and the progression of AIDS-associated immune suppression, although DPPIV does not serve directly as a co-receptor of HIV infection (Broder *et al.*, 1994) as was earlier postulated (Callebaut *et al.*, 1993). DPPIV is known to

cleave many chemokines such as the earlier mentioned SDF-1α/β, MDC (Struyf *et al.*, 1998; Mantovani *et al.*, 2000) and RANTES and regulate their biological functions. Intriguingly, cleavage of RANTES and SDF-1α, results in opposing effects regarding their anti-HIV activities. While truncation of RANTES by DPPIV increases its chemotactic activity via CCR5 and thereby prevents HIV infection (Oravecz *et al.*, 1997; Appay & Rowland-Jones, 2001), cleavage of SDF-1α by DPPIV leads to reduced chemotactic activity and consequently promotes HIV infection via the C-X-C chemokine receptor 4 (CXCR4) (Shioda *et al.*, 1998). The association of CXCR4 with DPPIV further supports the involvement of DPPIV in HIV infection (Herrera *et al.*, 2001). Furthermore, the association of DPPIV and ADA which promotes cell proliferation is inhibited by the HIV envelope glycoprotein gp120 (Blanco *et al.*, 2000).

Taken together, the exact roles played by DPPIV in HIV infection and progression of AIDS are poorly studied, but relate probably to its cleavage and alteration of the anti-HIV activities of chemokines such as RANTES and SDF-1α. The alteration of anti-HIV activities of SDF-1α and enhancement of the infection of humans by different viral strains is an unwanted process of DPPIV in the host and reflects one of the strategies by which HIV manipulates its host. Furthermore, the HIV1 transactivator of transcription, HIV1-TAT interacts with and inhibits the enzymatic activity of DPPIV (Gutheil *et al.*, 1994) which leads to a decrease in DPPIV-mediated T cell growth (Wrenger *et al.*, 1996; Wrenger *et al.*, 1997; Ohtsuki *et al.*, 2000).

It has been repeatedly observed that CCR5-using (R5) viruses are mainly transmitted (Carrington *et al.*, 1999) while CXCR4-using (X4) variants could be isolated from up to 50% of AIDS patients in subtype B infections and correlate with a more rapid loss of $CD4^+$ T cells and faster disease progression and death (Asjo *et al.*, 1986; Scarlatti *et al.*, 1997). CXCR4-using viruses emerge in most cases in the late phase of disease and colonize naïve T cell populations that were not infected by R5 viruses (Ostrowski *et al.*, 1999; Blaak *et al.*, 2000). The need for selection is therefore indispensable for the virus since the cause of AIDS and death of the host is unwanted. With effect, R5 HIV strains are preferentially transmitted and this seems to be controlled by the HIV1-TAT protein. This effect of HIV1-TAT seems to be mediated by several strategies, one of which involves the inhibition of DPPIV enzyme activity to ascertain a block of CXCR4 by intact SDF-1α. The other strategies evolved by the virus involve direct antagonistic binding of TAT to CXCR4 and inhibiting HIV infection via CXCR4 and also modulating the conformation of the HIV envelope protein gp120, thereby directly inhibiting or enhancing infection by particular HIV strains. A directed induction of co-receptor expression by TAT protein also grants preferential infection by specific viral strains due to availability of receptors (Huang *et al.*, 1998; Secchiero *et al.*, 1999; Ghezzi *et al.*, 2000).

However, it must be noted that depletion of $CD4^+$ T cells and AIDS occur in patients from which only R5- viruses (CCR5-using) could be isolated (de Roda Husman & Schuitemaker, 1998). In HIV-clade C infections, CXCR4-using variants have been detected in far fewer individuals in the late stages of disease (Morris *et al.*, 2001). Thus, AIDS and death presumably occurs in the absence of X4 HIV-variants for a substantial number of HIV^+ patients and is caused directly by R5 viruses though significantly less rapidly than in the case of X4 viruses. In both cases a significant decrease of the expression of DPPIV is noticed.

1.2.5.2.1 The HIV1 transactivator of transcription (HIV1-TAT)

The HIV1 genome constitutes nine viral genes, all of which are expressed from a single promoter located within the viral long terminal repeat (LTR) which flanks the 5' and 3' regions of proviral DNA (Coffin, 1995; Greene & Peterlin, 2002). The existence of a single and unique promoter makes transcription dependent on a single transactivator, TAT which is responsible for transcriptional activation and elongation of all the nine viral transcripts (Laspia *et al.*, 1989; Feinberg *et al.*, 1991; Kato *et al.*, 1992).

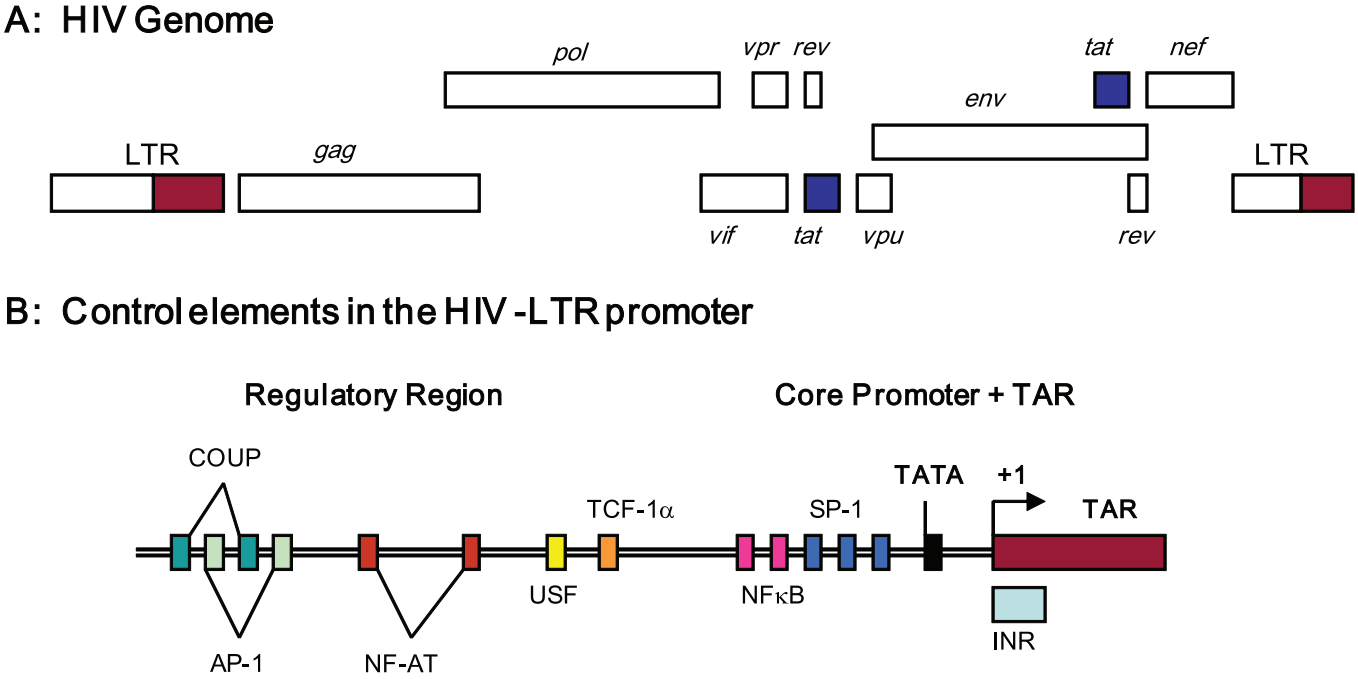

Figure 1.5: The HIV Genome and control elements in the HIV LTR

(A) The HIV Genome is made of 9 genes and a single promoter. The TAT gene is encoded by two exons which are highlighted in blue. **(B) Control elements in the HIV LTR:** The HIV promoter can be divided into the "core promoter" and the "regulatory" region. The core promoter region contains three tandem SP1 sites, a TATA element, and an initiator (INR) element. The "regulatory" region carries a series of binding sites for DNA transcription factors. Depending on the cell type, these factors can modulate HIV transcriptional activity. However, in contrast to the core promoter elements, the virus is still able to replicate when these elements are deleted. The diagram was modified according to (Karn, 1999).

HIV1-TAT is a small nuclear protein comprised of 86-101 amino acid residues depending on viral subtype, and is encoded by two exons. Though quite small, the TAT protein has a complex secondary structure and can be divided into five to six functional domains which are conserved in all Lentiviruses (Jeang *et al.*, 1991). The structural domains of TAT are as follows:

- The N-terminal domain is made up of the amino acids 1-22 and is rich in proline, with a proline residue on every third position when counting from the first methionine. The sequence X-X-Proline at the N-terminal of this domain makes TAT a natural inhibitor of DPPIV and suppressor of DPPIV-dependent T cell growth (Wrenger *et al.*, 1997).
- The cysteine-rich domain comprises residues 23-38 and contains seven cysteine residues which cause multimerization of the TAT protein (Frankel *et al.*, 1988).
- The core domain (residue 39-49) contains highly hydrophobic amino acids and is responsible for DNA-binding (Karn, 1999).
- The basic domain (residues 50-60) is rich in arginine and lysine, making up six arginines and two lysines within 11 residues. The domain contains a nuclear localisation signal and is responsible for binding to RNA and nuclear localization (Rana & Jeang, 1999).
- Residues 61-72 make up the glutamine-rich and last domain encoded by exon-1 of the TAT gene. This domain also plays a role in DNA-binding.
- Residues 73-101 make up the c-terminal domain which contains an RGD motive. This domain is involved in the recognition of transacting response element of an RNA stem loop called TAT-activation-RNA (TAR) and in the transactivation of all viral transcripts (Verhoef *et al.*, 1998). This domain also initiates binding to host extracellular matrix proteins such as fibronectin and vitronectin (Ruoslahti & Pierschbacher, 1987). Through its RGD motive it also binds to the integrin receptor α5β1 and αvβ3 (Barillari *et al.*, 1999).

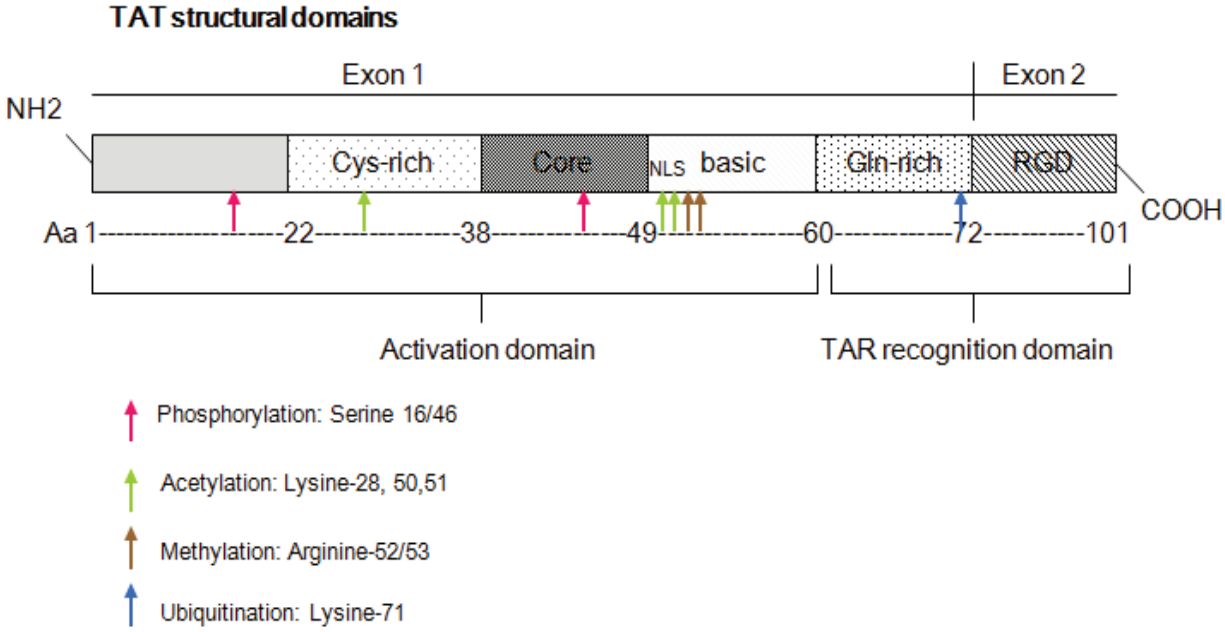

Figure 1.6: Structural domains of the HIV1-TAT protein

TAT protein comprises of 86-101 amino acid residues which make up distinct domains with typical functional roles in the cell. The residues which undergo co- or posttranslational modifications are indicated with coloured arrows.

1.2.5.2.2 Biological roles and effects of HIV1-TAT on its host

The primary role of HIV1-TAT is to transactivate the LTR promoter of HIV proviral DNA by binding to the transacting response element of TAT activation RNA (TAR). TAR forms a stable RNA stem-loop at the 5' end of all viral transcripts and its binding with TAT recruits a series of transcription factors to the promoter (Laspia *et al.*, 1989; Feinberg *et al.*, 1991; Kato *et al.*, 1992; Gatignol & Jeang, 2000).

Via its cysteine-rich domain, TAT binds the cyclin T1 component of the positive transcription elongation factor-b and cyclin dependent kinase 9 (CDK9), which facilitates viral transcription (Kim *et al.*, 2002; Brady & Kashanchi, 2005; Biglione *et al.*, 2007). Besides the recruitment of host cellular proteins and enzymes for transcriptional initiation, TAT protein binds a number of cofactors with intrinsic histone-acetyltransferase activity such as the p300/CBP, p300/CBP-associated factor (pCAF), TAFII250 and TAT-interacting protein 60, which regulate the chromatin structure located at the HIV promoter, thus allowing access to the LTR promoter (Chiang & Roeder, 1995; Dal Monte *et al.*, 1997). Furthermore, TAT induces remodelling of a nucleosome (nuc-1) which is positioned at the HIV promoter and probably stimulates transcriptional elongation of HIV, both by increasing the intrinsic ability of RNA-Pol II complex to elongate efficiently and by recruiting histone-modifying enzymes to remodel the elongation block caused by nuc-1. Hyperphosphorylation of the C-terminus of RNA-Pol II by CDK9 enhances elongation of transcription from the LTR promoter (Barboric & Peterlin, 2005; Brady & Kashanchi, 2005). In the absence of TAT protein, transcription of viral transcripts is low and results to production of shorter transcripts. Successful transcription transactivation of HIV LTR by TAT is regulated by posttranslational modifications of the TAT protein by host cellular proteins. These modifications include phosphorylation on serine-16 and -46 (Ammosova *et al.*, 2006), acetylation at lysine-28, -50, and -51 (Kiernan *et al.*, 1999; Berro *et al.*, 2006), ubiquitination at lysine-71 (Bres *et al.*, 2003), and methylation at arginine-52 and -53 (Boulanger *et al.*, 2005).

Acetylation of the basic domain on Lysine-28, -50, and -51 by CBP/p300 is crucial for TAT transactivation activity (Kiernan *et al.*, 1999; Berro *et al.*, 2006). The steps involved in the TAT-mediated transcription of viral genes are not fully understood yet. However, based on the findings available a model for TAT-mediated hyperphosphorylation of RNA-Pol II and the resulting transcription elongation is given in **Figure 1.7**.

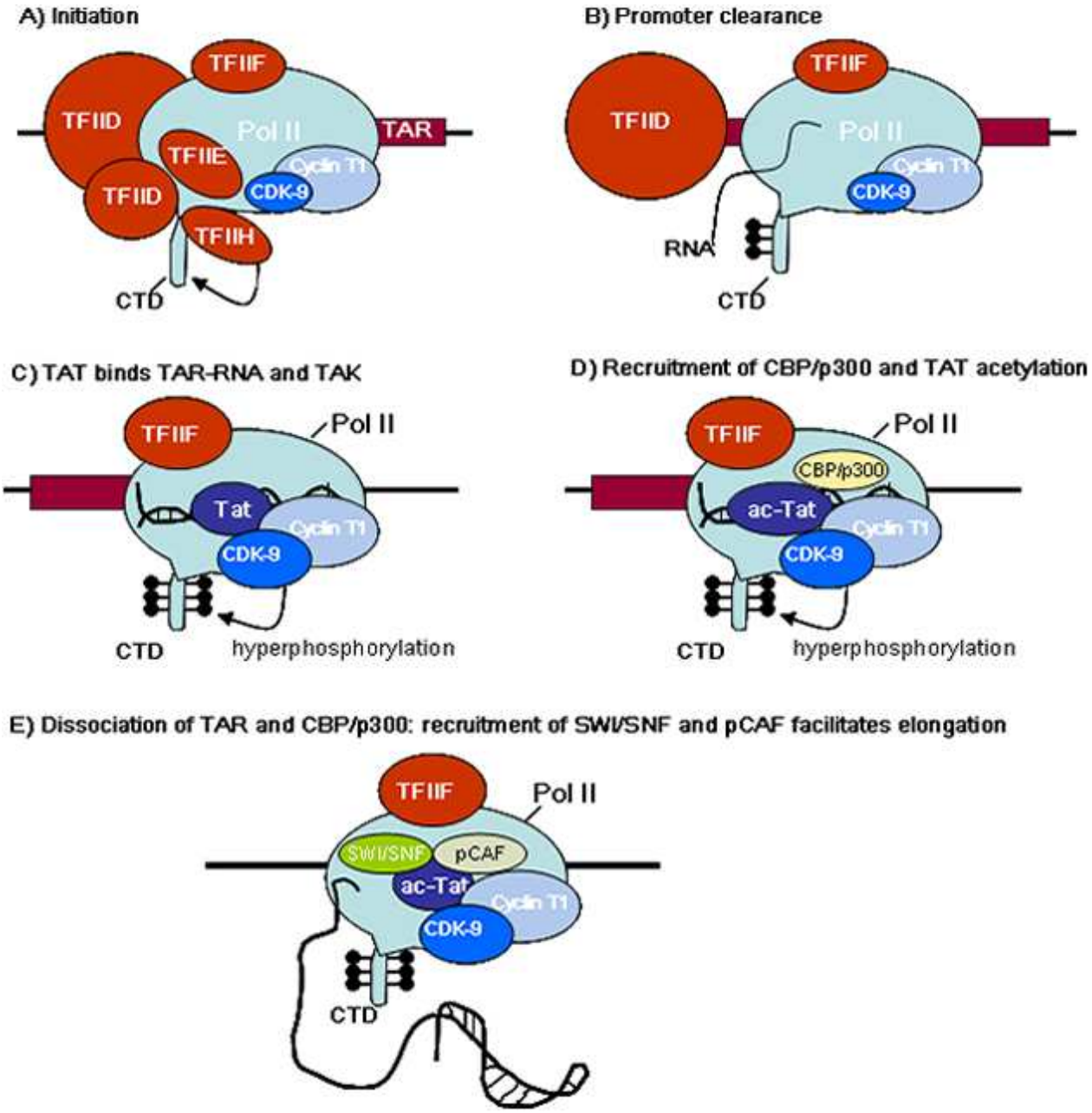

Figure 1.7: Model of TAT-mediated transcription elongation at the HIV LTR

(A) The RNA polymerase II holoenzyme is recruited to the HIV LTR through its interactions with TFIID and other components of the basal transcription apparatus. The CTD of the RNA-Pol II is phosphorylated by the CDK7 kinase found in TFIIH and the modified polymerase clears the promoter and begins transcription of TAR. **(B)** The nascent RNA chain corresponding to the TAR RNA transcript folds into its characteristic stem-loop structure and binds the RNA-Pol II. **(C)** Ubiquitination of TAT by Hdm2 activates TAT and causes its binding to the bulge sequence found near the apex of the TAR RNA structure and its formation of a ternary complex with Cyclin T1/CDK-9 (TAK). The activated TAK kinase catalyzes hyperphosphorylation of the Pol II-CTD. **(D)** Recruitment of CBP/p300 results in acetylation of TAT on K28, K50 and K51. **(E)** Following acetylation of TAT, TAT and CBP/p300 are displaced from TAR and transferred to the elongating RNA-Pol II complex. TAT recruitment of SWI/SNF and pCAF to the complex facilitates elongation. The activated transcription complex is able to transcribe the remainder of the HIV genome. Transcription complexes that have been activated by TAT show enhanced elongation capacity and are able to read through

a variety of terminator sequences, including RNA stem-loop structures with a high degree of efficiency. Arginine methylation of TAT by PRTM6 triggers the dissociation of acetylated TAT from the polymerase complex and pCAF at the end of the transcription cycle. Ubiquitination and dimethylation of arginines mark TAT for degradation. Monomethylation of TAT can be reversed by the action of TAT peptidyl arginine deaminase and ubiquitinated TAT can be recycled after deacetylation by SIRT1 into the transcription cycle. This model was modified with reference to information from (Karn, 1999; Hetzer *et al.*, 2005; Van Duyne *et al.*, 2008).

In HIV-infected patients, TAT protein is secreted from HIV infected cells by a poorly studied mechanism and is suggested to have paracrine effects on uninfected cells (Ensoli *et al.*, 1993; Huigen *et al.*, 2004). Extracellular TAT protein re-enters cells via lipid rafts and caveolar uptake (Vendeville *et al.*, 2004) by interacting with cell surface receptors such as heparan sulphate proteoglycans (Tyagi *et al.*, 2001), the integrin receptors $\alpha5\beta1$ and $\alpha v\beta3$ and the extracellular matrix proteins fibronectin and vitronectin (Ruoslahti & Pierschbacher, 1987; Barillari *et al.*, 1999). The subsequent outcome of such re-entry of TAT into cells is diverse and poorly studied. Studies with recombinant TAT protein reveal that extracellular TAT taken-up by cells, translocates to the nucleus where it modulates amongst others, the expression of a wide range of genes such as cytokines (Buonaguro *et al.*, 1994; Westendorp *et al.*, 1994), chemokine receptors (Huang *et al.*, 1998) and major histocompatibility complex (MHC) (Howcroft *et al.*, 1993; Verhoef *et al.*, 1998).
Reports testify that TAT could alter HIV co-receptor expression in lymphoid and myeloid cells (Huang *et al.*, 1998; Secchiero *et al.*, 1999; Xiao *et al.*, 2000). In monocytes/macrophages and T lymphocytes, TAT up regulates both CXCR4 and CCR5 expression. Furthermore, extracellular TAT is a specific antagonist of CXCR4 and selectively inhibits the entry and replication of X4 virus in peripheral blood mononuclear cells (Ghezzi *et al.*, 2000; Xiao *et al.*, 2000).
Several protein-protein interaction networks were developed for human and HIV proteins (Bandyopadhyay *et al.*, 2006) (http://www.ncbi.nlm.nih.gov/RefSeq/HIVInteractions/tat). With reference to the interaction network, TAT protein interacts with about 79 different proteins during the early stages of HIV latency. Amongst them, interaction with four groups of genes and proteins, namely tubulin associated genes (Chen *et al.*, 2002), transcription factors (Coyle-Rink *et al.*, 2002), collagen and fibronectin (Taylor *et al.*, 1992) and genes involved in the regulation of cell growth are particularly significant.
Taken together these reports indicate the role of HIV1-TAT in the regulation of HIV infection by its regulation of co-receptor usage and viral strain selection. Furthermore, it manipulates the host machinery by recruiting a series of molecules which ease transcription of the viral genes.
A series of research work support the active role of DPPIV and TAT in HIV infection and AIDS. Apart from being involved in cell migration and sharing common binding partners such as the HIV

co-receptor CXCR4, fibronectin and collagen-1, HIV-TAT and human-DPPIV are involved in lipid rafts, where they associate with various signalling molecules. Interestingly, HIV infection (Manes *et al.*, 2000; Liao *et al.*, 2003) and budding (Nguyen & Hildreth, 2000) take place in lipid rafts.

The eradication of HIV/AIDS can therefore only be successful if the mechanisms involved in infection and the progression of AIDS, and the structures underlying these mechanisms are characterized. The study of the interaction of human-DPPIV and the HIV1-TAT protein and the elucidation of the crystal structure of the complex between HIV1-TAT and human-DPPIV will contribute immensely towards the design of drugs to target the protein in HIV infected patients.

2 Aim of Work

1.) So far, the role played by DPPIV in HIV infection and AIDS and the mechanism of this role are poorly studied. Furthermore, the ligands involved in the DPPIV-HIV interaction are largely unknown. The HIV1-TAT protein which plays a crucial role for viral replication and transcription was described as a partial inhibitor of the enzymatic activity of DPPIV and peptides derived from the N-terminus of HIV1-TAT were shown to suppress DPPIV-dependent activation of T cell growth. However, a direct association of whole-length TAT protein and DPPIV has not been resolved.

Opposed to human-DPPIV protein, the tertiary structure of the multi-faceted HIV1-TAT protein has not been elucidated yet. The crystal structure of DPPIV in complex with the N-terminal nonapeptide of HIV1-TAT was resolved. From this structure, it was postulated that the interaction of the TAT N-terminus to DPPIV is weak and cannot be responsible for the overall inhibition effect of the TAT protein on DPPIV, implying that another binding site for TAT protein outside the active centre of DPPIV potentially plays a role in the inhibition.

The aim of the underlying work was as follows:

- Expression and characterization of recombinant TAT protein and its interaction with human-DPPIV.
- Verification of the inhibition effect of purified recombinant TAT protein on the enzymatic activity of DPPIV.
- The production and structural characterization of a DPPIV/TAT protein complex.

2.) Furthermore, the HIV1-TAT protein is secreted from infected cells of HIV-patients and re-enters uninfected cells by caveolar uptake. Caveolae and lipid rafts are centres for signal transduction. HIV infection and budding take place in these centres. The caveolae structural protein, Caveolin-1 was reported to associate with human-DPPIV in lipid rafts which may contribute to the role of DPPIV in signal transduction and HIV infection.

- The verification of the interaction of human-Caveolin-1 with human-DPPIV protein was a subproject of the underlying work.

3 Results I: Expression, Purification and Characterization of TAT protein

In order to verify the inhibitory effect of HIV1-TAT on the enzymatic activity of human-DPPIV and to confirm the importance of the N-terminus of TAT protein on this effect, TAT-cDNA from the HIV1-strain BRU, was cloned in different expression vectors in order to express the protein with different fusion tags. The fusion tags were to ease purification of the protein and also serve in some cases to block access of the N-terminus of TAT to the active site of human-DPPIV in subsequent investigations of their binding and inhibition of the enzymatic activity of DPPIV.

3.1 Expression and Purification of recombinant TAT proteins in *E. coli*

Recombinant TAT proteins with either N-terminal GST- or C-terminal 6xHis-tags were constructed and expressed in *E. coli* BL21 as stated under section **9.1.1.3**.

A schematic representation of the fusion protein constructs expressed and their respective names used in this work is given in

Figure 3.1.

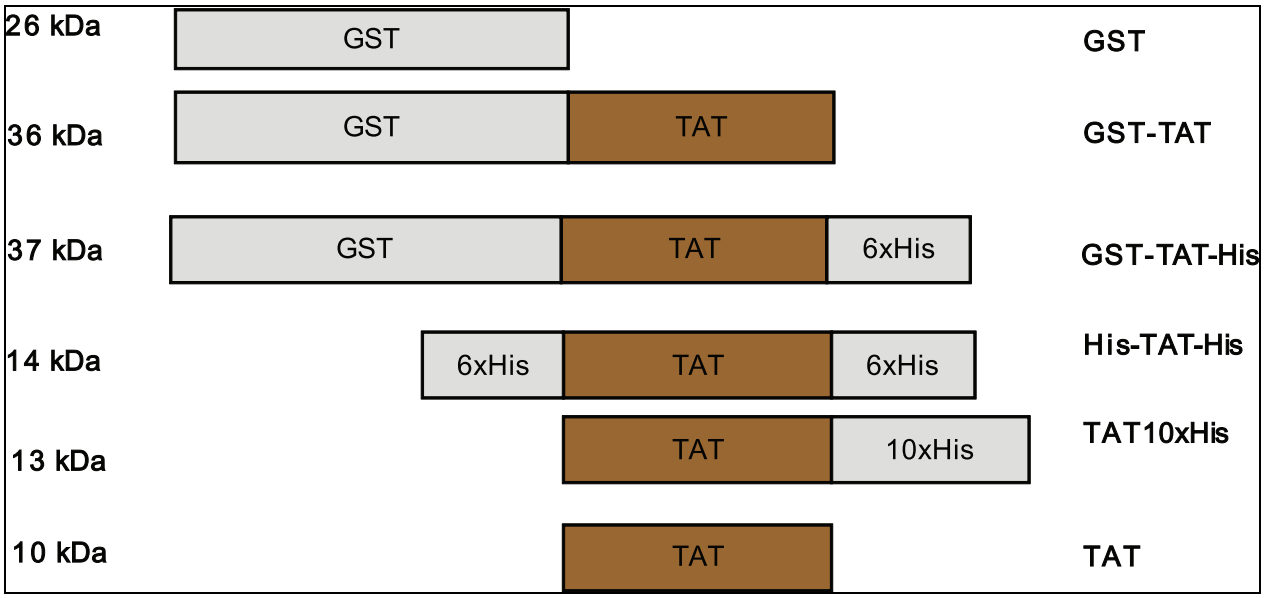

Figure 3.1: Schematic representation of TAT protein constructs expressed in *E. coli*

The recombinant TAT proteins with different fusion tags were assigned the names on the right. Only the assigned names shall be used in the following section of the work. The GST-TAT and GST-TAT-His both possess a linker of 7 residues between the GST and TAT which constitutes the recognition sequence for thrombin cleavage. The TAT10xHis also contains the thrombin recognition sequence between TAT and the 10x His tag. The TAT10xHis Protein was expressed and purified by our cooperation partners Dr. Eva Tauberger and Jacobo Martinez (AG Saenger, FU-Berlin).

3.1.1 Purification of GST-TAT-His protein

TAT fusion protein with N-terminal GST and C-terminal 6x His-tag (GST-TAT-His) was expressed in *E. coli* at 25°C for 3 h following induction with 2 mM final concentration of IPTG and purified in two steps by affinity chromatography and gelfiltration. All purification steps were carried out on ice with the use of aluminium foils to protect the protein from light. Furthermore, siliconized or Protein-Lobind-tubes (Eppendorf) were used to avoid protein loss due to the stickiness of TAT protein to surfaces. Purification of the fusion protein from cytosolic fractions was either by glutathione affinity chromatography or by Ni^{2+} affinity chromatography. High amounts of the protein could be purified (**Figure 3.2**B). To eliminate host proteins which are co-purified as a result of unspecific binding to the Nickel agarose and Glutathione sepharose used, fractions containing the GST-TAT-His protein were pooled and further purified by size exclusion chromatography on a Superdex 200 column.

From the elution profile, the main peak was at 9.33 ml retention volume (**Figure 3.2**C). With reference to protein standards used for size exclusion chromatography, the calculated molecular weight of proteins eluted at this retention volume was 1046 kDa. Theoretically, this peak corresponds to high molecular weight aggregates which cannot be separated accurately by the Superdex 200 column. Fractions of 500 µl each were collected and analysed by SDS PAGE (**Figure 3.2**D) and western blot (**Figure 3.2**E). Interestingly, the main peak corresponding to 1046 kDa proteins actually comprised of highly pure GST-TAT-His protein which could be reduced with DTT and SDS to its 37 kDa monomeric form. MALDI-TOF PMF of the 37 kDa band revealed GST-TAT-His, whereas the 75 kDa protein gave peptides which matched to the *E. coli* protein “ARNA_ECOLC”. This protein serves in *E. coli* to bind and neutralize the effect of strongly cationic molecules and therefore co-purified with the GST-TAT-His, but could be eliminated in SE-FPLC.

The fractions containing pure GST-TAT-His protein (fraction 6-10) were pooled and dialyzed against TAT storage buffer (50 mM Tris pH 8.0, 200 mM KCl, 5 mM DTT), placed in 10-20 µg aliquots in Protein Lo-Bind tubes and stored at -80°C well rapped in aluminium foils till further characterization of the protein.

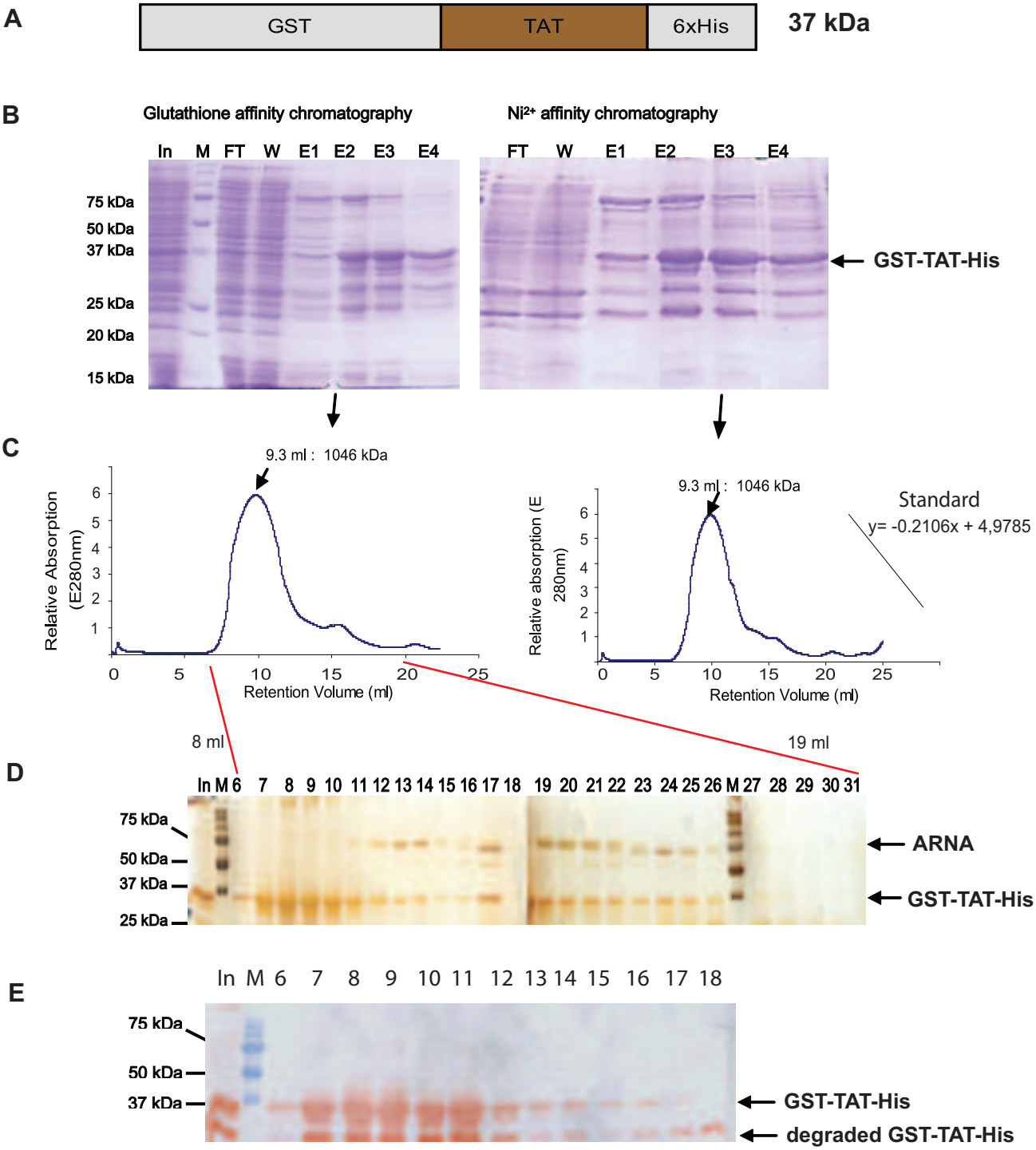

Figure 3.2: Purification of GST-TAT-His protein from *E. coli* BL21

(A) Schematic representation of the recombinant GST-TAT-His protein. **(B)** SDS PAGE and coomassie stain of protein (15 µl/ lane) purified by Nickel affinity chromatography and glutathione affinity chromatography respectively. In= Input, FT = Flow-through, W = wash fraction, E1-E4 are eluted fractions. **(C)** Elution profile of the GST-TAT-His protein purified by SE-FPLC on a Superdex 200. (**D) Analysis of GST-TAT-His after SE-FPLC**. 15 µl protein/ fraction were denatured and analysed by SDS PAGE and silver stain. **(E)** Samples were prepared like in "D". Gels were then blotted and probed with anti-TAT mAb then detected colorimetrically with the AEC substrate. The numbers refer to fractions collected at different retention volumes.

3.1.2 Purification of GST-TAT protein

The TAT fusion protein with N-terminal GST-tag was purified by glutathione affinity chromatography and analysed by SDS PAGE and stained with coomassie (**Figure 3.3**A). High amounts of the partially pure protein could be detected in the eluates. Further purification by size exclusion FPLC on a Superdex 200 column was done. The elution profile from SE-FPLC showed several main peaks with a double peak at 9.8 ml (821.5 kDa) and 10.7 ml (530.98 kDa) (**Figure 3.3**B). A second double peak of lower molecular weight fragments were seen at 14.7 ml (76.32 kDa) and 16.8 ml (27.56 kDa, corresponding to GST). The double peak corresponding to molecular weights ranging between 822 kDa and 530 kDa comprised of pure GST-TAT protein which could be detected as a double band of size 35-36 kDa by SDS PAGE (**Figure 3.3**C). Fractions containing the pure GST-TAT protein were pooled and dialyzed against TAT-storage buffer and used for verification of biological activity or stored at -80°C for later characterization.

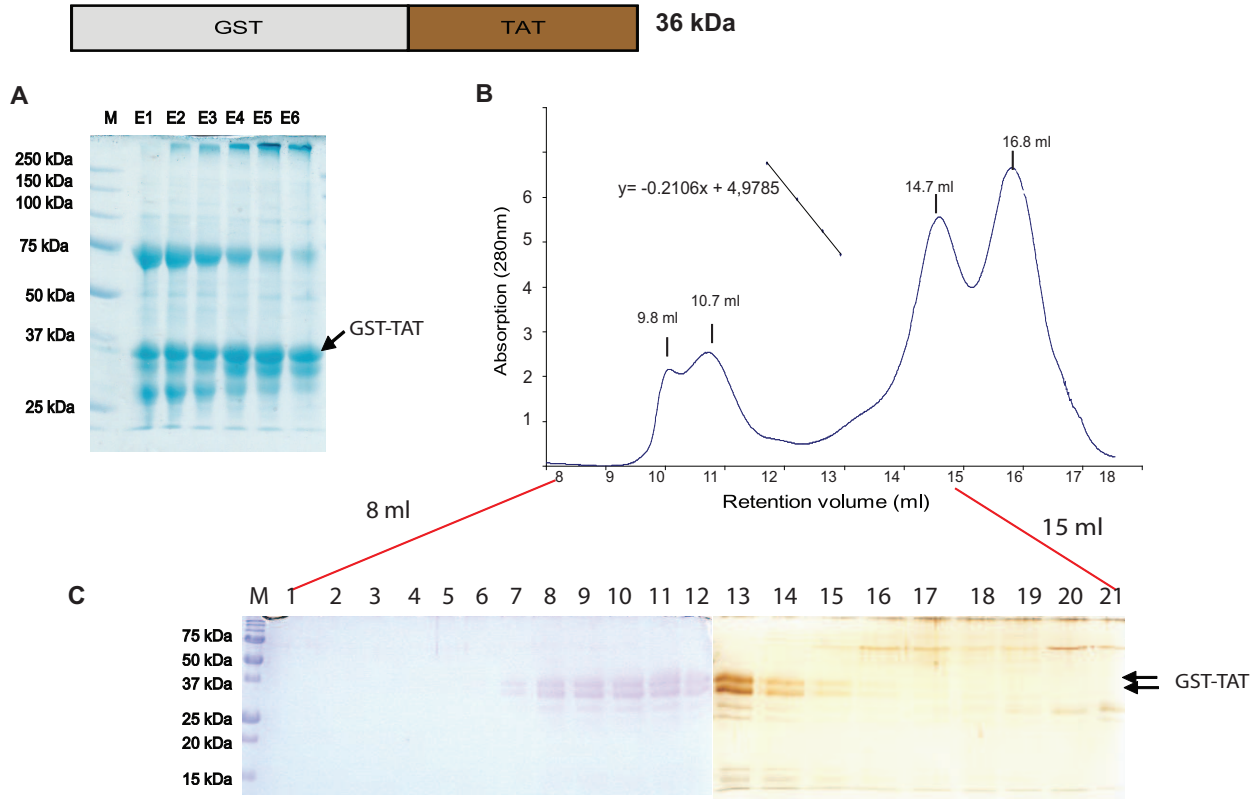

Figure 3.3: Two step purification of GST-TAT protein

(A) SDS PAGE analysis: 15 µl GST-TAT protein/ fraction were analysed by SDS PAGE and stained with coomassie solution. M: high molecular weight protein standards, E1-E6 are protein fractions eluted with 250 µl GST elution buffer each. **(B)** Elution profile of the GST-TAT protein purified by SE-FPLC on a Superdex 200. **(C)** Coomassie/ silver-stained SDS PAGE of GST-TAT protein after size exclusion FPLC. Numbers refer to fractions of 300 µl collected at different retention volumes.

3.1.3 Purification of His-TAT-His fusion protein

The expression of TAT fusion protein with N- and C-terminal 6x-His fusion tags was not as high as those with GST fusion tags. Also, purification by Ni^{2+} affinity chromatography yielded partially pure protein which however was more readily degraded. Purified protein was analysed by SDS PAGE and western blot (**Figure 3.4**B-C). Further purification by size exclusion chromatography on a Superdex 200 column was performed but yielded only low amounts of the pure protein. Although the calculated molecular weight of the fusion protein is about 14 kDa, the elution profile from SE-FPLC also revealed spectra corresponding to molecular weights higher than 670 kDa (result not shown).

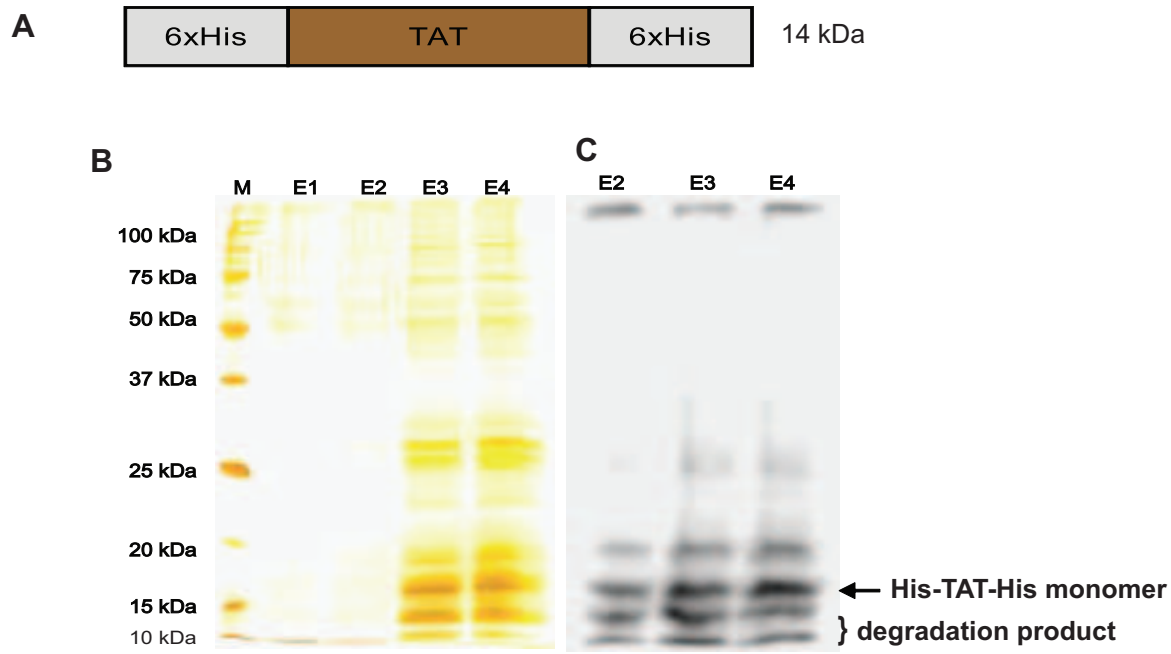

Figure 3.4: Analysis of purified His-TAT-His fusion protein

(A) Schematic diagram of the His-TAT-His protein. **(B)** 15 µl of protein sample per lane was analysed on a 12.5% SDS PAGE then stained with silver nitrate or **(C)** blotted and probed with anti-TAT mAb. M: Protein standard, E1-E4: fractions eluted with 100-, 200-, and 300 mM imidazol respectively.

3.1.4 Purification of TAT protein without fusion tags

The B-type HIV1-TAT cDNA (TAT-*BRU* strain) used in this work codes for an 86 residue TAT protein which is strongly hydrophobic, with a calculated isoelectric point of about 10.1. At buffer pH below this pI value, the untagged protein should carry a negative net charge and therefore bind strongly to cation exchangers. In the underlying work the recombinant TAT protein expressed in *E. coli* and *Sf9* cells did not bind strongly to such cation exchangers (SP- and S- sepharose), but rather bound to anion exchangers at pH 6.5. At this pH value, a high amount of host proteins also bound to

the anion exchanger (**Figure 3.5**A and B). A second purification step using immuno-affinity with anti-TAT mAb was not very successful as most of the bound protein could not be eluted with buffer pH values ranging between 3 and 10.8. At pH values below 3 and above 10.8 the immobilized antibody co-eluted with the protein. Subsequently, the TAT protein was purified in two-steps by combining ion-exchange chromatography and SE-FPLC. Protein elution from the anion-exchanger was performed with 10 mM -1 M salt (NaCl) concentration gradient, making a desalting step necessary. Fractions containing the TAT protein from several rounds of ion exchange chromatography were pooled, desalted on PD10 columns then concentrated with Vivaspin-5,000 MW columns (Vivascience). The concentrate was further purified by SE-FPLC on a Superdex 200. Similar to purification of the GST- and His-tagged TAT protein, the untagged TAT protein eluted at a retention volume corresponding to 708 kDa molecular weight (**Figure 3.5**C). Pure TAT containing fractions (6-9) were pooled and dialyzed against TAT storage buffer then analysed by western blot (**Figure 3.5**D) or stored in aliquots at -80°C for later characterization.

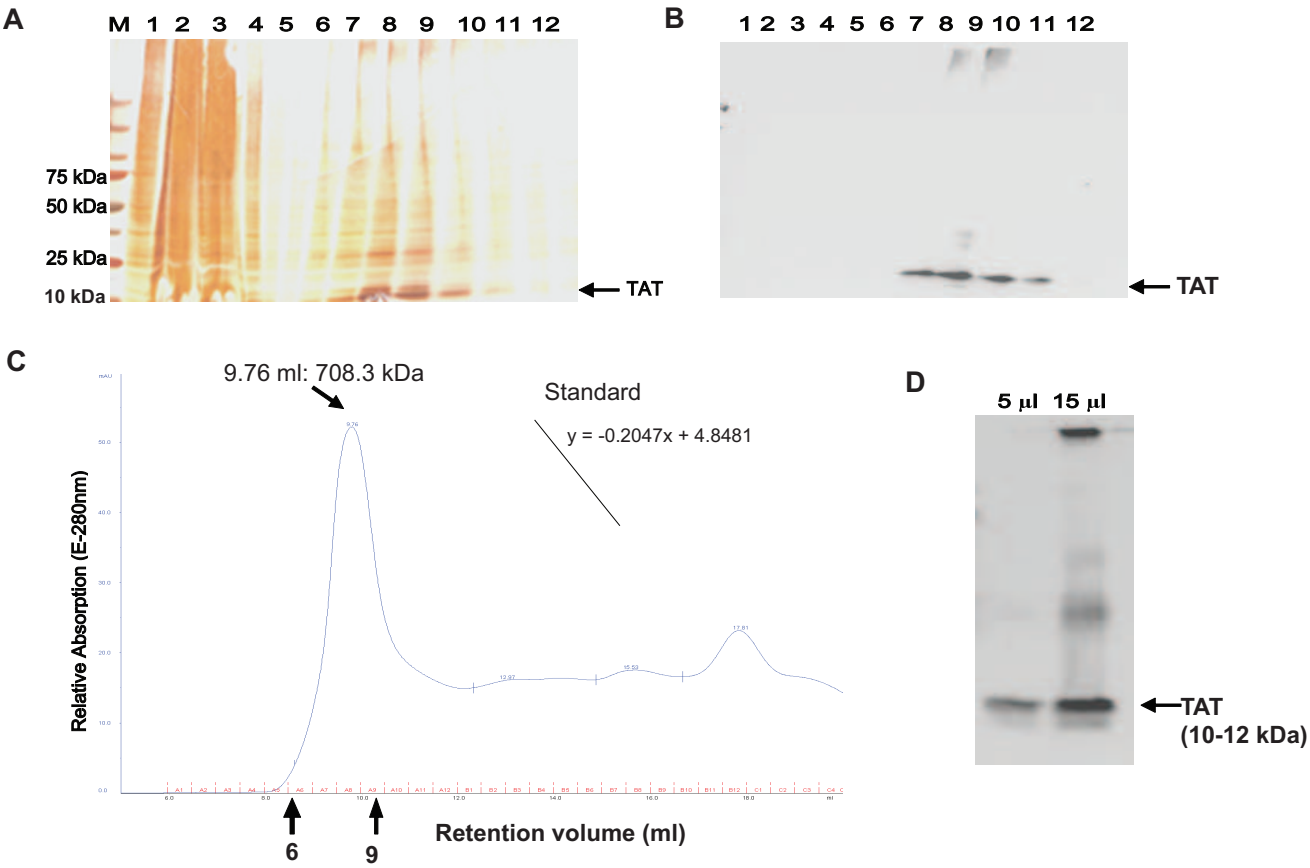

Figure 3.5: Analysis of purified recombinant TAT protein without fusion tags

(A) SDS PAGE: TAT protein was purified on an anion exchanger (HiTrap QF) and eluted with NaCl gradient. 15 µl samples per fraction were separated on 4-18% SDS gradient gels then stained with silver nitrate or **(B)** blotted and probed with anti-TAT mAb. 1-12 indicate fractions of 1 ml eluted with 10 mM- 1 M NaCl. **(C)** Elution profile of TAT protein purified by SE-FPLC on a Superdex 200 column. **(D)** Fractions

6-9 (500 µl each) from SE-FPLC were pooled, concentrated and buffer changed against TAT storage buffer then aliquots of 5 µl and 15 µl analysed by western blot and probed with anti-TAT mAb.

3.1.5 Purification of TAT fusion protein with reagents that prevent protein aggregation

The purification of GST-TAT-His, GST-TAT, His-TAT-His and non-tagged TAT protein under non-denaturing conditions revealed elution profiles of high molecular weight proteins in SE-FPLC. Assuming that this was a result of protein aggregation during purification it was necessary to modify the purification methods, since protein aggregation leads in many cases to inactivation. Reagents such as arginine and glutamate are reportedly accurate in hindering protein aggregation (Shiraki *et al.*, 2002). In the underlying work, using 5-10 mM arginine and glutamate as supplements in lysis-, washing-, and equilibration buffers partially reduced aggregation. However, it led to a rapid degradation of the recombinant TAT protein.

Also, a commercially available solution of short sugar chains called NV10 (Novexin, UK) was used to prevent aggregation of TAT fusion proteins during purification. These short carbohydrate chains supposedly, can block protein moieties which have the tendency to aggregate, thereby preventing protein aggregation. In the first step, purification of the GST-TAT-His protein by nickel affinity chromatography with NV10 in lysis-, wash- and elution buffers yielded high amounts of apparently monomeric protein as detected in SDS PAGE (**Figure 3.6**A). However, this protein became more rapidly degraded than those purified without NV10 in the buffers. This was consistent with the elution profile and yield of the protein during purification by SE-FPLC. Only a small amount of the protein still in aggregate form was eluted at 9.4 ml retention volume. Compared to the protein amount applied on the SE-FPLC this was a very low yield. A second peak corresponding to relatively high amounts of protein of molecular masses lower than 6 kDa could be detected (**Figure 3.6**B). Analysis of the other TAT constructs revealed identical results, making these reagents not suitable for use in the purification of TAT protein. Fractions collected from SE-FPLC and analysed by SDS PAGE revealed a small amount of the protein as aggregates and a large amount of smaller fragments (**Figure 3.6**C).

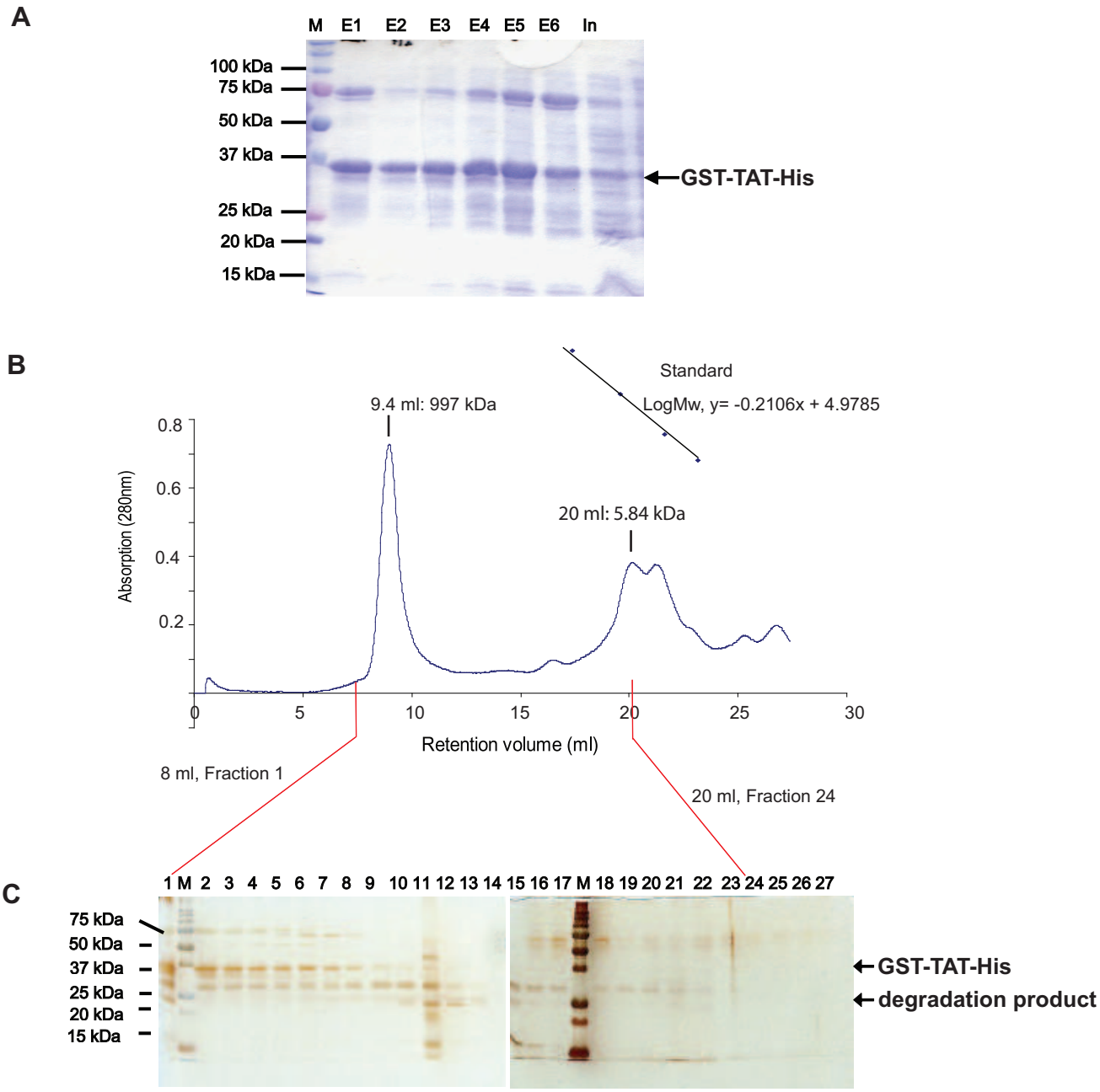

Figure 3.6: Analysis of GST-TAT-His purified with reagents that reduce protein aggregation

Buffers used in all purification steps were supplemented with NV10 at the ratio 1:10 (100 µl/ml). **(A) SDS PAGE:** After Ni^{2+}-affinity chromatography 15 µl proteins/ fraction were separated on a 12% SDS gel and stained with coomassie. In= cytosolic fraction, E1-E6 are fractions eluted with 200 mM imidazol. **(B) SE-FPLC:** Pre-purified GST-TAT-His protein was cast on a Superdex 200 column and purified by SE-FPLC with buffers containing NV10 and fractions of 500 µl collected. **(C) SDS PAGE after SE-FPLC**: 15 µl aliquot per fraction was analysed by SDS PAGE and stained with silver nitrate.

3.2 Expression and purification of TATGFP in stably transfected CHO cells

The cloning of TAT cDNA into the pEGFP-N1 vector which enables the expression of protein with a C-terminal GFP-tag in mammalian cell lines was done as described under section 9.1.1.3.

Transfection of the TAT-pEGFP-N1 in CHO cells and selection of stable clones was achieved over a period of three weeks with 600 mg/L neomycin. Selected clones were controlled by flow cytometry (**Figure 3.7**A) and fluorescence microscopy which revealed the protein predominantly in the nucleus (**Figure 3.7**B). Although the expression of recombinant protein in mammalian cell lines is generally low, about 30 µg of the protein could be purified from 10 large (Ø 15 cm) culture plates of confluently grown CHO-TATGFP cells. The recombinant TAT protein with C-terminal GFP-tag was purified by immuno-affinity chromatography on immobilised anti-GFP mAb and eluted by pH shift with 50 mM Diethylamine, pH 10.8. Eluted protein fractions were pooled and concentrated, then analysed by SDS PAGE and western blot. The immuno-purified protein was relatively pure and ran as a monomer of 36 kDa (**Figure 3.7**C). Further purification by SE-FPLC was not performed to avoid protein loss. The protein was stored at -80°C for later characterization.

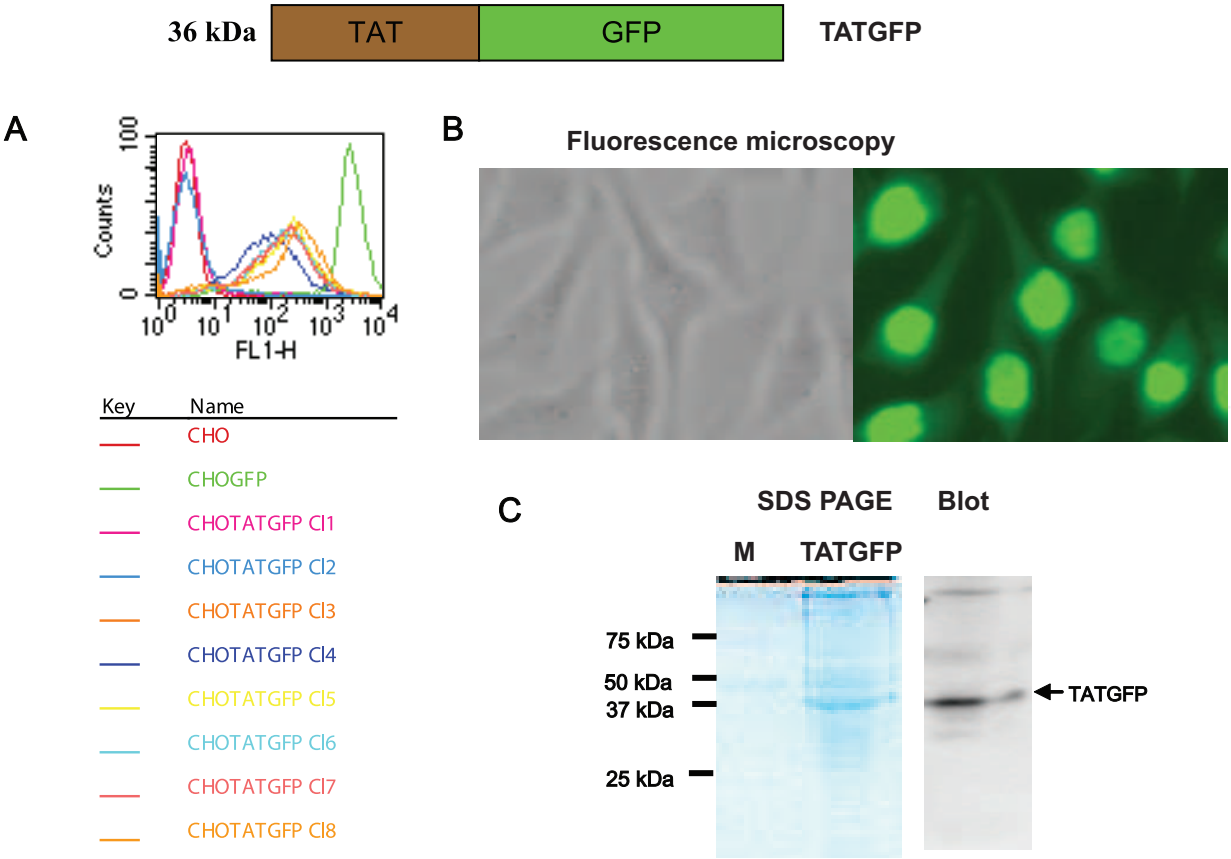

Figure 3.7: Expression and purification of TATGFP protein in CHO cells

(A) Flow cytometry: The level of expression of the TATGFP protein in selected clones was analysed. **(B) Fluorescence microscopy:** Images of a stably transfected CHO-TATGFP (clone 3) were made under a fluorescence microscope at a 40x magnification. **(C) SDS-PAGE and Western blot:** TATGFP protein purified by immuno affinity chromatography were analysed by SDS PAGE and stained with coomassie solution or blotted and probed with anti-TAT mAb.

3.3 Expression and purification of TAT protein in *Sf9* cells

3.3.1 Cloning, preparation and analysis of TAT-recombinant baculovirus

The HIV1-TAT1-86 cDNA was cloned in the pFastBac1^{TM} vector as described in section **9.1.1.2** and recombinant viruses for the protein constructs in **Figure 3.8**A were prepared. After transfection the primary recombinant baculovirus stocks in the culture medium were harvested and used for viral amplification. Cell pellets from the transfection step were lysed and the protein analysed by western blot. In all the samples TAT protein could be detected (result not shown). After the first viral amplification the cells infected with the TATHis recombinant baculovirus showed no further expression of the TATHis protein. This was strange since the initial transfected cells revealed the expression of the protein. After repeating the preparation of bacmid, transfection and viral amplification three times it was clear that the cells for an unknown reason could not express the TATHis fusion protein. Opposed to this, expression of the untagged TAT (*Sf9*-TAT) and the TATV5His bearing a V5-epitope tag between the TAT and the 6x His tag, were possible even after the second viral amplification. An analysis of the recombinant viruses also revealed that for some reason the TAT gene in the TATHis construct was lost during the viral amplification step (**Figure 3.8**B). Briefly, 1 ml of the primary viral stocks and the first amplifications were treated with SDS and Proteinase K. The bacmid DNA in the virus was then purified with the Zymoclean DNA clean and concentration kit and the eluted bacmid-DNA used as template for PCR with the primers For-pBAC vir and Rev-pBAC-vir as indicated under section **9.1.14.6**.

As detected on agarose gels, the TATHis DNA is present in the primary virus stock, but completely lacking in the first amplification sample. For the *Sf9*-TAT and TATV5His constructs the DNA was detected both in the primary viral stock and first amplification and was therefore suitable for use in expression of the respective fusion proteins in insect cells.

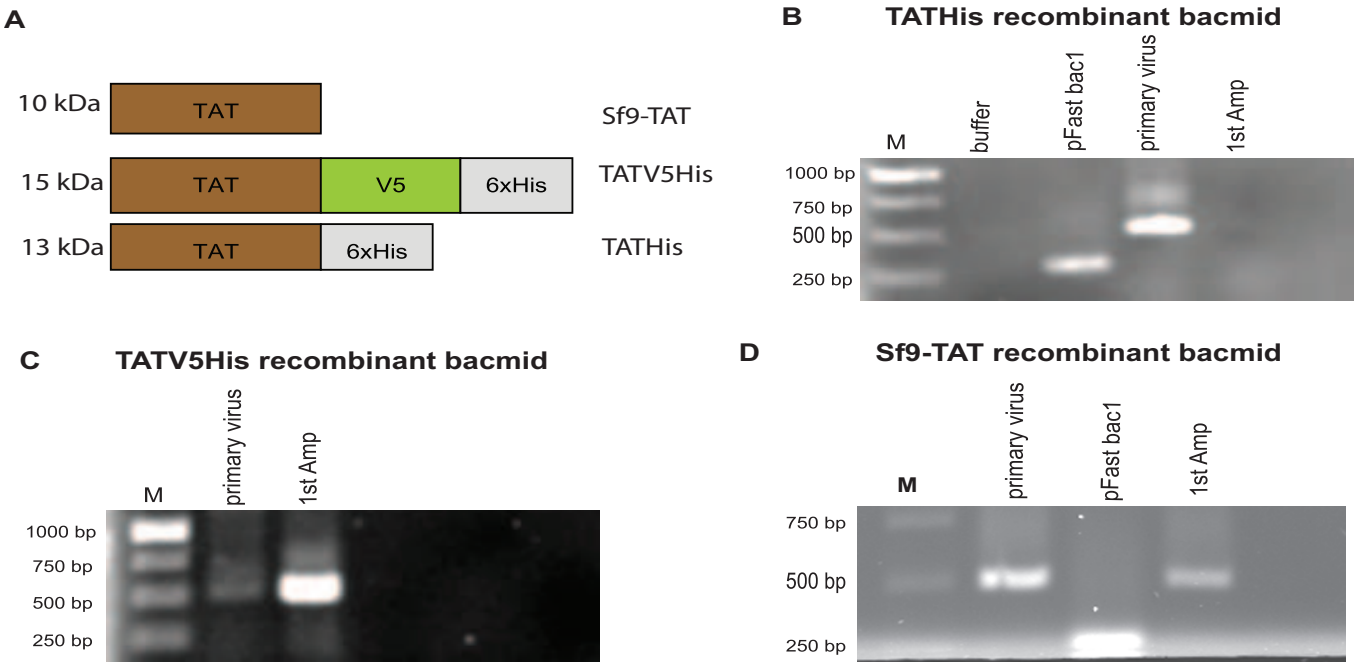

Figure 3.8: Expression of TAT fusion protein in *Sf9* cells

(A) Schematic representation of the TAT protein constructs expressed in *Sf9* insect cells and the given names used in this work. **(B-D**) Analysis of recombinant baculovirus: bacmid DNA for the different constructs were purified from the recombinant baculoviruses and verified by PCR and agarose gel electrophoresis for the presence of the TAT cDNA. **(B)** TATHis, **(C)** TATV5His, **(D)** *Sf9*-TAT. **M:** 1 kb DNA ladder, **"buffer":** negative control without template DNA, **primary virus:** viral stock after initial transfection, **pFastbac1:** shuttle vector used in the preparation of bacmid (positive control for PCR), **1st Amp:** first amplification of primary viral stock.

3.3.2 Expression of recombinant TAT protein in *Sf9* cells

Sf9 cells at a density 2 x 10^6cells/ml were cultured in serum-deficient medium and infected with the *Sf9*-TAT, TATHis and TATV5His recombinant baculoviruses then cultured at 27°C for 3 days. Harvested cells were stained anti-TAT mAb and Cy3-conjugated anti-mouse IgG then analysed by flow cytometry and fluorescence microscopy (**Figure 3.9**). In five independent assessments by FACS, the cells revealed high expression levels of the *Sf9*-TAT, whereas only very low amounts of the TATV5His protein were determined. The TATHis was not expressed at all by the cells, which was consistent with the fact that the recombinant baculovirus lost the TATHis recombinant bacmid as shown earlier by PCR analysis.

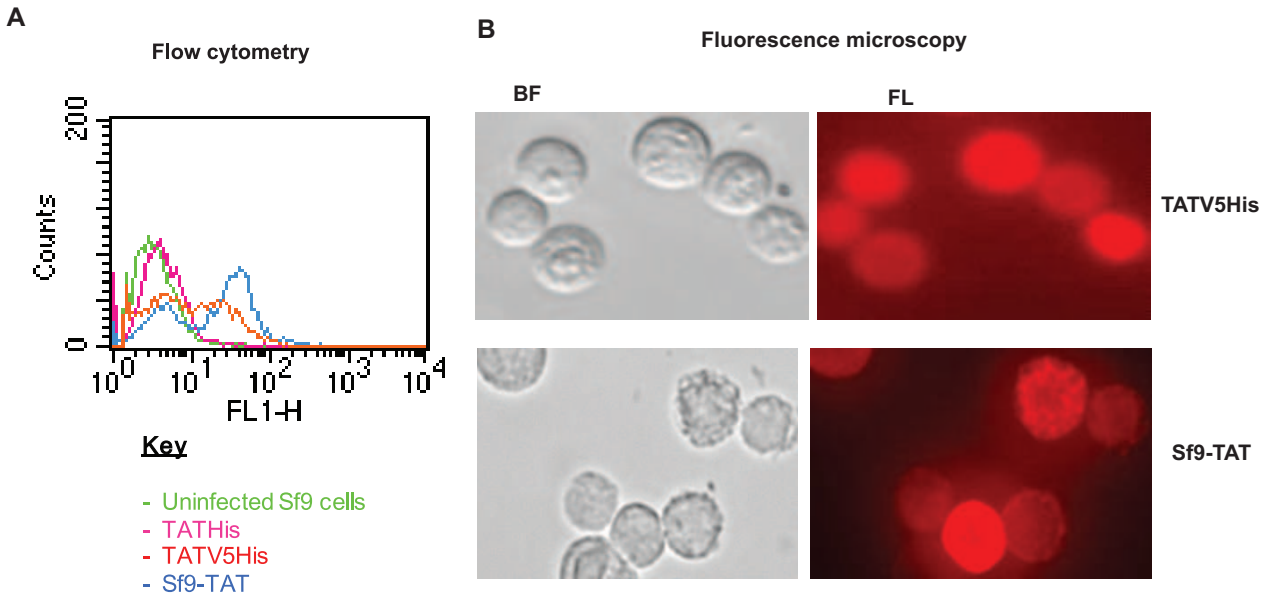

Figure 3.9: Analysis of TAT and TATV5His expression in *Sf9* Insect cells

(A) Flow cytometry: Uninfected cells and cells infected with the respective baculoviruses for 72 h were stained with the anti-TAT mAb and Cy3 conjugated anti-mouse IgG and analysed on a FACs scan. A total of 10000 events were scored. **(B) Fluorescence microscopy:** Stained cells were visualized under a fluorescence microscope (Zeiss) at 40x magnification and images made with the Axio-cam. BF: bright field, FL: fluorescence.

3.3.3 Purification of *Sf9*-TAT and TATV5His protein from *Sf9* cells

The purification of untagged TAT protein from insect cells by ion exchange chromatography on a HiTrap Q FF anion exchanger and SE-FPLC was under same conditions as described earlier (**3.1.4**). Despite the relatively high expression of the protein only a small fraction was purified to homogeneity by combining ion exchange chromatography and SE-FPLC. The final yield of the *Sf9*-TAT protein was 140 µg / 500 ml *Sf9* cells (2 x 10^6 cells /ml).

The TATV5His protein was purified in two steps by Ni^{2+}-affinity chromatography and SE-FPLC as reported earlier for the His-TAT-His (**3.1.3**). After Ni^{2+}-affinity purification moderate amounts of the partially pure protein could be detected by SDS PAGE and western blot (**Figure 3.10**A-B). A further purification by SE-FPLC yielded pure TATV5His protein. In this case as well, the retention volume of the TATV5His protein corresponded to 1047 kDa (**Figure 3.10**C). Fractions containing the pure TATV5His protein from SE-FPLC were pooled and dialyzed against TAT storage buffer and analysed by western blot. The pure protein could be seen predominantly as a 14 kDa protein with a fainter band of about 12 kDa. The rest of the protein was stored at -80°C for further characterization.

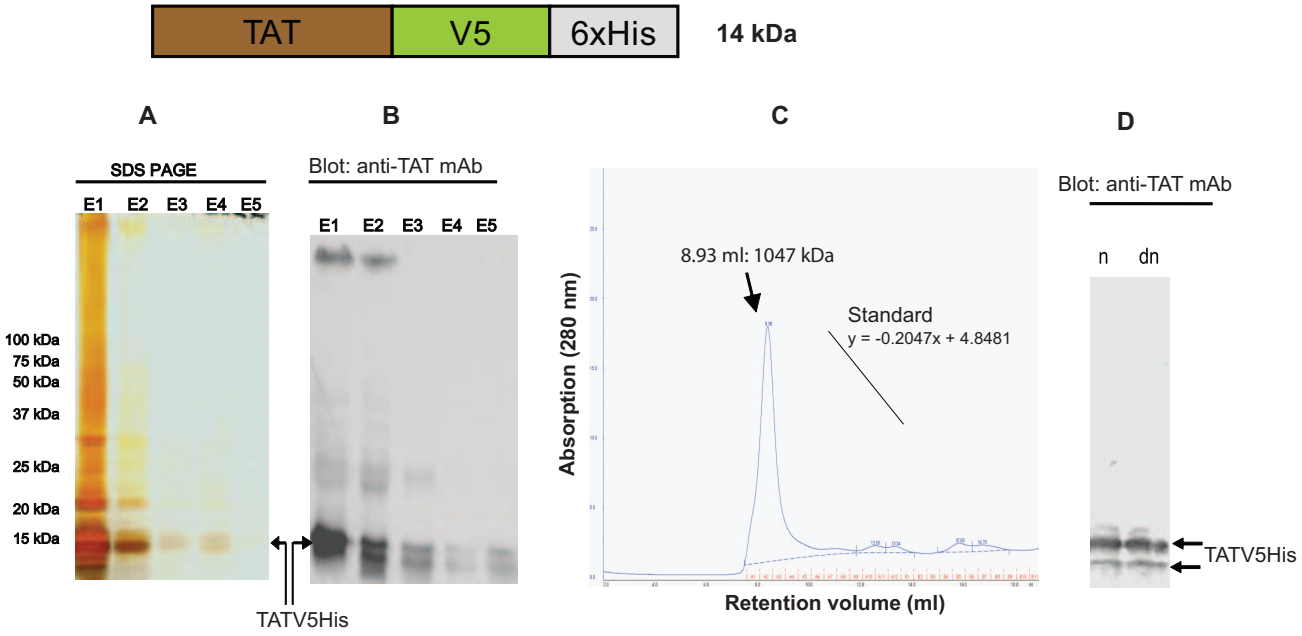

Figure 3.10: Two step purification of recombinant TATV5His protein from *Sf9* cells

(A) Fractions (15 µl) eluted from Ni^{2+}-affinity column were analysed by SDS PAGE and stained with silver nitrate or **(B)** blotted and probed with anti-TAT mAb. E1-E5: elution fractions. **(C)** Elution profile of TATV5His from SE-FPLC. **(D)** Western blot analysis of TATV5His after SE-FPLC. 15 µl of the concentrated TATV5His protein were either denatured by boiling with reducing sample buffer *(dn)* or mixed with non-reducing/ non-denaturing sample buffer *(n)* and analysed by western blot.

Summary I: Expression and purification of recombinant TAT protein

The expression levels of HIV1-TAT fusion proteins varied in all cell systems used. Coupled with this, the presence of fusion tags and the purification methods played a role in the yield and purity of the fusion protein. The relative expression and purification yield for each construct is given in **Table 3.1**.

Table 3.1: Expression and purification of recombinant TAT protein

Cell system	Construct	Relative expression level	Final yield
E. coli	GST-TAT	high, ca. 5-8 mg/L	570 µg/L
	GST-TAT-His	high, ca. 6 -10 mg/L	800 µg/L
	His-TAT-His	high, ca. 3-5 mg/L	200 µg/L
	TAT	high, ca. 5-6 mg/L	120 µg/L
Sf9	TATHis	no expression	
	TAT	high, ca. 2 mg/L	140 µg /500 ml 2x10^6c/ml
	TATV5His	low, ca. 1 mg/L	80 µg /500 ml 2x10^6c/ml
CHO (Epithelial)	TAT (pC63.4.1 Vector)	no detection	no detection
	TATGFP (Stable)	moderate	low (30 µg/ 10x Ø15 cm plates)
HeLa (Epithelial)	TAT (stable)	very low	

3.4 Characterization of purified recombinant TAT protein

The purified recombinant TAT protein have low endotoxin levels

Traces of endotoxin could be highly toxic to cells and tissues of mammalian origin thereby falsifying test results, when carried out with contaminated protein on mammalian cell lines.
In order to evaluate the biological activity and effect of the TAT fusion protein on the different cell lines CHO-CXCR4-GFP, Hek293-CXCR4GFP, Jurkat and HLCD4CAT, it was necessary to avoid the influence of protein contaminants such as endotoxins which are usually co-expressed in high amounts by *E. coli*. In this work the levels of endotoxin in the protein solution were evaluated with the commercially available endotoxin detection kit (Genscript). The assessed endotoxin levels are given in the table below. The endotoxin levels in the final protein solution were all in the range of 0.1 EU/µg and 0.08 EU/µg Protein. The acceptable level for intravenous injections of plasmid DNA is 0.1 EU/µg (Ferreira *et al.*, 2000) and 5 EU/Kg weight of recipient for recombinant proteins (Petsch & Anspach, 2000). Except for the GST-TAT protein, the endotoxin levels in all the purified protein samples were under the acceptable limit for use in cell culture assays.

Table 3.2: Evaluation of Endotoxin content of purified recombinant TAT protein.

	Endotoxin concentration in EU/µg protein				
Sample	**Lysate**	**Flow- through**	**Wash (pooled)**	**Eluates (before FPLC)**	**after FPLC (pooled fractions)**
GST-TAT-His	197.742	204.46	190.852	0.258	**0.0805**
GST-TAT	-	-	-	-	**0.175**
His-TAT-His	-	-	-	0.405	**0.0868**
TAT10xHis*	-	-	-	-	**0.0821**

*The TAT10xHis with a c-terminal deca-His fusion tag was purified from *E. coli* by our co-operation partners Dr. Eva Tauberger and Jacobo Martinez from the group of Prof. Saenger (FU-Berlin).

3.4.1 Evaluation of the biological activity of purified recombinant TAT protein

Purified recombinant-HIV1-TAT protein is highly susceptible to proteolytic degradation, oxidation and thermal and light inactivation. Added to these factors, the readiness of the protein to aggregate also contributes to the loss of its biological activity *in vitro*. Biologically active TAT protein has a series of roles which can be exploited in determining the activity of purified recombinant-TAT protein. HIV1-TAT is the only transactivator of transcription found in HIV. As such, it binds to the HIV 5'-long terminal repeat (LTR-) promoter found on all viral transcripts and transactivates their expression. In this work the ability of purified recombinant TAT-protein to induce the expression of

chloramphenicol acetyl transferase (CAT), under the control of the HIV-LTR promoter in the HeLa cell line HLCD4CAT was evaluated.

3.4.1.1 The purified recombinant TAT-protein transactivate the viral LTR promoter

HeLa cell lines carrying a stably cloned CAT gene under the control of the HIV-LTR promoter were treated with purified recombinant TAT proteins as described elsewhere. The cells were harvested and evaluated for the expression of CAT protein by use of the commercially available CAT-ELISA kit.

The amount of CAT expressed per / ml / µg TAT protein used is given in **Figure 3.11**. The purified GST-TAT-His, GST-TAT and TAT10xHis protein revealed the highest transactivation capacity. His-TAT-His fusion protein purified under the same conditions as GST-TAT-His was less active than equivalent concentrations of the latter. The TAT protein from Immuno-Diagnostics (TAT +ve) which served as a positive control revealed higher transactivation ability than the His-TAT-His, TATGFP, *Sf9*-TAT and TAT10xHis. However, the GST-TAT-His and the GST-TAT protein had higher transactivation abilities than this positive control. The TATGFP expressed in CHO cells and the *Sf9*-TAT protein expressed in *Sf9* cells both had low yields. Nevertheless, they could still activate the HIV-LTR and induce CAT expression. Compared to this, the commercial TAT_{47-57} peptide was unable to fully activate the HIV LTR, which is in accordance with the fact that recognition and binding of the HIV transacting response element on the LTR and activation requires other domains of the TAT protein.

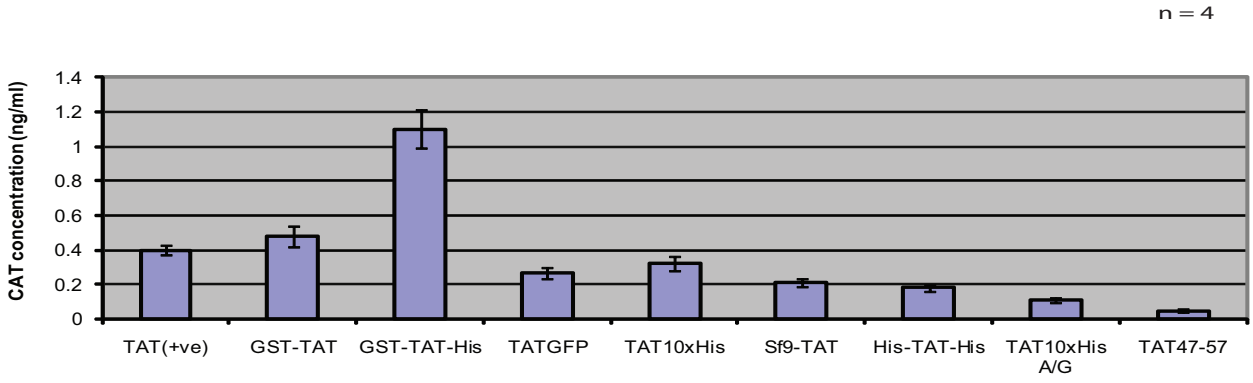

Figure 3.11: Quantification of TAT-induced expression of chloramphenicol acetyl transferase

The HeLa cell-line HLCD4CAT were treated with equivalent amounts of the respective recombinant protein then evaluated for the expression of CAT after 48 hours. The mean values of 4 independent assays ± standard deviation are given in the bar diagram. TAT(+ve) (TAT1-86, Immuno-Diagnostics USA), TAT10xHis A/G: TAT10xHis in buffer supplemented with arginine and glutamate, TAT47-57: TAT peptide from Genscript (negative control).

3.4.1.2 Purified TAT protein influences CXCR4-localisation in stably transfected cell lines

3.4.1.2.1 Analysis of CXCR4GFP expression in CHO and Hek293 cell lines

The human CXCR4 variant II cDNA was cloned in the pEGFP-N1 vector as described under methods section **9.1.1.4**. The CXCR4-pEGFP-N1 plasmid was transfected in CHO and Hek293 cells in parallel. Selection of stable clones was achieved over a period of two weeks with 600 mg/L and 500 mg/L neomycin for CHO and Hek293 cells respectively. Analysis of selected clones by flow cytometry, fluorescence and confocal microscopy, revealed a uniform expression of the CXCR4GFP protein. According to results from flow cytometry, the expression of CXCR4GFP in CHO is not as high as in the Hek293 cells. However, CXCR4 expression in all the selected CHO-clones is more uniform than in the Hek293 clones (**Figure 3.12**A and E). The Hek293 clones showed a mixture of cells with very strong expression and some cells with low levels of CXCR4GFP (**Figure 3.12**E). The expressed CXCR4GFP protein was located predominantly on the cell membrane with a minor fraction seen in vesicles. Relatively high amounts of the protein were also detected in western-blot analysis with the anti-GFP mAb (**Figure 3.12**D).

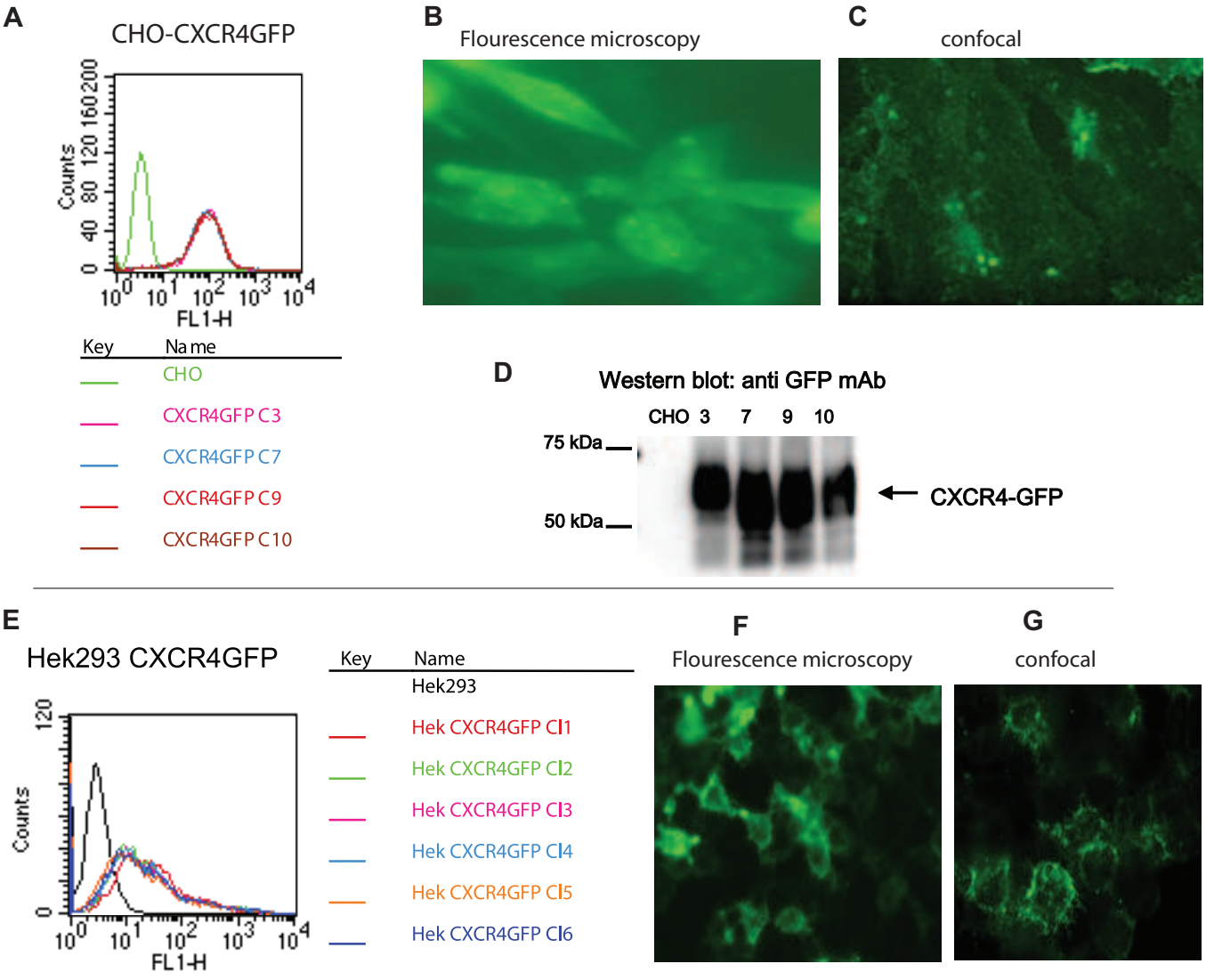

Figure 3.12: Analysis of stably transfected CHO-CXCR4GFP and Hek293-CXCR4GFP cell lines
(A) Flow cytometry of selected CHO-CXCR4GFP clones. **(B)** Fluorescence microscopy: Clone 9 of the CHO-CXCR4GFP cell lines was fixed on culture slides, washed once with PBS and visualized at a 40 fold magnification and images made. **(C)** Confocal laser scan of CHO-CXCR4GFP clone 3 imaged at a 63-fold magnification. **(D)** Western blot analysis of solubilised CXCR4GFP protein (5 µl lysates /lane) Numbers indicate selected clones 3, 7, 9 and 10. Probing was done with anti-GFP mAb. The selected Hek293-CXCR4GFP clones were also analysed by the same methods and presented in **E-G** respectively.

3.4.1.2.2 Purified TAT protein causes vesicular accumulation of CXCR4GFP

The stably transfected CHO-CXCR4GFP and Hek293- CXCR4GFP cell lines were treated with different recombinant TAT proteins and cultured for 48 h then assessed by flow cytometry and confocal microscopy. Controls were done with GST protein, the short TAT47-57 peptide and PBS. Analysis by flow cytometry revealed no significant change in the level of CXCR4GFP expression in the cell lines after application of the different TAT fusion proteins. However, assessment of the cells by fluorescence and confocal microscopy revealed a significant accumulation of the CXCR4GFP protein in vesicles following treatment of cells with some of the recombinant-TAT constructs. Compared to the PBS- and TAT_{47-57} treated Hek293-CXCR4GFP cell lines, vesicular accumulation of CXCR4GFP was quite significant in cells treated with GST-TAT-His, GST-TAT, TAT (Immuno-Diagnostics) and *Sf9*-TAT (**Figure 3.13**A). Opposed to this, treatment of the CHO-CXCR4GFP cell line with different TAT fusion proteins revealed a less significant effect of TAT on the cellular distribution of CXCR4GFP. A significant vesicular accumulation of the CXCR4GFP protein in CHO cells was only seen with TAT (Immuno-Diagnostics) and *Sf9*-TAT (**Figure 3.13**B).

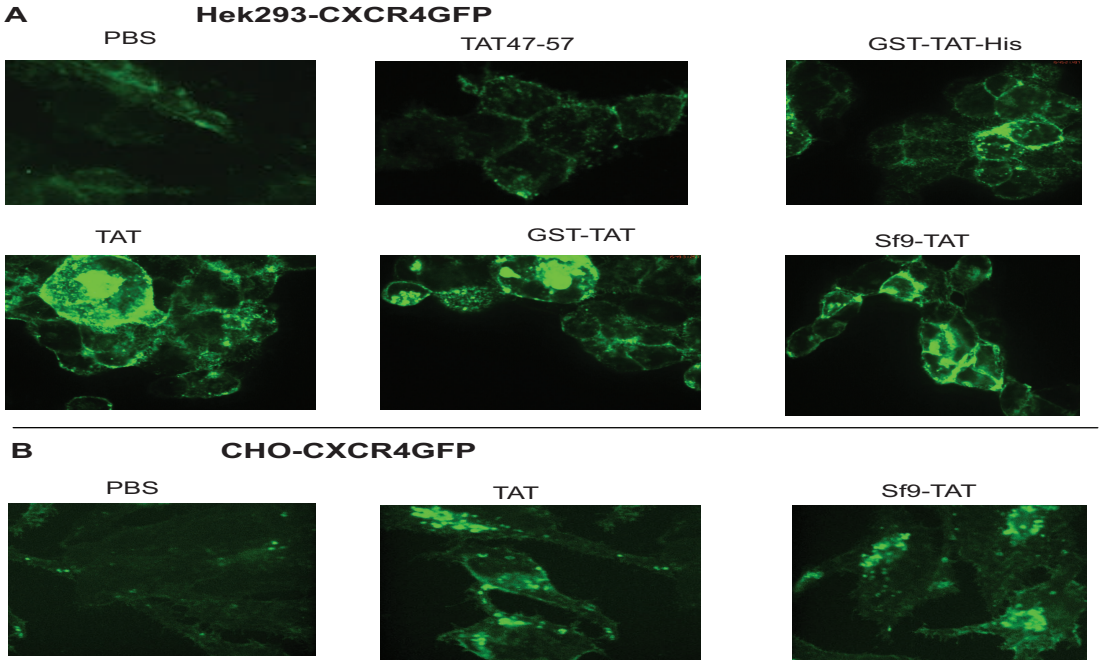

Figure 3.13: Effect of TAT on the distribution of CXCR4GFP in transfected CHO and Hek293
Stably transfected CHO and Hek293 cells were treated with TAT protein then washed and imaged by confocal laser scanning at a 63-fold magnification. TAT (Immuno-Diagnostics), *Sf9*-TAT (*Sf9* cells), GST-TAT-His and GST-TAT (*E. coli),* TAT47-57: TAT peptide (Genscript).

3.4.2 Effects of recombinant TAT protein on binding and inhibition of human-DPPIV

3.4.2.1 Recombinant TAT did not bind DPPIV in pull-down, immunoprecipitation or SPR

To investigate the binding of DPPIV and TAT, the recombinant TAT fusion proteins expressed in *E. coli* and *Sf9* cells and used in pull-down and immunoprecipitation assays or purified and used to verify their binding ability to DPPIV in SPR tests.

In pull-down assays, the GST-TAT-His and GST-TAT proteins were immobilized on Glutathione-Sepharose in batches and incubated for 30 min, 60 min and 90 min with lysates of *Sf9* cells expressing the human-DPPIV protein or with purified human-DPPIV protein. Unbound proteins were washed out and the bound protein fractions were analysed by SDS PAGE and western blot and probed with anti-DPPIV pAb. In all the tests conducted (n=4), there was no detection of bound DPPIV in the analysed resins, but rather in the wash fractions. Likewise, immobilizing DPPIV on anti-DPPIV antibody did not pull-down detectable amounts of any of the recombinant TAT proteins from lysates of TAT-expressing *E. coli* or *Sf9* cells.

The ability of purified HIV1-TAT fusion protein to bind to human-DPPIV was further investigated by surface plasmon resonance analysis. All the recombinant TAT proteins analysed (see section 9.4.1) did not bind to purified human-DPPIV that was immobilized on CM5 or C1 sensor chip, but rather precipitated on test- as well as control cells of the sensor chips. This was not due to the affinity of the TAT protein to the dextran film on the surface of the CM5 sensor chip, since the TAT proteins also precipitated on the C1 sensor chip which lacks the dextran film on its sensor surface.

3.4.2.2 Recombinant TAT retards the cleavage of a chromogenic substrate by DPPIV

It was verified whether recombinant TAT protein with varying fusion tags will inhibit DPPIV activity and if salt conditions played a role in this effect of TAT protein on DPPIV. In the initial experiments, the commercial whole length HIV1-TAT protein (TAT 1-86, Immuno-Diagnostics) was used. The commercial TAT protein was detected predominantly as monomer on SDS PAGE and western blot with a few aggregates (**Figure 3.14**C). The human-DPPIV protein used was purified from *Sf9* cells and analysed by SDS PAGE and western blot. The reduced DPPIV protein runs as a monomer at 96 kDa (**Figure 3.14**A) and under non-denaturing and non-reducing conditions, as a homodimer between 150 kDa and 188 kDa (**Figure 3.14**B).

The proteolytical cleavage of 100 nM of the chromogenic substrate H-Gly-Pro-pNA-HCl (Bachem) by purified DPPIV at different salt concentrations with or without addition of 50 nM final concentration of TAT protein was determined photometrically. In the absence of TAT protein, different NaCl concentrations in the reaction sample did not influence the cleavage of the chromogenic substrate by DPPIV (**Figure 3.14**D). However, in the presence of 50 nM TAT protein, DPPIV activity was reduced in a salt-dependent manner and increased with decrease in salt concentration. At NaCl concentrations between 10 mM and 40 mM, the cleavage of the chromogenic substrate by DPPIV was reduced to about 30-40% within the first 5 min. In the absence of NaCl, TAT protein showed no effect at all on the enzyme activity of DPPIV. Incubating the reaction mixtures for longer periods than 5 min resulted in a complete cleavage of the substrate, such that similar DPPIV activities were determined, irrespective of the presence of TAT protein.

Opposed to the untagged TAT protein, addition of up to 500 nM purified GST-TAT-His and GST-TAT fusion protein in DPPIV reaction assays did not affect the enzymatic activity of DPPIV. With 50 nM of the His-TAT-His, TAT10xHis and *Sf9*-TAT protein detectable but very low inhibitions were detected (result not shown).

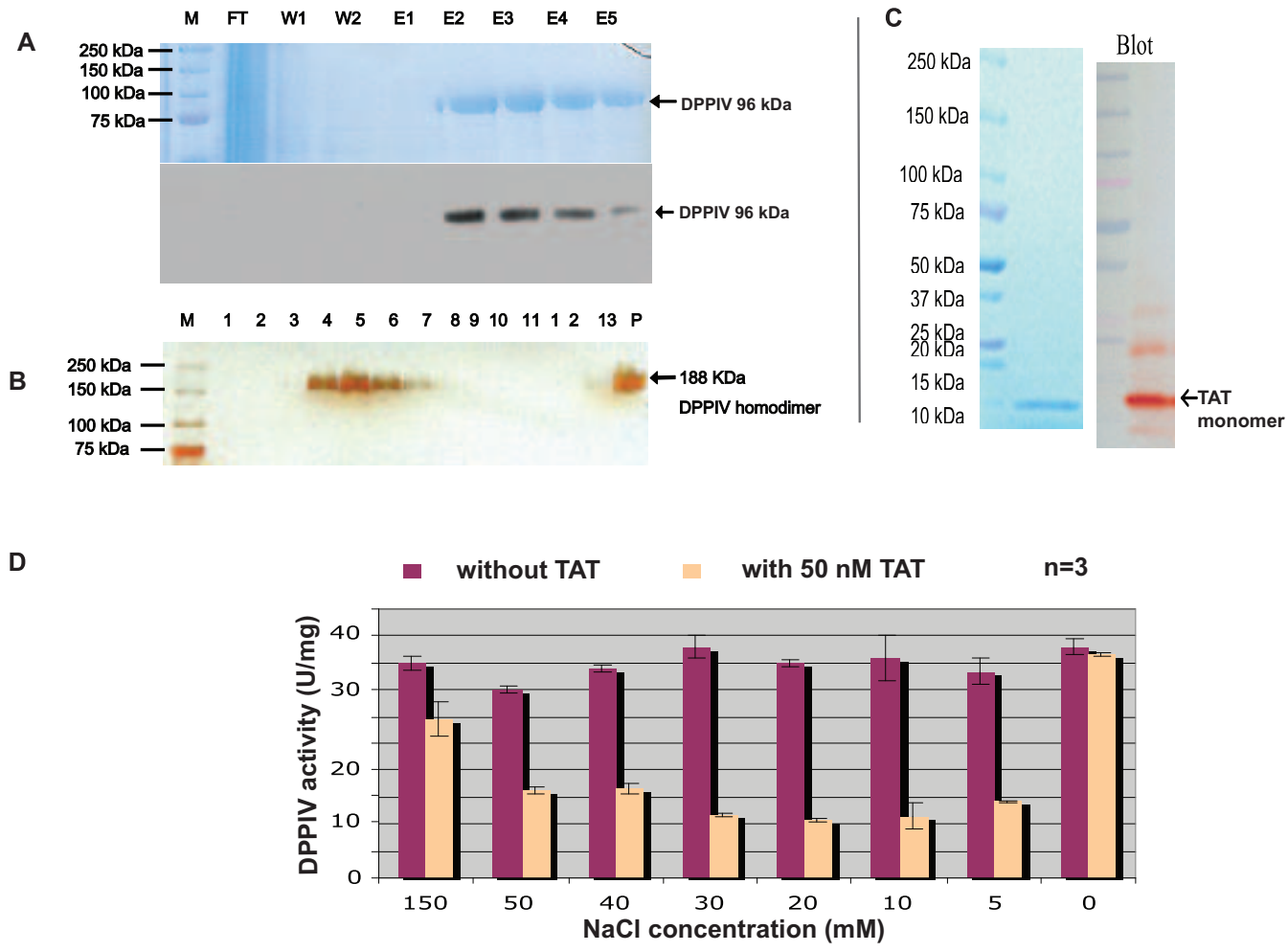

Figure 3.14: Effect of recombinant TAT on the enzyme activity of DPPIV

(A) SDS PAGE and western blot analysis of purified DPPIV. 10 µl DPPIV proteins / lane were analysed after purification by immuno-affinity chromatography. FT: flow-through, W1 /W2: wash, E1-E5: fractions eluted with 50 mM Diethylamine pH 10.8. **(B) Native PAGE of DPPIV protein after size exclusion FPLC.** 5 µg protein / fraction collected from the Superdex 200 column were analysed under non-denaturing and non-reducing conditions and stained with silver nitrate. Numbers refer to elution fractions, P: 5 µl of pooled fractions after protein concentration. **(C) SDS PAGE and western blot of TAT.** A 2 µg aliquot of the purchased TAT protein was separated on 4-16% SDS gradient gels and stained with coomassie or blotted and probed with anti-TAT mAb. **(D) Influence of TAT protein on DPPIV enzyme activity.** DPPIV was incubated with 100 nM substrate at 37°C for 5 min either without TAT protein or with 50 nM TAT protein per test, at different salt concentrations. The extinction was measured at 405 nm and used in determining the specific DPPIV activity given in U/mg in the bar diagram.

3.4.2.3 Recombinant TAT retards the cleavage of natural substrates by DPPIV

The chromogenic substrate H-Gly-Pro-pNA-HCl used in the above assay is not a natural substrate of DPPIV. However, the inhibition tests conducted with the substrate provided appropriate salt conditions at which TAT protein reveals significant inhibition effects on the enzymatic activity of human-DPPIV. Subsequent investigations on the effect of HIV1-TAT protein on the cleavage of natural substrates by purified human-DPPIV protein were conducted at 37 mM salt concentration. For this purpose, naturally occurring substrates of human-DPPIV such as glucagon-like-peptide 1 ($GLP1_{7-36}$), Neuropeptide Y (NPY_{1-36}) and glucose insulinotropic polypeptide 1 ($GIP1_{3-42}$) were used. These substrates do not give a colour change when cleaved by DPPIV, but the difference in the masses of cleaved and uncleaved form could be determined by MALDI-TOF mass spectrometry. For all the substrates used, an inhibition effect of the HIV1-TAT protein on DPPIV enzyme activity could be detected. The best spectra however, were got with GLP1. $GLP1_{7-36}$ has a mass of 3296 Da. When cleaved by DPPIV it becomes two residues shorter, ($GLP1_{9-36}$) with a mass of 3088 Da. With the use of MALDI-TOF MS, spectra of cleaved $GLP1_{9-36}$ versus uncleaved $GLP1_{7-36}$ were measured and their intensities compared at different time points of cleavage.

In initial assays without TAT protein, 16 nM DPPIV could cleave 31.25 µM GLP1 within 5 minutes, so that only the spectrum of cleaved GLP1 was determined (**Figure 3.15**A). With 1 µM TAT protein (Immuno-Diagnostics) in the assay mixture, about 60 % of the substrate was still uncleaved after 5 minutes (**Figure 3.15**B). TAT protein however only induces a retardation of the cleavage of GLP1 by DPPIV, since almost all the substrate was cleaved after 15 minutes. With 2-4 µM TAT protein the inhibitory effect was not remarkably different from that determined with 1 µM TAT (result not shown).

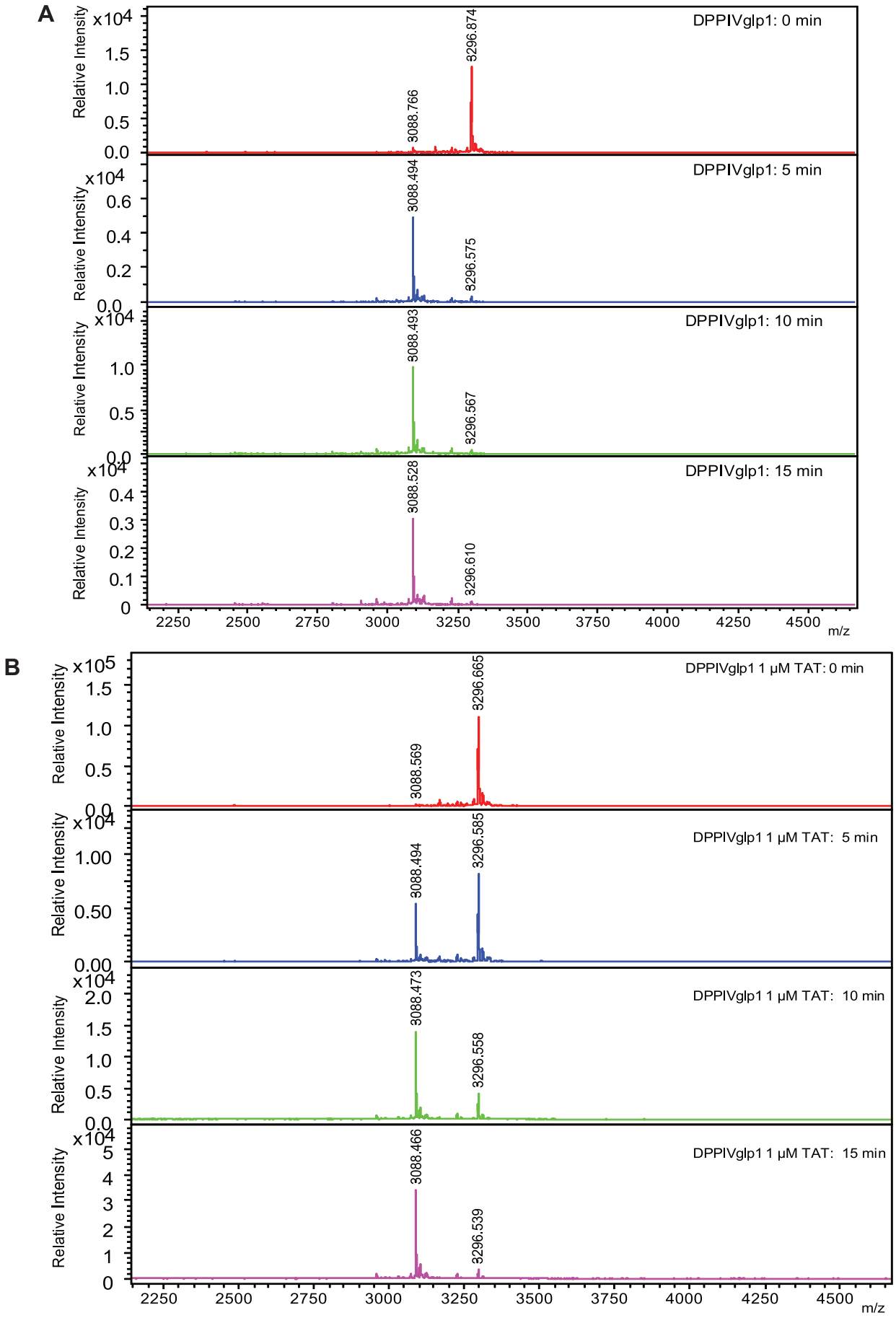

Figure 3.15: Mass spectra of GLP1 during cleavage by DPPIV

(A) DPPIV cleavage of GLP1 in the absence of TAT. 16 nM DPPIV was incubated with 31.25 µM GLP1 for 15 minutes at 37°C in 100 µl assay buffer pH 8.0, containing 37 mM salt. 5 µl aliquots were removed every 5 min and mixed with 0.5 µl 1% TFA to stop the reaction then used to determine the mass spectra of GLP1 by MALDI-TOF MS. **(B) DPPIV cleavage of GLP1 in the presence of 1 µM TAT.** DPPIV assays were conducted under same conditions with 1 µM purified TAT added in each test.

3.4.2.3.1 Recombinant *Sf9*-TAT, TAT10xHis and His-TAT-His retard cleavage of GLP1 by human-DPPIV

The untagged *Sf9*-TAT protein purified from *Sf9* insect cells and the TAT10xHis and His-TAT-His protein from *E. coli* significantly retarded the cleavage of GLP1 by DPPIV. At time 5 min and 10 min there was still uncleaved GLP1 in the reaction mixtures. With reference to the control experiments reported above, 16 nM purified DPPIV can cleave 31.25 µM GLP1 within 5 minutes. Addition of 1 µM *Sf9*-TAT resulted to about 40% of uncleaved GLP1 (mass 3296) after 5 min and about 10% after 10 min (**Figure 3.16**A). The TAT10xHis as well led to the accumulation of about 35% of uncleaved GLP1 in the reaction mixture after 5 min (**Figure 3.16**B).

With reference to reports that the amino-terminal X-X-Pro sequence of TAT is responsible for the inhibition of DPPIV enzyme activity, the GST-TAT-His, GST-TAT and His-TAT-His proteins with N-terminal GST or His-tag are not supposed to inhibit DPPIV enzyme activity. However, the His-TAT-His protein showed an inhibition effect on DPPIV activity (**Figure 3.16**C). During purification a relatively high level of degradation of the His-TAT-His protein was noticed (See **Figure 3.4**). Analysing an aliquot of the His-TAT-His sample by MALDI-TOF MS also revealed a spectrum of a 6.6 kDa protein fragment (result not shown), which might be responsible for the inhibitory effect seen in this sample. The GST-TAT-His and GST-TAT did not show significant retardation of the cleavage of GLP1 by DPPIV.

A **+ 1 µM Sf9-TAT**

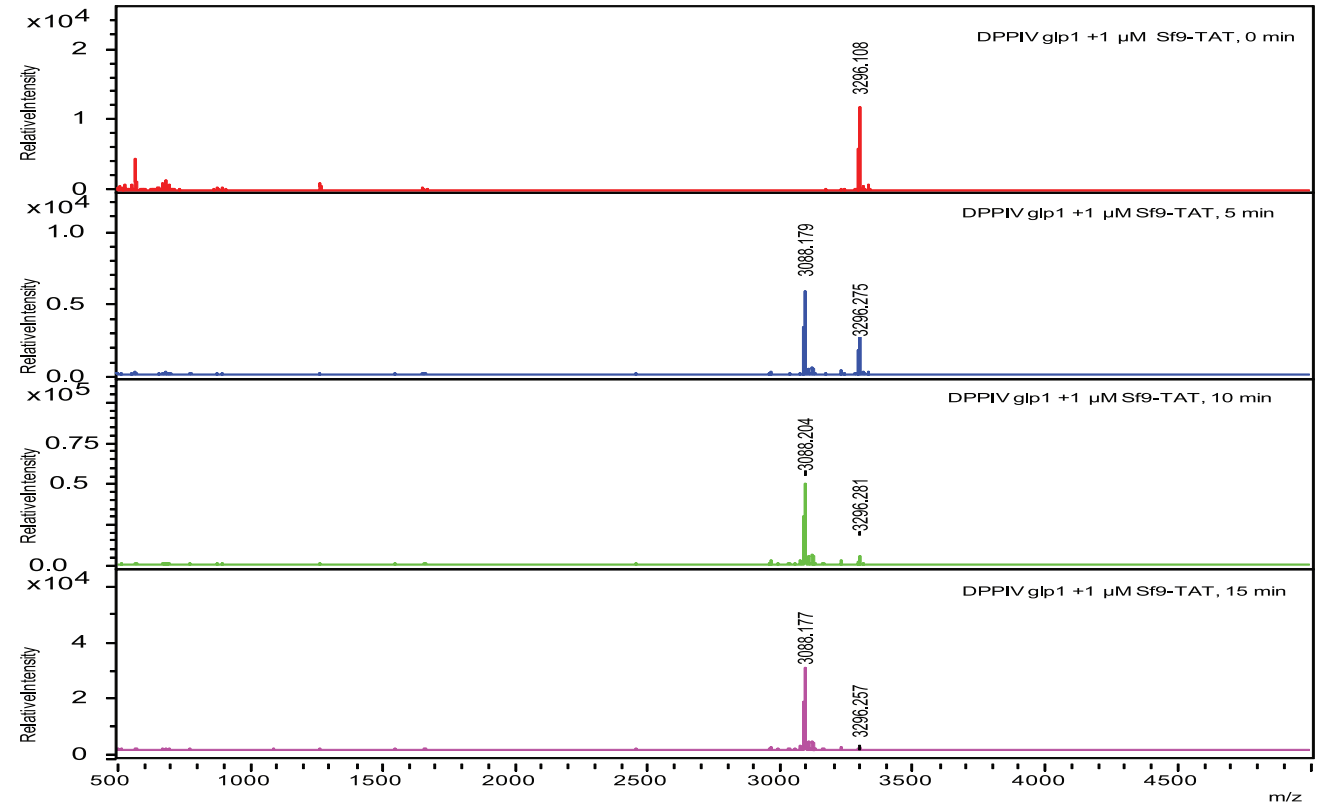

B **+ 1 µM TAT10xHis (*E. coli*)**

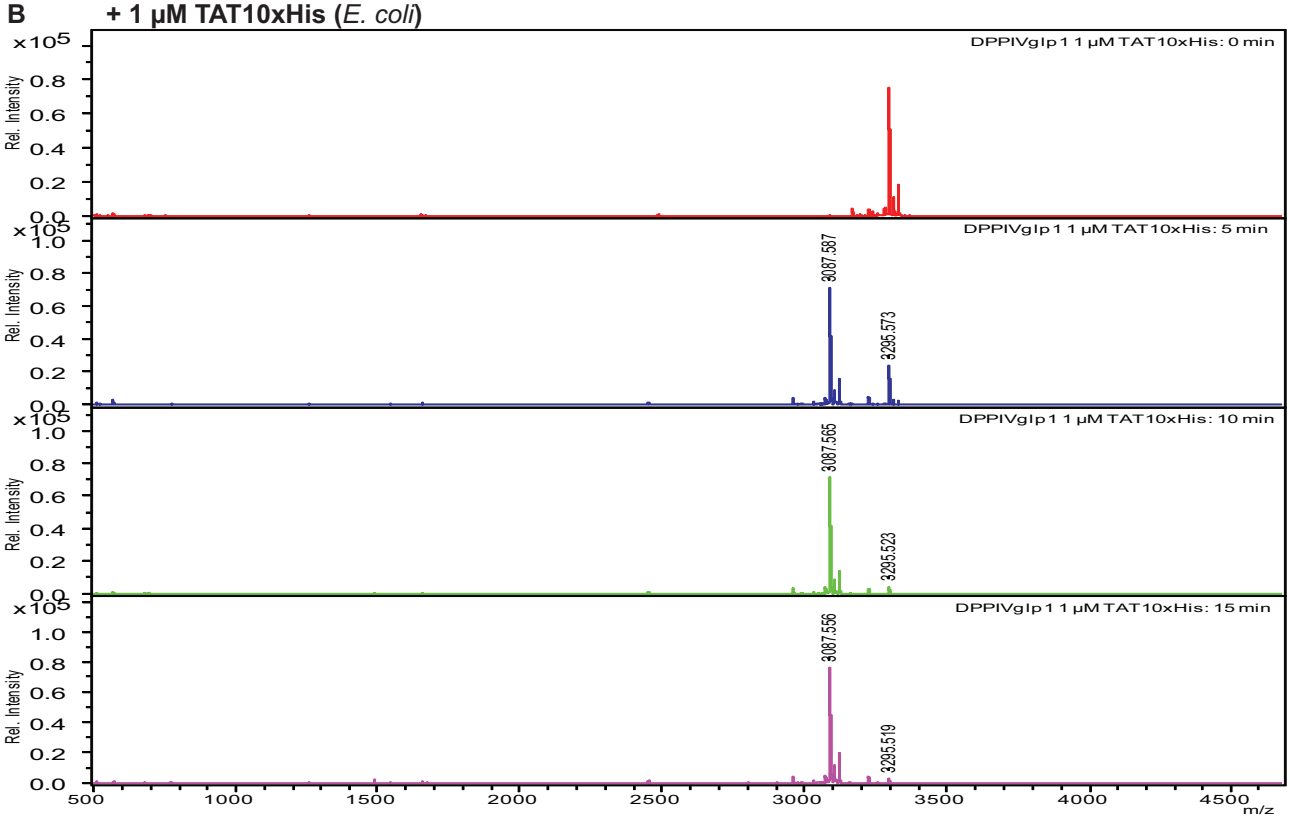

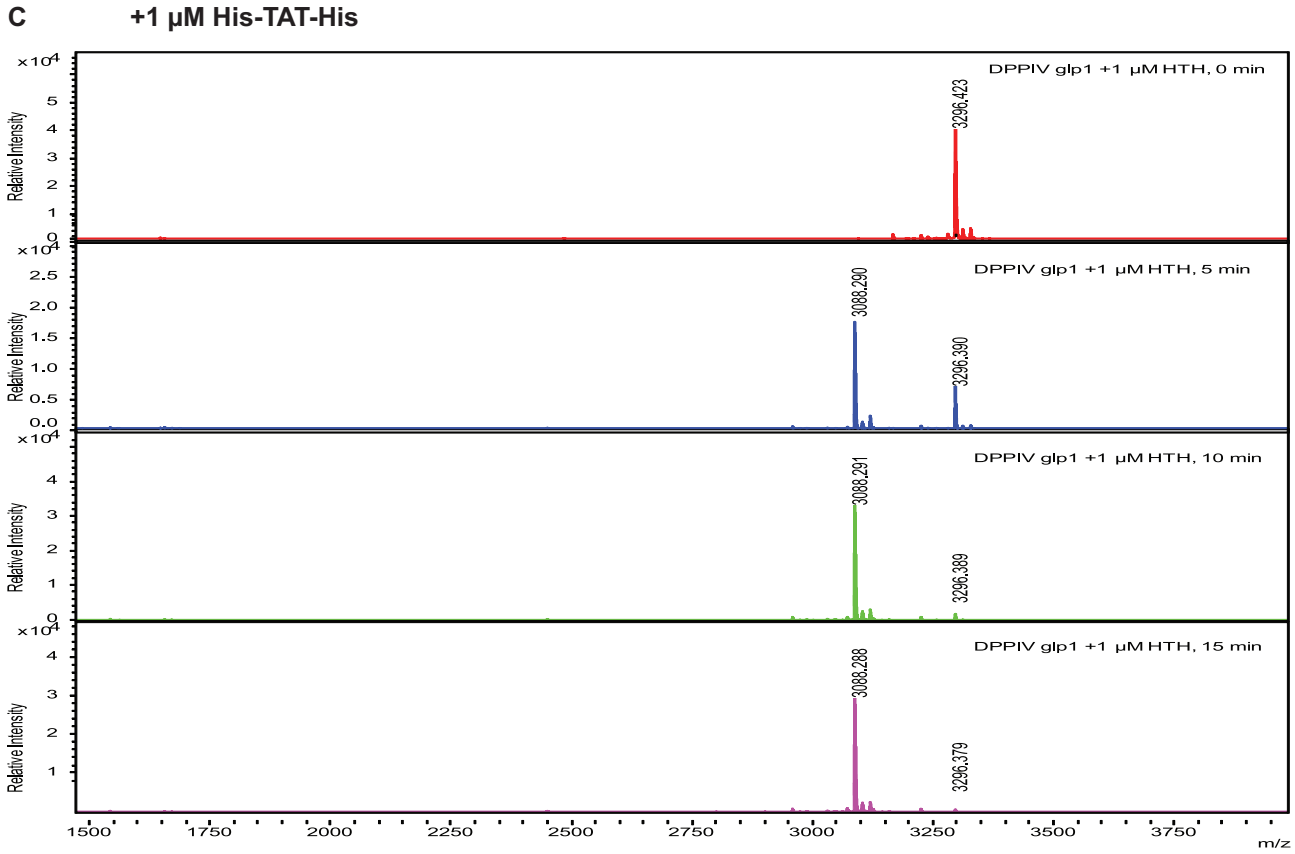

Figure 3.16: Effect of purified TAT fusion protein on the degradation of GLP1 by human-DPPIV

(A) DPPIV cleavage of GLP1 in the presence of 1 µM *Sf9*-TAT protein. **(B)** DPPIV cleavage of GLP1 in the presence of 1 µM TAT10xHis protein. **(C)** DPPIV cleavage of GLP1 in the presence of 1 µM His-TAT-His protein.

Table 3.3: Overview of the effect of TAT protein on the cleavage of GLP1 by human-DPPIV

Inhibitor	**Relative inhibition (% of uncleaved GLP1)**			
	5 min	**10 min**	**15 min**	**20 min**
TAT (Immuno-Diagnostics)	60	30	5	0
***Sf9*-TAT**	40	5	0	0
TAT10xHis	30	5	0	0
His-TAT-His	35	5	0	0
GST-TAT-His	≤ 5%	0	0	0

3.4.3 The HIV1-TAT reveal properties typical of intrinsically unstructured proteins

3.4.3.1 Gel-filtration spectra reveal an intrinsically unstructured nature of TAT protein

The recombinant TAT protein generated in this work revealed the tendency to elute from gel-filtration (SE-FPLC on a Superdex 200 column) at retention volumes corresponding to molecular weights which were many hundred folds higher than the actual molecular weights of the monomeric protein. This observation was unique, irrespective of whether the recombinant TAT was expressed

with a fusion tag or not. The actual molecular weights of the recombinant TAT protein ranged between 10 and 37 kDa depending on the fusion tag used. The eluted from the Superdex 200 column at retention volumes corresponding to molecular masses higher than 670 kDa reflects a characteristic of intrinsically unstructured proteins. An overview of the characteristic elution profiles of the GST-TAT-His (*E. coli*), TAT (*E. coli*), TATV5His (*Sf9*) and GST (*E. coli*) is presented in **Figure 3.17**A-D. GST protein and other His-tagged proteins do not give elution profiles of such high molecular masses in gel-filtration analyses (**Figure 3.17**C).

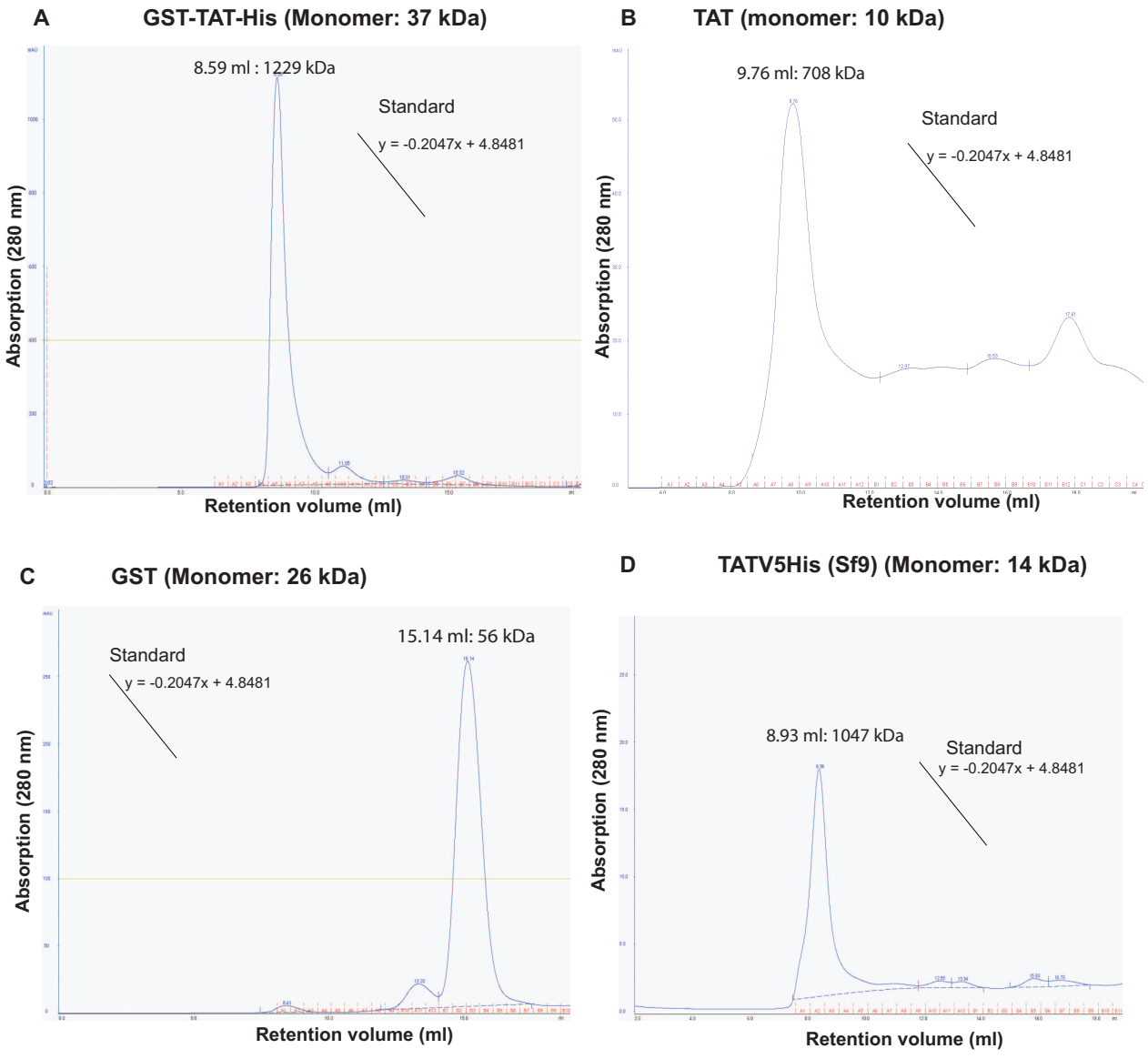

Figure 3.17: Elution profiles of recombinant TAT protein analysed by SE-FPLC

GST-TAT-His, TAT, GST and TATV5His were purified by SE-FPLC on a Superdex 200 column. The spectra for TAT and TATV5His are extracts from Figure 3.5 and Figure 3.10 respectively.

3.4.3.2 Electron micrographs of recombinant TAT reveal a mixture of oligomeric structures

To further substantiate the oligomeric states of the purified TAT protein, the homogeneity of the purified GST-TAT-His, GST and TAT10xHis was verified by electron microscopy via negative staining. GST-TAT-His was the most stable of the constructs purified and also revealed the highest transactivation of the HIV LTR-promoter. It was also the largest (37 kDa) of the recombinant TAT proteins purified in this work and therefore more suitable for analysis by electron microscopy.

The electron micrographs of the analysed GST-TAT-His and TAT10xHis protein revealed a mixture of oligomeric states. However, the investigation of TAT10xHis was only performed once with protein purified and stored for 1 week at -80°C before analysis and the results are therefore not presented here.

The electron micrograph of GST protein revealed uniform dots of the native protein and a few aggregates (**Figure 3.18**A). Opposed to this, the electron micrographs of GST-TAT-His revealed a mixture of single protein particles, large protein-aggregates and protein-clusters (**Figure 3.18**B). In samples lyophilized and stored, then resolved in water with or without 0.05% of the detergent n-octyl-β-D-glucopyranoside, the dots were similar to those observed with the freshly purified fusion protein (**Figure 3.18**C and D). In the freshly purified protein sample, “protein clusters” were more significant and almost disappeared completely after the protein was lyophilized and stored before resolving in water for analysis. The overall observation was the existence of a mixture of very large aggregates, protein clusters and other smaller oligomeric states. These forms portray a characteristic of natively unstructured proteins which likely interchange constantly and probably remain together by weak forces during gel-filtration, resulting in elution spectra of proteins with the large molecular masses observed with TAT protein.

A: GST (26 kDa) a few minutes after SE-FPLC

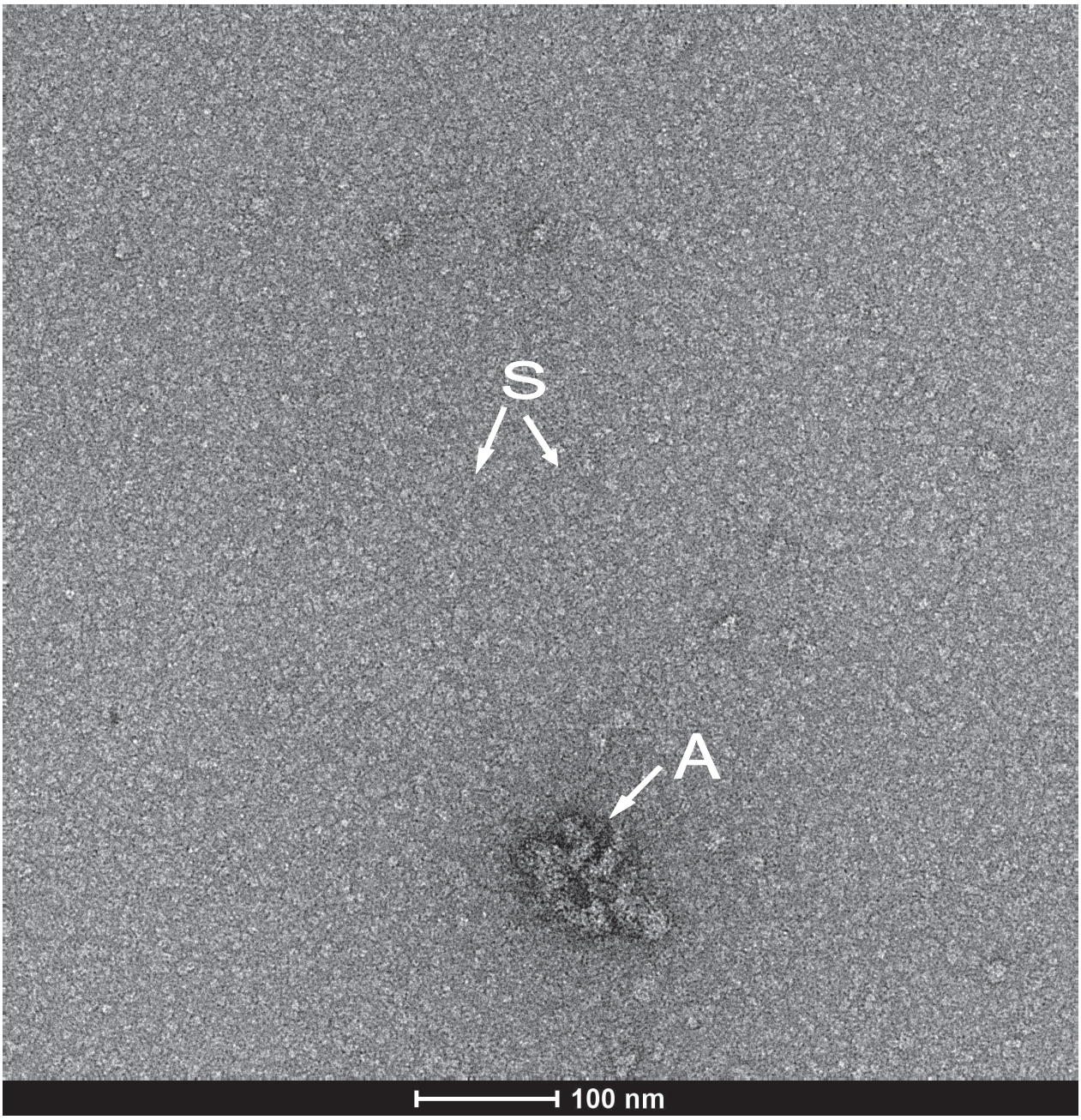

B: GST-TAT-His (37 kDa) a few minutes after SE-FPLC

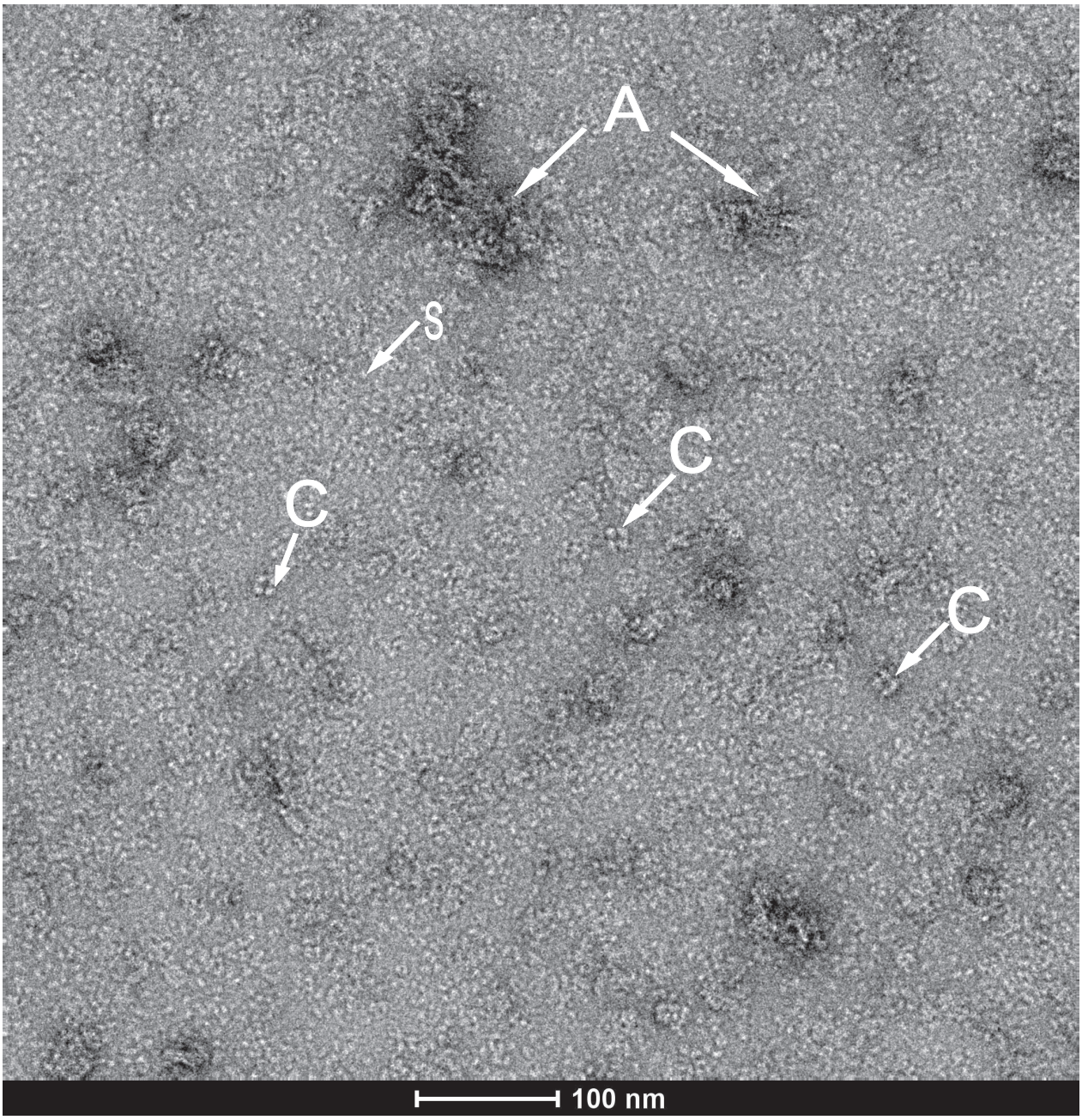

C: GST-TAT-His (37 kDa) lyophilized after SE-FPLC then resolved in water

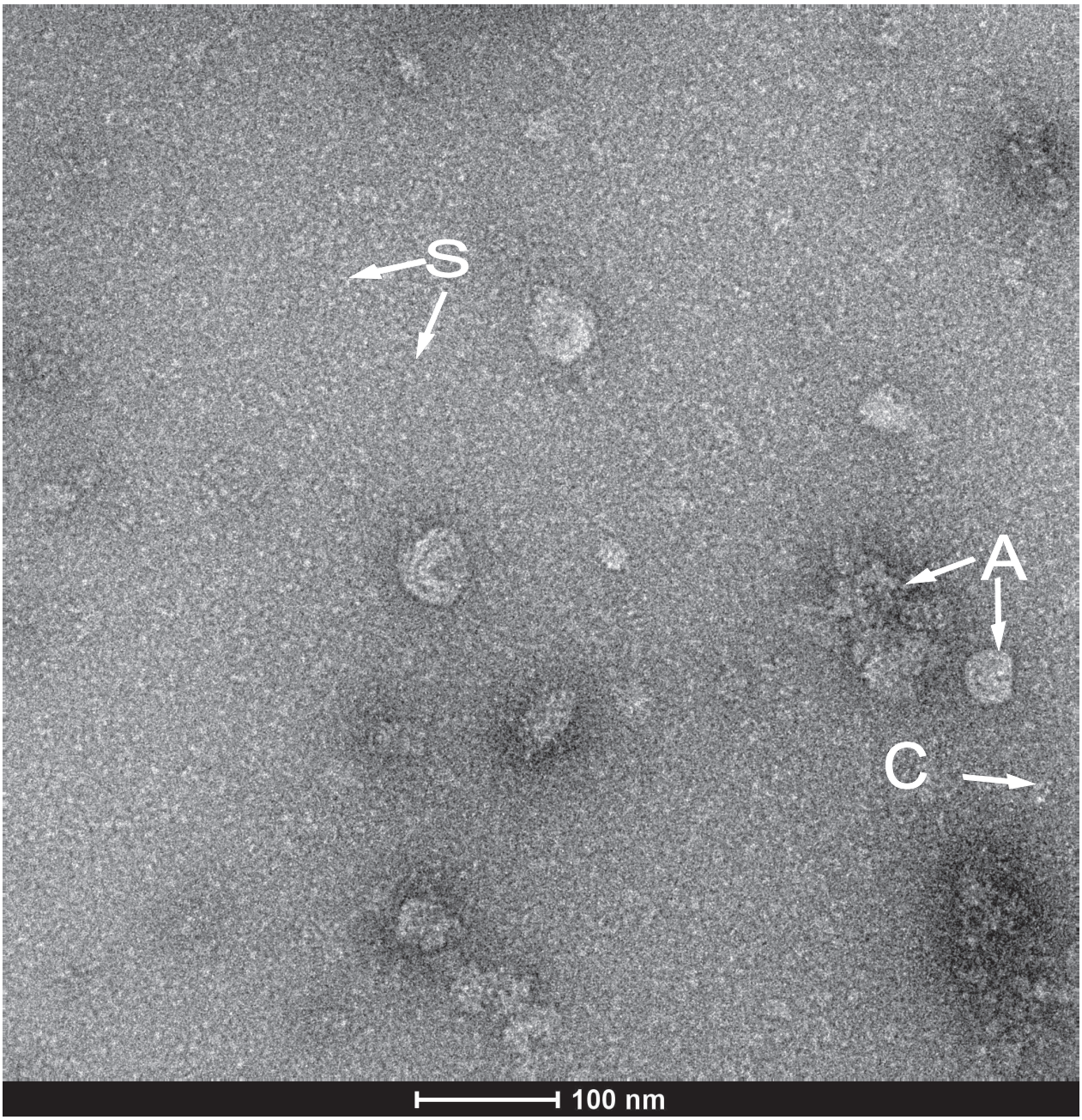

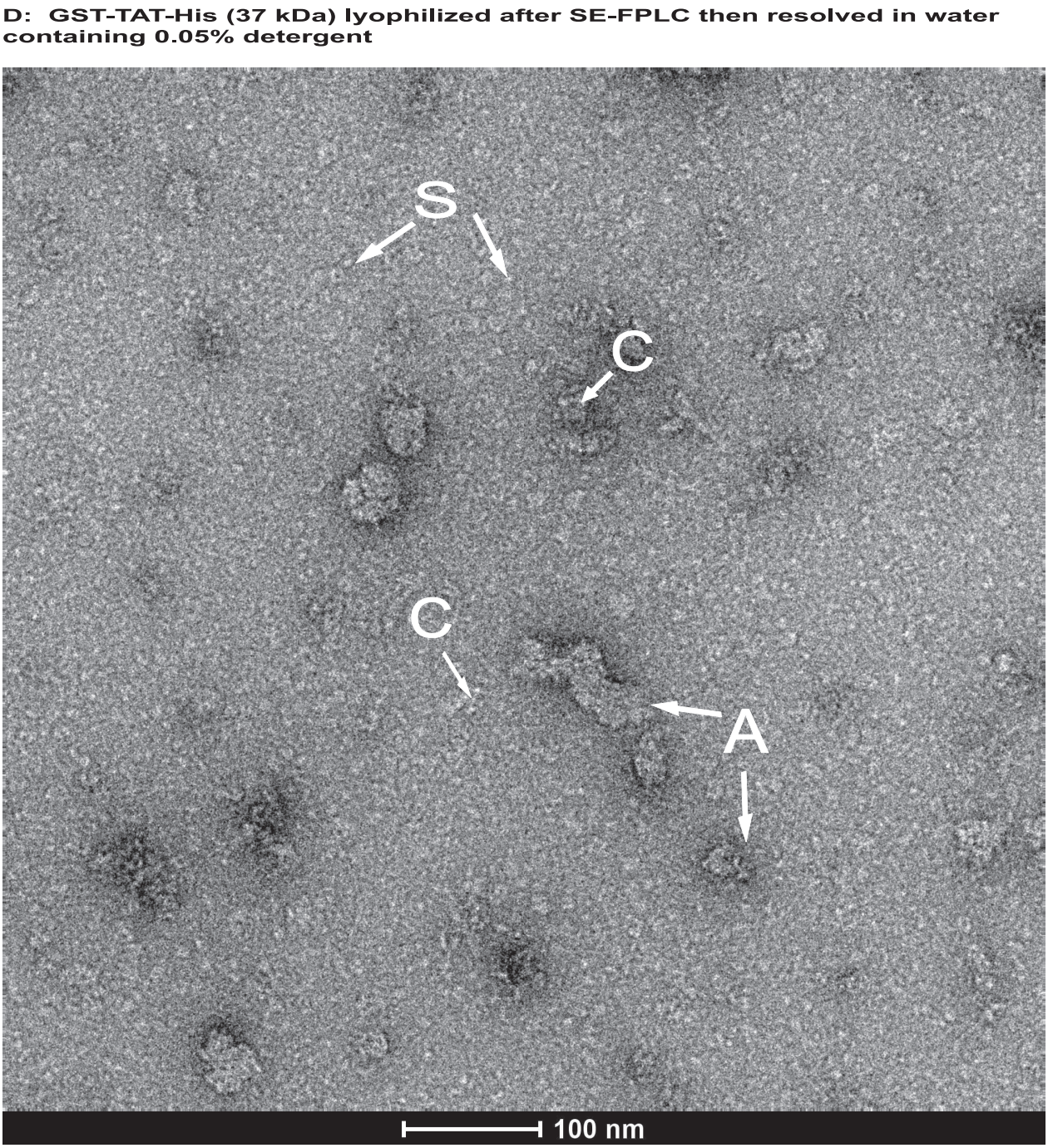

Figure 3.18: Electron micrographs of purified recombinant GST and GST-TAT-His protein

GST-TAT-His and GST proteins were prepared by negative staining and their electron micrographs documented. **(A)** GST analysed about 90 min after SE-FPLC. **(B)** GST-TAT-His analysed about 30 min after SE-FPLC. **(C)** GST-TAT-His lyophilized after SE-FPLC and stored at -80°C for 2 weeks then resolved in ddH_2O prior to negative staining. **(D)** GST-TAT-His lyophilized after SE-FPLC and stored at -80°C for 2 weeks then resolved in ddH_2O containing 0.05 % n-octyl-β-D-glucopyranoside prior to negative staining. **Arrows indicate the following**- S: single protein particles /units seen as white dots, A: large, non-uniform units of aggregates and C: uniform clusters of protein.

Summary II: characterization of purified recombinant TAT protein

The expression levels of HIV1-TAT fusion protein varied in all cell systems used. The purification methods also played a role in the yield and purity of the fusion proteins. All the protein constructs were able to transactivate the HIV LTR-promoter and induce the expression of CAT. However, only the TAT1-86 (Immuno-Diagnostics), GST-TAT-His, GST-TAT and *Sf9*-TAT could influence the localization of stably expressed CXCR4 in the human cell line Hek293. Tests with the stable CHO-CXCR4GFP cell line revealed vesicular accumulation of CXCR4GFP only when treated with the TAT (Immuno-Diagnostics) and *Sf9*-TAT. Furthermore, binding of immobilized TAT protein to DPPIV in pull-down and immunoprecipitation tests were not detected. Also, binding of the purified TAT fusion proteins to DPPIV protein immobilized on the surface of CM5 or C1 sensor chips could not be detected by SPR on a Biacore 2000 machine. Despite their inability to bind DPPIV, the purified TAT (*E. coli*), *Sf9*-TAT, TAT10xHis and His-TAT-His could retard the cleavage of GLP1 by DPPIV. GST-TAT-His and GST-TAT had no effect on DPPIV enzyme activity.

The recombinant TAT proteins revealed elution profiles characteristic of intrinsically unstructured proteins in gel filtration. Although the spectra obtained from gel filtration were quite unique, this uniformity was not reflected in the homogeneity of the oligomeric structures. In effect, the electron micrographs of GST-TAT-His and the TAT10xHis revealed a mixture of different oligomeric states which implies their existence as intrinsically unstructured proteins. Repeated attempts to crystallize the TAT10xHis fusion protein at concentrations 5-7 mg/ml under different buffer conditions did not yield crystals.

Table 3.4: Characterization of purified recombinant TAT protein

Cell system	Construct	Transactivation activity (LTR-CAT)	Influence on CXCR4	Binding to DPPIV (IP /Pull down)	Binding to DPPIV (SPR)	Inhibition of the activity of DPPIV
E. coli	GST-TAT	++	+	no	no	not tested
	GST-TAT-His	+++	+	no	no	no
	His-TAT-His	+	very low	no	no	+
	TAT10xHis	++	very low	no	no	+
	TAT	++	very low	no	no	++
Sf9 Insect	TAT	+	+	**++ (Co-IP)***	no	+
	TATV5His	+	+	no detection	no	not tested
CHO	TATGFP	+	+	no	not tested	not tested

***** Detection upon co-expression of TAT and DPPIV. A detailed result of the co-immunoprecipitation of *Sf9*-TAT with DPPIV is reported under part II of the results section.

4 Results II: Interaction of TAT and DPPIV in CHO and *Sf9* cells

4.1 Co-expression of TAT and DPPIV in CHO cells leads to DNA-fragmentation

Transfection of human-DPPIV or HIV1-TAT in the CHO cell line separately, resulted in the successful selection of stable clones. These clones grew normally in selection media and were still viable and could express the respective proteins after storage in liquid nitrogen for over two years. In images got from confocal laser scanning microscopy, the expressed human-DPPIV protein is seen predominantly on the cell membrane (**Figure 4.1**A), whereas the HIV1-TAT with a C-terminal GFP-tag is localized in the nucleus (**Figure 4.1**B). Although stable transfection of human-DPPIV and HIV1-TAT proteins separately in CHO cells were successful, it was not possible to doubly express them in CHO cells stably. An attempt to transfect stable CHO-DPPIV clones with the TAT-pEGFPN1 plasmid (for production of TATGFP) led to a rapid death of the cells, such that no stable CHO-DPPIV/TATGFP double transfectants could be selected. Transiently transfecting the stable CHO-DPPIV cell lines with the TAT-pEGFP-N1 plasmid or the pEGFP-N1 control vector (for GFP protein) revealed DNA-fragmentation in the CHO-DPPIV/TATGFP transient transfectants but not in the CHO-DPPIV/GFP transfectants. DNA-fragmentation occurred rapidly, and could be detected 48 h after transfection of stable CHO-DPPIV cells with the TAT-pEGFP-N1 plasmid (**Figure 4.1**C). Only a portion of the CHO-DPPIV cells expressed the GFP or TATGFP proteins. Despite this, DNA-fragmentation and cell death was not restricted to cells expressing both DPPIV and TATGFP, but rather also occurred in neighbouring cells. This was induced by a direct cell-cell contact of CHO-DPPIV cells with those expressing both DPPIV and TATGFP. In some cases only the contact of the long neurite-outgrowths formed by the CHO-DPPIV/TATGFP double transfectants with the CHO-DPPIV stable clones caused DNA-fragmentation (**Figure 4.1**C, white arrows). In CHO-DPPIV cells transiently transfected with the pEGFPN1 vector which enables the expression of GFP protein, DNA-fragmentation was not detected (**Figure 4.1**D). This implies that TAT protein is responsible for the induction of DNA-fragmentation seen in CHO-DPPIV/TATGFP transfectants. The fact that TAT does not cause DNA-fragmentation in CHO in the absence of DPPIV (**Figure 4.1**B) suggests that the underlying effect of TAT protein on CHO cells is dependent on DPPIV.

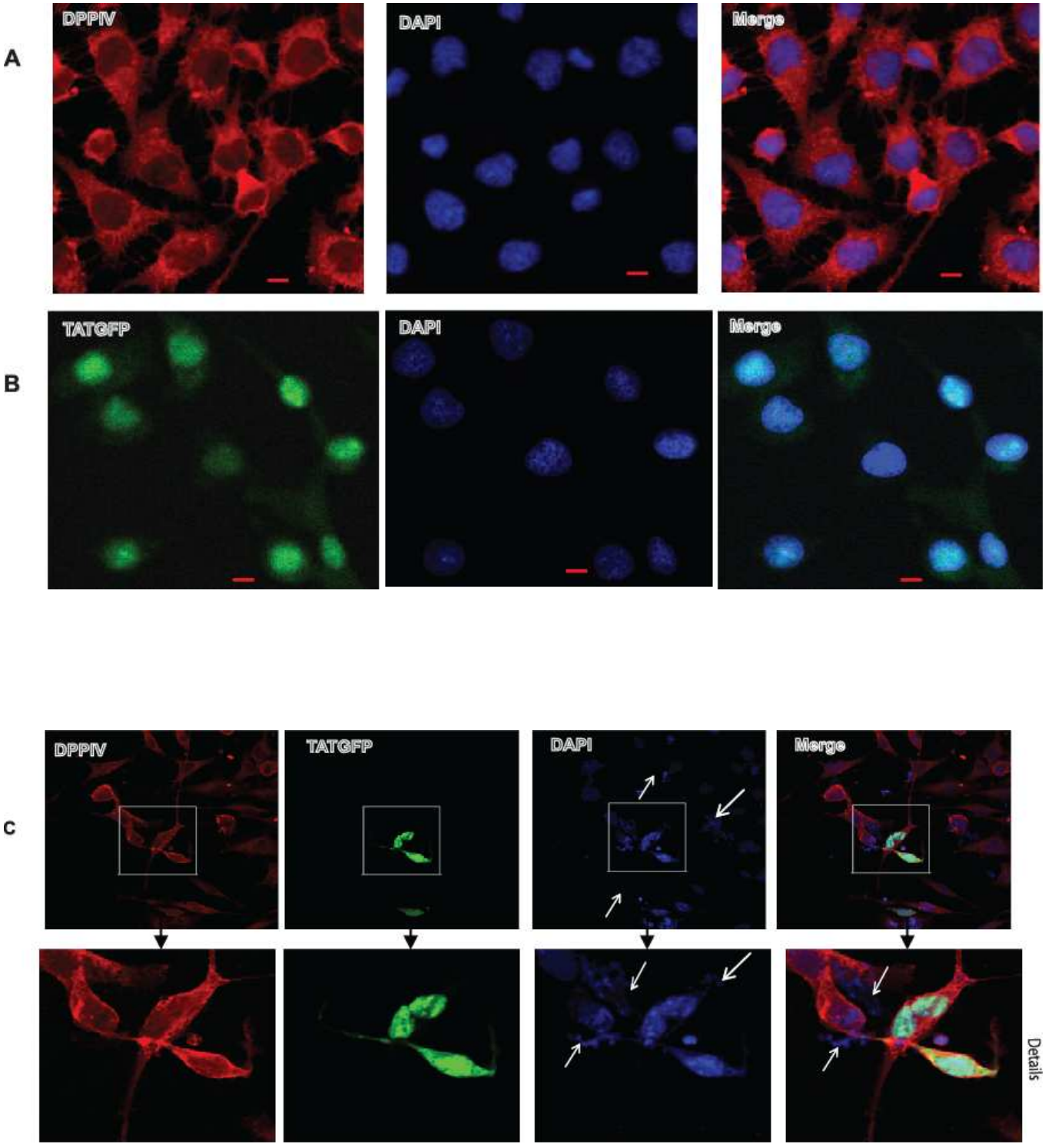
A
DPPIV
DAPI
Merge
B
TATGFP
DAPI
Merge
C
DPPIV
TATGFP
DAPI
Merge
Details

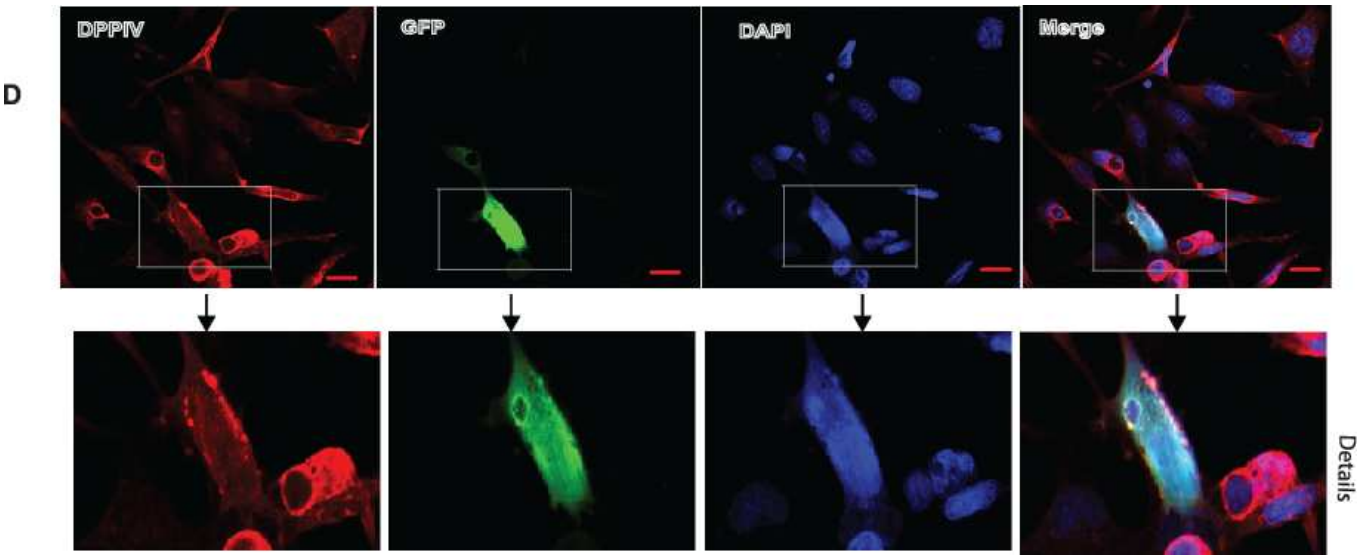

Figure 4.1: Analysis of DPPIV and TATGFP co-expression in CHO cells

(A) Stably transfected CHO-DPPIV cells were stained with a combination of anti-DPPIV pAb/Cy3-conjugated anti-rabbit IgG and DAPI then imaged by confocal laser scanning at a 40 fold magnification. **(B)** Stable CHO-TATGFP cells stained with DAPI and imaged at a 40 fold magnification. **(C)** The stable CHO-DPPIV cells were transiently transfected with the TAT-pEGFP-N1 plasmid and cultured for 48 h then stained with a combination of anti-DPPIV pAb/Cy3-conjugated anti-rabbit IgG and DAPI. Images were made at a 40 fold magnification and an extract of the cells at a 63-fold magnification (Details). White arrows point at DNA fragments. **(D)** The stable CHO-DPPIV cells were transiently transfected with the pEGFP-N1 vector and cultured for 48 h then stained and imaged similar to "C" (scale bar = 10 nm).

4.2 Co-expression of TAT and DPPIV in CHO cells leads to membrane inversion

To confirm whether the DNA-fragmentation and cell death observed in stable CHO-DPPIV cell lines following transient transfection with the TAT-pEGFP-N1 plasmid was due to apoptosis, the early events of apoptosis were further investigated. Under normal physiologic conditions the cell membrane component phosphatidylserine, (PS) is located predominantly in the inner, cytosol-facing leaflet of the membrane. During the early stage of apoptosis, PS loses its asymmetric distribution in the phospholipid bilayer and is translocated in part to the extracellular membrane leaflet. PS is a strong binding partner of Annexin-V. Therefore, Annexin-V conjugated with the fluorescent dye Allophycocyanin, (Annexin-V APC, from eBiosciences) was used to stain the cells followed by flow cytometry.

Analysing the cells 24-48 h after transfection revealed a lot of stained DNA, meaning that the integrity of the cell membrane was disrupted (result not shown). This implies that the cells were already in a later stage of apoptosis. Reducing the expression time to 22 h led to the detection of PS on the membrane of a small portion (8.9%) of intact CHO-DPPIV/TATGFP transfectants by

Annexin-V APC (**Figure 4.2**B and C). Opposed to this, the CHO-DPPIV/GFP transfectants revealed only 6% of intact cells with PS on the cell surface (**Figure 4.2**C). Reducing the expression duration to 9 h revealed a more significant portion (15.2%) of intact CHO-DPPIV/TATGFP transfectants with PS on the cell surface implying the onset of apoptosis in these cells (**Figure 4.2**A and C). A larger portion (16.4%) of the CHO-DPPIV/TATGFP transfectants was doubly detected by Annexin-V-APC and propidium iodide, which indicates a disruption of the cell membranes of this cell population (**Figure 4.2A** and C). However, the disruption of the cells in this population is not a result of apoptosis alone, as it can also be due to the transfection reagent used. In the CHO-DPPIV/GFP transfectants only 1.5% of intact cells exposed PS on the outer membrane after 9 h, whereas 30% of the cells could be detected with both Annexin-V-APC and PI which indicates the disruption of the cells in this population (**Figure 4.2**A and C). It is not clear why so many (30%) of the CHO-DPPIV/GFP cells are disrupted. However, it can be ruled out that this resulted from apoptosis, since the appearance of PS on the outer membrane leaflet is not detected in this CHO-DPPIV/GFP cell lines (only 1.5% intact cells detected with Annexin-V-APC). A portion of the CHO-DPPIV stable clones could also be doubly detected with Annexin-V-APC and PI following treatment with the transfection reagent alone (**Figure 4.2**A and B). An overlay of the overall intensity of PS detected with Annexin-V-APC against the total number of cells, revealed significantly higher levels of PS detection in the CHO-DPPIV/TATGFP transfectants compared to CHO-DPPIV and CHO-DPPIV/GFP cells. This significance was reduced after culturing the transfectants for 22 h (**Figure 4.2**A and B, overlay).

In a control CHO cell line stably transfected with a mutant of the alpha-1-anti-trypsin protein (CHO-A1AT), TATGFP did not induce apoptosis (**Figure 4.2**C, statistical values). This implies that the initiation of apoptosis by TAT in CHO-DPPIV cell lines is due to the presence of DPPIV.

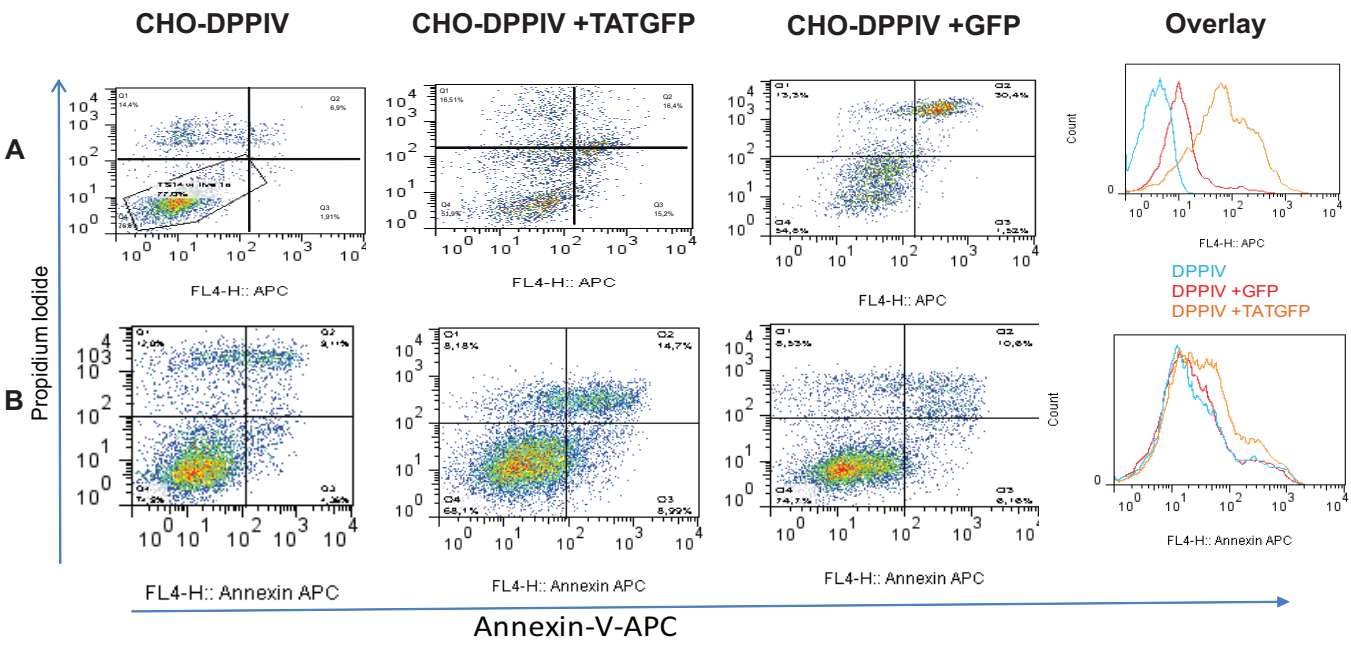

C

Q1	Q2
Q4	Q3

	Statistics	Q4	Q1	Q2	Q3
	Population (% total)	Live: An-/ PI-	Necrotic: An- PI+	Compensated: An+/ PI+	Apoptotic: An+ PI-
A 9h	DPPIV	76,8	14,4	6,9	1,91
	DPPIV +GFP	54,8	13,3	30,4	1,52
	DPPIV +TATGFP	51,9	16,51	16,4	15,2
	A1AT	100	0,025	0	0
	A1AT +TATGFP	52,7	9,05	37,4	0,825
A 22h	DPPIV	74,5	12	9,11	4,36
	DPPIV +GFP	74,7	8,1	10,6	6,16
	DPPIV +TATGFP	68,1	8,18	14,7	8,99
	A1AT	60,2	24,4	11,8	3,68
	A1AT +TATGFP	52,8	27,4	16,4	3,37

Figure 4.2: HIV1-TAT induces apoptosis in a DPPIV-dependent manner

The stable CHO-DPPIV cell line was transfected with TAT-pEGFPN1 plasmid or the pEGFPN1 vector then subsequently cultured for 9 h **(A)** or 22 h **(B)**. The cells were harvested, washed and doubly-stained with Annexin-V-APC and propidium iodide, then analysed immediately by flow cytometry, whereby 15,000 cells were gated in each case. The evaluation of the results was done with the FlowJo software. The difference in the intensity of cells stained with Annexin-V APC can be seen in the overlay of the results. **(C)** The percentage of the various cell populations was statistically determined with the FlowJo software. Apoptotic populations in the CHO-DPPIV cells transfected with the TAT-pEGFPN1 plasmid is highlighted in red. **CHO-A1AT**: CHO cells stably transfected to express alpha-I-antitrypsin protein was a kind gift from Dr. Mathias Kaup of Charite-Mitte.

Summary III: TAT induces apoptosis in CHO-DPPIV cell lines

The HIV1-TAT protein induced apoptosis in CHO cells in a DPPIV-dependent manner. This was revealed in the appearance of PS on the cell membrane of intact cells, 9 h after transfection of CHO-DPPIV cells with the TAT-pEGFP-N1 plasmid. The late stage of apoptosis was characterized by a high level of DNA-fragmentation which could be imaged by confocal laser scanning microscopy, 48 h after transfection of cells. The dependency of the apoptotic effect of TAT on

DPPIV was evident in the observation that TAT could be stably expressed successfully in CHO cell lines and also did not induce membrane inversion or DNA fragmentation in the stable CHO-A1AT cell line expressing a mutant of the alpha-1-anti-trypsin protein which was used as a control.
Due to the aggressive effect of HIV1-TAT protein on DPPIV-expressing mammalian cell lines, it was not possible to study the interaction of the HIV1-TAT with human-DPPIV in these cells.

4.3 Interaction of HIV1-TAT and human-DPPIV in *Sf9* cells

4.3.1 The level of human-DPPIV is increased upon co-expression with HIV1-TAT

To confirm whether HIV1-TAT protein has an effect on the enzymatic activity of human-DPPIV and whether the bulk expression of human-DPPIV is influenced by HIV1-TAT, TAT and DPPIV proteins were expressed separately or together in *Sf9* cells then analysed for the presence of DPPIV enzymatic activity and relative protein content. Photometric determination of the cleavage of 100 nM of the chromogenic substrate H-Gly-Pro-pNA-HCl by DPPIV containing lysates, revealed a higher enzyme activity in the lysates of TAT/DPPIV expressing *Sf9* cells than in the lysates of DPPIV being expressed alone (**Figure 4.3**A). This was intriguing, since HIV1-TAT is a known inhibitor of human-DPPIV. We further substantiated whether this increase in activity was due to an overall increase in the bulk expression of human-DPPIV protein in TAT/DPPIV-co-expressing cells, by additionally determining the protein content of human-DPPIV in the lysates. Aliquots of the cell lysates were subjected to polyacrylamide gel electrophoresis and western blot under non-reducing and non-denaturing conditions. The blots were either probed with anti-DPPIV pAb to determine the relative protein amounts or activity-stained with the synthetic DPPIV substrate, H-Gly-Pro-4-methoxy-β-naphthylamide in combination with Fast Garnet GBC diazonium salt (**Figure 4.3**C). Probing with anti-DPPIV pAb revealed stronger band intensities in TAT/DPPIV co-expression than in DPPIV being expressed alone at the respective expression durations (**Figure 4.3**B). The band intensities of antibody- and activity-stained DPPIV protein were determined with the QuantityOne software. To get the relative DPPIV proteolytic activity of each sample in percentage, the quotient of the band intensity from activity-staining and the corresponding band intensity from western blot was deduced for each sample and multiplied by 100 (**Figure 4.3**D). With respect to the relative activities, it could be seen that the enzymatic activity of DPPIV in each sample correlated to the level of DPPIV protein expressed. Only the TAT/DPPIV sample at 48 h expression duration revealed a lower relative activity compared to DPPIV being expressed alone for 48 h. This revealed that a very high DPPIV expression take place in the cells which compensates the inhibitory effect of TAT protein on DPPIV (**Figure 4.3**B, C and D). However, at 48 h

expression, the level of TAT in the TAT/DPPIV is also relatively high leading to an overall inhibition and lower relative activity at this stage of expression (see **Figure 4.3**D, 48 h).

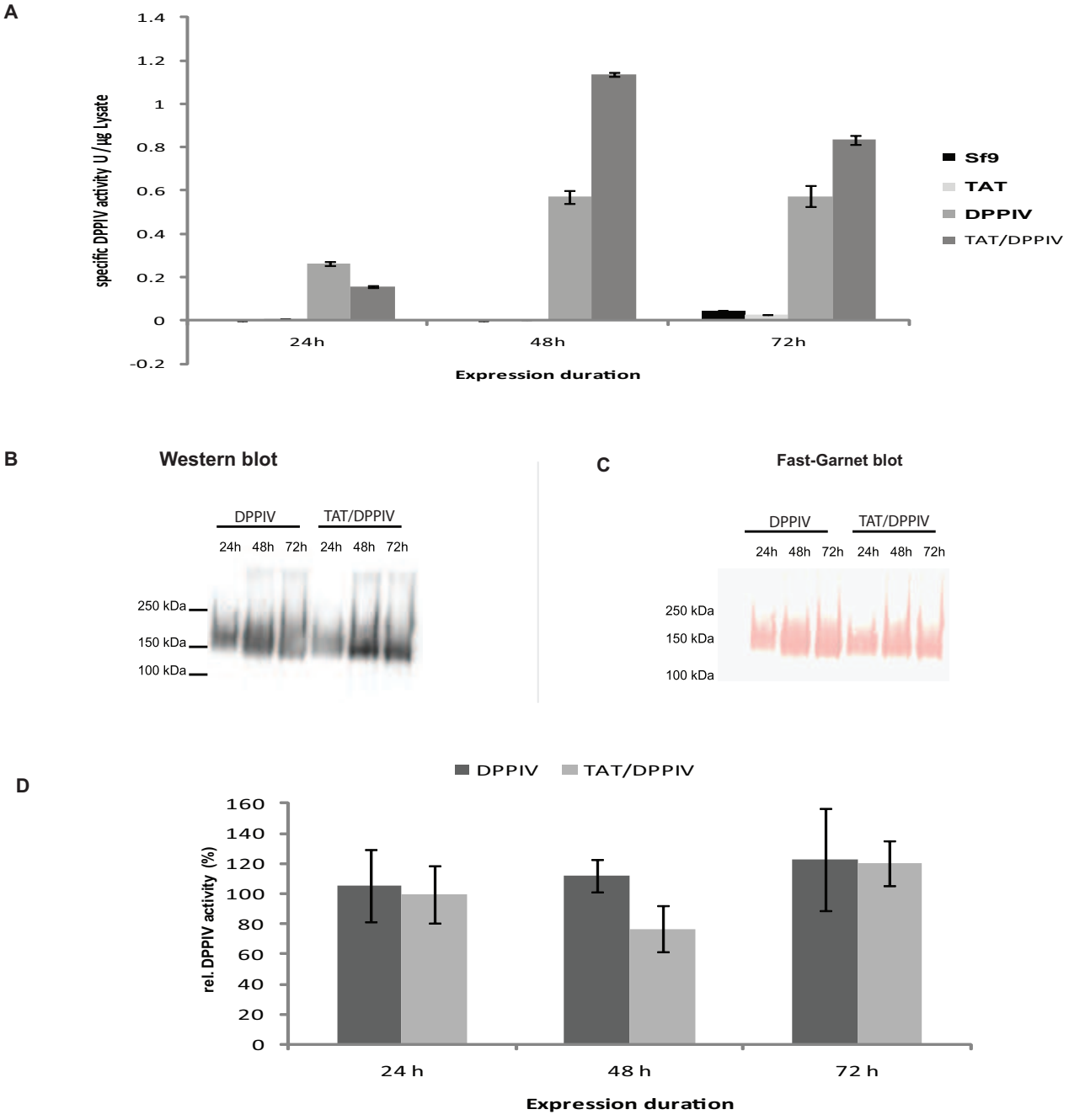

Figure 4.3: Determination of DPPIV enzymatic activity and total DPPIV in cell lysates

(A) Enzymatic activity of DPPIV was determined in cell lysates of indicated samples by photometrically monitoring the hydrolysis of 100 nM H-Gly-Pro-pNA-HCl by DPPIV at pH 8.0 and 410 nm. The specific activity of DPPIV/µg cell lysate was then deduced. Each bar represents specific DPPIV activity in U/µg lysate, derived as a mean of 3 independent experiments ± S.D. **(B)** Cell lysates (10 µg total proteins / sample) were separated under non-reducing and non-denaturing conditions on acrylamide gels and blotted, then subsequently probed with anti-DPPIV pAb. **(C)** Native DPPIV protein (10 µg cell lysates /sample), previously blotted on nitrocellulose membrane, was activity stained using Gly-Pro-4-methoxy-β-

naphthylamide and Fast Garnet GBC diazonium salt. **(D)** The band intensities of activity-stained DPPIV protein were quantified with the QuantityOne software and calibrated against the respective intensities of the antibody-stained DPPIV protein bands in "B". The resulting relative activities of the samples in percentages are presented in the bar diagram (n=3)**.**

4.3.2 Co-expression of TAT and DPPIV alters the cell surface expression of DPPIV in *Sf9* cells

To further verify whether the increased amount of DPPIV expressed in TAT/DPPIV expressing cells was reflected in its distribution on the cell membrane, non-permeabilized cells were stained with either anti-DPPIV pAb or anti-TAT mAb and analysed by FACS. The distribution of TAT on the cell surface was not influenced by its co-expression with human-DPPIV. Only a slight decrease of the level of TAT protein on the cell surface was noticed after 72 h co-expression with DPPIV, compared to TAT being expressed alone (**Figure 4.4**A). Opposed to the TAT protein, a high amount of human-DPPIV was detected on the membrane 24 h after infection of cells. This cell surface expression of DPPIV increased progressively till 72 h post infection (**Figure 4.4**B). Interestingly, 48 h and 72 h post infection, a portion of the cells co-infected with DPPIV and TAT recombinant baculoviruses showed a stronger fluorescence intensity of DPPIV protein than cells infected with DPPIV recombinant baculovirus alone. To verify if the variation in the cell surface distribution of DPPIV in co-infected cells was due to TAT and not the high titre of virus used in such co-infections, a recombinant baculovirus, prepared by transfecting pFastBac1-vector bacmid in *Sf9* cells, was used in co-infections with DPPIV. Assessment of the cell surface expression of DPPIV by FACS revealed no alterations in the level of cell surface DPPIV expressed (**Figure 4.4**C).

We further substantiated whether this increase in cell surface expression of DPPIV in TAT/DPPIV expressing cells correlated with DPPIV enzyme activity. DPPIV cell surface activity assay was implemented, by incubating whole cells with 100 nM of a chromogenic DPPIV substrate for 10 min at 37°C and monitoring its hydrolysis photometrically. In accordance with the mean values from 4 independent experiments, there was a progressive increase in DPPIV activity from 24 h to 72 h. Compared to DPPIV being expressed alone the specific activity of TAT/DPPIV expressing cells was higher at 48 h and 72 h expression. Taken together, the determined DPPIV specific activities correlated well with the cell surface expression of DPPIV assessed by FACS (**Figure 4.4**D).

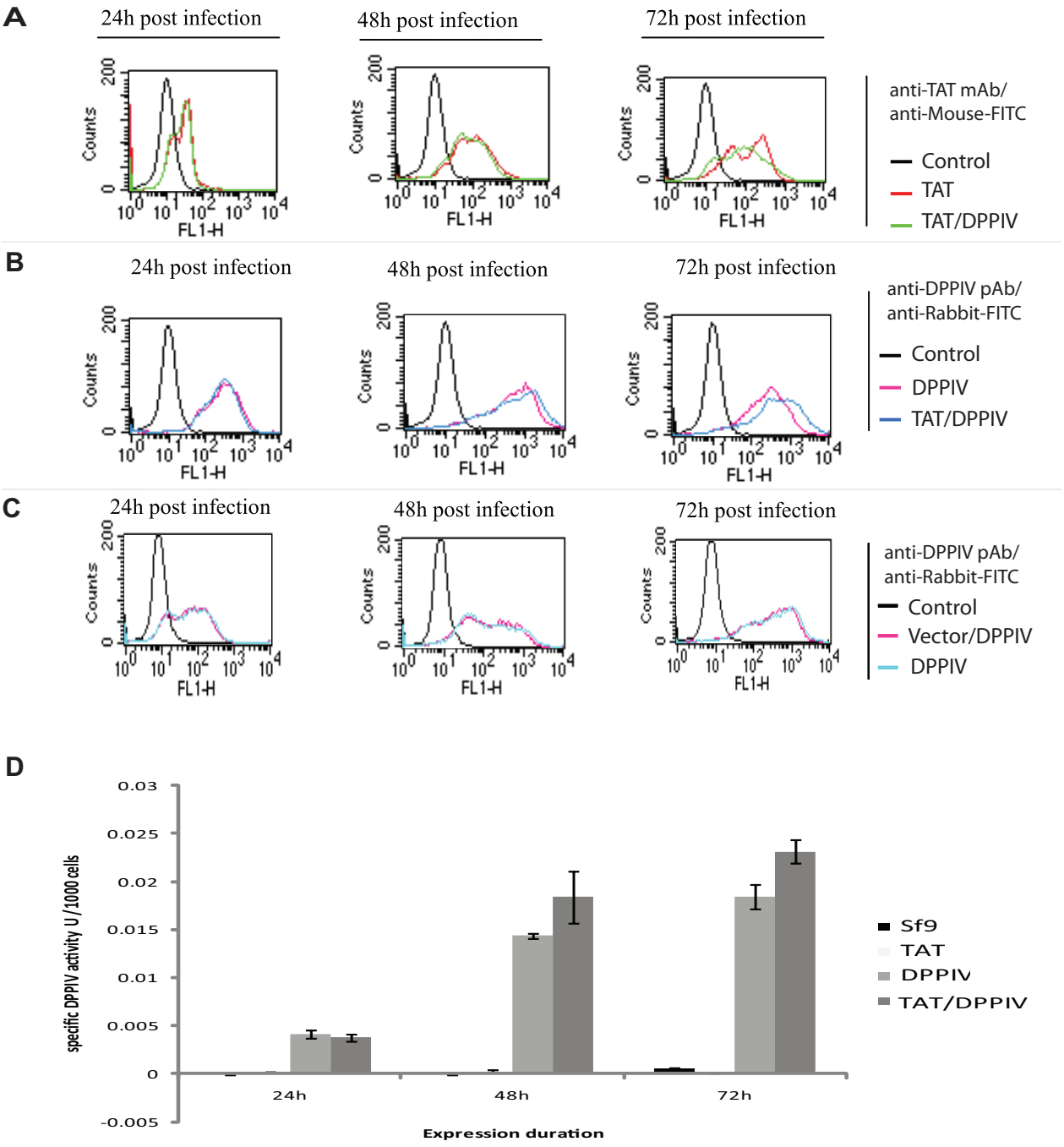

Figure 4.4: Analysis of TAT and DPPIV cell surface expression and DPPIV activity

(A) Cells infected with TAT recombinant baculovirus alone or co-infected with TAT and DPPIV recombinant baculovirus were harvested 24 h, 48 h and 72 h post infection, stained with anti-TAT mAb / FITC-conjugated anti-mouse Ab, then analysed by FACS. Cells infected with the pFastBac1 vector baculovirus alone were stained and used as control. **(B)** Cells infected with DPPIV recombinant baculovirus alone or co-infected with DPPIV- and TAT recombinant baculoviruses were harvested, stained for DPPIV using rabbit anti-DPPIV pAb / FITC-conjugated anti-rabbit antibody and subsequently analysed by FACS. **(C)** Co-infection of *Sf9* cells with DPPIV and the pFastBac1 recombinant virus was conducted and the cells were subsequently stained for DPPIV and analysed like in "B". **(D)** Harvested cells were washed and 1000 cells / sample were incubated with 100 nM H-Gly-Pro-pNA-HCl at pH 8.0 for 10 min then photometrically

monitored at 410 nm. The specific DPPIV activity in U/ 1000 cells were determined from the extinction values (n=4).

4.3.3 HIV1-TAT co-localizes with human-DPPIV in co-infected *Sf9* cells

To verify whether HIV1-TAT associates with human-DPPIV, *Sf9* cells were infected with the TAT or DPPIV recombinant baculoviruses or co-infected with both TAT and DPPIV recombinant baculoviruses. The cells were harvested 48 h or 72 h post infection, permeabilized with 0.3% Triton X100 in PBS and stained with specific antibodies towards the HIV1-TAT and human-DPPIV proteins. Stained cells were imaged by confocal laser scanning microscopy at a 63-fold magnification. Confocal microscopy detected the TAT protein predominantly in the nucleus and to a lesser extent in the cytosol and cell membrane after 48 h expression. Extending the expression duration to 72 h resulted in the translocation of a larger portion of TAT to the cytosol and cell surface (**Figure 4.5**A). This distribution was not altered nor influenced in cells expressing both TAT and DPPIV (**Figure 4.5**C).

As expected, DPPIV protein was located predominantly at the cell membrane after 48 h and 72 h expression (**Figure 4.5**B). In TAT/DPPIV expressing *Sf9* cells doubly stained for TAT and DPPIV, co-association of the proteins could be monitored at the cell surface of merged images as indicated with white arrows (**Figure 4.5**C).

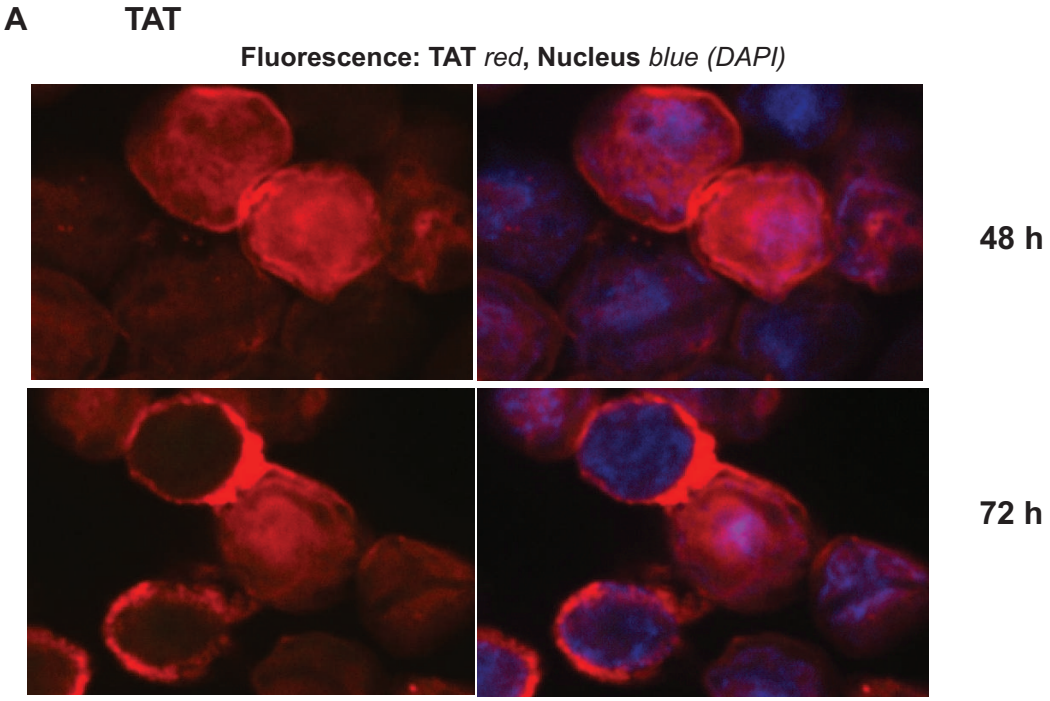

B DPPIV

Fluorescence: DPPIV *green*, **Nucleus** *blue (DAPI)*

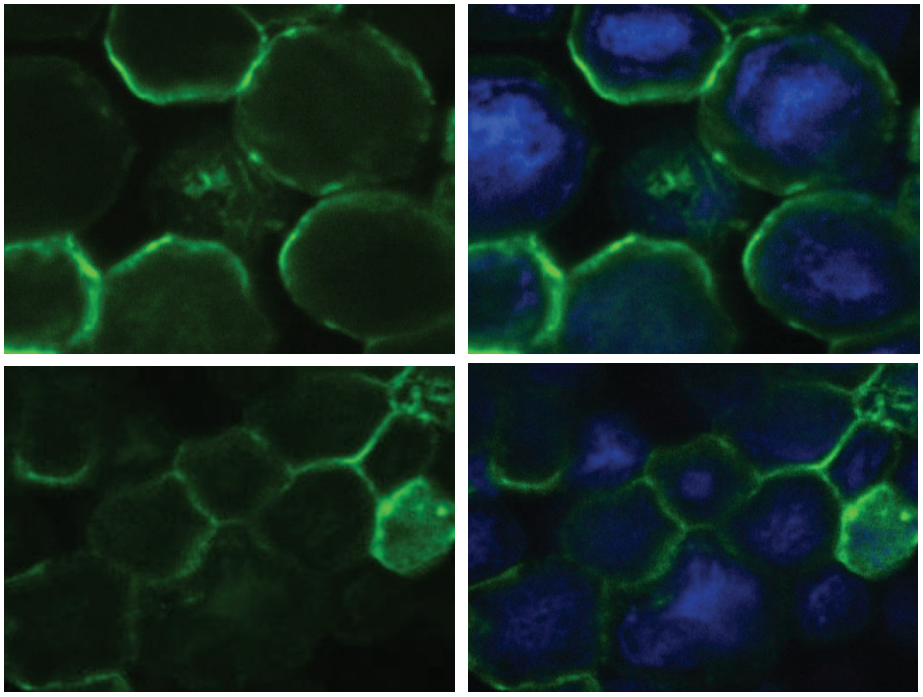

48 h

72 h

C.) Colocalization of TAT and DPPIV

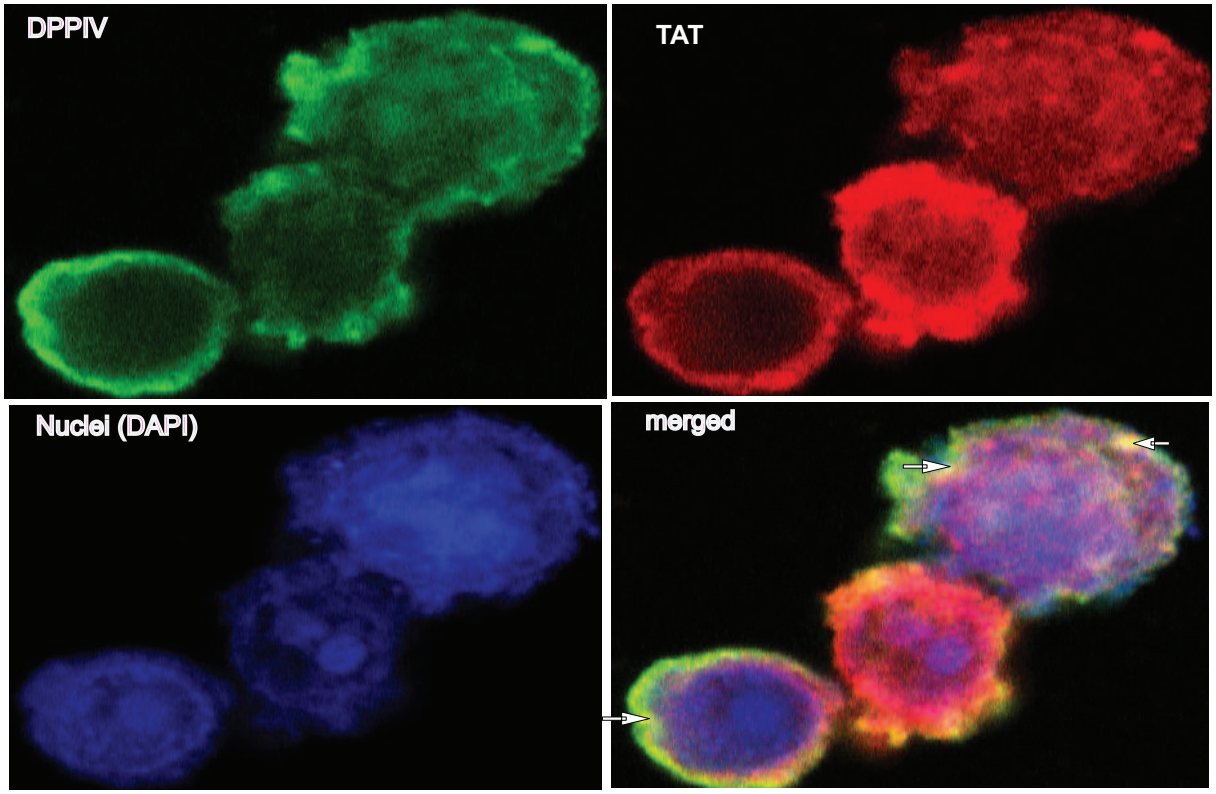

48 h

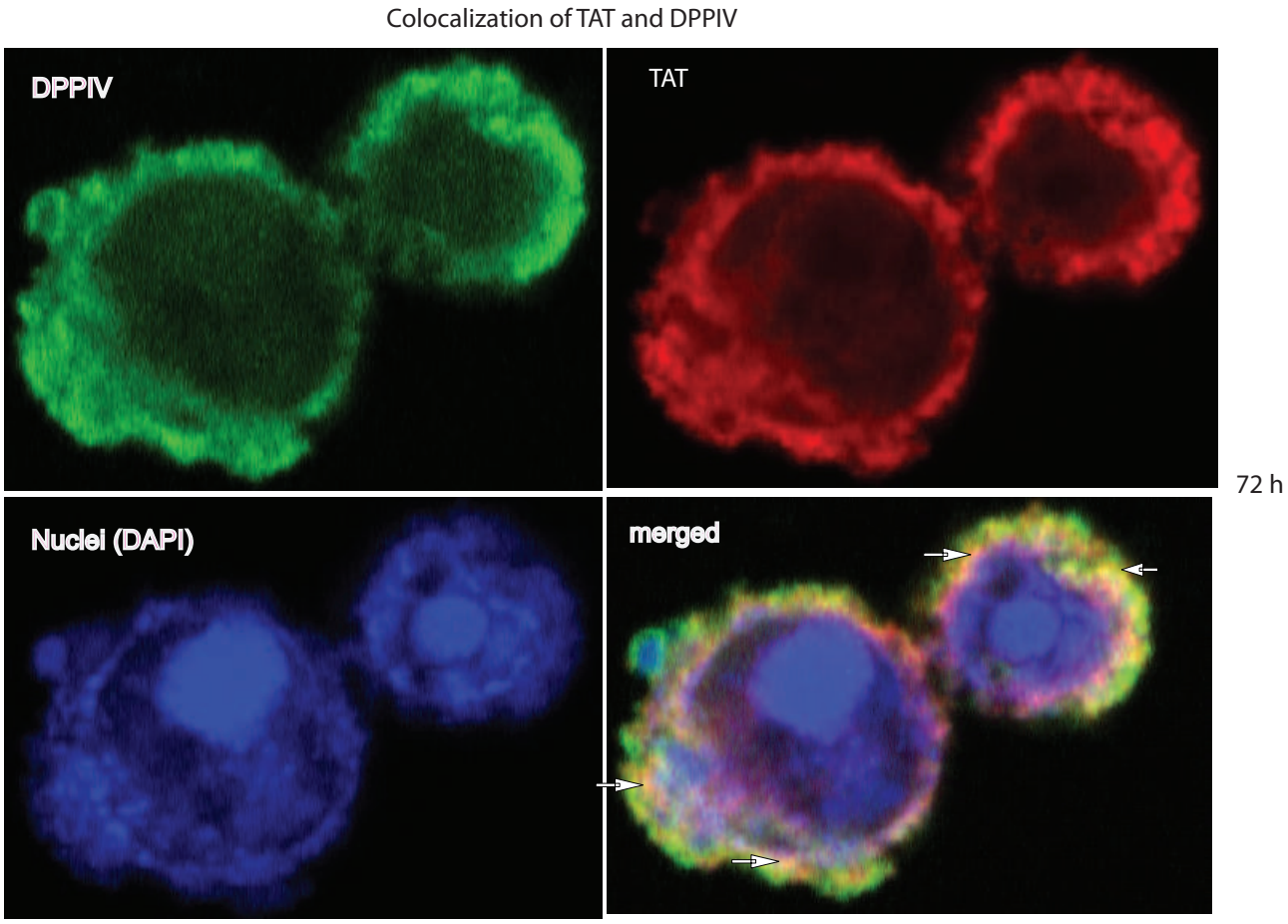

Figure 4.5: Localization of HIV1-TAT and human-DPPIV in *Sf9* cells

Sf9 cells either infected with the TAT or DPPIV recombinant baculoviruses or co-infected with both TAT and DPPIV recombinant baculoviruses were harvested at the indicated time, then fixed on culture slides and double-stained with the antibody combination: anti-TAT mAb / anti-mouse-Cy3 (*red*) and anti-DPPIV pAb / anti-rabbit-FITC (*green*). Nuclei stain was done with DAPI (*blue*). Images were made at a 63- or 100-fold magnification by confocal laser scanning microscopy. **(A)** Single expression of TAT. **(B)** Single expression of DPPIV. **(C)** Co-expression of TAT and DPPIV. Co-association of TAT and DPPIV protein is indicated with white arrows.

4.3.4 Human-DPPIV and HIV1-TAT co-immunoprecipitate from co-infected *Sf9* cells

The association of HIV1-TAT with human-DPPIV was further confirmed by co-immunoprecipitation tests. Implementing antibodies against TAT or DPPIV, both DPPIV and TAT protein could be co-immunoprecipitated from *Sf9* cells after 72 h co-expression (**Figure 4.6**). In control samples of single expressions, neither unspecific precipitation of TAT by the anti-DPPIV pAb (**Figure 4.6**A lane 1) nor of DPPIV by the anti-TAT mAb was seen (**Figure 4.6**B, lane 1). Furthermore, unspecific binding of the proteins to the protein-A-sepharose used was not detected, implying that TAT and DPPIV undergo binding which initiates their co-immunoprecipitation.

Expressing the HIV1-TAT and human-DPPIV proteins separately and using the lysates together in co-immunoprecipitation test did not yield any binding between the two proteins.

Immunoprecipitation of TAT with anti-TAT mAb always yielded a double band of molecular weight 10 kDa and 13 kDa, whereby the 13 kDa band was almost always more intensive than the 10 kDa protein band when TAT was expressed alone. Co-infecting *Sf9* cells with TAT and the pFastBac1 control virus, did not lead to a change in the intensities of the 10 kDa and 13 kDa TAT protein bands immunoprecipitated (**Figure 4.6**A lanes 2 and 4). Opposed to this, when TAT was co-expressed with DPPIV, immunoprecipitation with TAT or DPPIV specific antibodies yielded predominantly the 10 kDa protein band (**Figure 4.6**A, lanes 5 and 7). This suggests that the TAT protein due to co-expression with DPPIV, but not the high virus titre used in co-expression is predominantly the 10 kDa form.

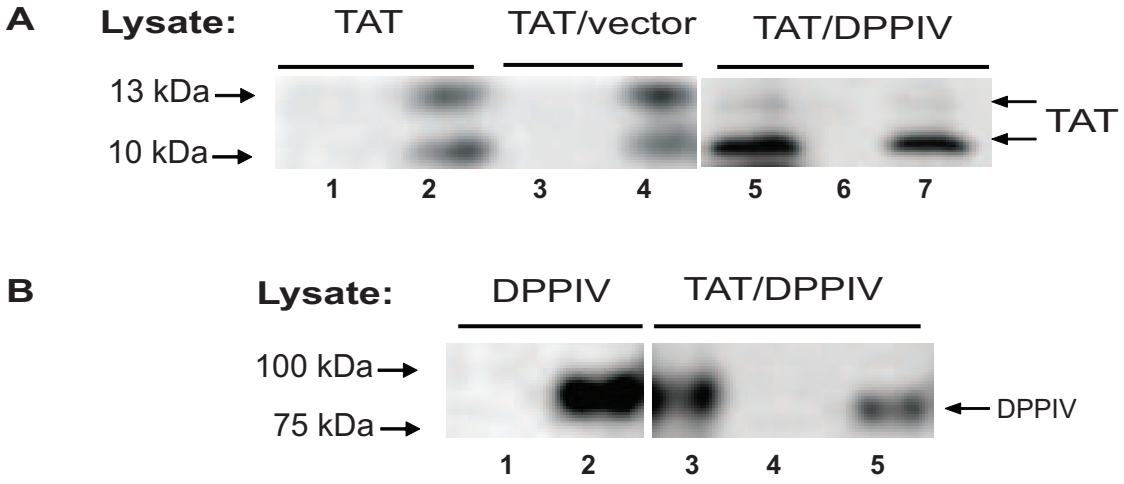

Figure 4.6: Co-immunoprecipitation of human-DPPIV and HIV1-TAT from *Sf9* cells

Single expression or co-expression of TAT with DPPIV was performed for 72 hours, afterwards the cells were solubilised and lysates subjected to immunoprecipitation, (IP). **(A)** IP was conducted with anti-TAT mAb (lanes 2, 4 and 5) or with anti-DPPIV pAb (lanes 1, 3 and 7). Lane 6 was control conducted with protein-A-sepharose without antibody. TAT/vector represents control cells co-infected with TAT and the pFastBac1 vector virus. Each immunoprecipitate was separated by SDS PAGE and the gels blotted and probed with anti-TAT mAb. **(B)** IP was conducted with anti-TAT mAb (lanes 1 and 5), with anti-DPPIV pAb (lanes 2 and 3) or with protein-A-sepharose without antibody (lane 4). The immunoprecipitates were subsequently blotted and probed for with anti-DPPIV pAb. The figure represents one of three independent experimental results.

4.3.5 Serine-phosphorylation of TAT in *Sf9* cells is reduced due to co-expression with DPPIV

To confirm whether the double TAT protein bands resulted from posttranslational modifications, we verified if TAT expressed in the *Sf9* cell system was phosphorylated. Precipitation of TAT protein from TAT- and TAT/DPPIV-expressing *Sf9* cells with anti-phospho-serine mAb was

achieved (**Figure 4.7**A, upper panel). Only the 13 kDa protein band was precipitated by the anti-phospho-serine mAb, opposed to both 10 kDa and 13 kDa TAT protein bands precipitated by the anti-TAT mAb from the same lysates (**Figure 4.7**A, lower panel). Furthermore, only a faint 13 kDa TAT protein band was precipitated from the TAT/DPPIV sample, suggesting that serine-phosphorylation of the HIV1-TAT protein was reduced due to its co-expression with DPPIV. Assuming that the level of phosphorylation of TAT protein being expressed alone for 72 h is 100 %, the phosphorylation level after 48 h was 59 % (**Figure 4.7**B). Only 22 % of phospho-TAT protein was realized after 72 h co-expression with DPPIV. Co-infecting *Sf9* cells with HIV1-TAT- and the control vector-virus did not influence the level of phosphorylation of TAT protein, suggesting that the decrease in the pool of phospho-TAT in TAT/DPPIV samples was not due to the high level of virus used in co-infection, but rather due to DPPIV.

To further confirm whether the 13 kDa band was precipitated due to phosphorylation and not unspecific binding to the antibody, lysates of HIV1-TAT protein being expressed alone or together with human-DPPIV for 72 h were either treated with alkaline phosphatase for 2 h at 37°C or left untreated, then subsequently immunoprecipitated with the anti-phospho-serine mAb (**Figure 4.7**C, upper panel) or anti-TAT mAb (**Figure 4.7**C, lower panel). The treatment of lysates with alkaline phosphatase abolished the immunoprecipitation of TAT protein with anti-phospho-serine mAb (**Figure 4.7**C, lane 2 and 3, upper panel), but not with the anti-TAT mAb (**Figure 4.7**C, lane 2 and 3 lower panel). The HIV1-TAT protein (TAT-BRU) expressed in this study has only one tyrosine residue (Y-47). Immunoprecipitation of TAT with anti-phospho-tyrosine mAb was not detected.

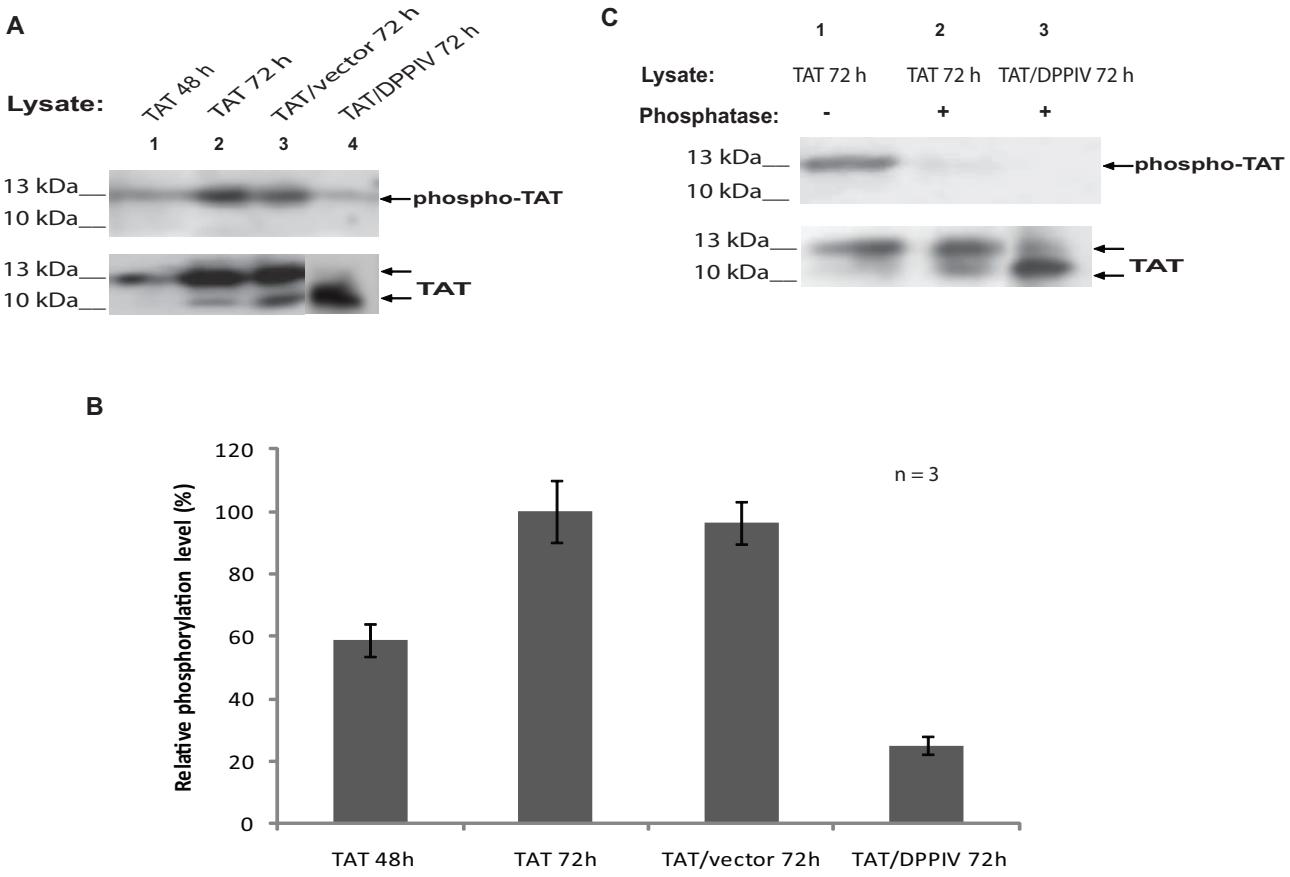

Figure 4.7: Serine-phosphorylation of TAT protein in *Sf9* cells

(A) Lysates of TAT-expressing *Sf9* cells harvested at the indicated time were subjected to IP with anti-phospho-serine mAb (upper panel) or anti-TAT mAb (lower panel). Each immunoprecipitate was separated by SDS PAGE then blotted and probed with anti-TAT mAb. **(B)** The intensities of phospho-TAT protein bands were determined with the QuantityOne software and calibrated against the respective intensities of the total protein detected with anti-TAT mAb. TAT being expressed alone for 72 h was taken as standard. Each bar represents the relative phosphorylation level deduced from 3 independent experiments ± standard deviations as a percentage of the standard. **(C)** Lysates of TAT-expressing *Sf9* cells were either treated with alkaline phosphatase (lanes 2 and 3) or left untreated (lane 1) then immunoprecipitated with the anti-phospho-serine mAb (upper panel) or anti-TAT mAb (lower panel). The immunoprecipitates were blotted and subsequently probed for with anti-TAT mAb.

4.3.6 The HIV1-TAT protein induces tyrosine-phosphorylation of human-DPPIV

To confirm whether tyrosine-phosphorylation of DPPIV takes place in *Sf9* cells and can be induced by TAT protein, we expressed DPPIV in *Sf9* cells for 50 h and subsequently treated a portion of the cells with the purified recombinant TAT protein, GST-TAT-His for 22 h. Parallel to this, *Sf9* cells were co-infected with TAT- and DPPIV-recombinant baculoviruses and incubated for 24 h, 48 h or 72 h. IP of phospho-proteins was performed with anti-phospho-tyrosine mAb and the immunoprecipitates blotted and probed with anti-DPPIV pAb. A small portion of DPPIV expressed

in *Sf9* cells was phosphorylated on tyrosine residues and could be immunoprecipitated with the anti-phospho-tyrosine mAb. The level of phosphorylation was significantly increased in the TAT-treated DPPIV samples and TAT/DPPIV expressing cells after 72 h co-expression (**Figure 4.8**A, lanes 4 and 7 upper panel). Compared to untreated DPPIV being expressed alone for 72 h (**Figure 4.8**A, lane 3), the phosphorylation of DPPIV after application of purified TAT protein was increased by 9 folds and that of TAT/DPPIV sample by 8 folds (**Figure 4.8**B). Co-infecting cells with DPPIV and the control vector virus for 72 h did not lead to an increase in the pool of phospho-DPPIV seen in TAT/DPPIV-expressing cells (**Figure 4.8**A, compare lanes 1 and 7), making it evident that HIV1-TAT and not the high titre of virus used in co-expressions is responsible for the induction of DPPIV phosphorylation.

To further verify the specificity of the TAT effect on phosphorylation of DPPIV and also the specificity of the antibody used, *Sf9* cells were infected with DPPIV recombinant baculovirus for 68 h then a portion of the cells subsequently treated with recombinant TAT (GST-TAT-His) or GST protein for 4 h. The cells were lysed and the lysates further separated in 2 equal parts. One part of each sample was then treated with alkaline phosphatase for 2 h at 37°C. Afterwards the lysates were subjected to IP with anti-DPPIV pAb or the anti-phospho-tyrosine mAb. Blotting the immunoprecipitates and probing for with anti-DPPIV pAb revealed a significant increase of phospho-DPPIV in TAT-treated samples. Treatment of the sample lysates with alkaline phosphatase prior to IP abolished the immunoprecipitation of DPPIV by the anti-phospho-tyrosine mAb, indicating that the antibody is specific for recognition of phosphorylated protein (**Figure 4.8**C, lanes 1 and 3).

Application of purified recombinant TAT protein to DPPIV expressing cells did not induce an increase in the overall expression level of DPPIV (result not shown). It was not clear if the higher intensity of phospho-DPPIV bands seen in the TAT/DPPIV co-expressing cells after 72 h (note that there was no increase in phosphorylation in the TAT/DPPIV co-expressing cells at 24 h and 48 h expression duration) was due to the bulk increase in DPPIV expression previously observed (see **Figure 4.3B**) or the presence of TAT in the culture medium as a result of translocation out of the cells. Interestingly, culturing TAT/DPPIV-expressing cells for only 44 h and application of purified TAT protein to the cells and culturing for a further 4 h (making a total of 48 h expression duration) resulted in an increase in tyrosine-phosphorylation of DPPIV (result not shown). This suggests that either extracellular TAT alone is responsible for the induction of tyrosine-phosphorylation or the concentration of TAT protein in the extracellular medium plays a role in the induction of DPPIV phosphorylation. This is in context with the observation that after 72 h co-expression of TAT and DPPIV residual amounts of TAT protein are detected in the culture medium which remain undetected after 48 h co-expression (result not shown).

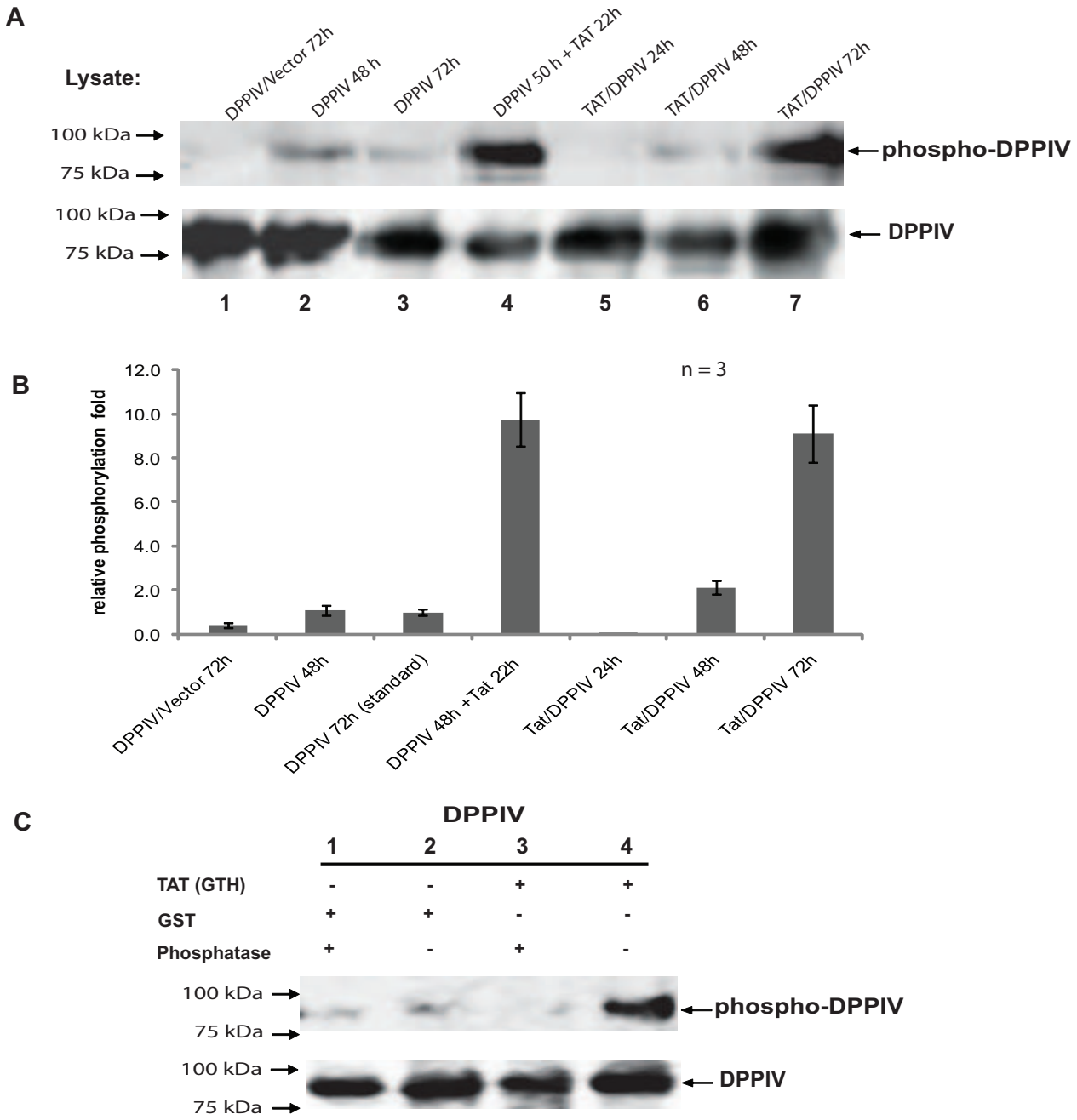

Figure 4.8: HIV1-TAT induces tyrosine-phosphorylation of human-DPPIV in *Sf9* cells

(A) *Sf9* cells were infected with the indicated recombinant baculoviruses. After 50 h a portion of the DPPIV-expressing cells were treated with 2.7 nM final concentrations of the purified GST-TAT-His protein and subsequently cultured for further 22 h. The cells were harvested, solubilised and the lysates were subjected to IP with anti-phospho-tyrosine mAb (upper panel) or anti-DPPIV pAb (lower panel). Each immunoprecipitate was separated by SDS PAGE then blotted and probed with anti-DPPIV pAb. DPPIV/vector represents control cells co-infected with DPPIV- and the control pFastBac1 recombinant virus. **(B)** The band intensities of phospho-DPPIV protein (in A, upper panel) were quantified with the QuantityOne software and calibrated against the total DPPIV protein (A, lower panel). The value of DPPIV being expressed alone for 72 h was set as standard (=1) and the relative phosphorylation fold of the other samples deduced as quotients of their calibrated band intensities and the standard. Each bar represents the relative phosphorylation fold deduced from 3 independent experiments ± standard deviations**. (C)** *Sf9* cells were infected with DPPIV recombinant

baculovirus and cultured for 68 h then subsequently treated with the GST-TAT-His or GST protein and cultured for further 4 h. After solubilisation, each lysate was divided into two equal portions and either treated with alkaline phosphatase for 2 h at 37°C (lanes 1 and 3) or left untreated (lanes 2 and 4). IP with anti-phospho-tyrosine mAb (upper panel) or anti-DPPIV pAb (lower panel) was performed. The immunoprecipitates were separated by SDS PAGE, blotted and subsequently probed with anti-DPPIV pAb. The figure represents one of three independent experimental results.

4.3.7 Human-DPPIV protein expressed in *Sf9* cells is O-glycosylated

Glycosylation and sialylation of DPPIV was reported to play a role in its binding to cationic peptides and proteins (Smith *et al.*, 1998). We verified the glycosylation pattern of purified human-DPPIV protein expressed in *Sf9* cells. After separation of the N-linked glycans (methods section 9.4.2.1), the o-linked glycans could be detected (**Figure 4.9**). Mass spectrometry of glycan fractions after extraction of N-glycans revealed galactose which implies its direct o-glycosidic linkage to serine or threonine residues. O-glycosylation of DPPIV is poorly studied. It still remains unclear whether this is cell-type specific and dependent on the *Sf9* cells used for expression or an unknown modification of DPPIV which is widely distributed. Further analysis to determine the positions of O-glycosylation are ongoing. Furthermore, glycosylation analysis of DPPIV purified from the liver of healthy Wistar rats is under process.

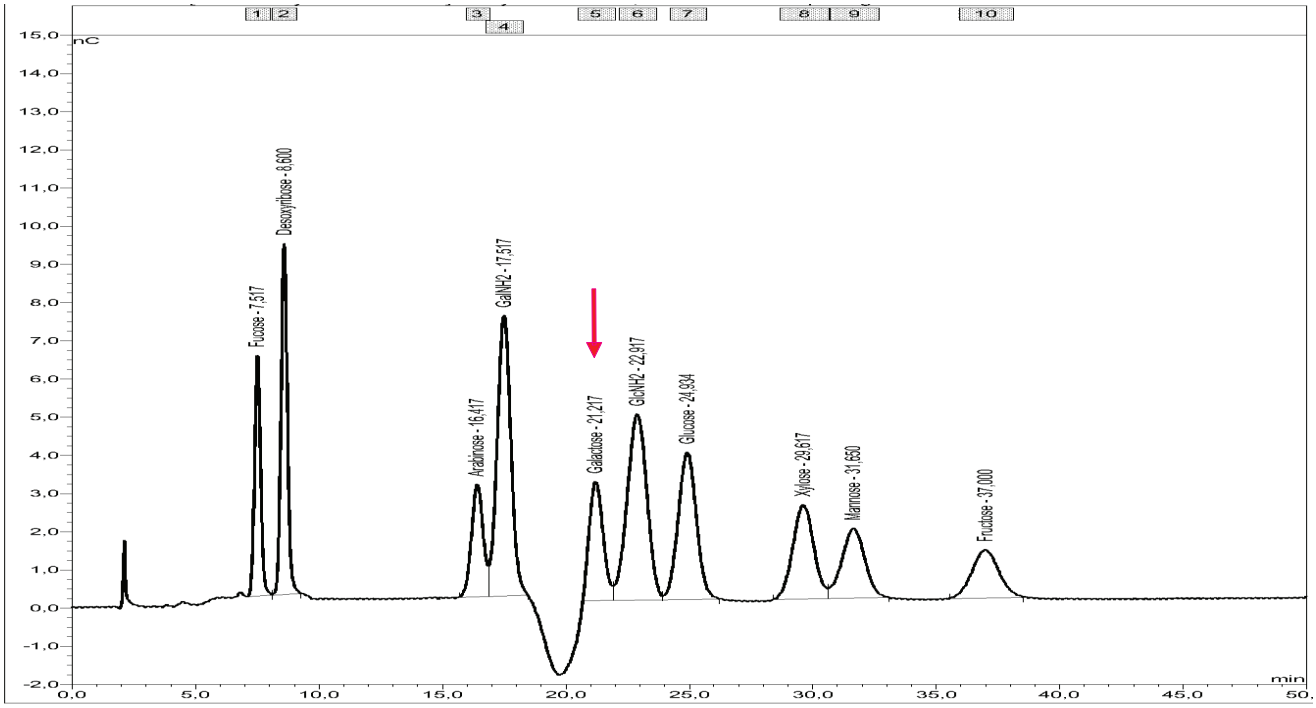

Figure 4.9: Mass spectra of O-glycans isolated from hDPPIV protein expressed in *Sf9* cells

The o-glycosidically linked galactose is indicated with a red arrow (n=2).

4.4 Purification and characterization of TAT/DPPIV protein complex *Sf9* cells

4.4.1 Purification by immuno-affinity chromatography

As demonstrated above, HIV1-TAT and human-DPPIV proteins co-expressed in *Sf9* cells associated in immunoprecipitation tests conducted with either the antibody against human-DPPIV or the HIV1-TAT protein. This ability to co-immunoprecipitate was exploited in the purification of the TAT/DPPIV protein complex from co-infected *Sf9* cells. Co-expression of TAT and DPPIV was performed in *Sf9* cells for 72 h. The cells were harvested, solubilised and lysates used for purification of protein. Immuno-affinity chromatography with specific antibody against human-DPPIV antigen was performed. High amounts of partially pure TAT/DPPIV protein complex could be eluted as detected in the elution fractions by western blot analysis with anti-DPPIV pAb (**Figure 4.10**A) and anti-TAT mAb (**Figure 4.10**B).

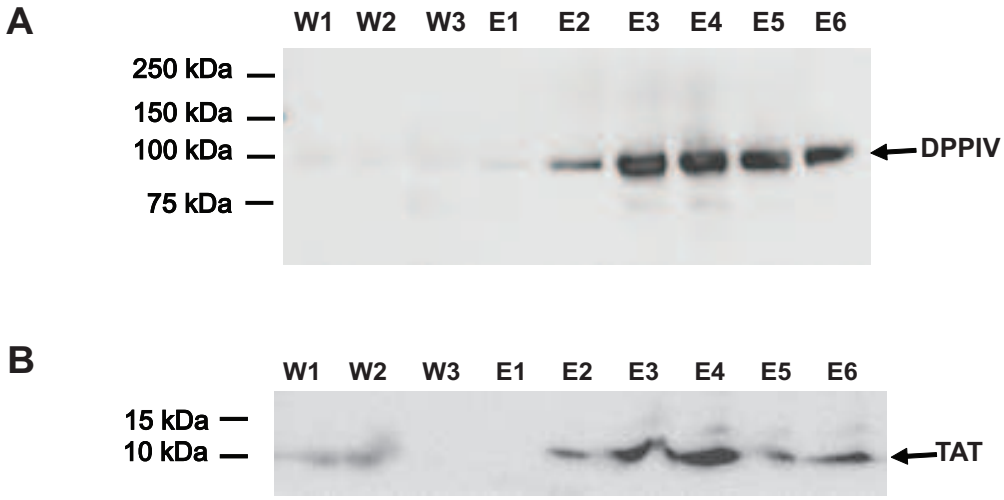

Figure 4.10: Western blot analysis of TAT and DPPIV purified in complex from co-infected *Sf9* cells
Lysates of TAT/DPPIV co-expressing cells were incubated on immobilised anti-DPPIV mAb for 8 h at 4°C. Unbound proteins were washed out (W1, W2) and the bound protein eluted with 50 mM Diethylamine pH 10.8 (E1-E6). The fractions were immediately equilibrated with 10% volume of 200 mM Tris pH 4,5. Aliquots (10 µg total protein/sample) of the protein were separated by either 8% or 4-14% gradient SDS PAGE. The gels were blotted and probed with **(A)** anti-DPPIV pAb or **(B)** anti-TAT mAb. FT: Flow-through.

4.4.2 Purification by size-exclusion FPLC

The TAT/DPPIV elution fractions collected from immuno-affinity purification were pooled and subjected to SE-FPLC on a Superdex 200 column. The elution profile of the TAT/DPPIV protein revealed a retention volume with a calculated molecular mass of 216 kDa (**Figure 4.11**A, TAT/DPPIV). DPPIV being expressed alone and purified under the same conditions revealed a retention volume corresponding to 193 kDa (**Figure 4.11**A, DPPIV). The calculated molecular

mass of the homodimeric human-DPPIV protein backbone is 176 kDa. The additional 16 kDa to the protein backbone of DPPIV being expressed alone is obviously a result of glycosylation.

The crystal structure of TAT nonapeptides in complex with DPPIV revealed that each homodimeric DPPIV binds two TAT peptides (Weihofen *et al.*, 2005). Based on this report, the calculated molecular mass of the TAT/DPPIV protein complex is 197.8 kDa, assuming that TAT protein is 10.9 kDa. The additional 18.2 kDa implies the presence of oligosaccharide side chains and other modifications.

Silver stained SDS-gradient gel revealed both DPPIV and TAT protein bands in the eluted TAT/DPPIV protein fractions (**Figure 4.11**B). After concentrating the TAT/DPPIV protein complex to a final concentration of 4.2 mg/ml, the protein could be detected as a heteromeric complex under non-denaturing and non-reducing conditions (**Figure 4.11**C).

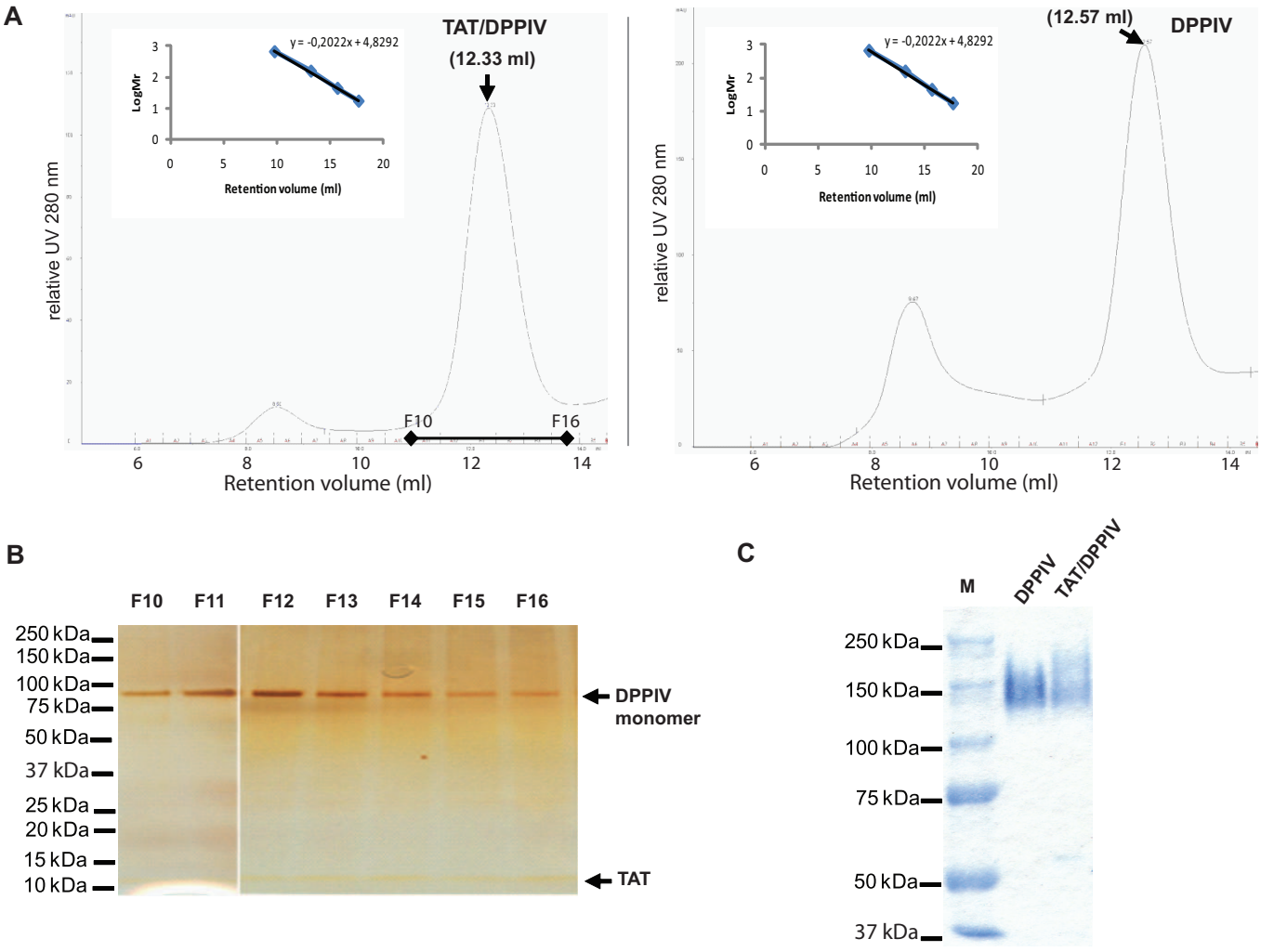

Figure 4.11: Purification of TAT/DPPIV protein complex by SE-FPLC

Fractions of TAT/DPPIV protein, which was pre-purified by immuno-affinity chromatography were pooled and further purified by SE-FPLC on a Superdex 200 column. **(A)** Elution profiles of TAT/DPPIV and DPPIV protein. The standard linear regression curve was generated by plotting the log of the molecular mass of different calibration proteins against their retention volumes (see inset). Components of the gel-filtration

standard (Bio-Rad) were: thyroglobulin (670 kDa), γ-globulin (158 kDa), ovalbumin (44 kDa) and myoglobin (17 kDa). **(B)** Fractions of 500 µl were collected from the main peak as indicated on the elution profile (F10-F16). Aliquots (15 µl / fraction) of the TAT/DPPIV protein were denatured by heating for 5 min at 98°C with reducing sample buffers and separated on a 4-20 % SDS gradient gel, then stained with silver nitrate. **(C)** Fractions 10-16 (**F10-F16**) were pooled and concentrated to 4.2 mg/ml then 5 µg/ sample were analysed under non-denaturing and non-reducing conditions on a 7.5% polyacrylamide gel. Both DPPIV and TAT/DPPIV were analysed 2 days after purification and storage at 4°C.

4.4.3 The purified TAT/DPPIV protein retained TAT and DPPIV specific activities

The purity and activity of the TAT/DPPIV protein complex was further confirmed by Tris-tricine SDS PAGE, MALDI-TOF peptide-mass fingerprinting and activity assays. Tris-tricine-SDS PAGE enables a more accurate separation of proteins with molecular masses ranging from 1-100 kDa on a single gel. Analysis of concentrated TAT/DPPIV protein complex on Tris-tricine gel revealed apparently homogenous DPPIV and TAT protein bands (**Figure 4.12**A). The intensity of the bands was not altered by treatment with TFA, a strong acid which usually causes unfolding of proteins. Using the QuantityOne software the intensities of the protein bands were quantified and used to determine the ratio of TAT protein to DPPIV in the purified complex. MALDI-TOF peptide mass fingerprints of the protein bands revealed peptides which matched to the HIV-TAT and human-DPPIV proteins respectively (see **11.3.2**).

The TAT portion of the TAT/DPPIV protein retained TAT-specific transactivation activity. This was determined in terms of the ability of the TAT/DPPIV protein to induce CAT expression under the control of the HIV-LTR promoter (**Figure 4.12**B). DPPIV protein being expressed alone did not induce CAT expression, making it evident that it is the TAT component of the TAT/DPPIV protein complex which specifically induced CAT expression. The DPPIV fraction of the TAT/DPPIV protein complex also retained 15.8 U/mg specific activities, which was evaluated in terms of cleavage of 100 nM of the chromogenic peptide substrate H-Gly-Pro-pNA-HCl (**Figure 4.12**C). The specific DPPIV activity of purified TAT/DPPIV (15.8 U/mg) was comparatively lower than that of DPPIV (28 U/mg) which was expressed alone and purified under similar conditions.

Following co-expression of DPPIV and TAT in 200 ml 2 x 10^6 cells/ml *Sf9* cells, 49 mg total protein was determined in the cleared lysates. The initial DPPIV activity determined was 1,070 mU/mg TAT/DPPIV lysate (**Table 4.1**). With reference to DPPIV proteolytic activity, the final purification step yielded a total purification factor of 14.7. The overall yield was 9.8%. After the final purification step, the estimated ratio (protein concentrations) of DPPIV to TAT protein was 6 µg DPPIV: 1 µg TAT. This was determined from coomassie-stained Tris-tricine gels of protein resulting from 4 independent purifications, by quantifying the band intensities with the QuantityOne software.

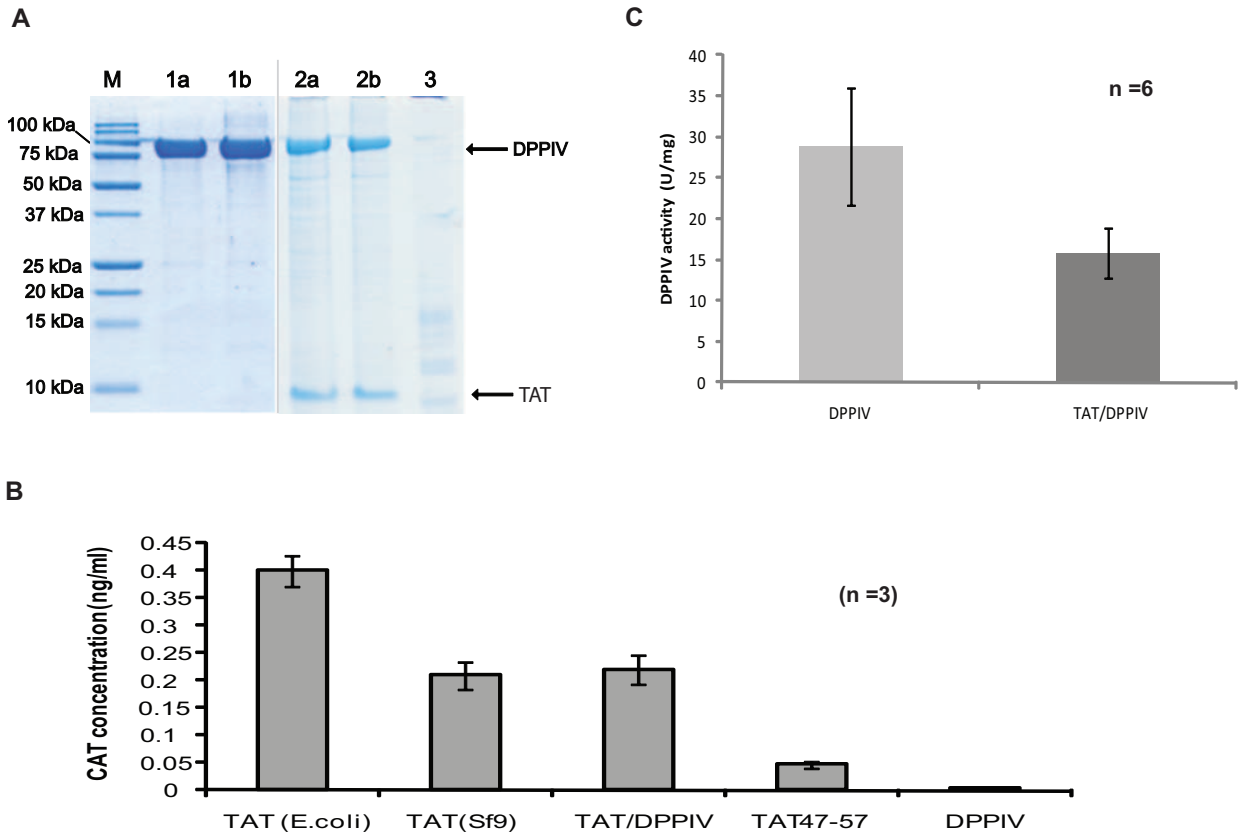

Figure 4.12: Evaluation of the purity and activity of purified DPPIV and TAT/DPPIV protein.

(A) Tris-Tricine SDS PAGE: Purified TAT/DPPIV or DPPIV protein (10 µg total protein / sample), were treated with 0.025% TFA or left untreated then analysed by 10% Tricine-SDS PAGE. **1a and 1b:** Untreated and TFA-treated DPPIV protein respectively. **2a and 2b:** Untreated and TFA-treated TAT/DPPIV protein. 3: TAT protein purified from *Sf9* cells. **(B) Specific transactivation activity of TAT protein:** The HLCD4CAT (HeLa) cell line stably-transfected with a CAT- gene under the control of the HIV1-LTR promoter was treated with 5 µg of the different TAT proteins indicated or with 20 µg of the purified DPPIV or TAT/DPPIV. Cells were harvested after 48 h and their CAT content quantified in duplicates and normalized to the total TAT protein used as inductor. It was assumed that the TAT content in 20 µg TAT/DPPIV complex was 3.5 µg (1 µg TAT: 6 µg DPPIV) Each bar represents the average amount of CAT protein / µg TAT used (n=3). TAT (E. coli) is TAT1-86 produced in *E. coli* (a kind gift from Prof. Dr. Paul Roesch, Bayreuth), TAT (*Sf9*) was purified from *Sf9* cells, and TAT47-57 peptide (Genscript). **(C) Specific proteolytic activity of DPPIV:** Purified DPPIV or TAT/DPPIV protein complex were incubated with 100 nM H-Gly-Pro-pNA-HCl at pH 8.0 for 5 min at 37°C. Afterwards the extinctions of proteolytically derived substrates were determined photometrically at 410 nm and used to calculate the DPPIV-specific proteolytic activities.

Table 4.1: Representative purification of TAT/DPPIV co-expressed in *Sf9* cells

(200 ml suspension culture, 2 x 10^6 cells/ml)

Sample	Total protein (mg)	DPPIV specific activity (mU/mg)	Total activity (mU)	Yield[a] (%)	Purification fold[a]	[b]Ratio DPPIV:TAT (µg)
Cleared lysate	49.0	1,070	52,430	100	1	
Immuno-affinity (pool)	1.733	8,100	14,037	26.8	7.6	4:1
Immuno-affinity (concentrate)	1.136	8,000	9,088	17.3	7.5	
SE-FPLC (pool)	0.408	16,000	6,528	12.5	15	
SE-FPLC (concentrate)	0.325	15,750	5,119	9.8	14.7	6:1

[a] based on DPPIV enzyme activity, [b] based on quantification with the QuantityOne software

4.4.4 Purified TAT/DPPIV protein revealed a heterogeneous distribution on 2D gels

Purified DPPIV or the TAT/DPPIV protein (10 µg/sample) were mixed with pH 3-10-BPG-sample buffer (Amersham) to 170 µl final volume and denatured by heating, then isoelectric-focused on wide range pH gradient gel strips (pH 3-10) and separated on 8-16% SDS gradient gels.

DPPIV protein being expressed alone, revealed a homogeneous distribution with a single spot at pH 5.7 and 96 kDa (**Figure 4.13**A). Opposed to this, part of the TAT/DPPIV protein is moved from pH 5.7 to a pH value between 7.0 and 8.0. Considering the calculated pI of TAT (10.1) and that of DPPIV protein (5.7), the resulting complex of TAT and DPPIV should exhibit pI values ranging between 7.0-8.0 (value 7.0 calculated with the pI/Mw tool of www.expasy.org) and the expected molecular weight should be about 198 kDa ([TAT/DPPIV2 heteromer). As a consequence of this pI and molecular weight, part of the complex which remained intact even after boiling in urea-containing sample buffer prior to isoelectric focusing, could be detected at a pH range between 7.0 and 8.0. The purified TAT/DPPIV protein revealed four main spots altogether, which are annotated with 1-4 (**Figure 4.13**B). An analysis of the spots by MALDI-TOF-PMF revealed DPPIV in spots 1, 2 and 3. Spot 3, is DPPIV which resulted from the dissociation of the intact complex seen in spot 4 during the second dimension (SDS PAGE). This is consistent with the observation that isoelectric focusing of TAT/DPPIV protein without boiling did not reveal a protein spot at the position of spot 3, but rather stronger band intensities of spot 4 (result not shown). Spot 4 has a molecular weight of about 225 kDa and is between pH 7.0 and 8.0. MALDI-TOF-PMF of this spot did not yield spectra intensities good enough for determination of the protein. The calculated pI of the TAT protein used here is 10.1 and the mass is approximately 10 kDa, which falls out of the detection range of the underlying analysis.

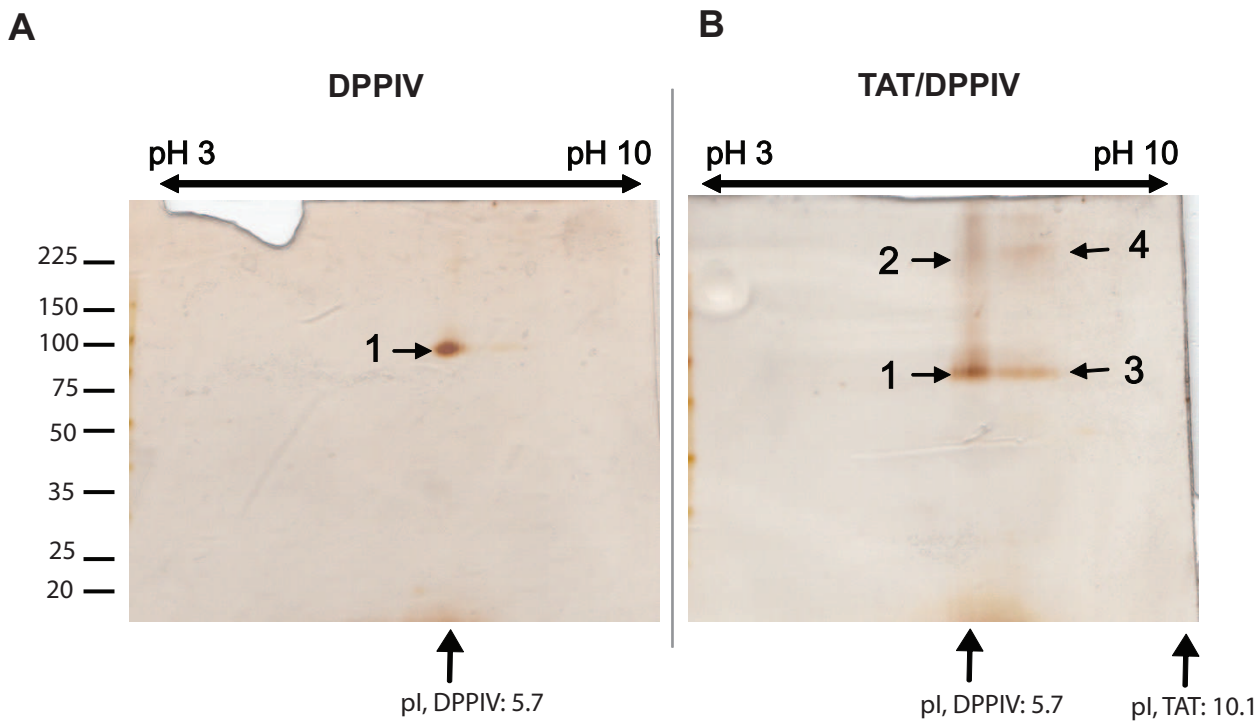

Figure 4.13: Characterization of purified human-DPPIV and TAT/DPPIV protein by 2D PAGE

10 µg of the purified protein samples were diluted with pH3-10 BPG-sample buffer to 170 µl final volumes then preheated at 99°C for 3 minutes. The samples were isoelectric focused on pH 3-10 gradient gel strips. The proteins were subsequently separated on 8-16% SDS gradient gels (Anamed GmbH). After separation the gels were stained with silver nitrate. **(A)** Purified DPPIV protein. **(B)** Purified TAT/DPPIV protein complex.

4.4.5 Crystallization screen of the purified TAT/DPPIV protein complex

Purified TAT/DPPIV protein complex at a concentration 4.2 mg/ml (in PBS pH 8.0) was used for crystallization screen in different crystallization buffers. For each screen, either 0.5 µl protein solution (sitting drop method) or 1 µl (hanging-drop method) were used. After incubation of the plates for a period of two weeks at 4°C the first rectangular crystals were visible. More than 20 crystals were picked. In **Figure 4.14** an image of some of the crystals is presented. The large crystals were used for initial X-ray analysis. The initial X-ray analyses revealed only mass densities corresponding to the DPPIV protein.

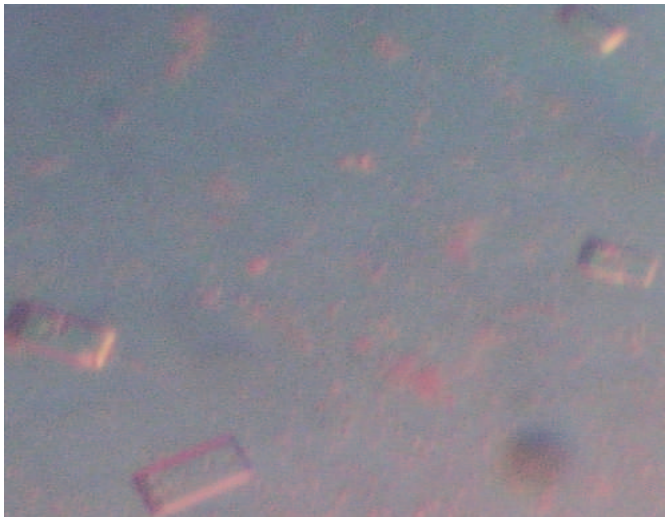

Figure 4.14: Microscopic images of crystals of purified TAT/DPPIV protein
The buffer in which the protein crystallized contained 100 mM Tris, 300 mM sodium acetate pH 8.0 and 22-28 % PEG-4000. Crystallization condition was 4°C via the hanging drop method. The protein concentration was 4.2 mg/ml in PBS pH 8.0.

Summary IV: DPPIV and TAT associate in co-infected *Sf9* cells

Co-expression of the HIV1-TAT and human-DPPIV protein in *Sf9* cells revealed an increase in the bulk of DPPIV protein expressed. Due to the co-expression serine phosphorylation of TAT protein was reduced and a direct binding of the TAT and DPPIV protein could be detected by immunoprecipitation. Furthermore, TAT-dependent induction of tyrosine phosphorylation of DPPIV could be detected which was independent of the inhibition of DPPIV enzyme activity. Purification of the TAT/DPPIV protein complex from co-infected *Sf9* cells was achieved. The protein complex revealed a heterogenic distribution on 2D gels but could be crystallised. However, X-ray analysis revealed only mass densities of the DPPIV protein and not the TAT protein.

5 Results III: Subproject Interaction of DPPIV and Caveolin-1

5.1 Amplification of Caveolin-1 cDNA from different human organs

Using the primers Cav1EcoFor and Cav1PstRev (see section **9.1.1.1** and section **11.2.2**) Caveolin-1 (Cav1)-coding cDNA was amplified from cDNA panels of 10 different human organs (Biochain Institute Inc) by RT-PCR. After repeating the RT-PCR, it was evident that the Cav1-coding cDNA was only expressed in the cDNA panels of human lung, heart, spleen, placenta, skeletal muscle, brain and colon (**Figure 5.1**). Quantification of the relative band intensities of the Cav1 cDNA was performed with the QuantityOne software. The highest levels of the Cav1 cDNA were seen in lung, placenta, skeletal muscle and colon. As a whole, the difference in the levels of Cav1 PCR product was not due to differences in the purity or concentration of the templates used for PCR, since the templates did not show remarkable differences in the levels of the housekeeping GAPDH cDNA.

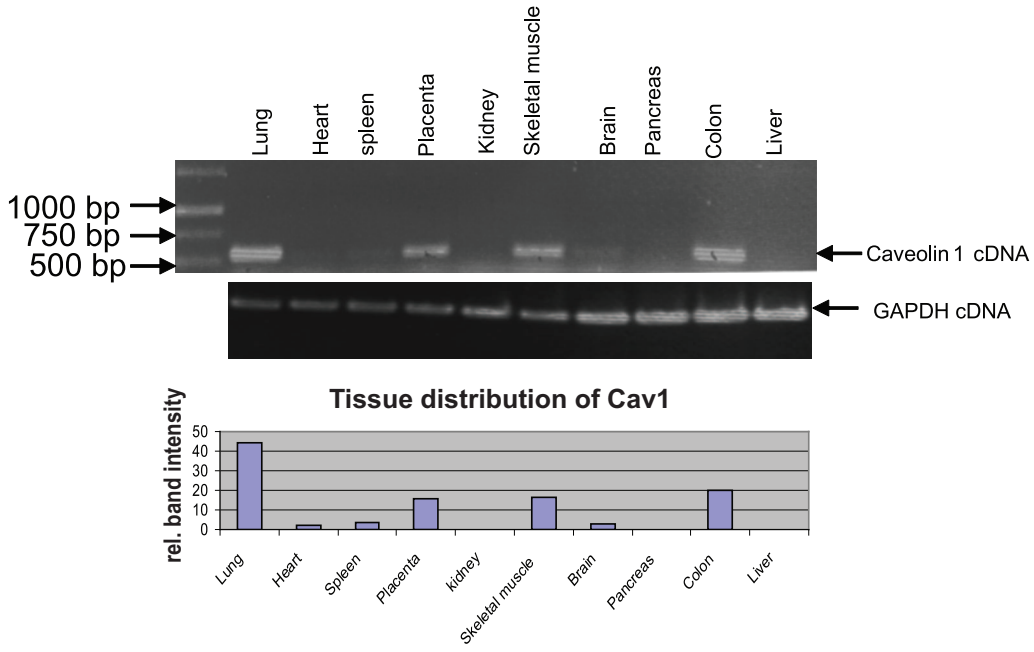

Figure 5.1: Amplification of Caveolin-1 coding cDNA from cDNA banks of different human organs
Using primers for the human Cav1 (upper panel) or GAPDH (lower panel) the respective cDNAs were amplified by PCR and analysed electrophoretically on 0.8% agarose gels. Quantification of the relative band intensities of the Cav1 cDNA was done with the QuantityOne software (bar diagram).

5.2 Expression and purification of GST-tagged Cav1 protein

5.2.1 Purification of GSTCav1 protein by affinity chromatography

In order to investigate the binding capacity of Cav1 with human-DPPIV, the Cav1 cDNA was cloned into the pGEX4T-2 vector and the GSTCav1 protein expressed as described under methods (section 9.2.15).

Expression was performed in the *E. coli* BL21-(DE3) strain. High optical densities of the cells as well as temperature affected the expression level and solubility of the GSTCav1 protein. For this reason the expression temperature was reduced from 37°C to 25°C. The cells were induced at an OD_{600nm} = 0.5-0.6, with 2 mM final concentration of IPTG. This condition enabled an increase in expression level and solubility of the protein. However, the *E. coli*-expressed GSTCav1 protein was still relatively insoluble and a large portion remained in the pellets of lysed cells. Solubilisation of the protein could only be achieved with the use of detergents. Harvested cells were solubilised with 20 mM HBS pH 7.4 supplemented with 1% n-dodecyl-β-D-maltoside and 5% polyethylenglycol, (PEG-400). The soluble proteins were fractionated by 60 min centrifugation at 18,000 rpm (29,703 x g) and coupled on Glutathione-Sepharose 4 Fast Flow (GE Healthcare) for 90 min at 4°C with head-over-tail rotation. The bound GSTCav1 was eluted with 10 mM reduced glutathione in 50 mM Tris buffer, pH 7.5 and analysed by SDS PAGE. The GST-tag has a molecular weight of ca. 26 kDa, whereas Cav1 has a molecular weight of 22 kDa. The calculated molecular weight of whole length monomeric GSTCav1 protein is 48 kDa as was evident on coomassie-stained SDS-gels (**Figure 5.2**B). Besides the monomeric GSTCav1, a high molecular weight form of the protein was detected at about 350 kDa. The identity of the eluted protein was confirmed by MALDI-TOF peptide mass fingerprinting after in-gel tryptic digestion. The detected masses of all peptides matched well with the theoretical masses expected from tryptically derived GSTCav1 protein (see section 11.3.1).

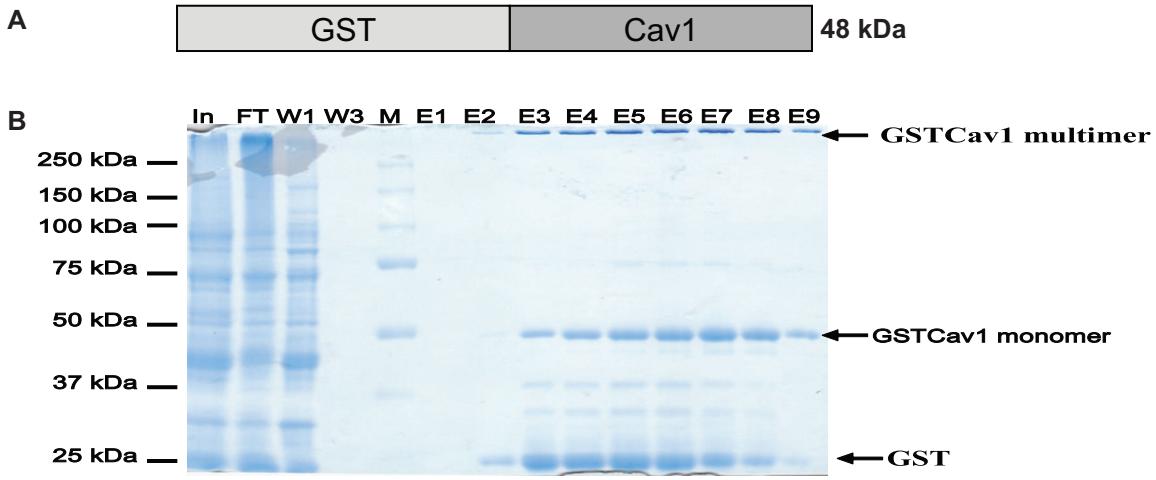

Figure 5.2: Analysis of purified GSTCav1 protein by SDS PAGE

(A) Schematic representation of the GSTCav1 fusion protein. A 7 residue linker constituting a thrombin recognition sequence separates the GST and the Cav1 protein. **(B)** SDS PAGE: Aliquots (10 µg/sample) of the protein fractions were denatured by boiling in reducing sample buffer and separated electrophoretically on an 8% SDS gel then stained with coomassie solution. M: High molecular weight protein standard, In: input- soluble protein fraction, FT: flow-through, W1/W3: Wash, E1-E9: eluted fractions.

5.2.2 Purification of GSTCav1 protein by SE-FPLC

After purification of the GSTCav1 protein by glutathione affinity chromatography the fractions E3-E9 containing the fusion protein were pooled and further purified to homogeneity by size-exclusion chromatography on a Superose-6 column.

The elution profile of the GSTCav1 protein revealed several peaks (**Figure 5.3**A), some of which contained the highly pure intact GSTCav1 protein. The purity of the protein was confirmed by SDS PAGE (**Figure 5.3**B) and western blot (**Figure 5.3**C). With reference to gel filtration standard, the peak corresponding to pure intact GSTCav1 protein eluted at a retention volume corresponding to a molecular mass of about 5800 kDa. Analysis of the fractions collected from this peak revealed a mixture of GSTCav1 multimers, faint bands of dimers and a majority of the protein as monomer. The peaks corresponding to 26 kDa proteins contained predominantly GST and Cav1 resulting from proteolytic degradation.

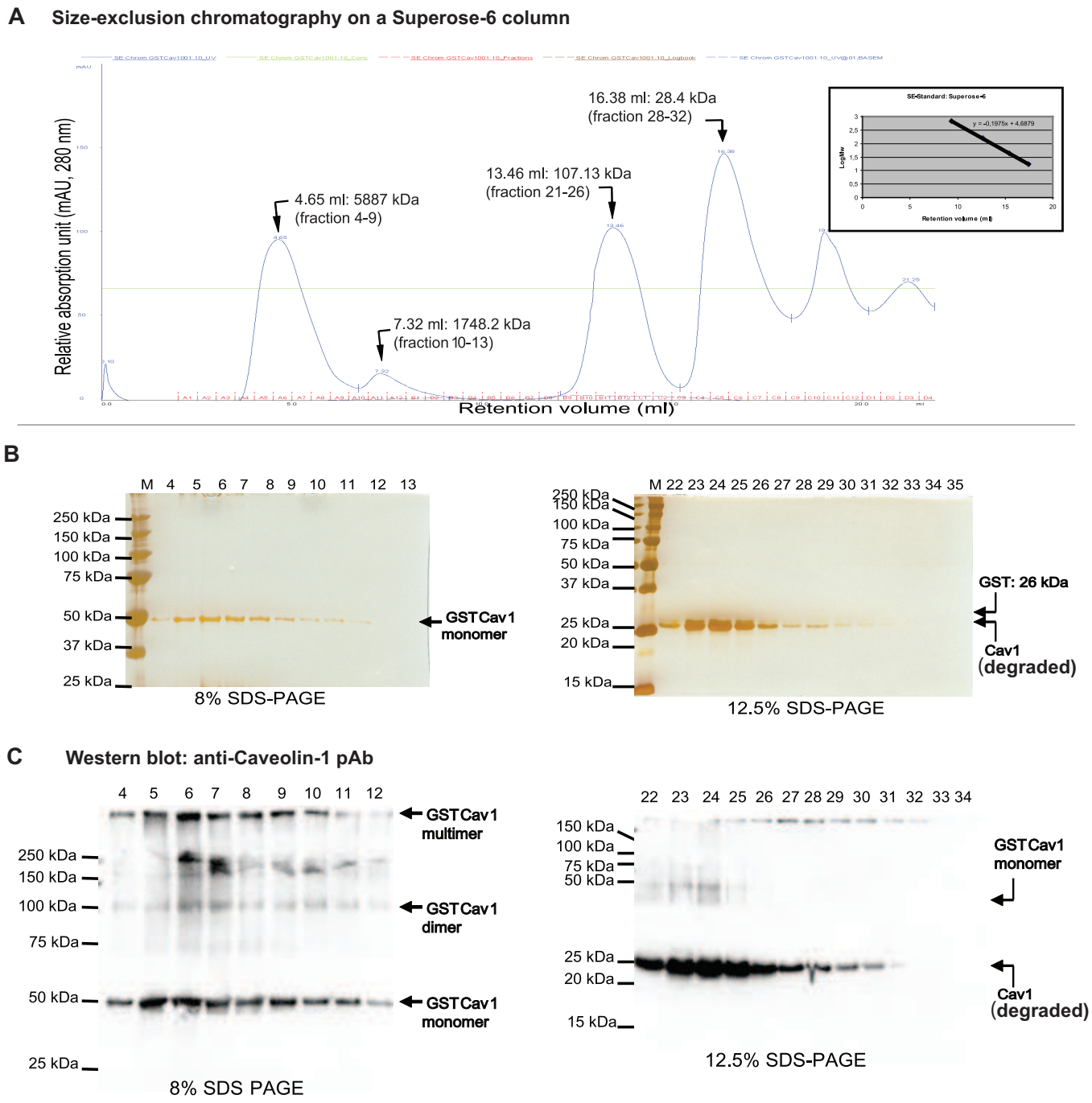

Figure 5.3: Purification of GSTCav1 by SE-FPLC

(A) Elution profile of GSTCav1 protein purified by SE-FPLC on a Superose-6 column. Fractions were collected and aliquots (15 µl) of each fraction were denatured by boiling with reducing sample buffer and separated on 8 % or 12.5% acrylamide gels then stained with silver nitrate solution **(B)**, or blotted on nitrocellulose membrane and probed with rabbit anti-human Caveolin-1 pAb **(C)**. 4-35 indicate the fraction number of samples collected at different retention volumes as indicated in 'A`.

5.3 GSTCav1 binds to human-DPPIV in immunoprecipitation test

To confirm whether Caveolin-1 protein binds to DPPIV, 20 µg of the purified proteins were subjected to IP. GSTCav1 bound to the immobilized DPPIV protein and could be detected by

western blot (**Figure 5.4**A, lane 4). Likewise, DPPIV bound to GSTCav1 that was immobilized on anti-Cav1 pAb (**Figure 5.4**B lane 1). In control tests, neither GSTCav1 bound to the anti-DPPIV pAb used (**Figure 5.4**A, lane 3) nor did DPPIV bind to anti-Cav1 pAb (**Figure 5.4**B, lane 2). This implies the precipitation of both proteins due to their direct binding and not unspecific binding to the antibodies used. Furthermore, incubating DPPIV protein with GST which was immobilized on anti-GST pAb did not lead to binding of DPPIV, which strengthens the fact that GSTCav1 binding to DPPIV is due to Cav1 and not the GST-Tag.

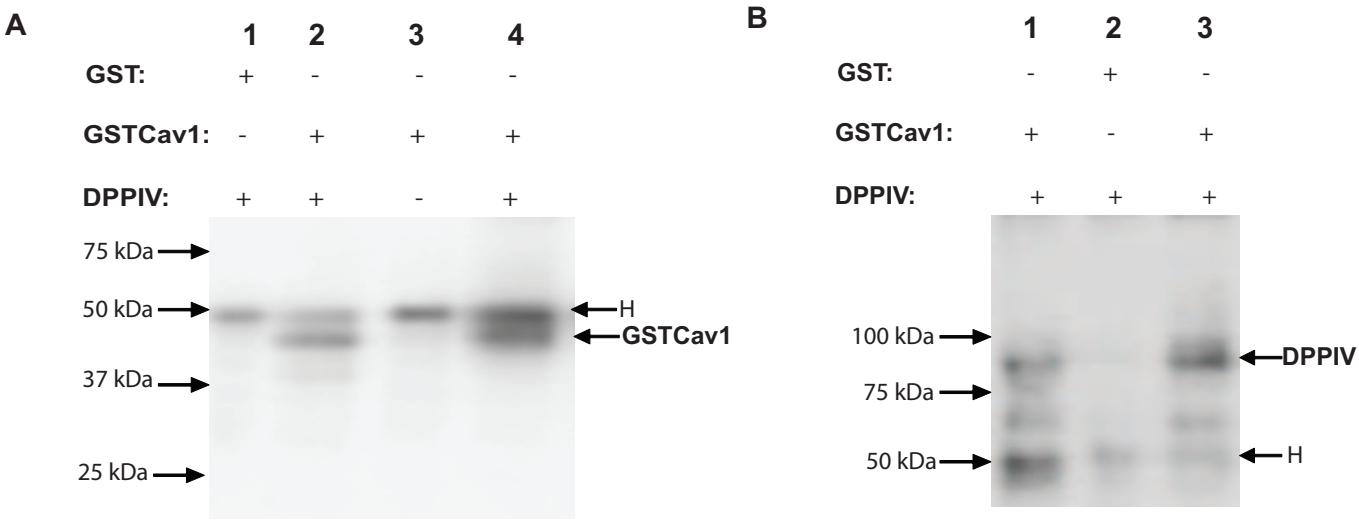

Figure 5.4: Western blot analysis of human-DPPIV and GSTCav1 binding

(A) Purified human-DPPIV and GSTCav1 proteins were subjected to IP with either anti-Cav1 pAb (lane 2) or anti-DPPIV pAb (lanes 1, 3 and 4) then analysed by western blot and probed with anti-GST pAb. **(B)** Purified human-DPPIV and GSTCav1 proteins were subjected to IP with either anti-Cav1 pAb (lane 1 and 2) or anti-DPPIV pAb (lane 3) then analysed by western blot and probed with anti-DPPIV pAb. H indicates the heavy chain of antibody used in IP.

5.4 GSTCav1 binds to DPPIV directly in SPR tests

To further confirm the binding of DPPIV and Cav1 and also determine their binding coefficients surface plasmon resonance analysis was performed. DPPIV was immobilized on the sensor surface of a CM5-Sensor chip (GE-Healthcare) and binding analyses were performed with different concentrations of purified GSTCav1 protein. The binding of GSTCav1 to immobilized DPPIV was quite weak and required relatively high concentrations of the protein. Detectable binding was only achieved with at least 200 nM GSTCav1 proteins (that is, 9.6 µg /100 µl running buffer). To minimize the buffer jump caused by the storage buffer of the protein during measurement, it was necessary that the GSTCav1 protein be concentrated to at least 1 mg/ml. At this concentration, only 9.6 µl GSTCav1 was added to 90.4 µl of the running buffer used in SPR to make up a 200 nM GSTCav1 protein solution. At lower concentrations of the protein stock, the buffer-jump was too

high and biased the overall results, since higher volumes of the protein solution had to be added to lower volumes of the running buffer. Unfortunately, the GSTCav1 protein stock could only be concentrated to 2 mg/ml after purification. Attempting to concentrate the protein higher than this led to precipitation of the protein. For this reason, the SPR measurements were only successful with 200 nM-500 nM GSTCav1 Protein.

In **Figure 5.5**A the sensorgrams of the total response measured with 500 nM GSTCav1 fusion protein is given. The GSTCav1 protein shows a slight affinity to the control cell without DPPIV. However, after deduction of the response given by GSTCav1 due to binding to the control cell, from the response given by GSTCav1 due to binding to DPPIV, an overall positive value was revealed as response difference (**Figure 5.5**B). The response differences were derived with the BIAevaluation software. The sensorgrams reveal a concentration-dependent binding of the GSTCav1 fusion protein to DPPIV. A saturation of the binding was not detected since the binding was relatively low and required higher concentrations of the GSTCav1 protein. GST protein used as control did not interact with DPPIV and gives no increase in response difference. Due to the poor dissociation of the protein, determination of the binding constant was not possible, since the dissociation rate is one of the factors that determine the binding constant.

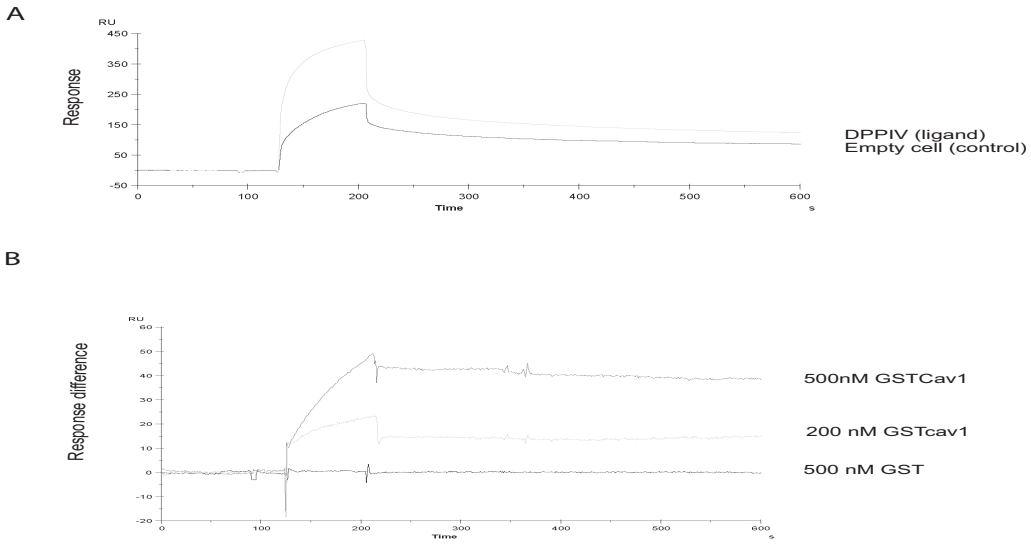

Figure 5.5: Surface plasmon resonance analysis of the binding of GSTCav1 and human-DPPIV

(A) DPPIV was immobilized on a CM5-Sensor chip and purified GSTCav1 proteins were injected and the response monitored. **(B)** The response difference derived with the BIAevaluation-software by subtracting the total response of the protein binding to negative cell from the response of binding to DPPIV is referred to as the total response due to specific binding of the analyte (GSTCav1 or GST) to the ligand (DPPIV).

6 Discussion

6.1 Purification of recombinant HIV1-TAT proteins

The HIV1-TAT protein is a very unstable protein which is light and temperature sensitive and also prone to aggregation *in vitro*. In the underlying work the HIV1-TAT protein was successfully expressed with different fusion tags in *E. coli* and *Sf9* cells and purified under various conditions. The length of the fusion tags used influenced the level of protein expressed and also the total amount and purity of the purified protein. Compared to the non-tagged TAT and His-TAT-His fusion proteins the expression level of GST-TAT-His and GST-TAT was higher. The length of the fusion tag used seemed to render the protein more stable during and after purification, which led to a higher yield and purity of the GST-TAT-His and GST-TAT fusion proteins. Furthermore, the condition of purification (e.g. temperature, light, handling / duration of purification) also played a vital role in the fusion protein's stability. In accordance with this, the GST-TAT-His purified in two steps (Ni-NTA affinity chromatography and SE-FPLC) within a period of approximately 6 h using aluminium foils to protect against light and performing all the steps on ice, revealed the highest yield and retained the highest level of TAT-specific transactivation activity. The GST-TAT fusion protein also showed high transactivation properties, though the protein was comparably less stable during purification than the GST-TAT-His as deduced from the higher level of GST-TAT degradation fragments in SE-FPLC. The high sensitivity of TAT protein to light and temperature could be seen in the fact that purification of the TAT10xHis protein in a hood with a regulated temperature at 4°C yielded high amounts of the pure TAT10XHis protein which was predominantly detected in the monomeric form on SDS PAGE after being concentrated to 7 mg/ml for crystallographic studies. However, the TAT10xHis protein was less stable upon storage than the GST-TAT-His and GST-TAT proteins. This was reflected in the low transactivation ability of the TAT10xHis protein compared to the transactivation activity of same molar amounts of GST-TAT-His and GST-TAT. This effect was due to a more rapid degradation of the TAT10xHis protein compared to the GST-TAT-His protein upon storage at -80°C, which strengthens the fact that the N-terminal GST- and C-terminal His-tag influenced the stability of the GST-TAT-His protein positively.

It was shown that the HIV1-TAT protein up regulates the expression of the HIV co-receptor, CXCR4 in T cells (Secchiero *et al.*, 1999). In the underlying work, the transactivation activities of the purified recombinant TAT proteins did not correlate with their ability to up regulate the expression of CXCR4 in Jurkat cells. Though all the purified TAT protein constructs revealed some extent of TAT-specific transactivation activity they could not up regulate the expression of CXCR4 protein in the Jurkat cell line. This could not be due to the lack of activity of the purified TAT

protein used, since all the purified TAT fusion proteins revealed TAT specific transactivation activity. The Jurkat cell line is a T cell leukaemia cell line and the effect of TAT protein on this cell line is probably different from its effect on healthy T cells or cells of HIV infected patients.

Interestingly, the purified TAT fusion proteins induced a significant accumulation of the CXCR4GFP protein in the cytosol and vesicles of stably transfected CHO and Hek293 cell lines, which could be monitored by confocal microscopy. However, the effects of TAT on the two cell lines did not correlate. Whereas only the TAT1-86 (Immuno-Diagnostics) and the *Sf9*-TAT provoked vesicular accumulation of CXCR4GFP in the CHO-CXCR4GFP cell line, four of the purified samples namely GST-TAT-His, GST-TAT, the *Sf9*-TAT and the TAT (Immuno-Diagnostics) induced vesicular accumulation of CXCR4GFP in the Hek-CXCR4GFP cell lines. These findings did not correlate directly with the TAT-specific transactivation property of HIV1-LTR promoter (compare **Figure 3.11** and **Figure 3.13**). The difference in the effect of TAT on CXCR4GFP in the two cell lines CHO and Hek293 are probably due to the general differences in their origin and nature. While the CHO cell line is derived from hamster ovaries, Hek293 is derived from human embryonic kidneys.

Furthermore, several reports have shown that different pathways mediate the cellular and viral effects of extracellular TAT protein. Accordingly, the cell growth-promoting effects of TAT peak at between 0.1 and 1 ng of purified recombinant protein per ml in the cell growth medium and do not increase with concentration (Ensoli *et al.*, 1993), whereas both the detection of nuclear-localized TAT taken up by cells and the transactivation of HIV1 gene expression or replication require higher TAT concentrations (>100 ng/ml), and all increase linearly with increasing amounts of the exogenous protein. Recent reports also revealed that the transactivation property of purified recombinant TAT proteins do not correlate with their signalling properties (Siddappa *et al.*, 2006). According to these findings, the signalling property of recombinant TAT proteins get lost or reduced *in vitro* due to conformational changes during purification and handling, whereas the transactivation property of the same protein sample is retained. This explains partly why the purified TAT fusion proteins despite the ability to transactivate the HIV LTR promoter revealed different effects on the vesicular accumulation of CXCR4GFP in transfected CHO and Hek293 cell lines.

6.2 HIV1-TAT protein reveal properties of intrinsically unstructured proteins

All the recombinant TAT protein constructs could be successfully purified by SE-FPLC on a Superdex-200 column. However, they all revealed spectra of molecular masses higher than 670 kDa, despite the actual molecular masses ranging between 10-12 kDa for the non-tagged protein and 37 kDa for the GST-TAT-His protein. Of immense interest, was the observation that the protein

fractions collected from these peaks revealed monomeric forms of the respective TAT fusion proteins on SDS PAGE. Strong TAT protein aggregates are not usually easily reduced to the monomeric protein components like observed with the freshly purified TAT protein. The molecular masses higher than 670 kDa in gel filtration and the readiness to be reduced to monomers revealed that the protein solutions were not composed of large strong aggregates which reflected one of the properties of natively unfolded proteins.

Although the FPLC spectra were quite unique, electron microscopy revealed the GST-TAT-His and TAT10XHis protein collected from these peaks as heterogeneous mixtures of different oligomeric states of the protein. These characteristics, (elution at very high molecular masses from gel filtration, existence in different/ large oligomeric states *in vitro*) coupled with the possession of a large net charge by the TAT protein, are typical properties of natively unfolded proteins. The observation that the purified TAT protein revealed properties significant of intrinsically unstructured (natively unfolded) proteins explained partly, why our attempts to crystallize the TAT10xHis protein solution after optimization of the expression (expression in 8 litre Fermenter at 18°C overnight) and purification (by His-Trap and SE-FPLC at 4°C in a hood), remained unsuccessful. The crystallization of a protein demands the existence of the protein in a monomodal form and at high concentrations. The protein used was highly pure and concentrated. However, with reference to the peaks observed in SE-FPLC and the electron micrographs of the protein, the protein was not in a monomodal form suitable enough for crystallography. In support of the observations in the underlying work, NMR studies recently revealed that TAT protein is a natively unfolded protein (Shojania & O'Neil, 2006). The only domain of TAT which seems to be structured is the cysteine-rich domain comprising residues 21-41. This is consistent with the structures of different HIV1-TAT protein which were characterized by NMR (**Figure 6.1**).

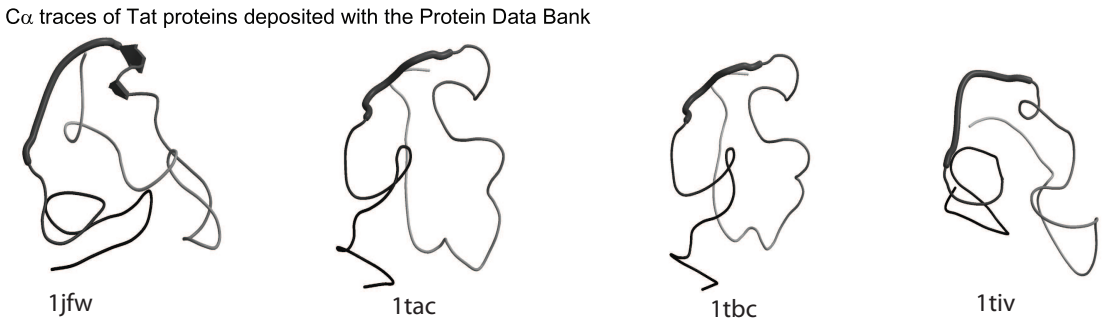

Figure 6.1: Structures of HIV1-TAT determined by nuclear magnetic resonance methods

and deposited with the Protein Data Bank under the codes 1jfw for TAT-Bru (Peloponese *et al.*, 2000) and 1tac, 1tbc and 1tiv for TAT Zaire 2 (HIV1Z2) (Bayer *et al.*, 1995). No secondary structure elements could be observed in the structures. Moreover, their Cα traces cannot be superimposed, although these proteins share more than 70% identity in sequence**.**

Intrinsically unstructured or natively unfolded proteins entirely lack ordered structure or contain domains which lack ordered structure under physiological conditions. They differ significantly in their primary sequence from small, globular, folded proteins (Uversky, 2002) and are quite common in nature (for example the human-β-amyloid peptide, tau protein and α-Synuclein) and share some few peculiarities ranging from the presence of numerous uncompensated charged groups resulting in a large net charge at neutral pH (Hemmings *et al.*, 1984; Weinreb *et al.*, 1996) like the one seen in HIV1-TAT protein. The functional importance of a protein being disordered has been intensively characterised. It has been shown that intrinsic flexibility represents an important prerequisite for effective molecular recognition. Natively unfolded proteins, therefore undertake a variety of biological roles including cell cycle control, transcriptional and translational regulation, modulation of activity and / or assembly of other proteins and even regulation of nerve cell function (Dunker *et al.*, 2001). The majority of natively unfolded proteins undergo a disorder-order transition upon functioning which provides them advantages over rigid globular proteins, for example the ability to bind several different targets (one-to-many signalling), the possibility of high specificity coupled with low affinity, the capability to overcome steric restrictions, the increased rates of specific macromolecular interactions, and the reduced lifetime of the disordered proteins in the cell as a mechanism to ensure rapid turnover of the important regulatory molecule (Dunker *et al.*, 1998; Uversky, 2010). Increased proteolytic degradation of natively unfolded proteins *in vitro* indirectly confirms their flexibility in solution (Markus, 1965).

The HIV1-TAT protein shares many of the above characteristics of natively unfolded proteins which were encountered as obstacles in realizing the crystals of the purified protein in the underlying work.

6.3 HIV1-TAT inhibits the proteolytic cleavage of GLP1 by human-DPPIV

One of the key goals of the underlying thesis was to verify if the HIV1-TAT protein inhibits the cleavage of natural substrates by human-DPPIV. Discrepancies in kinetic data obtained from *in vitro* tests with DPPIV and whole length TAT or TAT-derived peptides (Gutheil *et al.*, 1994; Wrenger *et al.*, 1996; Weihofen *et al.*, 2005) suggested another binding site independent of the N-terminus of TAT protein. However, pull down and immunoprecipitation tests with human-DPPIV and the recombinant TAT proteins expressed separately (GST-TAT-His, GST-TAT, His-TAT-His, TAT and TATV5His) did not yield detectable binding of TAT and DPPIV.

It was demonstrated that the proteolytic degradation of an artificial peptide substrate by DPPIV is inhibited by whole length HIV1-TAT protein in a salt-dependent manner (Gutheil *et al.*, 1994). A direct inhibition of the proteolytic cleavage of natural substrates of DPPIV by HIV1 TAT was not

reported. In the underlying work it could be demonstrated that the inhibition of the enzymatic cleavage of a chromogenic substrate of DPPIV by TAT protein is salt dependent and increases with decrease in salt concentration. The highest level of inhibition was determined with NaCl concentrations in the range between 20 mM and 40 mM.

Purified recombinant TAT protein also inhibited the cleavage of natural substrates of DPPIV to some extent. However, MALDI-TOF-MS revealed that the ability of the recombinant TAT protein to inhibit the cleavage of GLP1 by purified human-DPPIV is weak. DPPIV is a very active enzyme and despite the high molar ratio of TAT to DPPIV used in the assays (at least 1 µM TAT : 16 nM DPPIV), DPPIV could still cleave about 40 % of the GLP1 within the initial 5 min of the reaction and could cleave-up all the substrate (31.25 µM) within 15-20 min.

The purified GST-TAT-His and GST-TAT protein did not inhibit the cleavage of GLP1 by DPPIV. Interestingly, the purified GST-TAT-His, GST-TAT, HIS-TAT-His, TAT10xHis and TAT protein all retained TAT-specific transactivation activity. Furthermore, the retardation of the proteolytic cleavage of GLP1 by DPPIV was observed with the TAT10xHis, TAT and to a lesser degree with the His-TAT-His protein. With respect to this observation, the inability of the GST-TAT-His and GST-TAT proteins to inhibit the cleavage of GLP1 by human-DPPIV directly indicates that the interaction of the N-terminus of TAT with residues of the active site of human-DPPIV is vital for its inhibition of the enzymatic activity of DPPIV. This was blocked by the long GST tag of the GST-TAT-His and GST-TAT proteins. This observation and the observation that the TAT protein constructs did not bind DPPIV directly in pull down and SPR tests, implies that the contribution of other domains of the TAT protein other than its N-terminus, in the inhibition of the cleavage of GLP1 by DPPIV can be ruled out. However, it must be noted that the inhibition effect of TAT on DPPIV *in vivo* may be higher due to the adoption of different “disorder-order transitional states” by the TAT protein just like most natively unfolded proteins do.

Taken together the underlying work demonstrates that the HIV1-TAT also inhibits the cleavage of natural substrates of DPPIV and the N-terminus of TAT is important in this inhibition. The ability of the His-TAT-His protein to inhibit the cleavage of GLP1 by DPPIV could have resulted in part owing to a 6.5 kDa degradation fragment of the protein (see **Figure 3.4**).

6.4 HIV1-TAT protein induced apoptosis in CHO cells in a DPPIV-dependent manner

A typical observation in the infection of humans by HIV is the depletion of $CD4^+$ T cells and the deterioration of immune function in patients. The mechanism underlying this depletion of $CD4^+$ T cells in the pathogenesis of AIDS has not been resolved, yet. In the underlying work the HIV1-TAT protein induced apoptosis in CHO cells in a DPPIV-dependent manner. Stable transfection of CHO

cells with the TATGFP protein was successful without the induction of apoptosis. Furthermore, transfection of the CHO cell line stably transfected with the alpha-1-anti-trypsin protein (CHO-A1AT) with the TAT-bearing plasmids did not lead to the induction of apoptosis. Opposed to this, the transfection of stable CHO-DPPIV cells induced apoptosis, which was revealed in the appearance of phosphatidylserine on the outer leaflet of the cell membrane of intact cells 9 h after transfection and a high level of DNA fragmentation.

Interestingly, the induction of apoptosis in uninfected T cells and other human cell types by TAT protein has been documented (Li *et al.*, 1995; Campbell *et al.*, 2005). Generally, high expression of DPPIV is restricted to activated T cells and not resting T cells. DPPIV is detected in high levels during the early phase of HIV infection, a phase that is accompanied by rapid cell death and the depletion of $CD4^+$ T cells. Li *et al*. (1995) demonstrated that the TAT-induced apoptosis in uninfected T cells was associated with enhanced activation of cyclin-dependent kinases and could be inhibited by growth factors.

DPPIV is known to play a role in apoptosis. Consistent with this, it has been established that the expression of DPPIV is associated with haematological malignancies and apoptosis (Ohnuma *et al.*, 2002; Sato *et al.*, 2003) and inhibits the invasiveness of malignant melanoma cell lines (Pethiyagoda *et al.*, 2000). The activation of cyclin-dependent kinases by TAT protein may trigger the expression and signalling through DPPIV, which leads to the initiation of DPPIV-dependent apoptosis in CHO-DPPIV cell lines after transfection with TAT-bearing plasmids. However, this remains a hypothesis and can be further investigated by determining if TAT induces the activation of kinases in CHO cells in the presence or absence of DPPIV.

6.5 Co-expression of human-DPPIV and HIV1-TAT in *Sf9* insect cells

6.5.1 Co-expression of human-DPPIV and HIV1-TAT leads to an increase in membrane and total DPPIV protein in *Sf9* cells

Human-DPPIV and the HIV1-TAT protein were successfully co-expressed in the baculovirus-driven insect cell expression system at high levels. The bulk level of expression of the human-DPPIV protein and its distribution on the cell surface were significantly higher in the TAT/DPPIV co-expressing cells than in cells expressing DPPIV alone. The enzymatic activity of DPPIV on whole cells and cell lysates correlated with this expression pattern. Although the HIV1-TAT protein is a known inhibitor of DPPIV activity, the inhibition effect seemed to be compensated in part by the up regulation of DPPIV expression. Owing to this increase in DPPIV expression, the overall relative activity of DPPIV in cell lysates of DPPIV and TAT/DPPIV expressing cells were the same at corresponding expression durations. The only exception observed was a lower relative activity of

the TAT/DPPIV sample at 48 h compared to DPPIV being expressed alone for 48 h. This revealed that despite the fact that the highest intensity of DPPIV protein was detected in the TAT/DPPIV samples after 48 h expression (see **Figure 4.3B**), the high level of DPPIV could not completely compensate the inhibition effect of TAT on the enzymatic activity of DPPIV at this stage. This observation seems to be due to a higher amount of TAT protein after 48 h expression than in the other samples. Consistent with this, the intensity of TAT protein in *Sf9* cells imaged by confocal microscopy were stronger after 48 h than after 72 h expression (**Figure 4.5A**).

Altered levels of DPPIV expression, its cell surface distribution and altered enzymatic activity of DPPIV has been associated with several physiological processes as well as with the pathology of several diseases (reviewed in **Table 1.2**), including HIV infection and AIDS (Blazquez *et al.*, 1992; Vanham *et al.*, 1993). In HIV infected patients, the cell surface expression of DPPIV is down regulated in T-lymphocytes and patients exhibit a lower enzymatic activity in serum (Subramanyam *et al.*, 1993). However, these findings are based on results obtained from samples of HIV-infected patients that also displayed great variations in T cell activation due to their different stages of infection. Thus, the data may be biased, since high expression of DPPIV on T-lymphocytes is limited to activated $CD4^+$ and $CD8^+$ T-lymphocytes (Fox *et al.*, 1984) and T cell activation in HIV-infected patients is only high during the acute phase of HIV infection. However, secretion of TAT protein into the extra-cellular space peaks during the acute phase of infection of cultured T cells by HIV1 (Ensoli *et al.*, 1993), which might play a role in the up regulation of host proteins. Interestingly, an increased expression of DPPIV was reported in human cell lines upon stimulation with cytokines and bacterial components (Nemoto *et al.*, 1999). It has also been demonstrated that the HIV1-TAT protein modulates the function of some cytokines (Contreras *et al.*, 2005).

Taken together, the elevation of DPPIV expression levels in *Sf9* cells due to TAT is likely not an artefact in these cell system, but rather a characteristic effect of the TAT protein on several other proteins including DPPIV.

6.5.2 Human-DPPIV and HIV1-TAT associate in *Sf9* cells

HIV1-TAT and human-DPPIV co-localized at the membrane of co-infected *Sf9* cells. After 72 h co-expression, binding of both proteins could be determined by co-immunoprecipitation. However, this co-immunoprecipitation was only possible when whole-cell lysates were used. Using crude membrane extracts or mixed cell lysates of independently expressed human-DPPIV and HIV1-TAT protein revealed no binding of the proteins in immunoprecipitation tests. Furthermore, solubilisation of TAT/DPPIV co-expressing *Sf9* cells with Triton-X100 which destroys protein-protein contacts completely abolished their co-immunoprecipitation. Also, a direct binding of separately expressed TAT protein and DPPIV was not detected. Taking these observations into consideration, it is likely

that binding of TAT and DPPIV requires some modifications or factors which are only disposed when both proteins are co-expressed.

HIV1-TAT protein is natively unfolded (see point 6.1) and as such undergo disorder-order conformational transition during functioning which may contribute in its association with human-DPPIV. Posttranslational modifications of the HIV1-TAT protein may also contribute to its readiness to associate with human-DPPIV or not. This is consistent with the observation, that co-expression of TAT and DPPIV in *Sf9* cells resulted predominantly in a 10 kDa non-phosphorylated TAT protein. Opposed to this, expressing the TAT protein alone or together with an empty control vector in *Sf9* cells resulted to both the non-phosphorylated 10 kDa and phosphorylated 13 kDa TAT protein bands. In the underlying work, the significance of serine phosphorylation of TAT protein was not studied. It has been established earlier, that phosphorylation of TAT protein takes place on serine-16 and serine-46 and is important in regulating the level of transcription of HIV1 by TAT protein (Ammosova *et al.*, 2006). However, Ammosova *et al*. demonstrated in the same study that mutation of both serine-16 and serine-46 to alanine did not completely abolish the transactivation property of TAT protein, but rather only caused a 3-fold decrease in TAT transactivation activity. Besides phosphorylation, other post-translational modifications of HIV1-TAT protein such as acetylation, lysine-methylation and ubiquitination contribute in regulating TAT's function as a transcription activator (Kiernan *et al.*, 1999; Bres *et al.*, 2003; Boulanger *et al.*, 2005). Although the effect of DPPIV on the acetylation, methylation or ubiquitination of TAT protein in *Sf9* cells was not investigated, it seems likely that some if not all of these modifications are altered when HIV1-TAT is co-expressed with human-DPPIV. This is consistent with the observation that TAT being expressed alone yields predominantly the 13 kDa modified band but rather the 10 kDa protein predominantly when co-expressed with DPPIV. Phosphorylation alone (on serine-16 and serine-46) cannot result to the 3 kDa molecular mass difference observed in the TAT protein. This was also reflected in the observation that treatment of lysates of TAT expressing *Sf9* cells with alkaline phosphatase prior to immunoprecipitation with anti-TAT mAb, did not result in a significant decrease in the molecular mass of the 13 kDa TAT protein band (Figure 4.7C, lower panel), but abolished the precipitation of TAT by anti-phospho-serine mAb (Figure 4.7C, upper panel). These findings suggest that, not only phosphorylation but other unknown post-translational modifications of HIV1-TAT are altered due to its co-expression with human-DPPIV in *Sf9* cells. This implies that DPPIV may be involved in interfering with post-translational modifications of HIV1-TAT protein, thereby regulating TAT-induced transcription of HIV1. It also implies that the expression of TAT protein alone enables post translational modifications of the protein on residues which might be important in the TAT-DPPIV association. These modifications therefore prevent TAT's binding to DPPIV *in vitro*.

6.5.3 HIV1-TAT protein induced tyrosine-phosphorylation of DPPIV in *Sf9* cells

Tyrosine phosphorylation of human-DPPIV was up regulated by HIV1-TAT protein either added to DPPIV-expressing *Sf9* cells or as co-expression partner with DPPIV for 72 h. Treatment of cells with the purified recombinant GST-TAT-His, led to an increase in the pool of phospho-DPPIV protein. Control experiments with purified GST protein did not influence tyrosine phosphorylation of human-DPPIV in *Sf9* cells. This suggests that the inhibition effect of HIV1-TAT protein on the enzyme activity of human-DPPIV is not a prerequisite for the induction of the tyrosine-phosphorylation of DPPIV. Thus, N-terminal binding of HIV1-TAT protein to the active site of human-DPPIV may result in partial inhibition (Weihofen *et al.*, 2005), whereas interaction of HIV1-TAT protein to the glycan moieties may lead to tyrosine-phosphorylation of human-DPPIV respectively (Smith *et al.*, 1998). Interestingly, DPPIV-inhibitor dependent induction of tyrosine phosphorylation in resting T cells was reported earlier (Kahne *et al.*, 1998). HIV1-TAT protein is only a mild inhibitor of the enzymatic activity of DPPIV *in vitro* and its action on resting T cells is different from those of other known inhibitors of DPPIV. Consistent with this, the induction of apoptosis in CHO-DPPIV cells by TAT protein was observed in the underlying work. TAT-dependent induction of apoptosis in T cells was earlier demonstrated (Li *et al.*, 1995). Induction of apoptosis by other specific inhibitors of human-DPPIV has not been observed so far, which makes specific inhibitors of DPPIV suitable for therapeutic use in the treatment of diabetes mellitus type-2 (see introduction section **1.2.5.1**).

Interestingly, the inhibition effect of HIV1-TAT on DPPIV *in vitro* resembles that of Metformin, a known mild inhibitor of DPPIV used in the therapy of type-2 diabetes mellitus in combination with strong inhibitors of DPPIV. Although the effect of Metformin on tyrosine phosphorylation of DPPIV has not been studied yet, it is noteworthy that Metformin does not inhibit the cleavage of GLP1 by DPPIV *in vitro* or inhibit the binding of GLP1 to DPPIV in SPR tests (Hinke *et al.*, 2002), but significantly causes the elevation of blood GLP1 in obese non-diabetic subjects and also in type-2 diabetes patients in a poorly studied process associated with activation of protein kinases. The use of strong inhibitors of DPPIV in combination with Metformin is more effective in the therapy of type-2 diabetes mellitus than the use of strong inhibitors alone. The observation that the GST-TAT-His which due to the N-terminal GST tag was completely unable to inhibit the enzymatic activity of DPPIV *in vitro* could induce tyrosine-phosphorylation of DPPIV in cultured *Sf9* cells, suggests that the inhibition of DPPIV enzymatic activity by TAT may be involved, but is not a prerequisite in the induction of signalling cascades emerging from tyrosine phosphorylation of DPPIV.

Recently, insulin-dependent tyrosine phosphorylation of DPPIV in rat liver was demonstrated and the DPPIV protein levels were shown to be down regulated by 40% in both plasma membrane and Golgi/ER fractions after addition of the tyrosine phosphatase inhibitor bpV(phen) (Bilodeau *et al.*, 2006). These findings in rat liver revealed that tyrosine phosphorylation of DPPIV is not only involved in signalling platforms, but also associated with the stability and function of DPPIV.

In the underlying work, co-expression of TAT and DPPIV yielded only traces of tyrosine-phosphorylated DPPIV at expression durations 24 h and 48 h. At 72 h co-expression, the pool of tyrosine phosphorylated DPPIV increased significantly. At this stage of expression, traces of TAT protein were detected in the culture medium suggesting that extracellular TAT protein maybe responsible for the induction of tyrosine-phosphorylation of human-DPPIV in *Sf9* cells. Consistent with this, applying the recombinant GST-TAT-His protein to TAT/DPPIV-expressing *Sf9* cells after 44 h expression and further culturing for 4 h to achieve 48 h total expression duration, led to an increase in the pool of phospho-DPPIV in these samples. This indicates that the concentration of TAT protein in the culture medium may play a role in either up-take of TAT protein by the cells or signalling via association of TAT to other cell surface proteins. Selective activation of a variety of protein kinases by extracellular TAT protein in other cell systems has been documented (Borgatti P, 1997; Menegon A, 1997; Gibellini D, 1998).

6.5.4 Human-DPPIV protein expressed in *Sf9* cells is o-glycosylated

In the underlying work purified human-DPPIV protein expressed in *Sf9* cells revealed o-glycosidically linked glycan moieties in two independent purifications and analyses. O-glycosylation is a post translational modification of serine or threonine residues of proteins which takes place in the cis-Golgi (Varki, 1993). It has been established that this modification potentially plays a role in the biological function of glycoproteins and in conferring stability and protection against proteolytic degradation (Naim *et al.*, 1999). The functional analysis of N-glycan moieties of DPPIV protein was reported earlier (Aertgeerts *et al.*, 2004). However, O-glycosylation of DPPIV was not reported. Intriguingly, the crystal structure of human-DPPIV purified from an insect cell expression system revealed N-glycans on 7 of the 9 N-glycosylation consensus sites found in human-DPPIV (Aertgeerts *et al.*, 2004). Two sites, N321 and N219 were not identified in the crystal structure. Likewise no O-glycans were identified. It is worth noting that glycoproteins can lose some sugar moieties during purification. Added to this, X-ray analyses of crystals at times miss the mass densities of some sugar moieties although they are present on the protein crystal being analysed. This explains the detection of O-glycans by MALDI-TOF mass spectrometry studies, which are not detected in crystallographic studies. Although, it has been established that different strains of the insect cells used in protein expression produce variable forms of glycosylation (van

Die *et al.*, 1996; Lopez *et al.*, 1999), O-glycosylation of DPPIV in the underlying work is probably specific. In mammals o-glycosylation was suggested to play a role in the stability and protection of DPPIV protein against degradation (Naim *et al.*, 1999).

6.5.5 Purification of HIV1-TAT in complex with DPPIV and crystallization screen

The tertiary structure of the multifunctional enzyme DPPIV in complex with the nonapeptide of HIV1-TAT protein has been elucidated (Weihofen *et al.*, 2005). However, this structure alone does not reveal much about the tertiary structure of TAT protein. In order to do crystallization studies, a large quantity of biologically active and stable TAT protein is needed. Attempts to crystallize purified TAT10xHis protein remained unsuccessful. It could be shown by SE-FPLC spectra and electron microscopy, that the purified HIV1-TAT protein is intrinsically unstructured which leads to its high instability in aqueous solutions and its formation of different oligomeric forms. After unsuccessful attempts to crystallize the TAT10xHis fusion protein, we tried to stabilize the protein with Zn^{2+} and other buffer components which have been demonstrated to be able to stabilize protein structures. It has been reported that the binding of Zn^{2+} or other divalent metal ions induces partial folding of intrinsically unstructured proteins, such as thymosin α1 (Grottesi *et al.*, 1998), phosphodiesterase γ-subunit and human α-synuclein (Uversky, 2002) and stabilize them. With the use of Zn^{2+} ions the recombinant TAT proteins purified in the underlying work were not stabilized, but rather underwent more rapid degradation *in vitro*. The use of a different strategy in the stabilization of TAT protein for crystallographic studies was therefore necessary.

The ability of the HIV1-TAT and human-DPPIV to associate in immunoprecipitation test following their co-expression in *Sf9* cells was exploited in a simple strategy to purify the HIV1-TAT protein in complex with human-DPPIV. The idea behind this strategy was to stabilize the HIV1-TAT protein by the human-DPPIV during the purification and crystallization process.

The determination of suitable co-expression conditions for human-DPPIV and HIV1-TAT in *Sf9* cells was successful. Two-step purification by immuno-affinity and SE-FPLC yielded a total of 1.63 mg TAT/DPPIV protein complex/L *Sf9* cells. The purified complex retained both TAT-specific transactivation activity and DPPIV-specific proteolytic activity. The estimated concentration of the TAT-protein in the complex was approximately 0.27 mg. This estimate was based on the quantification of the intensities of protein bands seen on coomassie-stained gels. This method is less accurate in the estimation of protein concentrations than the conventional methods used in determining the concentration of protein solutions. However, the conventional methods are suitable for the determination of total protein concentrations, but not the concentration of each protein component of a mixture. The estimation of protein band intensities by use of the QuantityOne

software was therefore the only option at my disposal, to estimate the ratio of TAT and DPPIV concentration in the purified protein complex.

Based on the specific enzyme activity of DPPIV alone, the purification yield was 9.8%. Considering that the HIV1-TAT protein is a known inhibitor of DPPIV enzyme activity, it is likely that the TAT protein in the complex causes a decrease in the enzyme activity of DPPIV. This is consistent with the fact that human-DPPIV protein expressed alone in *Sf9* cells and purified under similar conditions has a yield of 19.8% after the final purification step, with a DPPIV activity of 28 U/mg (Dobers *et al.*, 2002). The final DPPIV activity of the TAT/DPPIV protein complex was 15.8 U/mg owing probably to the inhibition effect of TAT protein on DPPIV.

In an initial attempt, the TAT/DPPIV protein complex was concentrated to 7 mg/ml and used for crystallographic screen with different buffer conditions. At this concentration, precipitates of the protein could be observed prior to crystallographic screen. Crystallization screening with variable buffer, pH and salt components and incubating the crystallization plates for 3-5 weeks at 4°C did not yield any crystals. In further attempts, the TAT/DPPIV protein complex was concentrated to 4.2 mg/ml and used for crystallographic screen with several different buffer constitutions. At this concentration the purified TAT/DPPIV protein yielded crystals after 2 weeks, in buffers containing a range of 22-28% (v/v) PEG-4000. Intriguingly, X-ray analysis of the crystals revealed only mass densities corresponding to the human-DPPIV.

Although no further details of the crystals were established, the lack of mass densities of the TAT protein seems significant and can be due to one or several of the following reasons:

- For crystallization studies, the existence of a homogeneously pure and monomodal protein solution is essential. After SE-FPLC and concentration of the purified proteins, Tricine-SDS gels revealed apparently homogeneous DPPIV and TAT protein bands. However, the same TAT/DPPIV protein sample revealed several protein spots in 2D gels, whereas DPPIV being expressed alone had a unique spot at pH 5.7. This suggests that a portion of the TAT protein in the complex forms stable complexes with DPPIV, whereas the components in a portion of the TAT/DPPIV complex are not bound strongly. This results in a protein solution which is not of a monomodal oligomeric state. Crystallization therefore takes place in the most stable component of the protein solution.
- Considering that only some domains of the TAT protein associate with human-DPPIV, a large portion of the TAT protein is still exposed to the solution and the long periods of incubation at 4°C (crystallization condition) are less favourable for the TAT protein than human-DPPIV protein which readily crystallizes, leaving the dissociated TAT protein in solution.

- However, considering reports that X-ray crystallography defines missing electron density in many protein structures which correspond to intrinsically unfolded domains of crystallized proteins, the possibility that the mass density of TAT protein is missing due to its disordered nature cannot be completely ruled out. The increased flexibility of atoms in natively unfolded regions leads to a non-coherent X-ray scattering, making them unobserved (Bloomer *et al.*, 1978; Muchmore *et al.*, 1996; Worbs *et al.*, 2000; Uversky, 2010). In support of this, the crystal structure of human-DPPIV and the HIV1-TAT (1-9)-nonapeptide only revealed X-ray densities of the first 3 residues of TAT protein (Weihofen *et al.*, 2005).

- Shortly before this work was submitted, the crystal structure of HIV1-TAT protein in complex with the human positive transcription elongation factor, p-TEFb was elucidated following their co-expression by the same strategy and in the same cell system used in the underlying work (Tahirov *et al.*, 2010). This supports the fact that the cell system is suitable for the expression of the HIV1-TAT protein with binding partners of human origin and strengthens the fact that the protein modifications in the underlying research is due to TAT and its DPPIV binding partner used and not due to the cell system. Furthermore, in the report of Tahirov *et al*., the mass density of the residues 50-86 of TAT protein was not observed in X-ray analysis. This observation further supports the hypothesis that the intrinsically unstructured nature of TAT protein, contributed to the inability to determine its mass density in the crystal of the TAT/DPPIV complex.

6.6 Cloning, expression and purification of Caveolin-1

Caveolin-1 coding cDNA was successfully amplified from the cDNA panels of different human organs. Out of 10 different human organs, only 7 cDNA panels (lung, heart, spleen, placenta, skeletal muscle, brain and colon) contained the Caveolin-1-coding cDNA. Amongst them, the lung, placenta, skeletal muscle and colon revealed high levels of the Cav1 coding cDNA, whereas the heart, spleen and brain had only very low levels of the cDNA. The expression and distribution of Cav1, 2 and 3 in different cell types and organs is documented, amongst which high expressions were seen in the brain (Ikezu *et al.*, 1998).

Since the sequences of the amplified Cav1-coding cDNA from the different organs were identical, Cav1 coding cDNA from human-placenta was used for further cloning and expression of the protein. Optimization of the expression conditions resulted in the expression of high levels of Cav1 with an N-terminal GST tag in *E. coli* BL21-(DE3) strain.

The solubility of the GSTCav1 protein was improved by the use of 20 mM HBS pH 7.4 supplemented with 1% n-dodecyl-β-D-maltoside and 5% polyethylenglycol, (PEG)-400.

Approximately 1.2 mg of the partially pure GSTCav1 protein could be purified by glutathione affinity chromatography per litre *E. coli* culture. Compared to other proteins expressed in the *E. coli* BL21-(DE3) strain, this is a very low yield. However, considering that the protein is an intra-membrane protein and was expressed in a less soluble form, this result was quite satisfactory. A further purification of the GSTCav1 protein by SE-FPLC on a Superose-6 column yielded elution profiles with several protein peaks. One of the peaks contained the highly pure protein which formed very high-molecular-mass oligomers of about 5800 kDa with respect to the gel-filtration standards used. The identity and purity of the protein was proven by SDS PAGE, western blots and MALDI-TOF peptide mass fingerprinting which all revealed the monomer as a 48 kDa protein. The appearance of the GSTCav1 protein in elution spectra with a calculated molecular mass higher than 5000 kDa was not surprising. Using velocity gradient centrifugation, other researchers could demonstrate that Cav1 protein though a small molecule of only 22 kDa molecular mass could form high-molecular-mass oligomers of ≥ 400 kDa (Monier *et al.*, 1995; Sargiacomo *et al.*, 1995). It was also shown that the C-terminal domain of Cav1 is responsible for Caveolin-Caveolin interactions (Song *et al.*, 1997) which are important in the formation of caveolae and caveolin-dependent signalling in caveolae and lipid rafts.

6.6.1 Interaction of DPPIV and Caveolin-1

Using the GSTCav1 protein purified by SE-FPLC, it could be shown that human-DPPIV and Cav1 associate in immunoprecipitation tests. To further substantiate this association and also determine binding constants of the DPPIV-Cav1 interaction, surface plasmon resonance experiments were performed. The binding was quite weak and demanded very high molar ratios of the GSTCav1 to human-DPPIV protein. This observation signified that the association of DPPIV and Cav1 may take place in different ratios such that one DPPIV homodimer may associate with higher numbers of Cav1 subunits in a cluster. This is consistent with reports that Cav1 associates with DPPIV during antigen presentation after formation of a high molecular mass polymer due to its phosphorylation which is initiated upon antigen presentation (Song *et al.*, 1997; Ohnuma *et al.*, 2004).

7 Summary

Human-DPPIV is a multifunctional protein which is involved in several biological processes. The role played by DPPIV in HIV-infection and the outbreak of AIDS are poorly studied. Furthermore, the mechanisms and potential ligands involved in the DPPIV–HIV interaction are largely unknown. The HIV1-TAT protein which plays a crucial role for viral replication and transcription was described as a partial inhibitor of DPPIV and suppressor of the DPPIV-dependent activation of T cell growth. Opposed to human-DPPIV protein, the tertiary structure of HIV1-TAT protein which would reveal details about the protein and how to target the protein with drugs has not been elucidated.

In the underlying work the HIV1-TAT protein was functionally expressed and purified from *E. coli* and *Sf9* cells with variable fusion tags. The purified recombinant TAT proteins revealed TAT-specific transactivation activity. The combination of GST and a 6xHis tag influenced the protein stability positively such that the GST-TAT-His protein revealed the highest TAT-specific transactivation activity. Furthermore, it could be demonstrated that purified recombinant TAT, TAT10xHis, His-TAT-His and Sf9-TAT partially inhibit the proteolytic cleavage of GLP1 by human-DPPIV protein. GST-TAT-His and GST-TAT could not inhibit the enzyme activity of DPPIV, which authenticated that the free N-terminus of TAT is essential for its inhibition of DPPIV. The inhibition effect of TAT on DPPIV was weak and became saturated at a concentration of 1 µM TAT: 16 nM DPPIV.
A characterization of the recombinant TAT protein by gel-filtration and electron microscopy revealed that TAT protein is intrinsically unstructured, a property which hampered its crystallization.

Investigation on the interaction of HIV1-TAT and human-DPPIV in CHO cells revealed a DPPIV-dependent induction of apoptotic cell death by TAT. This effect of TAT on DPPIV-expressing CHO cells resembles the rapid cell death that leads to the depletion of $CD4^+$ T cells during the acute phase of HIV-infection and implies a possible role of the TAT-DPPIV-association in the depletion of cells during HIV-infection.

Also, HIV1-TAT and human-DPPIV were functionally co-expressed in *Sf9* cells by the BAC-TO-BAC® baculovirus system. Compared to DPPIV being expressed alone, TAT/DPPIV co-expressing cells revealed an increase in the overall level of DPPIV expression. Owing to this co-expression, co-association of HIV1-TAT and human-DPPIV protein was detected. Furthermore, a direct binding of the proteins following their co-expression could be demonstrated, which appeared to be

possible due to a reduced post-translational modification of the TAT protein. In effect, there was a 78% reduction of serine-phosphorylation of the HIV1-TAT protein as a result of its co-expression with human-DPPIV.
It could also be demonstrated with the purified recombinant GST-TAT-His protein which due to the N-terminal GST was unable to inhibit the enzymatic activity of DPPIV, that the inhibition of DPPIV enzyme activity may play a role, but is not a prerequisite for the induction of tyrosine-phosphorylation and hence signalling function of human-DPPIV.

One of the main aims of this work was the characterization of the TAT/DPPIV protein complex. As earlier mentioned the TAT protein is intrinsically unstructured. Moreover, it undergoes post-translational modifications when expressed alone in *Sf9* cells, which hindered its direct binding to separately expressed DPPIV protein *in vitro.* Through co-immunoprecipitation of TAT and DPPIV from TAT/DPPIV co-expressing cells it could be demonstrated that the production and purification of their complex can only be realized following their co-expression. The purification turned out to be quite tedious due to the instability of the TAT protein. Nevertheless, purification of a soluble active TAT/DPPIV protein complex under special care was achieved which could be used for crystallization. Many crystals could be picked after a couple of weeks. However, X-ray analyses of the largest crystals revealed only mass densities of the human-DPPIV protein. The observation that mass densities of natively unfolded proteins remain missing in X-ray analyses of crystals is well documented and at least explains why mass densities of the TAT protein in the complex could not be determined.
Taken together, it can be said that the TAT-DPPIV interaction is involved in mediating tyrosine-phosphorylation of DPPIV. Moreover, it plays a role in the initiation of signalling platforms which control TAT post-translational modifications such as serine-phosphorylation and regulate TAT-dependent induction of HIV gene-expression.

In the last part of this work the human-Caveolin-1 protein was successfully expressed in *E. coli* and purified in its soluble form. Its interaction with human-DPPIV protein could be demonstrated by immunoprecipitation and SPR. The analysis by SPR revealed that the binding of human-DPPIV with Caveolin-1 is weak and requires comparatively high molar ratios of the Caveolin-1 compared to lower amounts of the DPPIV protein.

7.1 Zusammenfassung

DPPIV ist ein multifunktionelles Protein, welches in vielen biologischen Prozessen involviert ist. Welche Rolle DPPIV bei der HIV-Infektion und dem Ausbruch von AIDS spielt, ist bisher jedoch weitestgehend unbekannt. Sowohl der Funktionsmechanismus als auch potentielle Liganden, die an der DPPIV-HIV-Interaktion beteiligt sein könnten, wurden bisher nicht beschrieben. Das HIV1-TAT-Protein, welches eine zentrale Rolle bei der viralen Replikation und Transkription spielt, wurde als Inhibitor der DPPIV-Enzymaktivität beschrieben. Demnach führt das HIV1-TAT-Protein zur Suppression der DPPIV-abhängigen Aktivierung der T-Zell-Proliferation. Im Gegensatz zum DPPIV-Protein, wurde die tertiäre Struktur des HIV1-TAT-Proteins, die zur Klärung näherer Einzelheiten über die Wechselwirkung des Proteins mit anderen Partnern bzw. Medikamenten beitragen würde, bislang nicht aufgeklärt.

In der vorliegenden Arbeit wurde das HIV1-TAT-Protein mit unterschiedlichen Fusions-Tags funktionell in *E. coli* und *Sf9*-Zellen exprimiert und aufgereinigt. Die aufgereinigten Proteinen zeigten die TAT-spezifische Transaktivierungsaktivität. Das rekombinante TAT-Protein mit einem N-terminalen GST- und C-terminalen His-Tag zeigte die höchste Stabilität und Transaktivierungsaktivität. Weiterhin konnte mit TAT10xHis, TAT, His-TAT-His und Sf9-TAT eine partielle Hemmung der proteolytischen Spaltung von GLP1 durch DPPIV nachgewiesen werden, was wiederum die Annahme bestätigt, dass der freie N-Terminus von TAT für die Inhibition essentiell ist. Die Hemmung von DPPIV durch TAT war schwach und erreichte bei einer Konzentration von 1 µM TAT: 16 nM DPPIV die Sättigung.
Die Charakterisierung der rekombinanten TAT-Proteine mittels Gelfiltration und Elektronenmikroskopie stellte das TAT-Protein als intrinsisch unstrukturiertes Protein dar, was die Kristallisation des Proteins verhinderte.

Untersuchungen zur Interaktion des HIV1-TAT-Proteins mit dem humanen-DPPIV-Proteins in CHO-Zellen zeigten eine DPPIV-abhängige Induktion der Apoptose durch TAT. Dieser Prozess ähnelt dem raschen Zelltod, der bei der Depletion der $CD4^+$-T-Zellen in HIV-infizierten Patienten auftritt und impliziert eine Beteiligung der TAT-DPPIV-Wechselwirkung bei der Depletion von T-Zellen in HIV-infizierten Patienten.
Desweiteren, wurden das HIV1-TAT- und das humane-DPPIV-Protein in *Sf9* Zellen über das BAC-TO-BAC® Baculovirus System co-exprimiert. Im Vergleich zur DPPIV, das allein in *Sf9* Zellen exprimiert wurde, konnte bei TAT/DPPIV-co-exprimierenden Zellen eine Erhöhung der Gesamt-DPPIV-Expression beobachtet werden. Aufgrund dieser Co-Expression konnte die Co-Assoziation und direkte Bindung des HIV1-TAT mit dem DPPIV-Protein nachgewiesen werden. Die Bindung

von TAT und DPPIV in TAT/DPPIV-co-exprimierenden *Sf9*-Zellen scheint durch eine Verminderung der post-translationalen Modifikationen des TAT-Proteins möglich zu sein. Es wurde eine 78%ige Verminderung in der Serin-Phosphorylierung von TAT in TAT/DPPIV-co-exprimierende *Sf9*-Zellen festgestellt. Mit dem GST-TAT-His Protein, das Aufgrund des N-terminalen GST-Tag nicht in der Lage war die enzymatische Aktivität von DPPIV zu hemmen, konnte eine TAT-abhängige Induktion der Tyrosin-Phosphorylierung von DPPIV gezeigt werden. Dies führte zu der Annahme, dass die Inhibition von DPPIV-Enzymaktivität keine Vorraussetzung für die Induktion der Tyrosin-Phosphorylierung und somit das Einschalten von Signalkaskaden durch phosphoryliertes DPPIV darstellt.

Einer der Hauptziele dieser Arbeit war die Charakterisierung des TAT/DPPIV-Protein-Komplexes. Wie bereits erwähnt konnte im Laufe dieser Arbeit festgestellt werden, dass das TAT-Protein intrinsisch unstrukturiert ist. Desweiteren haben post-translationale Modifikationen des in Abwesenheit von DPPIV exprimierte TAT-Proteins zur Folge, dass die Bindung mit getrennt exprimierten DPPIV *in vitro* deutlich schlechter ist. In Ko-Immunpräzipitations-Versuchen konnte gezeigt werden, dass die Herstellung und Aufreinigung eines Komplexes beider Proteine nur nach deren Ko-Expression möglich ist. Jedoch stellte sich bei der Aufreinigung des TAT/DPPIV-Protein-Komplexes heraus, dass das TAT-Protein sehr instabil war. Dennoch konnte unter besonderen Vorsichtsmassnahmen ein aktiver TAT/DPPIV-Protein-Komplex aufgereinigt und für die Kristallisation eingesetzt werden. Mehrere Kristalle konnten geerntet werden. Die Röntgenstrukturanalyse der größten Kristalle zeigte allerdings keine Massendichte des TAT-Proteins, was zumindest auf seine Eigenschaft als intrinsisch unstrukturiertes Proteins zurückzuführen ist. Es konnte nur die Massendichte des DPPIV-Proteins gemessen werden.

Zusammenfassend lässt die vorliegende Arbeit schlussfolgern, dass die TAT-DPPIV-Wechselwirkung bei der Vermittlung der Tyrosin-Phosphorylierung von DPPIV eine Rolle spielt. Darüber hinaus werden Signalkaskaden initiiert, die gezielt die post-translationalen Modifikation wie beispielsweise die Serin-Phosphorylierung von TAT-Proteinen kontrollieren und somit die TAT-abhängige Induktion der HIV-Genexpression regulieren können.

Im letzten Teil dieser Arbeit wurde das humane-Caveolin-1-Protein in *E. coli* exprimiert und in seiner löslichen Form aufgereinigt. Die Interaktion des humanen-Caveolin-1-Proteins mit dem humanen-DPPIV-Protein wurde mittels Immunpräzipitation und SPR bestätigt. Die Bindungsanalyse mittels SPR liess darauf schliessen, dass die Binding von DPPIV mit Caveolin-1 relativ schwach ist und eine höhe Menge an Caveolin-1 gegenüber einer geringeren Menge an DPPIV benötigt wird.

8 Materials

8.1 Vectors

Table 8.1: Vectors for cloning and Protein over expression in Bacteria

Vector	Bacteria Selection	Purpose	Source
pRSET	Ampicillin	Over expression of 6x His recombinant protein	Invitrogen (Karlsruhe Germany)
pCR-Blunt-Vector	Kanamycin	Cloning of PCR products	Invitrogen (Karlsruhe Germany)
pGEX-4T	Ampicillin	Over expression of GST recombinant Protein.	Amersham (Freiburg, Germany
pQE-60	Ampicillin	Over expression of 6x His recombinant Protein.	Qiagen (Hilden Germany)
pFastBac1™	Ampicillin	Cloning for preparation of recombinant Baculovirus	Invitrogen

Table 8.2: Vectors for Protein expression in eukaryotic cells

Vector	Selection		Purpose	
	Bacteria	Cell culture		
pEGFP-N1	Kanamycin	neomycin	Expression of GFP fusion protein	BD Biosciences (Heidelberg Germany)

8.2 Cell lines

8.2.1 Bacteria cell lines

E. coli INVα F’ Invitrogen
E. coli (one shot®) TOP10 Invitrogen
E. coli DH10 BAC Cells Invitrogen
E. coli BL21 star™ (DE3) Invitrogen
E. coli BL21 star™ (DE3) pLysS Invitrogen

8.2.2 Insect cell lines

Sf9 cells Invitrogen

8.3 Media and cell Culture

For the preparation of media and solutions, distilled, deionised water was used. Solutions and Media were sterilised either by autoclaving at 121°C for 20 minutes or sterile filtered through a 0.22 µm Filter.

8.3.1 Media for Bacteria culture

Except otherwise indicated all Bacteria cells and cell lines were cultivated at 37°C as suspension cultures in a shaking incubator (HAT-Infors, Switzerland) at 225 rpm or on agar plates in a culture incubator (Model B; Memmert, Germany). Storage of cells for short periods up to 2 months was done at 4°C. For storage over longer periods cells were cultured to an OD_{600} of 0.3 -0.6 and glycerol was added to a final concentration of 20% (v/v). The cultures were then frozen at -80° and stored in liquid nitrogen. Frozen cells could be thawed on ice and recultured in fresh media when needed.

SOC-Medium:
20 g/l Peptone (Invitrogen)
5 g/l Yeast-Extract (Invitrogen)
0.5 g/l NaCl (Roth, Karlsruhe)
186 mg/l KCl (Roth, Karlsruhe)
10 ml 50% Glucose (sterile filtered) is added when autoclaved medium cools down to 60°C.

LB- Medium:
10 g/l Peptone
10 g/l NaCl
5 g/l Yeast extract
15 g/l Agar (only for plates)

After sterilisation of media by autoclaving and cooling down to 60°C, respective antibiotics are added for selection purposes.

Antibiotic stock Solutions:
50 mg/ml Ampicillin
35 mg/ml Chloramphenicol
50 mg/ml Kanamycin
10 mg/ml Tetracycline
7 mg/ml Gentamycin
25 µg/ml Zeocin

For blue-white selection of colonies the following substances were added:
40 mg/ml IPTG
200 mg/ml Bluo-gal

8.3.2 Media for Insect cell culture

Insect cells are cultured at 27°C either as suspension cultures in shakers (Multitron; HAT-Infors, Switzerland) at 115 rpm or as monolayer cultures in culture incubators (Heraeus, Germany). For long term storage of insect cells, cells were cultured in suspension pelleted and resuspended at a density of 2 x 10^8 cells /ml in 90% FCS (v/v) and 10% (v/v) DMSO. Cryotubes were filled with aliquots of 1 ml, frozen gradually (1°C/ml) in - 80°C and stored in liquid nitrogen. When needed frozen cells were thawed at room temperature and cultured in fresh media on plates for 24 h. Dying non-adhering cells were then removed by aspiration and viable adhering cells cultured in fresh media in suspension.

***Sf*9-cells:** *Sf*900 II medium (Invitrogen)
10 ml/l 200 mM Glutamine (Invitrogen)
100 ml/l FCS (PAA, Austria)

8.4 Mammalian cell culture

Mammalian cells and modified mammalian cell lines were cultivated as monolayer cultures on plates at 37°C, 95% humidity and 5% $C0_2$.

8.4.1 Media and reagents for cell culture

Fetal calf serum	Kraeber	(Wedel, Germany)
L-Glutamine	BioWest	(Essen, Germany)
Penicillin/streptomycin	Biochrom	(Berlin,Germany)
G418 sulfate	PAA laboratories GmbH (Linz, Austria)	

8.4.2 Mammalian cell lines and respective culture media

All the media used were from Biochrom (Berlin, Germany)

CHO: (Chinese hamster ovary cells; Epithelial): MEM Alpha, with ribonucleoside (G, 2.5 mg, A, C, T, 5 mg in 500 ml)

Hek293 (human embryonal kidney cell line) DMEM-high glucose,

HLCD4CAT (HeLa/ cervical cancer cells; epithelial with stable CD4 and HIV1-LTR/CAT): RPMI 1640

HeLa TAT III (HeLa, with stably transfected HIV1-TAT): RPMI 1640

Jurkat cell line (human leukaemia T cell line) ATCC-Nr. TIB-152: RPMI 1640

8.5 Primer and oligonucleotides used for PCR and Sequencing

Unless otherwise indicated, all the primers used were from MWG Biotech (Ebersberg, Germany).

Table 8.3 Sequencing primers

Name	Sequence	Modification
T7	5'-TAATACGACTCACTATAGGGC -3'	5' IRD 700
M13 For	5'-GTAAAACGACGGCCAG -3'	5' IRD 700
M13 Rev	5'-CAGGAAACAGCTATGAC -3'	5' IRD 700
PQE-60 Seq1C	5'-GTGAGCGGATAACAATTTCACACAG-3'	5' IRD 700
PQE-60 Seq2R	5'-GGAGTCCAAGCTCAGCTAATTAAGC-3'	5' IRD 800
pGEX 5'sequencing primer	5'-GGGCTGGCAAGCCACGTTTGGTG-3'	5' IRD 700
pGEX 3'sequencing primer	5'-CCGGGAGCTGCATGTGTCAGAGG-3'	5' IRD 800

Table 8.4: Primers and linkers for cloning and modification of vectors

Given name	Sequence	Purpose
TAT-His2 cod	5’CTAGAGCATCATCACCATCACCATTA-3'	“Sense” linker for modification of TAT-pFastBac1 vector with 6 x His-Tag
TAT-His2RevK	5’AGC**TTA**ATGGTGATGGTGATGATGCT-3'	“Antisense” linker for modification of TAT-pFastBac1 vector with 6 x His-Tag
Cav1EcoFor	5’GAATTC**ATG**TCTGGGGGCAAATAC-3'	Forward primer for amplification of Caveolin-1 cDNA
Cav1PstRev	5’GACGTCTATTTCTTTCTGCAAGTTGATGC-3'	Reverse primer for amplification of Caveolin-1 cDNA
For pBAC Vir	5’-AGATCATGGAGATAATTAACC-3’	Forward primer for PCR verification of inserts in BACMID DNA
Rev pBAC Vir	5’GTATGGCTGATTATGATCC-3’	Reverse primer for verification of inserts in BACMID DNA
CXCR4EcoFor	5’ACTATAGGGCGGCCGCGAATTC-3’	Forward primer for the amplification of CXCR4 cDNA
CXCR4XbaI-Rev1	5’GCATCTAGACTGGAGTGAAAACTTGAA-3’	Reverse primer for the amplification of CXCR4 cDNA

The underlined bases are recognition sequences of respective restriction endonucleases. The bases in bold code for start codon or stop codon respective.

8.6 Kits, Marker and Enzymes

8.6.1 Kits

T7 Sequencing™ kit	Amersham Biosciences (Freiburg, Germany)
Plasmid Midi-Kit	Qiagen (Hilden, Germany)
Plasmid Maxi-Kit	Qiagen (Hilden, Germany)
Original TA Cloning Kit	Invitrogen
Accuprime pfx Supermix kit	Invitrogen
ECL-Luminol-kit	AG Reutter-charite Berlin

8.6.2 Marker

High-Molecular-weight Protein standard	Bio-Rad
Prestained all Blue/Dual colour Standard	Bio-Rad
1 Kb DNA ladder	Fermentas, St. Leon Rot, Germany

8.6.3 Enzymes

CIAP	Fermentas
T4-DNA-Ligase	Fermentas
Taq- (*pfu*-) Polymerase	Invitrogen
All Restriction endonucleases	Fermentas

8.7 Antibodies

Anti-HIV1-TAT monoclonal antibody:	ARP352 (NIBSC, Centre for AIDS Reagents)
Monoclonal/polyclonal anti-GFP Ab:	AG Fan/Reutter (Charite Berlin)
Monoclonal/polyclonal anti-DPPIV Ab:	AG Fan/Reutter (Charite Berlin)
Monoclonal anti-phospho-tyrosine antibody:	P3300, Clone PT-66 (Sigma-Aldrich)
Monoclonal anti-phospho-serine antibody:	P3430, clone PSR-45 (Sigma-Aldrich
Monoclonal antibody to CXCR4:	ARP3101 (NIBSC, Centre for AIDS Reagents)
Rabbit polyclonal anti-Caveolin-1 Ab:	ab2910 (Abcam)
Peroxidase conjugated rabbit-anti-GST Ab:	Sigma
Peroxidase conjugated Goat anti Mouse:	Sigma
Peroxidase conjugated Goat anti rabbit:	Sigma
Peroxidase conjugated Rabbit anti mouse:	Sigma
HRP-anti-Mouse:	EnVision+® system DakoCytomation
HRP-anti-Rabbit:	EnVision+® system DakoCytomation
FITC-conjugated anti-Mouse/ Rabbit IgG:	Sigma
Cy3-conjugated anti-Mouse/ Rabbit IgG:	Sigma

8.8 Synthetic peptides

All peptides were from Genscript Corporation.

Glucagon-Like-Peptide 1:	GLP_{7-36} amide, human.
Gastric Inhibitory Peptide:	GIP_{1-42}, human
Neuropeptide Y:	NPY_{1-36}, human
Mutant TAT2-M1:	TAT_{47-57} peptide, HIV

8.9 Solutions for the purification and analysis of nucleic acids and proteins

8.9.1 Solutions for small scale purification of plasmids from Bacteria

Mini lysate solution 1:	25 mM Tris-HCl 50 mM Glucose 10 mM EDTA 2 mg/ml RNase A pH 8.0
Mini lysate solution 2:	0.2 M NaOH 1 % SDS (w/v)
Mini lysate solution 3:	3 M NaOAc, pH 4.8

8.9.2 Solutions for the electrophoretic analysis of nucleic acids

TAE-buffer:	0.04 M Tris 5 mM Na-acetate 2 mM EDTA pH 8.0

TE-buffer:
10 mM Tris-HCl, pH 8
1 mM EDTA

5x Sample buffer:
25 % Glycerine
50 mM EDTA
0.1 % Bromo-phenol blue

8.9.3 Solutions for the purification and analysis of proteins

8.9.3.1 Buffers for cell lysis and solubilisation of Protein

RIPA:
50 mM Tris-HCl pH 7.2
150 mM NaCl
1% Triton-x-100
1% Na-Deoxycholate
0.1% SDS

Prewash:
10 mM Tris-HCl pH 7.2
1 M NaCl, 0.1% Triton-x-100

DPPIV native solubilisation buffer:
10 mM Tris pH 7.8
150 mM NaCl,
1 mM $CaCl_2$
2% CHAPSO
Trasylol (500 KU)

DPPIV native washing buffer 1:
50 mM Tris pH 7.2
1M NaCl,
0.5% n-octyl-β-D-glucopyranoside
Trasylol (500 KU)

DPPIV native washing buffer 2:
10 mM Tris pH 7.2
150 mM NaCl,
0.1% n-octyl-β-D-glucopyranoside
Trasylol (500 KU)

DPPIV Elution buffer:
50 mM Diethylamine pH 10.8

CXCR4GFP native solubilisation buffer:
10 mM Tris pH 8.5
100 mM $NH_4(SO_4)_2$,
10 % glycerol
2% (w/v) n-dodecyl-β-D-maltoside
0.5% CHAPS
Protease inhibitors and 1 mM DTT

CXCR4GFP Elution buffer:
50 mM Diethylamine pH 11.2

HIV1-TAT solubilisation buffer:
20 mM Tris pH 7.4
150 mM NaCl
0.5 % (v/v) Triton X100

	+ 1 mM of DTT, EDTA, PMSF Trasylol (1:1000) as protease inhibitor
Caveolin 1 solubilisation buffer:	20 mM Tris pH 7.4 150 mM NaCl 1% (w/v) n-dodecyl-b-D-maltoside 10 % PEG-400 + 1 mM of DTT, EDTA, PMSF Trasylol (1:1000) as protease inhibitor

8.9.3.2 Solutions and buffers for SDS PAGE and western blot

SDS PAGE

Solution A:	30 % acrylamide (w/v) 0.8 % N, N' Methylenbisacrylamide (w/v)
Solution B:	0.2 % SDS (w/v) 1.5 M Tris-HCl, pH 8.8
Solution C:	0.4 % SDS (w/v) 0.5 M Tris-HCl, pH 6.8
10 x running buffer:	0.25 M Tris-HCl, pH 8.0 1.92 M Glycin 1 % SDS (w/v)
5x Sample buffer (reducing)	0.3 M Tris HCl, pH 6.8 15 % SDS (w/v) 50 % Glycerine (v/v) 0.015 % Bromo phenol blue (w/v) 25 % beta Mercapto ethanol (v/v) 5 mM DTT

5x Sample buffer (non-reducing)
Like reducing buffer, without SDS and DTT

Western blot

Transfer buffer:	160 mM Glycine 20 mM Tris-HCl, pH 8.3 10 % Ethanol
Ponceau-S-Staining solution:	0.2 % Ponceau Red (w/v) 1.5 % TCA (v/v) 1.5 % Sulfosalicylic acid (v/v) 0.1 % citric acid (v/v)
Coomassie staining solution:	40 % Methanol (v/v) 10 % citric acid (v/v) 1 g/l Serva-Blue G-250

Washing buffer for western blots

PBS:	1.5 mM KH2PO4 8 mM Na_2HPO_4 140 mM NaCl 3 mM KCl pH 7.4
PBS-Tween:	0.1 % Tween 20 (v/v) in PBS

ECL Solution for blot development:

Luminol A:	6.8 mM p-Cinnamic acid in DMSO
Luminol B:	1.25 mM Luminol in 0.1 M Tris-HCl, pH 8,5
Luminol C:	3 % H_2O_2 (v/v)

8.10 Chemicals and other materials

All chemicals except otherwise indicated were from Sigma Aldrich (Munich, Germany), Roth (Karlsruhe, Germany), Merck (Darmstadt, Germany), Boehringer Ingelheim (Ingelheim, Germany),

Aminoacids	Sigma, Munich
Ampicillin/Kanamycin	Boehringer, Mannheim
N, N'-Bisacrylamide	Serva, Heidelberg
BSA Standard	Pierce, Rockford USA
4-Hydroxycinamic acid	Sigma, Munich
G418 Sulphate	PAA, Austria
Luminol	Sigma, Munich
β-mercapto ethanol	Roth, Karlsruhe
Nitrocellulose-Membrane	Schleicher and Schüll, Dassel
PEG-3350	Sigma, Munich
PEG-400	Sigma, Munich
PMSF	Sigma, Munich
TCEP-HCl	Sigma, Munich

Other reagents and materials used as well as their sources are indicated in the methods section.

8.11 Instruments and Apparatuses

Name of instrument	**Type**	**Manufacturer**
UV-Table	Gel-Print 2000i	MWG-Biotech
Autoclave	Varioklav	Sauter-Schubert
Incubator	BK 6160,	Heraeus
Sterile bench	Faster 1,	BioFlow-Technik
Gel electrophoresis Tanks	B1A, B2	Bio-Rad
Luminescent-Image- Analyser	Universal Hood II	Bio-Rad
Microplate reader	Spectra Rainbow	TECAN, Austria
Heating block	Thermomixer 5336,	Eppendorf
Hybaid Thermocycler	Touch-Down	MWG-Biotech

Cool centrifuge	Centrikon H-401,	Kontron Instruments
Membrane-Vacuum pump	Vacuubrand	
Microwave	RZV2G,	Sharp
Pipettes	Eppendorf Research,	Eppendorf
Power Supply Systems	Power-Pac 1000,	Bio-Rad
SDS PAGE system	Mini-Protean II,	Bio-Rad
MALDI-TOF-MS analyser	Bruker Ultra Flex III	Bruker Daltonics
Sequencer	LI-COR 4200	MWG-Biotech
SE-Chromatography system	ÄKTA purifier	GE Healthcare
Spectral photometer	Ultrospec 3000	Pharmacia
Centrifuge	Biofuge Pico	Heraeus
Vortex	Vortex-genie 2	Bender and Hobein
Centrifuge	Megafuge 1.0	Heraeus
One shot cell disrupter	Constant cell disrupting system	Constant systems Daventry, UK
Sonicator	Labsonic	Braun Biotech GmbH
Confocal microscope		Zeiss
pH meter	pH 211	Hanna instruments
Flow cytometer	FACScan	Becton Dickinson
BIACORE	Biacore$^{(R)}$ 2000	GE Healthcare

9 Methods

Most of the methods used in this work, are routine methods used in normal molecular biology and biochemistry laboratories with little or no modifications. A detailed outline of all the methods is not reported in this section. A more detailed outline of the methods used and their references are stated in Ausubel *et al.* (2002): Current Protocols in Molecular Biology, Vol.1+2 and Maniatis *et al.* (1989): Molecular cloning: a laboratory manual Vol. 1-3.

9.1 Molecular biology methods

9.1.1 Cloning and preparation of plasmids for protein expression

9.1.1.1 Cloning of human Caveolin-1 in pGEX4T-2 vector

The full length human-Caveolin-1 cDNA was amplified by RT-PCR from the cDNA panels of different human organs as described under section **9.1.7.1.** The PCR product were purified by gel-elution then cloned into the pCR-blunt vector. The Cav1 cDNA was then excised via the EcoRI and PstI sites and cloned into the pGEX4T-2 vector which was linearised with EcoRI and PstI enzymes (**Figure 9.1**). The resulting GSTCav1 protein contains a seven residue linker between GST and the Cav1 protein which constitutes part of the recognition sequence for thrombin cleavage.

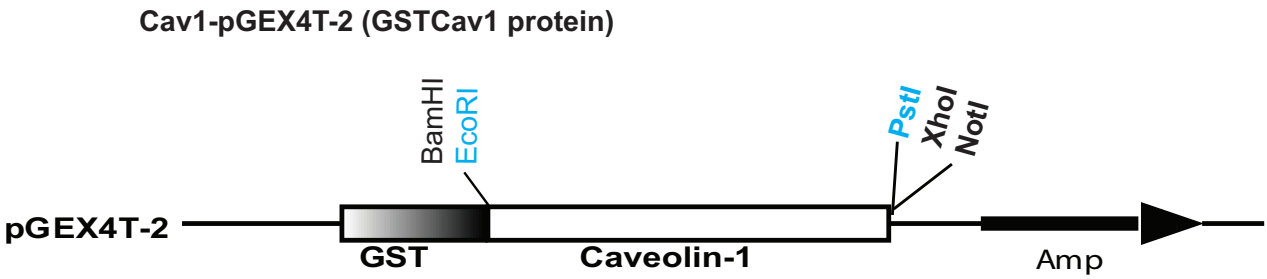

Figure 9.1: Extract of the Cav1-pGEX4T-2 plasmid construct

9.1.1.2 Cloning of TAT in pFastBac1 vector

The TAT-pFastBac1 plasmid was available in the group of Dr. Fan at the beginning of this work. To insert a 6xHis Tag to the vector the linker primer, TAT-His-cod and TAT-HisRev2K (see section 8.5) were annealed by heating at 99°C for 10 min then left to cool gradually at RT. The annealed "Xba1-6xHis-HindIII linker" was then ligated into the XbaI and HindIII site of linearised TAT-pFastBac1 plasmid. This resulted to the TATHis-pFastBac1 plasmid (**Figure 9.2**A-B). In order to have more recognition sites for cloning, the TAT6xHis was excised from the TATHis-pFastBac1 plasmid with EcoRI and DraI enzymes and re-ligated in the EcoRI and StuI site of the original pFastBac1 vector. This resulted to the TATHis-pFastBac1-MCS plasmid (**Figure 9.2**C).

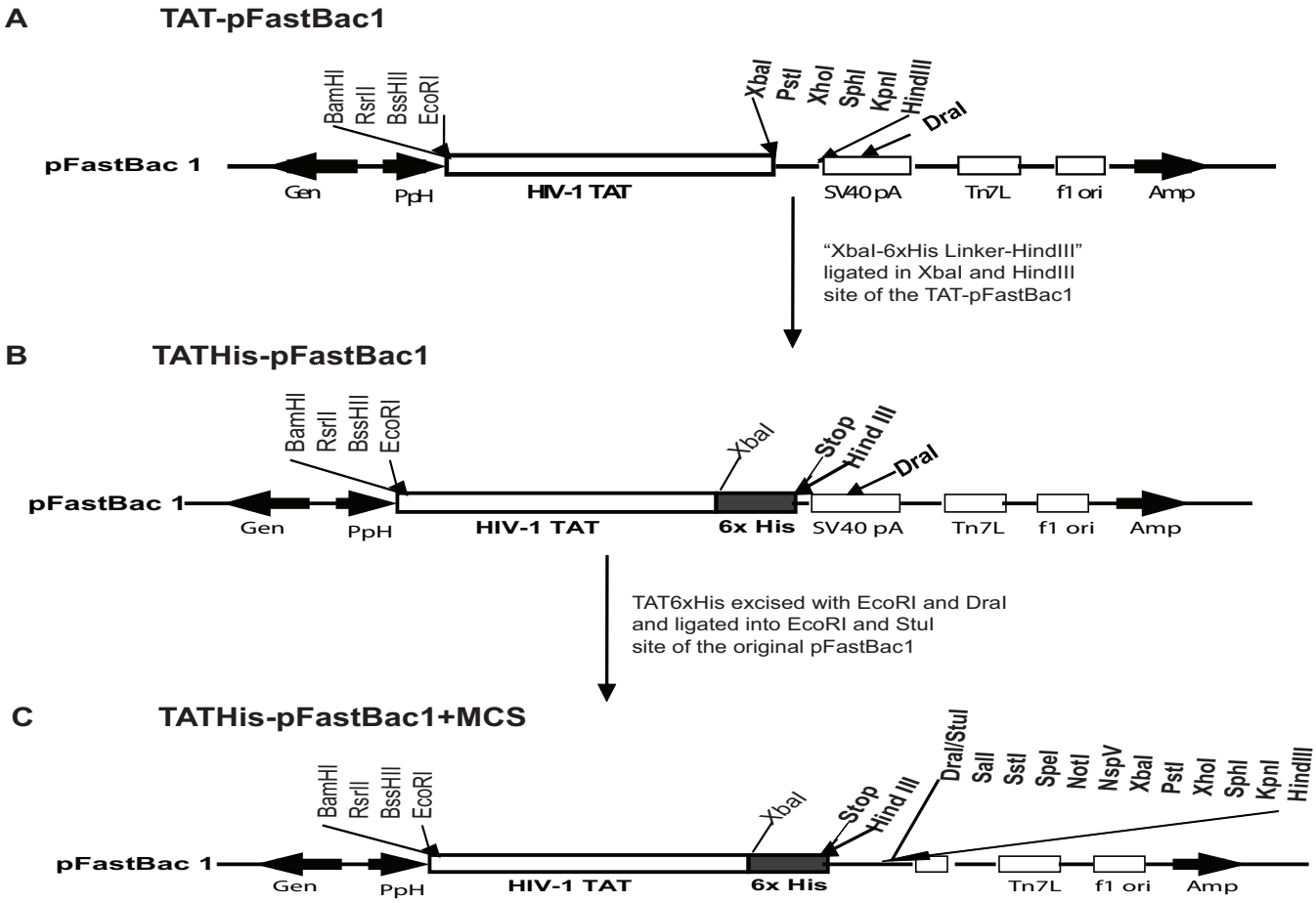

Figure 9.2: Constructs of TAT in pFastBac1

9.1.1.3 Cloning of TAT in pGEX4T-3, pRSET-B, pQE-60 and pEGFP-N1

TAT cDNA was excised from the TAT-pFastBac1 plasmid with the EcoRI and XhoI restriction enzyme and cloned into the EcoRI/XhoI linearised pGEX4T-3 vector. This resulted in TAT-pGEX4T-3 for the expression of GST-TAT protein with a thrombin cleavage linker of 7 residues between GST and the TAT protein (**Figure 9.3**B). The TATHis DNA was excised from the TATHis-pFastBac1-MCS plasmid with the EcoRI and DraI restriction enzymes and ligated into the EcoRI/StuI-linearised pGEX4T-3 vector. This resulted to the TATHis-pGEX4T-3 plasmid for the expression of GST-TAT-His protein with a linker of 7 residues between GST and the TAT protein which constitutes the thrombin recognition sequence (**Figure 9.3**A).

TATHis cDNA was restricted from the TATHis-pFastBac1 plasmid with the EcoRI and HindIII endonucleases and ligated into the EcoRI/HindIII linearised pRSET-B vector. TATHis-pRSET-B plasmid for the expression of the His-TAT-His protein resulted (**Figure 9.3**C).

The TAT-pEGFP-N1 plasmid was constructed by excising the TAT cDNA from the TAT-pFastBac1 plasmid with EcoRI and KpnI enzymes and ligating into the EcoRI/kpnI-linearised pEGFP-N1 vector (**Figure 9.3**D).

The original TAT1-86 cDNA was got from the Centralised Facility for AIDS Reagents, in the mammalian vector pC63.4.1. The cDNA carried an NcoI site next to its start codon and a stop

codon within the BamHI restriction site. The TAT cDNA was excised from this vector with the NcoI and BamHI enzymes and ligated in the pQE-60 vector which was linearised with the same enzymes. This resulted to the TAT-pQE-60 plasmid which was used in expressing the TAT1-86 (untagged due to stop codon at the end of TAT) in *E. coli*,(**Figure 9.3**E).

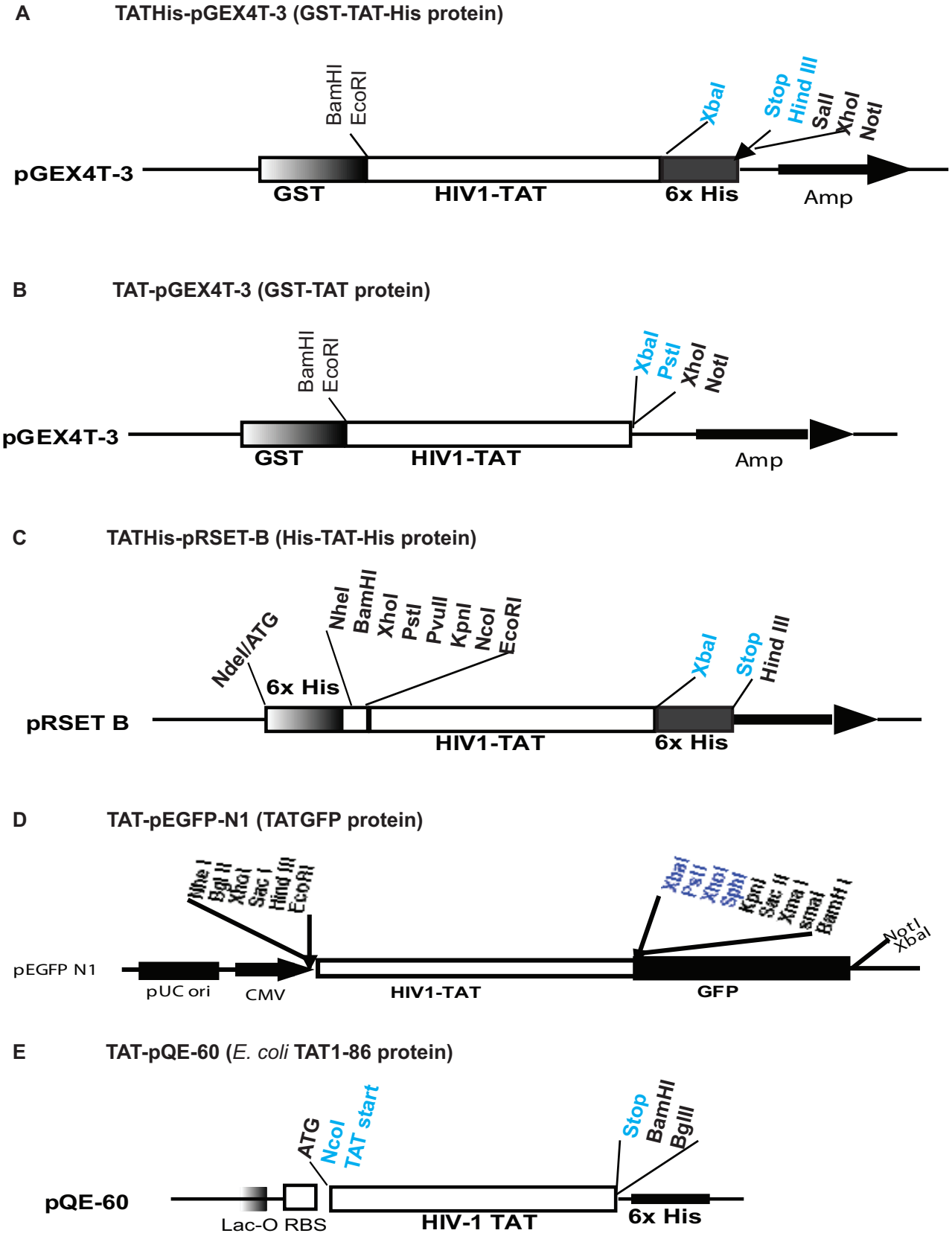

Figure 9.3: Constructs of TAT in pGEX4T-3, pRSET-B pEGFP-N1 and pQE-60 vectors

9.1.1.4 Cloning of CXCR4 in pFastBac1 and pEGFP-N1

The plasmid bearing the cDNA of human-CXCR4 variant II was got from OriGene Technologies Inc (Rockville). The CXCR4-coding cDNA was amplified by PCR with the primers CXCR4EcoFor and CXCR4XbaI-Rev1 then purified by gel elution and cloned in the pCR-Blunt vector. The cDNA was then excised with the EcoRI and XbaI restriction enzymes (see cDNA sequence under **11.2.1**) and ligated in the pFastBac1 vector. This provided the CXCR4-pFastBac1 plasmid (**Figure 9.4**A). The CXCR4-cDNA was excised from the CXCR4-pFastBac1 plasmid with the EcoRI and KpnI restriction enzymes and ligated into the pEGFP-N1 vector which was linearised with the same enzymes. The resulting CXCR4-pEGFP-N1 vector was used in expression of CXCR4GFP in the mammalian cell lines CHO and Hek293 (**Figure 9.4**B).

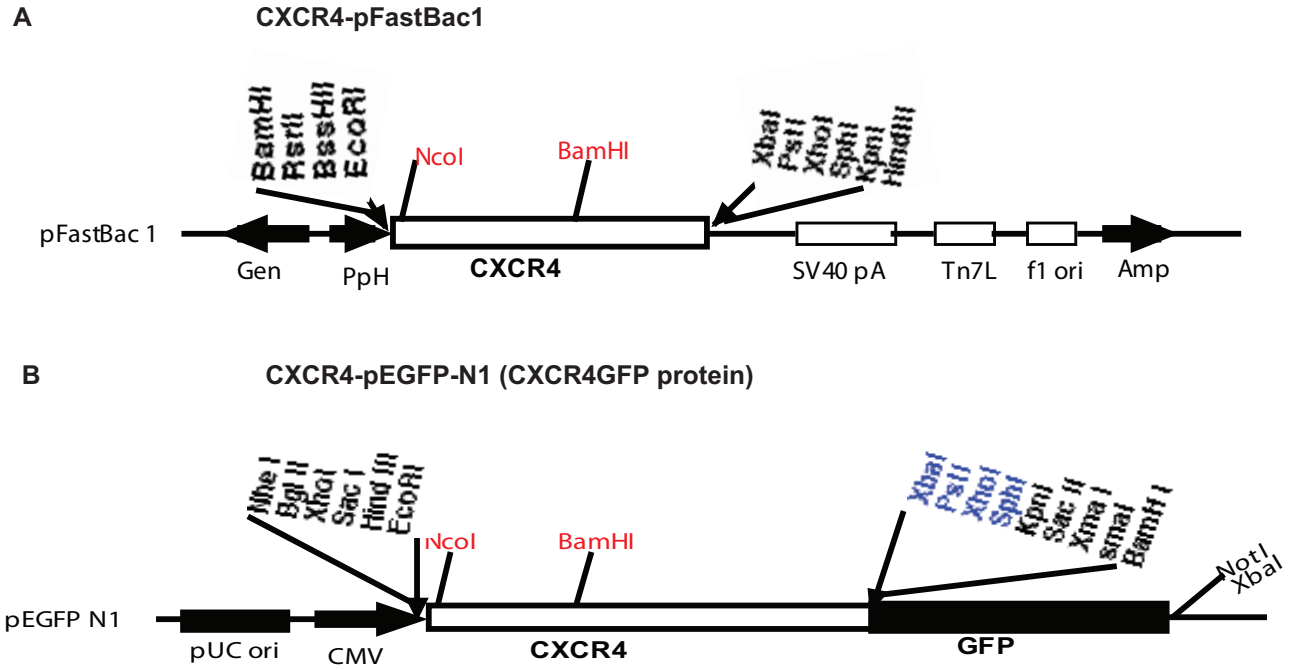

Figure 9.4: Cloning of CXCR4 in pFastBac1 and pEGFP-N1 vectors

9.1.2 Plasmid preparation

After preparation of *E. coli* overnight cultures, 2 ml were aliquoted in reaction tubes and centrifuged at 8000 rpm for 5 minutes. The bacteria pellets were then homogeneously resuspended in 200 µl buffer 1 (50 mM Tris-HCl, pH 8, 10 mM EDTA, 100 µg/ml RNase A). 200 µl of buffer 2 (0.2 M NaOH, 1% SDS) was added and mixed carefully. Incubation was done at room temperature for 5 minutes and 200 µl cold buffer 3 (3 M Na-acetate pH 5.5) was added. The suspensions were mixed carefully and incubation done on ice for 10 minutes. Following this, the samples were centrifuged for 10 minutes at 13000 rpm and 4°C to pellet cellular proteins and DNA, the supernatants decanted in clean tubes and the centrifugation step was repeated. Supernatants from this centrifugation were put in clean tubes, mixed thoroughly with 450 µl isopropanol and incubated

at -20° C for 15 minutes to precipitate the plasmid DNA. The precipitated DNA was pelleted by a 10 minutes centrifugation at 13000 rpm at 4°C and the DNA pellet washed with 500 µl of 80% ice cold ethanol. The plasmid DNA was then air dried, resuspended in 50 µl sterile ddH_2O and the concentration determined. Storage was done at -20°C. For such small scale plasmid preparation, about 500 -1000 µg total Plasmid-DNA/ml Bacteria culture was extracted. For the extraction of larger amounts of plasmid DNA, 50- 200 ml overnight cultures were used and the extraction done with the Qiagen Maxi-preparation kit (Qiagen, Hilden) according to the user manual.

9.1.3 Determination of DNA concentration

The concentration of a DNA solution is determined by spectral photometric measurements of their absorption at 260 nm. The extinction value = 1 in such measurements represent 50 µg/ml double stranded DNA. The purity of the DNA probe can be deduced from the ratio of its absorption from 260 nm to 280 nm. Pure DNA solutions have an extinction quotient of about 1.8.

9.1.4 Enzymatic modification of DNA with restriction endonuclease

For restriction purposes, 1-50 µg DNA was digested for 1 to 4 h at 37°C with 0.1-1 U of appropriate restriction enzymes from Fermentas (St. Leon-Roth, Germany) or Invitrogen (Karlsruhe, Germany) in their respective buffer. The digested DNA was then analysed by agarose - gel electrophoresis and the detected bands excised from the gel and purified by gel elution with the Gel Extraction II kit (Macherey and Nagel).

9.1.5 Dephosphorylation of DNA

For ligation purposes, plasmid DNA linearised with only one enzyme was dephosphorylated with calf intestinal alkali phosphatase (CIAP, Invitrogen) to prevent re-ligation of the vector. A dephosphorylation reaction composed of 1 pmol 5'-DNA-end, 5 µl CIAP, 10 µl 10x dephosphorylation buffer and ddH_2O to a final volume of 50 µl. Incubation was carried out for 1 h at 65°C. The reaction was stopped by heating for 15 minutes at 85 °C and the DNA cleaned up with the QIAquick PCR-purification kit (Qiagen, Hilden).

9.1.6 Ligation of DNA fragments

Ligations were done with T4-DNA-Ligase (Fermentas, St. Leon-Roth) over night at 14°C A standard ligation reaction composed of digested DNA (500 ng insert :100 ng vector, 1 µl T4-DNA-Ligase (10 U), 2 µl 10x ligation buffer and sterile ddH_2O to 30 µl final volume. 15 µl of the ligation reaction was used to transform competent *E. coli* cells.

9.1.7 Polymerase Chain Reaction (PCR)

PCR enables the exponential amplification of defined DNA fragments *in vitro* (Mullis & Faloona, 1987). For each reaction, two oligonucleotide primers are needed which are complementary to the 5' and 3' ends of the template DNA. The 5'-primer is usually in a sense orientation whereas 3'-primer is reverse complementary to the amplified DNA. The DNA polymerase amplifies from each of the primers in a 5' - 3' direction, such that a sense and an antisense strand are produced in each cycle of the reaction. A single reaction cycle begins with denaturation of the DNA into single strands then the binding (annealing) of the primer to the single strands at primer-suitable temperatures, followed by amplification of the DNA matrix by the polymerase. Heat stable DNA-polymerase from thermophilic bacteria e.g. *Taq*- polymerase from *Thermos aquaticus*, are used which can withstand the high temperatures reached during DNA denaturation.

PCR reactions for cloning purposes were carried out with the *pfu* polymerase (Invitrogen) which produces DNA blunt ends suitable for direct self ligation or ligation in a PCR blunt vector. The *pfu* polymerase from the thermophilic archae-bacterium, *Pyrococcus furiosus* has a 3'- 5' exopolymerase proofreading activity which enables the recognition and elimination of wrongly inserted nucleotides.

In this work all PCR for cloning purposes were done with the Accuprime-*pfx*-Supermix kit (Invitrogen) according to the manufacturer's instructions. In such PCRs a standard reaction sample of 25 µl total volume composed of the following:

Template DNA:	1- 200 ng
Primer (forward and reverse):	200 nM each
Accuprime pfx Supermix:	22.5 µl

The reaction was carried out in a Touch-Down-Thermo cycler (Hybaid, MWG-Biotech) with the following program (with slight modification of annealing temperatures depending on primer used):

Denaturation	1 cycle:	94°C,	3 min
	24-30 cycles:		
Denaturation		94°C,	30 sec
Annealing		45-60°C	1 min
Elongation		68°C	2 min pro kb of the amplified DNA
Proofreading	1 cycle:	68°C	5 min

Standard control PCRs were done with *Taq* DNA polymerase (Fermentas) according to the manufacturer's instructions. In such PCRs, a standard reaction sample of 50 µl total volume composed of the following:

Template DNA	1- 100 ng
Primer (forward and reverse):	20 pmol each
dNTP	2 mM
$MgCl_2$	2 mM

10x Taq buffer	5 µl
Taq polymerase	0.6 µl
dd H_2O to 50 µl final volume	

The reaction was carried out in a Touch-Down-Thermo cycler (Hybaid, MWG-Biotech) with the following program (with modification of annealing temperatures depending on primer used):

Denaturation	1 cycle:	94°C,	3 min
	25-30 cycles:		
Denaturation		94°C,	30 sec
Annealing		45-60°C	30 sec
Elongation		72°C	1 min pro kb of the amplified DNA
	1 cycle:	72°C	5 min

Primers used in the amplification of DNA by PCR are listed under the materials section of this work. After each PCR, analysis of a 5 µl aliquot was done by agarose gel-electrophoresis.

9.1.7.1 Reverse Transcription-Polymerase Chain Reaction (RT- PCR)

RT PCR as the name goes is a reverse transcription reaction, whereby mRNA is isolated from a tissue then “reverse transcribed” into its complementary DNA form. For this reaction a DNA-polymerase with reverse transcriptase activity is used.

In this work the RT-PCR method was applied to amplify Caveolin-1 cDNA from a panel of cDNAs of 10 different human organs (heart, liver, lungs, kidney, placenta, skeletal muscle, colon, brain and spleen). The primers used were Cav1EcoFor and Cav1PstRev which dock the first 18 and the last 23 bases of the ORF of Cav1 respectively. Additional bases coding the recognition sites of EcoRI and PstI restriction enzymes were linked to the primers respectively. The human cDNA panels (Biochain Institute Inc.) were a kind gift from Prof. Stephan Hinderlich. A comparison of RT PCR products from different tissues was quantified for expression levels of Caveolin 1 in these human organs or tissues. The Accuprime pfx Supermix kit (Invitrogen) was used for the RT PCR according to the manufacturer’s instructions. A 50 µl PCR sample was made up of the following components:

1 µl	template DNA (100 ng)
1 µl	Cav1EcoFor primer (100 pM)
1 µl	Cav1PstRev primer (100 pM)
45 µl	Accuprime pfx Supermix
2 µl	dd H_2O

After pippetting the samples on ice the tubes were spinned briefly then inserted in a PCR cycler and subjected to the following program.

Denaturation	1 cycle:	94°C,	1 min
	30 cycles:		

Denaturation		94°C,	30 sec
Annealing		54°C	1 min
Elongation		68°C	2 min pro kb of the amplified DNA
Proofreading	1 cycle:	68°C	5 min

After the reaction, DNA sample buffer was added and the samples analysed by agarose gel-electrophoresis. The DNA bands were excised from the gel and purified by gel elution. The purified PCR products (with blunt ends) were then ligated into the pCR-blunt vector (Invitrogen) and used to transform *E. coli* INVαF' or *E. coli* Top10 cells. Plasmids were prepared form the cells and then sequence verified.

9.1.8 DNA Sequencing

All the cDNA constructs used in this work were sequenced by the Sanger dideoxy method, whereby a controlled termination of enzymatic replication of the constructs are analysed. The Thermo Sequenase Primer Cycle Sequencing Kit (Amersham Biosciences, Uppsala, Sweden) was used according to manufacturer's instructions. Primers used for sequencing are listed in the materials section of this work. The sequencing primers are labelled with infrared fluorescent dyes (IRD700 and IRD800).

In a typical sequencing reaction the DNA to be sequenced serves as matrix for the polymerisation of a fluorescent labelled complementary strand. For this purpose 1.3 µg DNA was mixed with 1 µl of a 2 picomolar primer solutions and sterile distilled water added to 13 µl final volumes. 3 µl of this mixture was transferred to four tubes containing 3 µl of one of the sequencing reagents A, C, G or T. Besides the dNTPs (Deoxynucleoside triphosphate) each of the reagents contains an excess of one of the dNTPs (Dideoxynucleoside triphosphate) which leads to the interruption of the polymerisation reaction. The reaction was run in a Touch-Down-Thermocycler (Hybaid, MWG-Biotech) with the following program:

Denaturation	94°C,	3 min	1 cycle:
Denaturation	94°C,	20 sec	
Annealing	45-60°C	20 sec	
Elongation	72°C	20 sec	
	Total number of cycles:	24	

To stop the reaction 5 µl stop solution was added and run for 3 min at 72°C.

The reaction product were separated on a 6% acrylamide gel and analysed in an automatic sequence analyser (Licor 4000 L, MWG-Biotech Munich Germany).

9.1.9 Agarose gel electrophoresis

The separation of linear DNA fragments in a given sample by agarose gel-electrophoresis is enabled by their sizes. The flow speed of the DNA molecules on the agarose gel is inversely proportional to

the logarithms of their molecular weights. The higher the molecular weights of the linear DNA fragments, the lower their speed on agarose gels.

In this work agarose gel electrophoresis was applied for molecular weight determination of DNA fragments after enzymatic cleavage, purification of DNA fragments and quality control of DNA fragments from PCR. DNA molecules ranging between 300-10000 bp were separated horizontally on a 0.5 to 2 % (w/v) agarose gels. The agarose (Amersham Biosciences) were dissolved in TAE buffer and boiled to a homogeneous transparent gel. After cooling down to 60°C the gels were poured in electrophoresis tanks provided with gel combs and left at room temperature to solidify. After solidification the combs are removed. The gels are then immersed in TAE running buffer in an electrophoresis tank. Samples premixed with bromo-phenol blue-loading buffer are then loaded in the slots. In each case a 1 Kb DNA standard (Invitrogen) is loaded for size determination.

The electrophoresis is then run with 70-80 volts (5 V/cm) for 45- 60 min. The gels are then stained for visualization by incubating the gels for 5 – 10 min. in an ethidium bromide bath (0.5 µg/ml in TAE buffer). Ethidium bromide intercalates in the DNA and fluoresces thus making the DNA fragments visible under UV light (366 nm).

9.1.10 Extraction of DNA from agarose gels by gel elution

After electrophoresis, DNA fragments needed for further cloning can be isolated from the gel by melting the gel piece containing the fragment in a suitable buffer and purification of the DNA from this gel-buffer mixture. For this purpose known DNA fragments were excised from gels under a UV lamp and the DNA purified with the Nucleospin Gel Extract II kit (Macherey und Nagel) according to manufacturer's instructions. The buffers contained in the kit make it possible for the agarose to melt at temperatures as low as 50°C and also lead to a suitable DNA conformation, enabling DNA binding to the silica gel membrane provided in the kit. The bound DNA is washed on the column, thereby assuring elimination of contaminants like oils, salts, enzymes, ethidium bromide and agarose. Elution of the purified DNA is done with 20- 50 µl elution buffer depending on the intensity of the DNA band as seen under UV lamp.

9.1.11 Preparation of competent *E. coli* cells

Competent *E. coli* cells are cells which are able to take up circular DNA lying free in their vicinity. Treatment of E. coli cells with $CaCl_2$ makes their plasma membranes permeable for DNA molecules (Dagert and Ehrlich, 1979). The *E. coli* cell lines Top10, InvαF' or BL21 (BL21 star^{TM} (DE3) pLysS) were made competent for transformation by treatment with $CaCl_2$. Briefly, 100 ml SOB medium was inoculated with 2 ml overnight culture of the cells and grown at 37°C and 225 rpm aeration, to an OD_{600} of 0.3 to 0.4. The cells were harvested by centrifugation at 4000 rpm for 10

min. The cell pellets were then resuspended in 20 ml ice cold 100 mM $CaCl_2$ and incubated on ice for 30 min. A further centrifugation of the cells and incubation in 1 ml cold 100 mM $CaCl_2$ for 1 h rendered the cells competent and ready for transformation. The cells were either used immediately for transformation or mixed with 20% glycerol (v/v) and stored at -80°C in aliquots of 100 µl each.

9.1.12 Transformation of competent *E. coli* cells with plasmid DNA

The incorporation of foreign DNA molecules by *E. coli* leads to the modification of their total genetical material, thereby to their transformation. Competent *E. coli* cells were transformed to either amplify a known plasmid DNA for further isolation (*E. coli* cell lines Top10 and InvαF'), for the preparation of bacmid for transfection in insect cells (*E. coli* cell line DH10 BAC) or for protein expression (*E .coli* BL21 star™ (DE3) pLysS).

For the transformation of 100 µl competent cells, 100 ng plasmid-DNA or 10-20 µl ligation products were added to the cells on ice and incubated for 30 min. After heat shocking the cells at 42°C for 45 sec and regeneration on ice for 2 min. 250 µl SOC medium was added and mixed briefly. The cells were incubated for 1 h at 37°C in a thermomixer with mixing at 500 rpm. 100 µl aliquots were plated on solid LB-agar medium supplemented with respective antibiotics and the plates incubated over night at 37°C.

9.1.13 Expression of recombinant protein in *E. coli*

The expression of GST fusion proteins in *E .coli* was done according to instructions of the manufacturer of the expression vector pGEX-4T (Amersham Biosciences), whereas the expression of 6x His fusion proteins were according to instructions of the manufacturer of the pRSET and pQE-60 (Qiagen) expression vectors.

E .coli BL21 star™ (DE3) pLysS cells (Invitrogen) were transformed with the expression vector constructs carrying the open reading frame of the gene of interest and positive clones selected by virtue of their growth on solid LB-medium containing the antibiotics ampicillin/ chloramphenicol. To determine which of the clones express the highest rate of the fusion protein, 5x 5 ml LB-medium containing the former antibiotics were inoculated with 5 distinct colonies and grown overnight at 37°C with shaking at 225 rpm. For each of the colonies 20 ml LB medium was inoculated with 150 µl overnight culture and grown at 37°C to an OD_{600} of 0.4- 0.6. At this exponential growth phase induction of protein expression was done by addition of 1 mM IPTG. Incubation then continued at 37°C for 3 hours. The cells were harvested by 10 min centrifugation at 4000 rpm, washed with PBS buffer then resuspended in PBS lysis buffer (PBS containing 1 mM DTT, 1 mM EDTA and 1 mM PMSF). Cell lysis was done by sonication or with a Constant cell disruption system (Constant systems, Daventry, Northants- UK) and the cytosolic fractions containing the fusion proteins were

separated from other cell debris by 30 min centrifugation at 15000 rpm, 4°C. The cytosolic supernatant were then analysed by western blots for the presence of the fusion protein.

From a comparison of the western blot analysis of the 5 colonies, it could be seen if the expression rate is same for all colonies or if some had higher rates. In each case a colony with the highest rate was chosen for further large scale expression. For such large scale expressions 2- 5 litres LB selection medium were inoculated with 50- 250 ml overnight cultures and grown at 37°C till the exponential growth phase was reached. Induction of protein expression was then done by addition of IPTG to a final concentration of 1- 4 mM depending on the fusion protein and expression vector. The cells were then incubated for 3- 4 hours then harvested by centrifugation as stated above and the cell pellets stored at -20°C for eventual purification of the fusion protein.

9.1.14 Expression of recombinant proteins in insect cells

In this work the expression of recombinant protein in *Sf9* insect cells was done by use of the BAC-TO-BAC™- Baculovirus expression system. The system is based on the transposition of a gene of interest from a donor plasmid into a Bacmid which is then inserted into insect cells with the help of Baculovirus particles as displayed on the picture below.

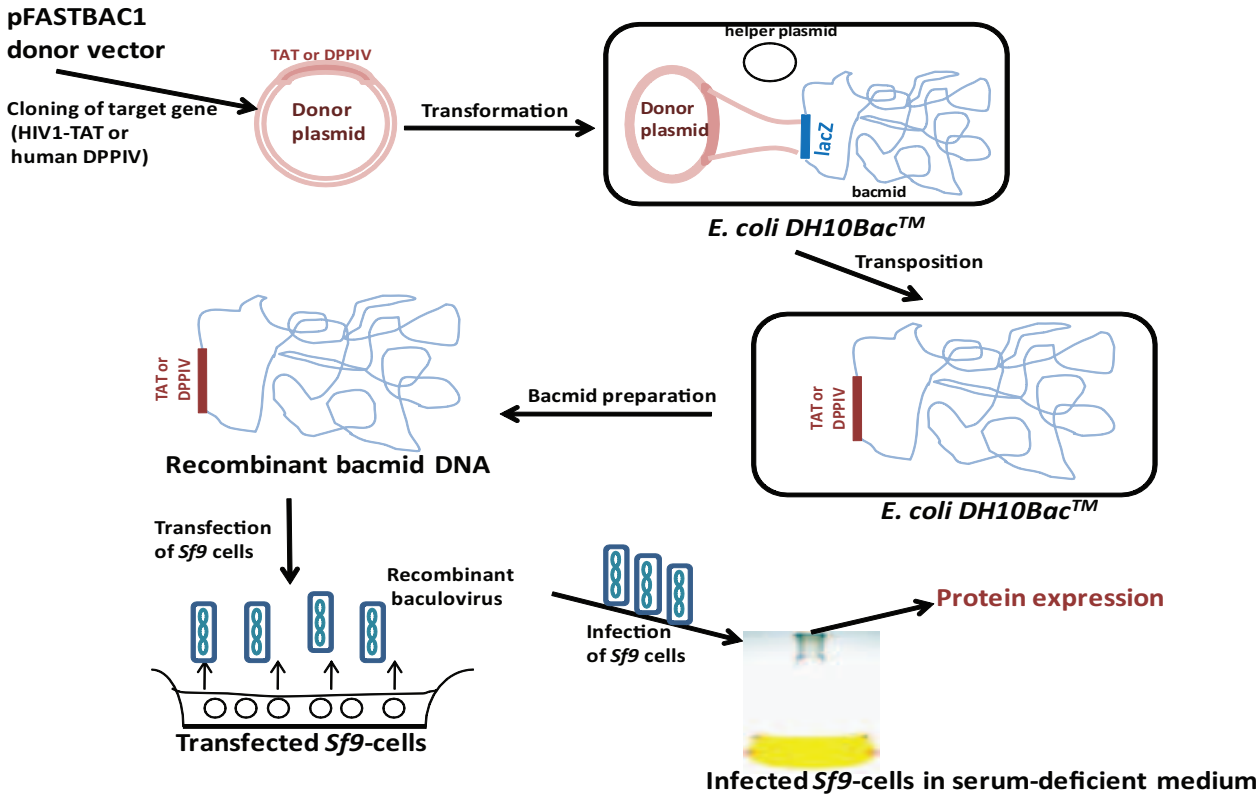

Figure 9.5: Expression of HIV1-TAT and h-DPPIV by the BAC-TO-BAC baculovirus expression system

9.1.14.1 Transformation of *E. coli* DH10-Bac cells and preparation of Bacmid DNA

For the purpose of protein expression in insect cells the gene of interest is cloned into a donor plasmid carrying the mini Tn7 elements from *E. coli* on both sides of its MCS. Transformation of *E. coli* DH10Bac cells (carry helper plasmids and Bacmid with the mini attTN7 sites) with the donor plasmids enables transposition of the gene of interest into the Bacmid. A recombinant bacmid bearing the gene of interest is then produced and can be isolated from the DH10Bac cells.

In this work the preparation of DPPIV and TAT recombinant Bacmid DNA for further transfection in *Sf9* cells, was done by first cloning the cDNA into the MCS of the pFastBac1 donor vector as described earlier (**9.1.1.2**). The plasmids were transform in the *E. coli* cell line DH10Bac (Invitrogen) according to the user manual. Blue white selection was done and positive (white) clones in which transposition of the gene of interest took place into the host LacZ gene, (cells lose the ability to express the enzyme β-galactosidase which cleaves the bluo gal substrate to a blue homolog) were used for culturing in liquid media. Bacmid preparation was performed with the Plasmid purification kit (Qiagen). Since the recombinant Bacmid DNA are very large (23000 bp) special care is taken during purification in order to avoid destruction of the Bacmid DNA.

The recombinant baculovirus of human DPPIV was available, so only that of the HIV1-TAT were prepared.

9.1.14.2 Analysis of Bacmid DNA

After purification of the Bacmid DNA it is necessary to analyse them for their purity and also intactness. After determining the bacmid DNA concentration 1 µg of the DNA was loaded on 0.6 % agarose gels and electrophoretic separation carried out at 20v overnight (16-19 h). Visualisation of the DNA bands was done under UV after staining in ethidium bromide. A λDNA digested with Hind III was used as standards for determination of molecular weights.

A second analysis of the recombinant Bacmid DNA was done by PCR with specific primers for the gene of interest (DPPIV, HIV1-TAT) in order to verify their presence in the Bacmid DNA.

9.1.14.3 Generation of recombinant virus

In order to get recombinant virus for expression in insect cells, transfection of the pure recombinant Bacmid is necessary. For each transfection probe, 2 ml of a $4.5x10^5$ cells/ml *Sf9* cell stock were pipetted in 6 well plates (Falcon, USA) and incubated for at least 1h at 27°C for the cells to adhere to the plate. During this time 5 µg of each Bacmid-DNA sample was diluted in 100 µl *Sf*900-II medium without additives like serum. Parallel to this, 6 µl cellfectin reagents was mixed with 100 µl *Sf*900-II medium without additives and vortexed vigorously. Both mixtures were then pooled and mixed carefully. An incubation of 45 min at RT enables the formation of a DNA-lipid complex in

the transfection mixture. After the incubation 800 µl *Sf*900-II medium without additives is added to each transfection mixture and mixed lightly.

Meanwhile the adhered *Sf9* cells are removed from the incubator and the culture medium aspirated carefully without damaging the cells. The cells (in each well) are washed once with 2 ml *Sf*900-II medium without additives and the transfection mixture added to the cells. For transfection to take place the plates must be incubated for at least 5 h at 27°C. After 5 h the cells were aspirated carefully and 2 ml/well *Sf*900-II medium containing glutamine and serum was added to the cells. The cells were then incubated for 5 days at 27°C to generate the recombinant virus. After 5 days recombinant virus produced in the cells and budded off are found in the medium. The medium containing the recombinant virus particles are therefore removed carefully and transferred to sterile reagent tubes. Storage of the virus (now called first virus stock) for further use is done at 4°C.

9.1.14.4 Amplification of recombinant virus

For high expression of recombinant protein in insect cells, higher amounts of virus are needed than the one produced during the first transfection. To produce high enough virus titre for this purpose, 30 ml $0.5x10^6$ cells /ml *Sf9* cell suspension is infected with 0.5 ml of the first virus stock and incubated for 5 days at 27°C with shaking at 115 rpm. The cell medium containing recombinant virus (first virus amplification) was got by removing the supernatant after centrifugation for 5 min at 2000 rpm. To make sure that the virus solution is cell-free a second centrifugation step is done. The pure recombinant virus is then stored at 4°C for further use.

9.1.14.5 Determination of virus titre

For an optimal expression of recombinant protein in insect cells it is important that all the individual cells are infected with the recombinant virus bearing the gene of interest. In order to achieve this knowing the concentration of the virus in a given stock is necessary. In this work the titre of the first virus amplificate was determined by plaque assay. For the plaque assay, 1.5×10^6 *Sf9* cells per well were transferred to a 6 well plate and incubated for 1 h at 27°C for the cells to adhere to the plate. The recombinant virus stock to be analysed were diluted stepwise with Sf900-II medium, to get the dilutions 10^{-1} to 10^{-7}. The incubated cells were then aspirated and 500 µl of the virus dilutions 10^{-3} to 10^{-7} were added carefully. As a negative control Sf900-II medium without virus was added to one of the wells. The plate was then incubated for 2 h at room temperature. While incubation was going on, 14 ml Sf900-II medium was warmed at 45°C and 7 ml solution of a 3% sterile sea-plaque agarose (Biozym) was prepared. After cooling the temperature of the agarose was maintained at 45°C by placing it in an incubator preheated to the given temperature.

The virus supernatant and the medium from control well were aspirated after 2 h incubation. The 14 ml pre-warmed medium and 7 ml agarose were then mixed thoroughly and 3 ml/well was used to cover the aspirated cells homogeneously and incubated at RT till the agarose solidified. To prevent the cells from dehydrating, the solid agarose was covered with 1 ml Sf900-II medium per well. The plates were then incubated for 5 days at 27°C for plaque formation. In order to visualize the plaques for correct counting and quantification the medium was aspirated from the wells and 200 µl of a sterile 5 mg/ml MTT (thiazolyl blue) solution was added per well. A last incubation of the plates for 2 h at 27°C followed after which the colourless plaques in each well were counted.
By applying the formula:

$$\text{Virus titre} = \frac{\text{number of plaques counted}}{\text{dilution coefficient x (infection volume per well in ml)}}$$

the virus titre in pfu (plaque forming units) was deduced.

9.1.14.6 Preparation and analysis of bacmid DNA from recombinant baculovirus

After determination of viral titre it was still necessary to verify the presence of the gene of interest in the recombinant baculovirus stocks. This is possible by PCR with primers that flank both ends of the pFastbac1 vector region which lies within the region of transposition as indicated in **Figure 9.6**. The DNA is first purified to get rid of the protein coating the baculovirus.
Briefly, 1 ml of the first viral stocks and the first and second amplifications were aliquoted and treated with SDS and Proteinase K. The mixture was cleared by centrifugation and the DNA content of the virus was then purified with the Zymoclean DNA clean and concentration Kit (Zymo Research, Germany). The eluted DNA was used as template for PCR with primers Pvir For and Pvir Rev which anneal to the ends of the MCS of the pFastbac1 cloning vector as demonstrated in the following figure. Analysing the virus DNA by PCR reveals if the recombinant baculovirus carries the cDNA of interest or not.

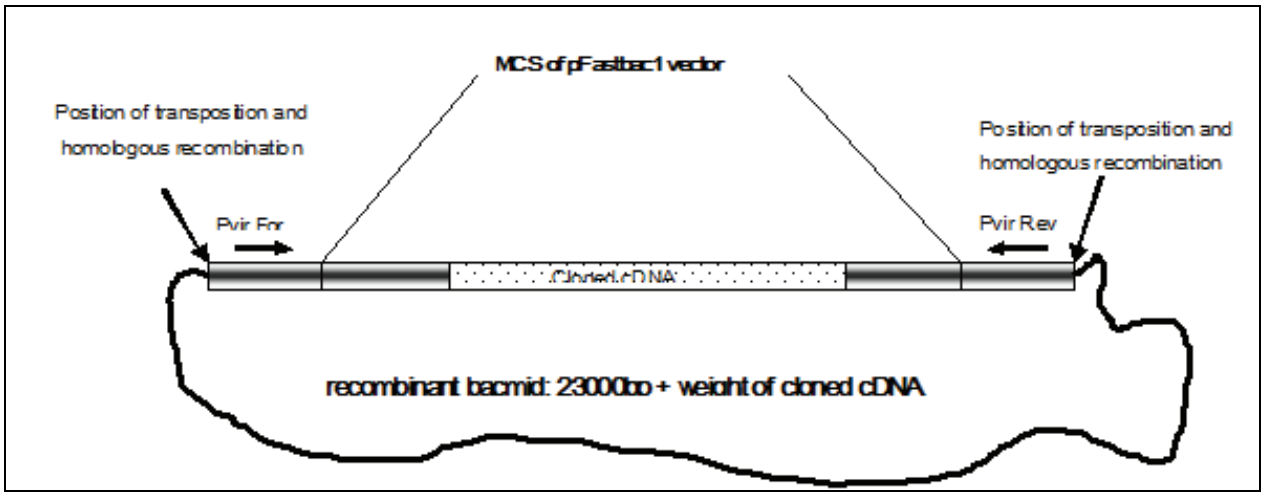

Figure 9.6: Schematic diagram of the recombinant bacmid with position of transposed cDNA.
MCS: multiple cloning site, Pvir-For and Pvir -Rev show annealing sites for the forward and reverse primers used in PCR analysis of recombinant Bacmid purified from either *E. coli* DH10Bac cells or the recombinant baculovirus.

9.1.14.7 Infection of *Sf9* cells and protein expression in serum-free media

Insect cells at a density of 2 x 10^6 cells /ml were used for the expression of recombinant protein. For this purpose cells were infected with the recombinant virus to final MOI rate 1, then incubated at 27°C and shaking at 115 rpm for 2-3 days. The cells were then harvested by 5 min centrifugation at 2000 rpm and analysed for the presence of the recombinant protein.

9.2 General biochemical methods

9.2.1 Determination of protein concentration

9.2.1.1 According to Bradford

Coomassie-brilliant –blue G-250 reacts with proteins, leading to the formation of a complex which has an absorption maximum at 595 nm (Bradford, 1976).

To determine the concentration of a protein solution, 5 µl of the solution was added to 995 µl Bradford reagent (10% (v/v) ethanol, 5% (v/v) phosphoric acid, 0.1% (w/v) Coomassie G-250) and mixed thoroughly. After 1 min incubation at RT the extinctions of the samples were measured at 595 nm. Purified bovine serum albumin (Pierce, Rockford USA) of known concentrations were used as standards.

9.2.1.2 Determination by Bicinchonin Acid (BCA) method

The BCA method is based on the reduction of Cu^{2+} to Cu^{+} by protein. The Cu^{+} then builds complexes with bicinchonin acid (BCA) which can be measured at the wavelengths 562nm or 570 nm. The intensity of the complex built is equivalent to the amount of Cu+ present which is equivalent to the concentration of protein in the solution used.

For the determination of concentrations of glycosylated proteins or proteins in a buffer which contains substances not suitable for the Bradford method, the BCA method was applied. The BCA protein assay kit (Pierce, Rockford, USA) was used and the procedures were according to the manufacturer's instructions.

Briefly, 20 µl dilutions (1µg/20 µl to 10 µg/20 µl)of a BSA standard (Pierce, Rockford, USA), or distilled water as blank were transferred into wells of a 96-well microplate in triplicate. Respectively, 20 µl diluted samples of the protein to be quantified were also put in doubles to distinct wells on the microplate. 200 µl BCA working reagent (Reagent A and B at a ratio 50:1) was added to each well and the plate incubated at 37 °C for 30 min. The extinction of the samples was then determined at 570 nm on a microplate reader (TECAN, Austria). The protein concentrations were calculated with reference to a standard curve.

9.2.2 Sodium dodecyl sulphate- polyacrylamide gel electrophoresis (SDS PAGE)

Just like for the separation of DNA by agarose gel-electrophoresis, proteins can be separated by SDS PAGE. In a protein solution denatured with the detergent sodium dodecyl sulphate (SDS), the protein molecules are bound on their hydrophobic moieties by the anionic SDS molecules which make them anionic. The anionic nature of the protein molecules and the fact that they have different molecular weights makes it possible to separate them electrophoretically. The concentration of acrylamide in the gels, determine the pore size of the gels. Under an electric field, movements of the protein molecules are inversely proportional to the logarithm of their molecular weights.

In this work the vertical SDS PAGE method was applied according to Laemmli (1970). The Bio-Rad Mini-Protean II system was used. The electrophoretic separation was done at a constant flow rate at 150 V. For size determination of the protein molecules, high molecular weight standards (Bio-Rad) were used.

Discontinuous gels of variable concentrations were prepared according to values in the following table.

Table 9.1: Preparation of restoring gels with different acrylamide concentrations. (Values given in the table are for 2 minigels (Bio-Rad mini Protean II system))

gel concentration (%)	**4**	**4.25**	**4.5**	**5**	**6**	**7**	**7.5**	**10**	**11**	**12,5**	**15**	**20**
Solution A (ml)	1.2	1.275	1.35	1.5	1.8	2.1	2.25	3	3.3	3.75	4.5	6
Solution B (ml)	2.25	2.25	2.25	2.25	2.25	2.25	2.25	2.25	2.25	2.25	2.25	2.25
dd H_2O (ml)	5.55	5.475	5.4	5.25	4.95	4.65	4.5	3.75	3.45	3	2.25	0.75

Stacking gels: (values for 2 gels)
1.85 ml water
0.75 ml Solution C
0.4 ml Solution A

12 µl APS
3 µl TEMED

Solution A: 30% Acrylamide (w/v), 0.8% N, N'-Methylenbisacrylamide
Solution B: 1.5 M Tris-HCl, pH 8.8, 0.2% SDS (w/v)
Solution C: 0.5 M Tris-HCl, pH 6.8, 0.4% SDS (w/v)

To modify the restoring gels by 1%, 0.3 ml acrylamide was either added or reduced. In each case equivalent volumes of water was used to subsidize the reduction or addition.

To enhance polymerisation of the acrylamide gels, 50 µl 10% (w/v) APS and 5 µl TEMED was added per 2 gels. After mixing the solution thoroughly, 3.55 ml was cast on a gel tank, covered with a layer of water and incubated at RT for 20-30 min to polymerise to a solid gel. Afterwards, the water above the gels were poured out and 1.2 ml stacking gel solution cast and combs with the required number of slots inserted. After 20 min incubation at RT the polymerised gel was ready for use. The combs were then removed and protein samples loaded in the slots and the electrophoresis started. Complete separation of the protein molecules is achieved if the staining solution in the sample buffer is seen almost running out of the gel. The electrophoresis is then stopped and the gel either stained for visualisation of the protein bands or used for western blot analysis.

For non-denaturing gels the preparation was done as above but without SDS in the buffers and the electrophoresis ran at 100 V constantly.

In order to separate protein mixtures with very high (above 100 kDa) as well as very low (10 kDa) molecular weight molecules, gradient gels were used. To cast such gels, solutions were prepared for 16%, 12.5%, 10%, 7.5% and 4% gels. These solutions were used to cast five gels by loading 1 ml of each solution after the other, starting with the highest concentration. After loading the lowest concentration (4%) combs were inserted immediately and the gels left for polymerisation at RT. The gels were used after polymerisation as stated above.

9.2.3 Tricine-SDS PAGE

With the Tris-Tricine- System, proteins with molecular weights between 1-100 kDa, are conveniently separated on the same gel. The stacking and the restoring gels are prepared parallel and cast after each other before letting polymerisation to take place.

Separation is done in the stacking gel at 60 V and in the restoring gel at a maximum of 120 V.

Solutions for Tricine-gel system:

Anode buffer: 0.2 M Tris-HCl, pH 8.9.

Cathode buffer: 0.1 M Tricine;
0.1% SDS

	0.1 M Tris-HCl, pH 8.3 (pH is not adjusted).
Gel buffer:	0.3% SDS 3 M Tris-HCl, pH 8.45
Acrylamide stock solution:	30% Acrylamide (w/v) 0.8% N,N´Methylenbisacryl-amid (w/v).
Values for 4 mini gels:	
Restoring gel:	3.1 ml Acrylamide stock solution 5 ml gel buffer 1.5 ml Glycerine + dd H_2O to 15 ml 75 µl APS (10%) 7.5 µl TEMED
Stacking gel:	1 ml Acrylamide stock solution 3.1 ml gel buffer + dd H_2O to12.5 ml 100 µl APS (10%) 10 µl TEMED

Stacking gel is loaded immediately after loading of restoring gel solution then the gel left to polymerise.

9.2.4 Staining proteins on acrylamide gels

9.2.4.1 Staining with coomassie-blue solution

Just like in the Bradford test protein molecules embedded in gels react with coomassie G250 to a blue complex. Nevertheless the method is not so sensitive and protein bands with less than 200-400 ng are not detectable. The Biosafe coomassie (Bio-Rad) was used in this work. After electrophoresis, the gels were removed and washed 3 times 5 min with distilled water. After washing, each gel was immersed in 25 ml Biosafe Coomassie solution and incubated on a shaker at RT for 1 h. The staining solution was then removed and the gel washed with water till the bands were seen clearly and no background was left.

9.2.4.2 Staining with silver nitrate

Ag^+ ions react and build complexes with Glu-, Asp- and Cys- rests of proteins. Reducing the Ag^+-complexes with formaldehyde leaves silver metal, which is then visualised where the protein bands are located. Opposed to coomassie stain, staining with silver nitrate is very sensitive and protein bands with only 10 ng protein are detectable. Unfortunately, nucleic acids, lipopolysaccharides, lipids and glycolipids on the gel are stained, making silver staining of protein unspecific. The method used here was modified according to (Heukeshoven & Dernick, 1988). After electrophoresis the gel was incubated for 30 min in 20 ml fixation solution at RT, then washed 3 x 20 sec with ddH_2O. Incubation for 1 min in sensitizer solution followed, after which the gel was washed 3 x 20 sec with ddH_2O. The gel was then incubated for 20 min in silver nitrate solution and

washed again as before. To visualise the bands the gel was incubated in developing solution till protein bands were visibly gold brown. The reaction was then stopped with fixation solution and the gel washed with water.

Fixation solution: 50% ethanol, 12% acetic acid in ddH_2O

Sensitizer solution: 0.02% sodium thiosulphite in ddH_2O

Silver nitrate solution: 0.1 g $AgNO_3$
0.02% formaldehyde,
Filled to 50 ml with ddH_2O

Developer: 3% sodium carbonate
0.05% formaldehyde
0.0005% sodium thiosulphite

9.2.5 Western-blot

Protein transfer from gels to nitrocellulose membrane was performed by the Semi-Dry-Method in a Bio-Rad blot apparatus.

After complete separation of protein by electrophoresis the gels were sandwiched between filter paper and nitrocellulose membrane in blot buffer, such that there were no gas bubbles between them. Due to negativity of the protein molecules post SDS PAGE, they therefore move from the gel (cathode end) towards the membrane (anode end) of the blot system when blotted in buffer (150 mM glycine, 20 mM Tris-HCl, pH 8.3, 10% ethanol (v/v)). The transfer procedure is performed at 4°C with constant current at 250 mA for 60 min.

9.2.5.1 Staining protein on nitrocellulose membrane

After the transfer process, the blot membrane is removed from the sandwich and a control of the transfer process performed by staining the membrane for 1 min with the reversible protein dye Ponceau-red. Washing the membrane with water reduces background stain and makes protein bands visible. 5x Ponceau red stock solution (2% Ponceau-red (w/v), 30% TCA (v/v), 30% Sulfosalicylic acid (w/v). Working solution was diluted 1:5.

In cases where unstained molecular weight standards were used, ponceau stained marker-bands were marked on the membranes with a pencil, then the membranes destained with PBS-T.

9.2.5.2 Immuno-histochemical detection of protein on nitrocellulose membrane

9.2.5.2.1 Chemiluminescence detection

Proteins transferred to nitrocellulose membranes can be detected by their specific antibodies, if the membranes are incubated in a solution of the antibodies. To avoid unspecific binding of other

proteins by the primary and secondary antibodies, membranes are first of all incubated in PBS with 5% (w/v) non fat milk powder for 1- 2 h at RT or overnight at 4°C. After the blocking step membranes are washed 2 x 5 min with PBS-T then incubated in primary antibodies in PBS-T overnight at 4°C. The primary antibody is then removed and the membrane washed 2 x 5 min with PBS-T. Horse-raddish peroxidase coupled secondary antibody in PBS-T is put on the membrane and incubated for at least 1 h at RT. After washing 2 x 5 min with PBS-T and 1x 5 min with PBS to remove residual Tween-20 which interferes with the ECL reaction, the membranes were then prepared for ECL reaction in transparent plastic foils and molecular weight standard bands marked with a fluorescent wax. The ECL reaction was initiated by incubating the membrane in the luminol reaction mix (1 ml Luminol B, 10 µl luminol solution A and 3 µl luminol solution C). Visualisation and documentation of the chemiluminescence was performed with the digital Fujifilm LAS-1000 Imaging-System and captured on a CCD-camera. Images were then converted to a photoshop compatible format and transferred for further processing.

9.2.5.2.2 Colorimetric detection with AEC substrate

Besides the chemiluminescence method, the detection of the peroxidase coupled antibody on western blots could be established by colorimetric staining with the commercially available AEC detection kit (Pierce). For this detection 1 ml 10x AEC reaction buffer was added to 8.8 ml ddH_2O. 200 µl of the 50x substrate was added and the solution mixed shortly by vortexing. The blot membranes were then incubated in the reaction mixture till the reddish-brown protein bands were visible.

9.2.6 Purification of Ab from sera of immunized rabbits and cell culture supernatant

Blood was collected from rabbits immunized with human-DPPIV protein or GFP protein every one to two weeks and centrifuged for one hour at 3000 rpm. The supernatant was then collected and used for purification of polyclonal antibodies to human-DPPIV or GFP.

Anti-GFP mAb was purified from cell culture supernatants of hybridoma cells. The purification procedure was performed with the Affi-Gel® Protein A MAPS® II Kit (BioRad) according to manufacturer's instructions. A 1x 10 cm Econo-column chromatography column (Bio-Rad) was packed with 1 ml of the Affi-Gel protein-A-agarose, equivalent to bind 6-8 mg/ml IgG_1. The resin was equilibrated with 5x 1 ml pH 9 binding buffer (prepared as stated in the product manual). 2 ml cell culture medium from the hybridoma cells (or 1 ml rabbit serum) were diluted with 2 ml of binding buffer then transferred to the columns and incubated for 15 min at RT with rocking. Unbound components were washed away with 15 times 1 ml binding buffer and the respective antibodies eluted with 10 x 700 µl pH 3.0 elution buffer. Eluates were neutralized immediately by

adding 100 µl of a 1M Tris HCl, pH 9.0 in each tube in which eluates were collected. After elution the column was washed with 5 x 1 ml regeneration buffer and stored in PBS containing 0.05% (w/v) sodium azide.

The eluates were pooled and desalted as well as concentrated in a Vivaspin column (Vivascience) at 4°C and 3000 rpm and the concentrations and purity determined by BCA and SDS PAGE respectively.

9.2.7 Preparation of immuno-affinity columns

150 mg Affi-gel 10 protein-A-sepharose (Amersham Pharmacia, Uppsala, Sweden) was loaded on a 10 ml disposable chromatography column and washed twice with 1 ml ice cold double distilled water. About 3 mg purified antibody in 15 mM sodium phosphate buffer pH 8.0 was put on the resin and the columns incubated for 3-6 h at RT (or overnight at 4°C) for covalent binding to take place. Subsequently, unbound antibodies were collected as flow through and the sepharose washed once with 1 ml 1 M ethanolamine pH 8.0. Blocking of the sepharose is performed with 3 ml 1M ethanolamine pH 8.0 for 2 h at RT. Finally the sepharose coupled with antibody was washed three times with 15 mM sodium phosphate buffer pH 8.0. For later use of the affinity columns, 1 ml PBS with 0.02% NaN3 was added to the sepharose and stored at 4°C.

9.2.8 Purification of DPPIV from *Sf9* insect cells

9.2.8.1 Purification by immuno-affinity

Cells were washed once with PBS and resuspended in solubilisation buffer (10 mM Tris pH 7.8, 150 mM NaCl, 1mM $CaCl_2$, 2% (w/v) CHAPSO containing Trasylol (1:1000) and 0.5 mM DTT as protease inhibitor and reducing agent respectively). After a 6 x 30s sonication step the cells were incubated overnight at 4°C with agitation. The solubilised protein was fractionated by 45 min centrifugation at 18,000 rpm. Supernatants containing soluble DPPIV were used directly for immuno affinity chromatography. Protein coupling on the column was performed overnight at 4°C with agitation. Unbound protein was collected as flow through and the resin washed once with 1 ml DPPIV native washing buffer 1(50 mM Tris pH 7.2, 1 M NaCl, 0.5% (w/v) n-octyl-b-D-glucopyranoside) and twice with 1 ml washing buffer 2 (10 mM Tris pH 7.2, 150 mM NaCl, 0.1% (w/v) n-octyl-b-D- glucopyranoside). Elution of DPPIV was done with 6x 250 µl elution buffer (50 mM Diethylamine pH 10.8).

9.2.8.2 Purification of protein by size-exclusion fast protein liquid chromatography

Fractions containing the immuno-purified DPPIV were pooled and further purified by SE-FPLC on a Superdex 200 column (GE Healthcare) which had been equilibrated with PBS. Elution of the

protein was performed with PBS containing Trasylol (1:1000) as protease inhibitor at a flow rate of 0.3-0.5 ml/min. Size exclusion standards were run under same buffer conditions. A standard linear regression curve was generated by plotting the log of the molecular mass of the different calibration proteins against their retention volumes. Components of the gelfiltration standard (BioRad): thyroglobulin (670 kDa), γ-globulin (158 kDa), ovalbumin (44 kDa), and myoglobin (17 kDa).

9.2.9 Determination of DPPIV enzyme activity

9.2.9.1 By photometric determination

To verify if the purified DPPIV protein was enzymatically active, a colorimetric enzyme assay was performed. 5 µl DPPIV sample of known dilution was used per 100 µl assay. 100 nM (1 µl) of the chromogenic substrate, H-Gly-Pro-p-NA-HCl, (Bachem, Bubendorf, Switzerland) was used. Briefly, enzyme and substrate were pipetted into wells of a 96 well plate and 94 µl reaction buffers (100 mM Tris pH 8.0) were added. The plates were incubated at 37°C for 5 min and the absorbance measured at 405 nm with the Spectra Rainbow microplate reader (TECAN, Austria). The enzyme activity of DPPIV was calculated by the formula:

$$C = \frac{E_{405}-E_{blank} \text{ x dilution factor}}{\varepsilon.d.t \text{ (min)}} \qquad \varepsilon = 14.4 \text{ cm}^2/\mu\text{mol and d} = 0.266 \text{ cm}$$

C/total protein used in µg, gives the enzyme activity in U/µg

9.2.9.2 Determination by colorimetric on-blot detection

For the evaluation of DPPIV enzyme activity on blot membranes the protein were separated on acrylamide gels under non-reducing conditions and blotted. The blot membranes were washed once with 100 mM Tris pH 8.0. The membranes were then incubated for 2 h at 37°C in 0.1 mg/ml of the substrate Gly-Pro-4-methoxy-β-naphthylamide-HCl (Bachem) in 100 mM Tris pH 8.0. After washing the membrane once with 10 mM sodium acetate buffer pH 4.5, detection of the cleaved methoxy-β-naphthylamide was performed with 0.25 mg/ml GBC Fast Garnet diazonium salt (Sigma) in sodium acetate buffer. Reaction of GBC Fast Garnet diazonium salt with the cleaved methoxy-naphthylamide gives a reddish product on the positions of cleavage.

9.2.9.3 Monitoring HIV1-TAT influence on DPPIV cleavage of GLP1, GIP1 and NPY by MALDI-TOF MS

DPPIV cleavage of GLP1, GIP1 and NPY was evaluated by measuring the spectra of cleaved substrate at different time points by MALDI-TOF mass spectrometry. To proof the inhibitory effect

of the HIV1-TAT protein on DPPIV enzyme activity, *E. coli* expressed, full length (1-86) HIV1-TAT protein from Immuno-Diagnostics, USA was used. The GLP1 (7-36), GIP1 (3-42) and NPY peptides used were from Genscript Corp.

A 100 µl assay sample composed of (final concentrations) 17 mM Tris pH 7.5, 20 mM KCl, 15 mM NaCl, 0.5 mM DTT, 1.4 µg DPPIV (16 nM), 10 µg GLP1 (31.25 µM) and 10 µg TAT (1 µM; Mw: 10 KDa). The substrate was added last in each test. For assays without HIV1-TAT, equivalent volumes of TAT storage buffer (50 mM Tris pH 7.5, 5 mM DTT and 200 mM KCl) were added to the mixture.

After pipetting all assay components, 5 µl was quickly removed and added to a 0.5 µl 1% TFA to stop the reaction. This sample was at time t = 0. The assay mixture was incubated at 37°C and aliquots of 5 µl removed at 5 minutes intervals (for 15 minutes) and stopped with TFA.

1 µl of the reaction mixtures at time-points t = 0, 5, 10 and 15 minutes were spotted on a MALDI target and 1 µl of the matrix ACCA (alphacyano cinnamic acid) was added to each spot. The target was left for a short while at RT to get dried after which detection of the mass spectra in a MALDI TOF MS (Bruker Ultra Flex III) analyser followed.

9.2.10 Co-expression of human-DPPIV and HIV1-TAT in *Sf9* insect cells

In order to monitor a possible co-localisation and binding of human-DPPIV and HIV1-TAT, *Sf9* insect cells were co infected with DPPIV- and HIV1-TAT recombinant baculoviruses. Briefly, 1 ml DPPIV- and 0.5 ml HIV1-TAT recombinant baculoviruses (final MOI ratio, 1:1 pfu/cell) were put on 20 ml *Sf9* cells at a density 2 x 10^6 cells / ml and incubated with shaking at 27°C for 2 days. Cells were harvested by 5 minutes centrifugation at 2000 rpm, washed once with PBS and evaluated by flow cytometry, fluorescence microscopy and immunoprecipitation as described below.

9.2.11 Evaluation of DPPIV and TAT co-expression by flow cytometry

DPPIV and TAT co expression in *Sf9* cells was evaluated in single fluorescence staining by using the anti-TAT mAb or anti-DPPIV pAb (9/9) together with FITC-conjugated anti mouse and anti rabbit secondary antibodies (Sigma) respectively. The cells were then analysed on a fluorescence activated cell sorter, FACS Scan (Becton-Dickinson, San Jose, CA).

9.2.12 Analysis of DPPIV and TAT co-expression by indirect immunofluorescence

9.2.12.1 Immuno staining and fluorescence microscopy

After expression of respective proteins, washed insect cells were fixed on slides with 3% formaldehyde in PBS. Except otherwise indicated, cells were permeabilized with 1% Triton X100

in PBS washed three times and incubated for 1 hour in blocking buffer (PBS with 0.5% BSA and 1% non fat milk). Cells were then incubated overnight in either monoclonal antibody against HIV1-TAT or polyclonal antibody against DPPIV as primary antibodies. Secondary antibodies were either Cy3 conjugated anti mouse or FITC conjugated anti rabbit antibodies respectively. Co-localisation of the proteins was investigated by staining co-infected cells with both antibodies. After incubation in respective antibodies the cells were washed twice with PBS buffer. Finally the cells were air dried, embedded in mounting solution and observed under the Axio observer fluorescence microscope (Carl Zeiss GmbH, Germany) and images made with the Axio Cam. Cells co-expressing DPPIV and CXCR4GFP were only stained with the anti-DPPIV pAb and Cy3 conjugated anti rabbit antibodies.

9.2.12.2 Confocal microscopy

Harvested cells were washed, fixed on culture slides and permeabilized with 0.3% Triton X100 and blocked with 1% BSA and 1% non-fat milk in PBS. Double staining with a combination of anti-TAT mAb/ anti Mouse-Cy3 (red) and anti-DPPIV pAb / anti Rabbit-FITC (green) was performed. The cells were assessed by confocal laser scanning microscopy (Carl Zeiss LSM 410) at 63-fold magnification.

9.2.13 Co-immunoprecipitation of human-DPPIV and HIV1-TAT from *Sf9* cells

After co expression cells were analysed for binding of DPPIV and TAT. Immunoprecipitation (IP) tests were performed parallel to this with samples prepared by infecting cells with either of DPPIV and HIV1-TAT baculoviruses. After 2-3 days incubation at 27°C with shaking, cells were harvested by 5 minutes centrifugation at 2000 rpm, washed once with PBS and resuspended in solubilisation buffer (PBS with 2% CHAPSO or DDM, Trasylol as protease inhibitor and 1 mM DTT). The cells were then sonicated (4 x 30 sec) and incubated for 3 hours at 4°C with rocking. After centrifugation for 1 hour at 15000 rpm the supernatant containing solubilised protein was used for immunoprecipitation or co immunoprecipitation. For each test 2 µg monoclonal antibody to HIV1-TAT (from Centralised facility for AIDS Reagents) and polyclonal antibody to human DPPIV (produced in our laboratory) were used respectively. Briefly, 10 mg protein-A- sepharose (per test) was swelled and washed with PBS and 2 µg of the respective antibodies in 1 ml PBS were added and rocked overnight at 4°C. After washing the sepharose twice with 1 ml PBS the solubilised protein were incubated on the antibodies for 4 hours at 4°C. Unbound protein was removed and samples washed 3 times with PBS-0.5% n-octyl-β-D-glucopyranoside containing 1mM DTT and 1x with PBS-0.1% n-octyl-β-D-glucopyranoside containing 1 mM DTT. Denaturing sample buffer was

added to the pellets mixed and cooked for 4 min at 99°C. Analysis was done by western blots and detection with respective antibodies.

9.2.13.1 Immunoprecipitation of phospho-DPPIV and phospho-TAT from *Sf9* cells

2 µg of the respective antibodies anti-phospho-serine mAb (Sigma, P3430 clone PSR-45) and anti-phospho-tyrosine mAb (Sigma, P3300 Cl-66) were put in 500 µl PBS and immobilized on 10 mg protein-A/G-sepharose per test by rocking overnight at 4°C. Unbound antibody was removed by washing twice with 1 ml PBS and analyte protein lysates were added and incubated for 10-16 h at 4°C. Unbound protein was removed and samples washed several times with native washing buffer (PBS-0.5% n-octyl-β-D-glucopyranoside with 0.5 mM DTT). The pellets were mixed with reducing, denaturing sample buffer then heated for 4 min at 99°C and analysed by western blot.

9.2.14 Expression and purification of recombinant HIV1-TAT protein

9.2.14.1 Expression in *Sf9* insect cells

The HIV1-TAT cDNA was cloned in the pFastBac1 donor plasmid as described under section **9.1.1.2**, and used for the preparation of bacmid and recombinant virus as described above. The recombinant virus was used for infection at an MOI of 0.1-1.0.

9.2.14.2 Expression and Purification of TAT protein with GST / His-Tags from *E. coli*

Cloning of the TAT cDNA in appropriate expression vectors were performed as described under section **9.1.1.3**. The plasmids were transformed into *E. coli* BL21. Expression of TAT fusion protein in *E. coli* BL21 (DE3) pLysS was induced with 3 mM IPTG for 3 hrs at 25°C. Cell lysis was performed in TAT lysis buffer (PBS + 5 mM DTT, 1 mM EDTA and 1 mM PMSF, 0.2% Triton-X100) in a constant cell disrupting system (Constant Systems, Daventry-Northants UK). Lysed cells were cleared by centrifugation at 18,000 rpm and supernatants either used for glutathione affinity chromatography (Constructs with GST-tag) or Ni-affinity chromatography (constructs with His-Tags).

Briefly, a 10 cm Econo-column chromatography column (BioRad) was loaded with 250 µl of either Glutathione Sepharose (Amersham Biosciences/GE Healthcare) or Nickel-NTA-Agarose (Qiagen) and washed twice with 1 ml PBS. The soluble fraction of the corresponding fusion protein was then added to the resin and incubated by rocking at 4°C for 90 min. Unspecific protein from glutathione affinity columns was removed with PBS containing 1 mM DTT and EDTA. For Ni-chromatography, washing was done with NiNTA standard washing buffer (20 mM Sodium phosphate pH 8.0, 300 mM NaCl, 20 mM imidazol).

Protein elution from glutathione affinity chromatography was with GST-elution buffer (50 mM Tris pH7.5, 10 mM reduced glutathione). For Nickel-affinity chromatography, elution buffer was 20 mM sodium phosphate with 200 mM imidazol. After affinity chromatography eluates were pooled and desalted on a PD10 desalting column (Amersham Biosciences). Protein fractions were pooled again and further purified by size exclusion FPLC as described under section **9.2.8.2**. SE-FPLC buffer for TAT was TBS pH 8.0 + 1-2 mM DTT.

9.2.14.3 Purification of untagged TAT and TATGFP fusion protein

9.2.14.3.1 Preparation of immuno affinity columns with anti-GFP and anti-TAT mAb

Immuno affinity columns of anti-GFP pAb, anti GFP mAb and TAT mAb were prepared as described for the DPPIV antibody above. Since enough anti-GFP antibodies are prepared in our laboratory, columns were prepared with about 2- 6 mg anti-GFP antibody each. Purified anti-TAT mAb in limited concentrations was from CFAR (centralised facility for AIDS reagents). For the anti-TAT affinity columns, only a maximum of 800 µg antibody was coupled on the column.

9.2.14.3.2 Purification of HIV1-TAT protein by immuno-affinity chromatography

Full length TAT (1-86) was cloned into the EcoRI and Kpn1 sites of the pEGFP-N1 vector as described under **9.1.1.3** and used for the expression of TATGFP protein in mammalian cell lines. The sequence-verified plasmid was stably transfected in CHO cells and expression of TATGFP analysed by fluorescence microscopy and FACS analysis. Stable clones were cultured to 90% confluency on 10 large Ø15 cm plates then lysed by sonication in TBS pH7.5, with 1% Triton X100, 2 mM DTT, 1 mM EDTA and HALT! Protease inhibitor-cocktail (Pierce). After clearance by centrifugation supernatants were packed on immobilised anti-GFP mAb columns and incubated overnight at 4°C with agitation. Unbound protein was washed out with 3 x 1 ml TBS-1 mM DTT and bound protein eluted with either high pH elution buffer (50 mM Diethylamine pH 10.8) and equilibrated immediately with HCl or low pH TAT-elution buffer (100 mM Glycine pH 3.0). TAT protein is a very cationic molecule (isoelectric point of untagged protein is 9.8-10.13; calculated by Expasy.org pI/Mw tool), but the protein is rather more stable at a pH lower than 6.

The untagged TAT protein expressed in *Sf9* cells, *E. coli* BL21 were purified by anti-TAT immuno affinity chromatography under same binding, washing and elution conditions or by ion exchange chromatography on the HiTrap Q FF anion exchanger and HiTrap SP cation exchangers (GE-Healthcare Germany).

9.2.15 Expression and purification of recombinant Caveolin-1 protein

Expression of the Caveolin-1 fusion proteins in *E. coli* BL21 (DE3) pLysS was induced with 2 mM IPTG for 4 hrs at 30°C. Cell lysis was performed in Cav1 lysis buffer (HBS = 20 mM HEPES, 140 mM NaCl pH 7.4, containing: 10% PEG-400, 1% n-dodecyl-β-D-maltoside (DDM), 1 mM DTT, 1 mM EDTA and 1 mM PMSF) in a constant cell disruption system. Lysed cells were cleared by centrifugation at 18,000 rpm and supernatants used for glutathione affinity chromatography.
Elution from glutathione affinity chromatography was done with GST elution buffer. After affinity chromatography eluates were pooled desalted on a PD10 desalting column and further purified by size exclusion FPLC as described above. SE-FPLC buffer for Cav1 was HBS pH 7.4 containing 200 KE Trasylol and 0.5 mM EDTA.

9.2.16 Co-immunoprecipitation of DPPIV and Caveolin-1 fusion protein

To verify if Caveolin-1 protein binds to DPPIV in immunoprecipitation tests 20 µg purified GSTCav1 proteins were immobilized on anti Caveolin-1 polyclonal antibody then 10 µg purified DPPIV in PBS was added and incubated for 2 hours. Likewise, 10 µg purified DPPIV protein were immobilized on anti-DPPIV pAb and 20 µg GSTCav1 protein added and incubated for 2 hours. After washing several times with PBS reducing sample buffer was added and the resins boiled for 5 min at 98°C then blotted and probed for with either anti-GST pAb or anti-DPPIV pAb.

9.2.17 Analysing protein structure by chemical cross linking

During interaction and/or binding, proteins come close to each other in biological systems. In most cases these *in vivo* protein-protein interactions and binding occur very briefly to facilitate signal transductions for example. In order to capture these complexes together it is necessary to covalently link them with each other by use of chemical cross linkers. Using chemical cross-linking agents is suitable to determine near-neighbour relationships, analyse protein structure and distance between interacting molecules
In this work the chemical cross linker DSP (Dithiobis succinimidyl propionate) and its analog DSS (disuccinimidyl suberate) (Pierce/Thermo scientific) were used to analyse the structure of TAT protein *in vivo* and also to study the interaction of TAT and DPPIV. Both are homobifunctional cross-linkers with N-hydroxysuccinimide (NHS) esters as reactive groups which react with primary amines at pH 7-9. DSS and DSP are membrane permeable. DSS forms non cleavable covalent bonds between amine groups of nearby proteins, whereas DSP forms thiol-cleavable bonds between amine groups of the proteins being studied. The water insoluble cross linkers were first dissolved in DMSO then diluted with PBS pH 8.1 before use. The structure of the cross-linkers DSS and DSP are given in **Figure 9.7**.

TAT-structure- and DPPIV-TAT binding analysis: To study DPPIV-TAT binding by cross-linking, co expression of DPPIV and TAT was performed in *Sf9* insect cells. After 2 days of culture the cells were harvested by centrifugation, washed twice with PBS pH 8.0 and incubated for 60 min at RT with 12,5 µg/ml DSS in PBS (pH8.1) or 20 µg/ml DSP in PBS pH8.1. The cells were not permeabilised before treatment since the cross linkers are membrane permeable. The reactions were stopped by addition of 1 ml 0.1 M Tris pH 8.0 for 15 min. The cells were then centrifuged and washed once with PBS. Cell lysis was done by sonication in PBS containing 2% n-dodecyl-β-D maltoside and Trasylol as protease inhibitor. Solubilisation was performed by incubating the lysed cells for 4 hrs at 4°C with head over tail rotation. Soluble proteins were fractionated by centrifugation at 18000 rpm for 30 min. The soluble supernatant fractions were processed by immuno precipitation or analysed directly by western blots.

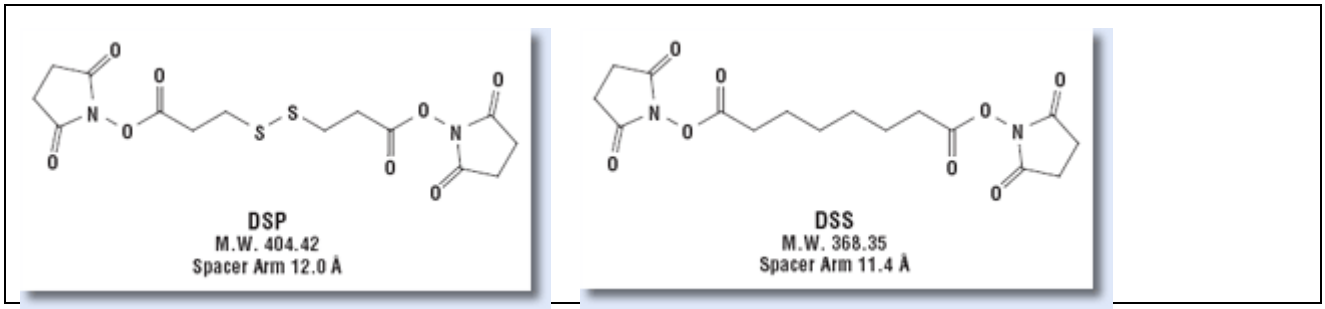

Figure 9.7: Structure of the chemical cross-linkers DSS and its analog DSP
DSS is homobifuntional and forms non-cleavable covalent bonds whereas DSP forms thiol-cleavable bonds (Pierce/Thermo Scientific).

9.2.18 Analysing protein complexes by two-dimensional polyacrylamide gel electrophoresis

Two-dimensional gel electrophoresis is suitable for the analysis of protein complexes since it enables the separation of the protein molecules according to their net charge (first dimension; isoelectric focusing), and the separation according to their molecular weights (second dimension: SDS PAGE). 2D PAGE was used to analyse purified DPPIV and TAT/DPPIV protein complex. For the first dimension, 10 µg DPPIV or 10 µg TAT/DPPIV protein complexes in TBS were mixed with IPG-sample buffer (pH 3-10, Amersham Pharmacia Biotech AB, Uppsala- Sweden) to 170 µl final volumes. The samples were denatured by heating at 99°C for 3 min then isoelectric-focused overnight on wide-range immobilized pH gradient gel strips (pH 3-10; GE-Healthcare). The second-dimension, SDS-PAGE was performed on 8-16% bis-Tris gradient gels (Anamed GmbH, Germany). The gels were stained with either silver nitrate for visualization or with Coomassie brilliant blue solution (Bio-Rad) for analysis by MALDI-TOF- peptide mass fingerprinting.

9.3 General cell culture techniques

9.3.1 General culture conditions

Unless otherwise mentioned, all mammalian cells were cultured in a cell culture chamber (Heraeus 6000, Kendro Laboratory Products) at 37°C in suitable medium with 5% CO_2 in a fully humidified atmosphere. The cell lines used in this work and the respective culture media are listed in the material section.

In each case cells were grown to 70-90% confluency and passaged every 2-3 days. To passage the cells, culture medium was removed by aspiration and cells diluted in PBS containing 0.05% EDTA. Aliquots of the cells were then transferred to fresh medium on new culture plates. When necessary, cells were diluted with Trypan blue and counted in a Neubauer-chamber or in a Coulter Particle Counter Z1. General cell culture materials were from BD Biosciences, Discovery Lab ware (Bedford, USA), Biochrom KG (Berlin), Corning (New York, USA), Nunc (Wiesbaden), PAA (Cölbe) and TPP (Trasadingen, Switzerland).

Cryo-cultures: Mammalian cells usually have a finite number of cell multiplications after which they stop dividing when regularly sub cultured for a long period. In order to always have viable cells or transfected cell lines cryo-cultures were prepared and stored at -175°C in liquid nitrogen? For this purpose cells were pelleted and pellets diluted in FCS/10% DMSO (dimethyl sulfoxide) and transferred in 1 ml aliquots to cryogenic vials. The vials were wrapped in tissue paper and frozen for at least 2 h at -20°C, 24 h at –80°C then finally transferred to a liquid nitrogen storage tank. The cells are viable for years when stored this way.

To re-culture the cells, vials were removed from the nitrogen and thawed immediately at 37°C, briefly centrifuged and then aspirated. The cell pellets were then transferred to 37°C warm culture media and cultured as above.

9.3.2 Transfection of CHO cells with TAT-pEGFPN1 and CXCR4-pEGFPN1 and selection of stable clones

CHO cells at a density 1x 10^5 cells/ml were plated and grown overnight to reach 80-90% confluency, then transfected with 5-10 µg TAT-pEGFPN1 or CXCR4-pEGFPN1 plasmid DNA with the Superfect transfection reagent (Qiagen) according to the user manual. Briefly, cells were aspirated and washed then the transfection complex added and kept at room temperature for 10 min. Culture medium (w/o serum and antibiotics, supplemented with 2 mM Glutamine) was added and the cells cultured for 5 h. Subsequently, medium was replaced with alpha MEM medium containing 10% FCS and 1% penicillin and streptomycin and grown for 48 h. The culture medium was then

removed by aspiration and the cells further grown in selection medium containing 600 mg/l G418. Medium was changed every day in the first week and every two days in the second week. Two weeks later, cells were diluted into different microplate such that only single cells / well was present. After growing and observing the cells under fluorescence microscope positive clones could be selected by virtue of their fluorescence. Selected clones were analysed by flow cytometry till there were no false-positive clones present. Cells were maintained in alpha MEM medium (Biochrom KG, Berlin, Germany) supplemented with 10% heat-inactivated FCS (Biochrom KG), 0.2 mg/ml penicillin/streptomycin, and 0.1% (w/v) L-glutamine (Biochrom KG) at 37°C in a 5% CO_2 fully humidified atmosphere.

9.3.3 Transfection of Hek293 cells with CXCR4-pEGFPN1

Except for the use of higher cell densities, Hek293 cells were transfected with CXCR4-pEGFPN1 plasmid same as indicated for the CHO cells. Selection of stable clones was achieved with 500 mg / L G418 (neomycin).

9.3.4 Expression and purification of CXCR4GFP from CHO and Hek293 cells

Cells were plated at a density of 1x 10^6 cells /ml on large (Ø15 cm) plates and grown for 3 days in selection medium. The medium was removed by aspiration and the cells removed with PBS-EDTA and centrifuged. Cell pellets were lysed by sonication and solubilised overnight in CXCR4 solubilisation buffer (see **8.9.3.1**). Soluble proteins were fractionated by centrifugation at 18,000 rpm for 45 min and used for purification by anti-GFP affinity chromatography as described earlier.

9.3.5 Verification of TAT-specific transactivation activity

The HIV-TAT protein is the only transactivator protein found in HIV. It is highly conserved within different subtypes of HIV. Its main role is the transactivation of transcription of viral transcripts, through its binding to the TAR RNA region on the HIV long terminal repeat (LTR) promoter and the induction of transcription. In **Figure 1.6** in the introduction section, a diagram of the HIV LTR-promoter and the position of elements involved in the transcription of HIV transcripts is presented. Cloning a reporter gene of interest downstream of the LTR-promoter provides a reliable means by which the transactivation activity of HIV-TAT protein can be assessed. In the underlying work the bacterial chloramphenicol acetyl transferase (CAT) was used as reporter gene.

9.3.5.1 Induction of CAT expression

To know if the TAT protein purified from the various expression systems are biologically active, their ability to activate the HIV promoter on the 5’ LTR (long terminal repeat) was made use of.

The cell line HLCD4CAT (centralised facility for AIDS reagents), which contains the CAT (chloramphenicol acetyl transferase) reporter gene linked to the 5'LTR of HIV1 was used. Cells were cultured on 6 well plates and grown for 24 h to achieve 80% confluency. Prior to TAT treatment the medium was aspirated and the cells washed once with 1 ml PBS. The TAT fusion protein were removed from -80°C and diluted immediately with PBS to a final concentration 0.1 µg/µl. Aliquots were mixed with culture medium to a final concentration 125 ng /ml then added to the test cell line. After culturing for 24 h the medium was changed against fresh medium and the cells subjected to a further incubation for 48 h. Purified TAT fusion protein from Immuno-Diagnostics-USA was used as positive control and TAT storage buffer, GST protein and the TAT translocation peptide TAT47-57 were used as negative controls. After induction for 72 h the cells were harvested and evaluated for the expression of CAT protein by use of the commercially available CAT-ELISA kit.

9.3.5.2 Evaluation of TAT induced CAT expression by ELISA

After induction cells were harvested in PBS-EDTA, washed once with PBS and quantified for CAT protein expressed per well, for each TAT protein construct. The CAT-ELISA kit (Pierce, Rockford, USA) was used according to manufacturer's instructions. Briefly, cells were lysed with the lysis buffer included in the kit then fractionated by centrifugation. The soluble fraction containing CAT was used. The total protein concentration of each sample was determined by BCA method as described earlier and equivalent protein concentrations per sample were used for CAT assay according to manufacturer's instructions.

9.3.6 Induction of CXCR4 up regulation by purified TAT recombinant protein

The HIV-TAT protein is known to up regulate the expression of CXCR4 in T-lymphocytes and monocytes. In this work the characterization of purified recombinant TAT proteins was also evaluated by virtue of their ability to up regulate CXCR4 expression in non-transfected Jurkat cell lines and also in CHO and Hek293 cell lines transfected to stably express CXCR4GFP.

Similar to the transactivation test, the purified TAT fusion protein were added to the cell lines Jurkat, CHO-CXCR4GFP and Hek293-CXCR4GFP. Negative controls were done with equivalent concentrations and volumes of GST protein, the mutant TAT47-57 and also TAT storage buffer. After 24 h incubation with the fusion proteins the culture medium was changed against fresh media and the cells incubated for further 24 h. Harvested cells were washed with PBS and analysed by fluorescence/confocal microscopy and flow cytometry. For the Jurkat cell line immuno stain of CXCR4 was performed with the anti-CXCR4 mAb (Number ARP3101 from NIBSC, Centre for AIDS Reagents) and FITC conjugated anti-mouse antibody (Sigma).

9.4 General biophysical methods

9.4.1 Evaluating protein–protein binding by Surface Plasmon Resonance analysis

Biomolecular interactions can be efficiently investigated by surface plasmon resonance analysis, a phenomenon that occurs in thin conducting films at an interface between media of different refractive index. The principle of the Biacore systems used in this work is quite simple. The media of variable refractive index are the glass of a sensor chip and the sample solution, whereas the conducting film is a thin layer of gold on the sensor chip surface. An interacting partner protein is immobilised on the surface of a sensor chip and several putative binding partners of the protein are then passed over the surface in solution. If binding takes place between the test protein and the putative binding partner there will be a total increase in mass on the surface. An overall response is generated on the surface which is proportional to the bound mass. What is measured is the total reflection angle of a polarised light of defined wavelength at the border between the glass and thin gold film. Despite total internal reflection, light incident on the reflecting interface leaks electric field intensity (evanescent wave field) across the interface into the medium of lower refractive index, without actually losing net energy. The amplitude of this evanescent wave field decreases exponentially with distance from the surface so that the effective penetration depth in terms of sensitivity to refractive index is about 20% of the wavelength of the incident light. At a certain wavelength, the incident light excites plasmons (electron charge density waves) in the gold film. As a result a characteristic absorption of energy via the evanescent wave field occurs and SPR is seen as a drop in intensity of the reflected light. Changes in solute concentration e.g. through protein-protein binding at the surface of the sensor chip results to changes in the refractive index of the solution which can be measured as changes in the SPR conditions. This is possible since Protein-protein binding on the surface leads to changes in the total refractive index of the light reflected on the other side of the gold film.

The Biacore technology is very sensitive and detects changes in mass bound as low as a few picograms per square millimetre on the sensor surface. This corresponds to concentrations in the picomolar and nanomolar range in the bulk sample solution.

In this work hDPPIV purified from *Sf9* cells was attached covalently to either a CM5 sensor chip or a C1 sensor chip (BIAcore AB, Uppsala, Sweden) with the Amine Coupling Kit (BIAcore AB, Uppsala, Sweden) and the following putative binding partners passed over the surface to test or proof their binding capacity to hDPPIV.

Table 9.2: Putative binding partners of DPPIV used in SPR binding assay

Protein Name	Expression system	Purification (Company)	Purpose
TAT	*E. coli*	(from Immuno-Diagnostics)	test
TAT	*E. coli*	(from Prof. Roesch)	test
TAT	*E. coli /Sf9*	Immuno affinity/SE-FPLC	test
GST-TAT-His	*E. coli*	NiNTA/SE-FPLC	test
TAT10xHis	*E. coli*	NiNTA/SE-FPLC	test
TATV5His	*Sf9* insect cells	NiNTA/SE-FPLC	test
GST-TAT	*E. coli*	Glutathione affinity/SE-FPLC	test
GST-Cav1	*E. coli*	Glutathione affinity/SE-FPLC	test
GST	*E. coli*	Glutathione affinity/SE-FPLC	negative control
ADA	swine		positive control
gp120-Flag	*Sf9* insect cells	Anti-Flag affinity chromatography	negative control

The coupling procedure was performed at a flow rate of 5 µl/min. Briefly the surface of the sensor chip was activated with 35 µl 100 mM N-ethyl-N´-(Dimethylaminopropyl) carbodiimid hydrochloride/400 mM N-hydroxysuccinimide. Immediately prior to immobilisation, 80 µl (20 µg) DPPIV was diluted in 10 mM sodium acetate, pH 4.5 in order to assure a positive net charge of the protein (iso-electric point of the DPPIV is 5.67) then injected into the Bia2000 system. The positive net charge of the protein enables covalent attachment of the protein to the dextran on the sensorchip surface. After immobilisation of the DPPIV protein the sensor chip was washed with 35 µl 1M ethanolamine hydrochloride (pH 8.5) to clear unbound protein and also deactivate the surface against unspecific binding. Final rinsing of the chip was done with HCl. Protein-protein interaction analysis was performed with HBS running buffer (10 mM HEPES, pH 7.4, 150 mM NaCl, 1 mM EDTA) at variable flow rates ranging from 10-30 µl/min depending on the test protein on a BIAcore® 2000 (BIAcore AB, Uppsala, Sweden).

Regeneration of the surface after test injections was done with 20 µl of 1M NaCl containing 0.02% Tween 20.

9.4.2 Analysis and identification of protein by MALDI-TOF-MS

With the aid of MALDI-TOF MS (Matrix-Assisted Laser-Desorption-Ionization Time-Of-Flight Mass Spectrometry) protein fragments with blocked n-termini or which are available only in limited concentrations can be easily analysed. In this work the GST and His fusion proteins (TAT and Caveolin-1) expressed and purified from *E. coli* were analysed by Mass- fingerprinting.

For this purpose purified fusion proteins were separated by SDS PAGE and the gels stained with Biosafe coomassie as described earlier. Corresponding protein bands were then excised from the gel

neatly with a clean scalpel, cutting as close to the edge of the band as possible to avoid contaminations. All solutions and buffers used were prepared with sterile pure HPLC grade water (Milli-Q® Water filter apparatus, Millipore, Schwalbach).

In-gel tryptic digestion of proteins:

The excised bands were cut into very tiny fragments (1x1 mm) to ease distaining and transferred to sterile 1.5 ml Eppendorf tubes. After rinsing the gel fragments once with 100 µl sterile distilled water, the gel was distained. For that, 20 µl (for small bands) and 100 µl (for big bands) of a 1:1 mixture of acetonitrile and 100 mM NH_4HCO_3 was added and the tubes incubated for 15 min at RT with rocking. The tubes were centrifuged briefly and the supernatants removed. 20 µl (100 µl) acetonitrile was added and the tubes incubated for 5 min or till the gel fragments became milky white. The supernatant were removed again and the gel fragments lyophilised for 10 minutes. 20 µl (100 µl) of a 1:1 100 mM DTT and 100 mM NH_4HCO_3 was added and the tubes incubated for 30 min at 56°C. After this incubation the tubes were centrifuged briefly, supernatants removed and their volumes determined and noted. The expanded gel fragments were again shrinked by incubating in same volumes of acetonitrile as before then centrifuged and supernatants removed. The milky white gel cubes were then incubated in 20 µl (or 100 µl) iodoacetamide solutions (55 mM iodoacetamide/100 mM NH_4HCO_3 for 20 min at RT in the dark. After a brief centrifugation supernatants were removed and the gel fragments washed with 20 µl (or 100 µl) 100 mM NH_4HCO_3 for 15 min at RT. Supernatants were removed again after a brief centrifugation and the fragments shrinked for 5 min at RT with same volumes of 100% acetonitrile as before. The fragments were lyophilised and exact volumes (as those of the supernatants noted earlier + 3 µl) of trypsin solutions (12.5 ng/µl bovine Trypsin sequencing grade, in 100 mM NH_4HCO_3) were added. The tubes were then incubated on ice for 30 min then overnight at 37 °C with light shaking, for tryptic digestion of the protein to take place.

On the next day the tubes were briefly centrifuged and checked if enough supernatant for analysis was present. If there was no supernatant pure milli-Q water was added and tubes incubated at RT for 30 min. after a brief centrifugation the supernatant with trypsin digested protein fragments were removed and 1 µl used for analysis. To make sure that the protein fragments were isolated totally from the tubes, 10 µl 40% acetonitrile/0.1% TFA was added to the gel fragments after removing the first tryptic supernatant and the tubes incubated for several hrs at RT with shaking. The supernatants were then transferred after a brief centrifugation to clean Eppendorf tubes and 1 µl used for MALDI-Mass fingerprinting analysis. Unused rest were lyophilised and stored at -20°C.

MALDI-TOF-MS analysis: The MALDI Mass Fingerprinting was performed by Dr. Chris Weise (FU Berlin) on a Bruker-Biflex Reflex Mass spectrometer and by Dr. Veronique Blanchard (Charite-Mitte) on a Bruker Ultra Flex-III MALDI-TOF mass spectrometer (Bruker Daltonics,

Bremen Germany) in reflector-mode with α-cyano-4-hydroxycinnamic acid (ACCA, 10 mg / ml in 70% acetonitrile and 0.1% TFA) as matrix. Ionisation was enhanced with a 337 nm-ray of a Nitrogen-Laser. The peptide masses were determined by calibration with the PAC peptide calibrant standard. Evaluation and identification of the mass spectra were performed with help of the internet search software Mascot (Perkins *et al.*, 1999).

9.4.2.1 Determination of O-glycans on human-DPPIV expressed in *Sf9* cells

In order to verify if DPPIV is O-glycosylated, the protein was purified to homogeneity by immunoaffinity chromatography and SE-FPLC. The protein was cleaved to shorter fragments with trypsin, which enables the exposure of the glycan moieties to glycosidases in further steps of the isolation. The spatial structures of protein usually hinder the detection of the sugars by glycosidases and strongly reduce the yield of isolated sugars. Specific glycosidases e.g. PNGase F for the cleavage of N-glycans are available. PNGase F specifically cleaves the bond between asparagin and GlcNAc (Tarentino *et al.*, 1985; Nuck *et al.*, 1990). For the cleavage of O-glycans, very few and rare specific enzymes are available. The isolation and characterisation of O-glycans are therefore processed by chemical methods.

Beta (β)-elimination was used to hydrolyse the N and O-glycans. This chemical method results in the release of the glycans completely lacking reactive reducible termini. The glycans therefore cannot be further derivatised after β-elimination.

Separation of N-and O-Glycans

β-elimination results in the release of N and O glycans from proteins. In order to characterise the N- and O-glycans, their separation is required. In the first step the N-glycan cleavage with PNGase F is performed and the samples purified on a C18 column. Proteins and glycoproteins bind irreversibly with high affinity to the matrix of the C18 column meanwhile free sugars have no affinity and cannot bind to the matrix. The PNGase F released N-glycans are therefore collected in the flow-through and wash fractions, whereas the peptides with o-glycosidically linked glycans remain on the column and can be eluted with acetonitrile. After desalting and drying the samples separately (flow-through versus eluted samples), β-elimination is performed. Analysis of both samples is conducted by MALDI-TOF mass spectrometry and the masses from both samples compared since same glycans may occur in both sample as a result of incomplete cleavage by PNGase F in the first step. Spectra that appear in both samples are therefore N-glycans whereas those that appear only in the second sample (eluted from C18) are O-glycosidically linked glycans.

9.4.3 Analysis of protein homogeneity by transmission electron microscopy (negative staining)

Droplets of the sample (5µl) were applied to hydrophilised (glow discharged in a BALTEC MED 020 (BAL-TEC AG, Liechtenstein) for 60s at 8W) carbon covered microscopical copper grids (400 mesh) and supernatant fluid was removed with a filter paper until an ultrathin layer of the sample was obtained. A droplet of contrasting material (1% uranyl acetate) was added, blotted again and air-dried. Imaging was performed using a FEG equipped Tecnai F20 TEM (FEI Company, Oregon) at 160 kV accelerating voltage under low-dose conditions. Micrographies were recorded following the low-dose protocol of the microscope at a primary magnification of 62,000 x. The defocus value was chosen to correspond to a first zero of the contrast transfer function (CTF) at ~ 15 Å.

9.4.4 Crystallization screen of purified TAT10xHis and TAT/DPPIV protein

Biological macromolecules such as proteins are stable under different conditions depending on their primary and secondary structures. This makes the initial screen to identify crystallization conditions very exhaustive, since it demands testing different buffer components and pH values. In order to identify suitable crystallization conditions for the TAT10xHis protein, the commercially available Hampton crystal screen buffer series were used in 98 well micro plates (sitting-drop method). The protein solution at a concentration 5-7 mg/ ml in 50 mM Tris pH 8.0, 300 mM KCl, 5 mM DTT) was used, whereby 1 µl was pipetted for each buffer condition. The trays were then incubated for over six weeks at 4°C and observed every two weeks for the appearance of protein crystals.

The human-DPPIV crystal structure was solved earlier. However, no knowledge about the crystallization of the HIV1-TAT protein alone or in complex with another biological macromolecule is available. The purified TAT/DPPIV protein complex at a concentration 4.2 mg/ml (in PBS pH 8.0) was therefore used for crystallization screen in different Hampton crystallization buffers (sitting-drop method). Part of the protein solution was used in a series of buffers from literature, which were reported as suitable crystallization conditions for DPPIV. For this preparation the hanging-drop method was applied. After putting all components together, the plates were sealed and incubated for a period of four weeks at 4°C and observed every 2 weeks under a microscope for the appearance of crystals. The buffer series used for the screen was composed of 100 mM Tris, 300 mM Sodium acetate pH 8.0, containing different concentrations (18-29%) of PEG-4000.

10 References

Abbott C A, Baker E, Sutherland G R and McCaughan G W. **1994.** Genomic organization, exact localization, and tissue expression of the human CD26 (dipeptidyl peptidase IV) gene. *Immunogenetics*, **40**:331-338.

Abbott C A, McCaughan G W and Gorrell M D. **1999.** Two highly conserved glutamic acid residues in the predicted beta propeller domain of dipeptidyl peptidase IV are required for its enzyme activity. *FEBS Lett*, **458**:278-284.

Abbott C A, Yu D M, Woollatt E, Sutherland G R, McCaughan G W and Gorrell M D. **2000.** Cloning, expression and chromosomal localization of a novel human dipeptidyl peptidase (DPP) IV homolog, DPP8. *Eur J Biochem*, **267**:6140-6150.

Aertgeerts K, Ye S, Shi L, Prasad S G, Witmer D, Chi E, Sang B C, Wijnands R A, Webb D R and Swanson R V. **2004.** N-linked glycosylation of dipeptidyl peptidase IV (CD26): effects on enzyme activity, homodimer formation, and adenosine deaminase binding. *Protein Sci*, **13**:145-154.

Aertgeerts K, Ye S, Tennant M G, Kraus M L, Rogers J, Sang B C, Skene R J, Webb D R and Prasad G S. **2004.** Crystal structure of human dipeptidyl peptidase IV in complex with a decapeptide reveals details on substrate specificity and tetrahedral intermediate formation. *Protein Sci*, **13**:412-421.

Ahren B, Simonsson E, Larsson H, Landin-Olsson M, Torgeirsson H, Jansson P A, Sandqvist M, Bavenholm P, Efendic S, Eriksson J W, Dickinson S and Holmes D. **2002.** Inhibition of dipeptidyl peptidase IV improves metabolic control over a 4-week study period in type 2 diabetes. *Diabetes Care*, **25**:869-875.

Ajami K, Abbott C A, Obradovic M, Gysbers V, Kahne T, McCaughan G W and Gorrell M D. **2003.** Structural requirements for catalysis, expression, and dimerization in the CD26/DPIV gene family. *Biochemistry*, **42**:694-701.

Alpern R J. **1990.** Cell mechanisms of proximal tubule acidification. *Physiol Rev*, **70**:79-114.

Amemiya M, Loffing J, Lotscher M, Kaissling B, Alpern R J and Moe O W. **1995.** Expression of NHE-3 in the apical membrane of rat renal proximal tubule and thick ascending limb. *Kidney Int*, **48**:1206-1215.

Ammosova T, Berro R, Jerebtsova M, Jackson A, Charles S, Klase Z, Southerland W, Gordeuk V R, Kashanchi F and Nekhai S. **2006.** Phosphorylation of HIV-1 Tat by CDK2 in HIV-1 transcription. *Retrovirology*, **3**:78.

Appay V and Rowland-Jones S L. **2001.** RANTES: a versatile and controversial chemokine. *Trends Immunol*, **22**:83-87.

Aran J M, Colomer D, Matutes E, Vives-Corrons J L and Franco R. **1991.** Presence of adenosine deaminase on the surface of mononuclear blood cells: immunochemical localization using light and electron microscopy. *J Histochem Cytochem*, **39**:1001-1008.

Arndt M, Reinhold D, Lendeckel U, Spiess A, Faust J, Neubert K and Ansorge S. **2000.** Specific inhibitors of dipeptidyl peptidase IV suppress mRNA expression of DP IV/CD26 and cytokines. *Adv Exp Med Biol*, **477**:139-143.

Asjo B, Morfeldt-Manson L, Albert J, Biberfeld G, Karlsson A, Lidman K and Fenyo E M. **1986.** Replicative capacity of human immunodeficiency virus from patients with varying severity of HIV infection. *Lancet*, **2**:660-662.

Augustyns K, Bal G, Thonus G, Belyaev A, Zhang X M, Bollaert W, Lambeir A M, Durinx C, Goossens F and Haemers A. **1999.** The unique properties of dipeptidyl-peptidase IV (DPP IV / CD26) and the therapeutic potential of DPP IV inhibitors. *Curr Med Chem*, **6**:311-327.

Baggiolini M. **1998.** Chemokines and leukocyte traffic. *Nature*, **392**:565-568.

Baggiolini M. **2001.** Chemokines in pathology and medicine. *J Intern Med*, **250**:91-104.

Bandyopadhyay S, Kelley R and Ideker T. **2006.** Discovering regulated networks during HIV-1 latency and reactivation. *Pac Symp Biocomput*:354-366.

Barboric M and Peterlin B M. **2005.** A new paradigm in eukaryotic biology: HIV Tat and the control of transcriptional elongation. *PLoS Biol*, **3**:e76.

Barillari G, Sgadari C, Fiorelli V, Samaniego F, Colombini S, Manzari V, Modesti A, Nair B C, Cafaro A, Sturzl M and Ensoli B. **1999.** The Tat protein of human immunodeficiency virus type-1 promotes vascular cell growth and locomotion by engaging the alpha5beta1 and alphavbeta3 integrins and by mobilizing sequestered basic fibroblast growth factor. *Blood*, **94**:663-672.

Batterham R L, Cowley M A, Small C J, Herzog H, Cohen M A, Dakin C L, Wren A M, Brynes A E, Low M J, Ghatei M A, Cone R D and Bloom S R. **2002.** Gut hormone PYY(3-36) physiologically inhibits food intake. *Nature*, **418**:650-654.

Bauvois B. **2004.** Transmembrane proteases in cell growth and invasion: new contributors to angiogenesis? *Oncogene*, **23**:317-329.

Bayer P, Kraft M, Ejchart A, Westendorp M, Frank R and Rosch P. **1995.** Structural studies of HIV-1 Tat protein. *J Mol Biol*, **247**:529-535.

Berger E A, Murphy P M and Farber J M. **1999.** Chemokine receptors as HIV-1 coreceptors: roles in viral entry, tropism, and disease. *Annu Rev Immunol*, **17**:657-700.

Bernard A M, Mattei M G, Pierres M and Marguet D. **1994.** Structure of the mouse dipeptidyl peptidase IV (CD26) gene. *Biochemistry*, **33**:15204-15214.

Berro R, Kehn K, de la Fuente C, Pumfery A, Adair R, Wade J, Colberg-Poley A M, Hiscott J and Kashanchi F. **2006.** Acetylated Tat regulates human immunodeficiency virus type 1 splicing through its interaction with the splicing regulator p32. *J Virol*, **80**:3189-3204.

Bertin J, Wang L, Guo Y, Jacobson M D, Poyet J L, Srinivasula S M, Merriam S, DiStefano P S and Alnemri E S. **2001.** CARD11 and CARD14 are novel caspase recruitment domain (CARD)/membrane-associated guanylate kinase (MAGUK) family members that interact with BCL10 and activate NF-kappa B. *J Biol Chem*, **276**:11877-11882.

Bertotto A, Gerli R, Spinozzi F, Muscat C, Fabietti G M, Crupi S, Castellucci G, De Benedictis F M, De Giorgi G, Britta R and et al. 1994. CD26 surface antigen expression on peripheral blood T lymphocytes from children with Down's syndrome (trisomy 21). *Scand J Immunol*, **39**:633-636.

Biemesderfer D, Pizzonia J, Abu-Alfa A, Exner M, Reilly R, Igarashi P and Aronson P S. **1993.** NHE3: a Na+/H+ exchanger isoform of renal brush border. *Am J Physiol*, **265**:F736-742.

Biglione S, Byers S A, Price J P, Nguyen V T, Bensaude O, Price D H and Maury W. **2007.** Inhibition of HIV-1 replication by P-TEFb inhibitors DRB, seliciclib and flavopiridol correlates with release of free P-TEFb from the large, inactive form of the complex. *Retrovirology*, **4**:47.

Bilodeau N, Fiset A, Poirier G G, Fortier S, Gingras M C, Lavoie J N and Faure R L. **2006.** Insulin-dependent phosphorylation of DPP IV in liver. Evidence for a role of compartmentalized c-Src. *FEBS J*, **273**:992-1003.

Bischoff A and Michel M C. **1998.** Neuropeptide Y lowers blood glucose in anaesthetized rats via a Y5 receptor subtype. *Endocrinology*, **139**:3018-3021.

Bjelke J R, Christensen J, Nielsen P F, Branner S, Kanstrup A B, Wagtmann N and Rasmussen H B. **2006.** Dipeptidyl peptidases 8 and 9: specificity and molecular characterization compared with dipeptidyl peptidase IV. *Biochem J*, **396**:391-399.

Blaak H, van't Wout A B, Brouwer M, Hooibrink B, Hovenkamp E and Schuitemaker H. **2000.** In vivo HIV-1 infection of CD45RA(+)CD4(+) T cells is established primarily by syncytium-inducing variants and correlates with the rate of CD4(+) T cell decline. *Proc Natl Acad Sci U S A*, **97**:1269-1274.

Blaese R M, Culver K W, Miller A D, Carter C S, Fleisher T, Clerici M, Shearer G, Chang L, Chiang Y, Tolstoshev P, Greenblatt J J, Rosenberg S A, Klein H, Berger M, Mullen C A, Ramsey W J, Muul L, Morgan R A and Anderson W F. **1995.** T lymphocyte-directed gene therapy for ADA- SCID: initial trial results after 4 years. *Science*, **270**:475-480.

Blanco J, Valenzuela A, Herrera C, Lluis C, Hovanessian A G and Franco R. **2000.** The HIV-1 gp120 inhibits the binding of adenosine deaminase to CD26 by a mechanism modulated by CD4 and CXCR4 expression. *FEBS Lett*, **477**:123-128.

Blazquez M V, Madueno J A, Gonzalez R, Jurado R, Bachovchin W W, Pena J and Munoz E. **1992.** Selective decrease of CD26 expression in T cells from HIV-1-infected individuals. *J Immunol*, **149**:3073-3077.

Bleul C C, Farzan M, Choe H, Parolin C, Clark-Lewis I, Sodroski J and Springer T A. **1996.** The lymphocyte chemoattractant SDF-1 is a ligand for LESTR/fusin and blocks HIV-1 entry. *Nature*, **382**:829-833.

Bloomer A C, Champness J N, Bricogne G, Staden R and Klug A. **1978.** Protein disk of tobacco mosaic virus at 2.8 A resolution showing the interactions within and between subunits. *Nature*, **276**:362-368.

Bloomgarden Z T. **2007.** Exploring treatment strategies for type 2 diabetes. *Diabetes Care*, **30**:2737-2745.

Boggiano M M, Chandler P C, Oswald K D, Rodgers R J, Blundell J E, Ishii Y, Beattie A H, Holch P, Allison D B, Schindler M, Arndt K, Rudolf K, Mark M, Schoelch C, Joost H G, Klaus S, Thone-Reineke C, Benoit S C, Seeley R J, Beck-Sickinger A G, Koglin N, Raun K, Madsen K, Wulff B S, Stidsen C E, Birringer M, Kreuzer O J, Deng X Y, Whitcomb D C, Halem H, Taylor J, Dong J, Datta R, Culler M, Ortmann S, Castaneda T R and Tschop M. **2005.** PYY3-36 as an anti-obesity drug target. *Obes Rev*, **6**:307-322.

Bohm S K, Gum J R, Jr., Erickson R H, Hicks J W and Kim Y S. **1995.** Human dipeptidyl peptidase IV gene promoter: tissue-specific regulation from a TATA-less GC-rich sequence characteristic of a housekeeping gene promoter. *Biochem J*, **311 (Pt 3)**:835-843.

Bongers J, Lambros T, Ahmad M and Heimer E P. **1992.** Kinetics of dipeptidyl peptidase IV proteolysis of growth hormone-releasing factor and analogs. *Biochim Biophys Acta*, **1122**:147-153.

Boonacker E and Van Noorden C J. **2003.** The multifunctional or moonlighting protein CD26/DPPIV. *Eur J Cell Biol*, **82**:53-73.

Borgatti P Z G, Colamussi ML, Gibellini D, Previati M, Cantley LL, Capitani S. **1997.** Extracellular HIV-1 Tat protein activates phosphatidylinositol 3- and Akt/PKB kinases in CD4+ T lymphoblastoid Jurkat cells. *Eur J Immunol*, **11**:2805-2811

Bosi E, Camisasca R P, Collober C, Rochotte E and Garber A J. **2007.** Effects of vildagliptin on glucose control over 24 weeks in patients with type 2 diabetes inadequately controlled with metformin. *Diabetes Care*, **30**:890-895.

Boulanger M C, Liang C, Russell R S, Lin R, Bedford M T, Wainberg M A and Richard S. **2005.** Methylation of Tat by PRMT6 regulates human immunodeficiency virus type 1 gene expression. *J Virol*, **79**:124-131.

Bouras M, Huneau J F, Luengo C, Erlanson-Albertsson C and Tome D. **1995.** Metabolism of enterostatin in rat intestine, brain membranes, and serum: differential involvement of proline-specific peptidases. *Peptides*, **16**:399-405.

Brady J and Kashanchi F. **2005.** Tat gets the "green" light on transcription initiation. *Retrovirology*, **2**:69.

Bres V, Kiernan R E, Linares L K, Chable-Bessia C, Plechakova O, Treand C, Emiliani S, Peloponese J M, Jeang K T, Coux O, Scheffner M and Benkirane M. **2003.** A non-proteolytic role for ubiquitin in Tat-mediated transactivation of the HIV-1 promoter. *Nat Cell Biol*, **5**:754-761.

Broder C C and Collman R G. **1997.** Chemokine receptors and HIV. *J Leukoc Biol*, **62**:20-29.

Broder C C, Nussbaum O, Gutheil W G, Bachovchin W W and Berger E A. **1994.** CD26 antigen and HIV fusion? *Science*, **264**:1156-1159; author reply 1162-1155.

Broxmeyer H E and Carow C E. **1993.** Characterization of cord blood stem/progenitor cells. *J Hematother*, **2**:197-199.

Brubaker P L and Drucker D J. **2004.** Minireview: Glucagon-like peptides regulate cell proliferation and apoptosis in the pancreas, gut, and central nervous system. *Endocrinology*, **145**:2653-2659.

Buonaguro L, Buonaguro F M, Giraldo G and Ensoli B. **1994.** The human immunodeficiency virus type 1 Tat protein transactivates tumor necrosis factor beta gene expression through a TAR-like structure. *J Virol*, **68**:2677-2682.

Cahir McFarland E D, Hurley T R, Pingel J T, Sefton B M, Shaw A and Thomas M L. **1993.** Correlation between Src family member regulation by the protein-tyrosine-phosphatase CD45 and transmembrane signaling through the T-cell receptor. *Proc Natl Acad Sci U S A*, **90**:1402-1406.

Callahan P X, McDonald J K and Ellis S. **1972.** Dipeptidyl aminopeptidase I: application in sequencing of peptides. *Fed Proc*, **31**:1105-1113.

Callebaut C, Krust B, Jacotot E and Hovanessian A G. **1993.** T cell activation antigen, CD26, as a cofactor for entry of HIV in CD4+ cells. *Science*, **262**:2045-2050.

Campbell G R, Watkins J D, Esquieu D, Pasquier E, Loret E P and Spector S A. **2005.** The C terminus of HIV-1 Tat modulates the extent of CD178-mediated apoptosis of T cells. *J Biol Chem*, **280**:38376-38382.

Carrington M, Dean M, Martin M P and O'Brien S J. **1999.** Genetics of HIV-1 infection: chemokine receptor CCR5 polymorphism and its consequences. *Hum Mol Genet*, **8**:1939-1945.

Chang W J, Ying Y S, Rothberg K G, Hooper N M, Turner A J, Gambliel H A, De Gunzburg J, Mumby S M, Gilman A G and Anderson R G. **1994.** Purification and characterization of smooth muscle cell caveolae. *J Cell Biol*, **126**:127-138.

Charbonneau H and Tonks N K. **1992.** 1002 protein phosphatases? *Annu Rev Cell Biol*, **8**:463-493.

Chen D, Wang M, Zhou S and Zhou Q. **2002.** HIV-1 Tat targets microtubules to induce apoptosis, a process promoted by the pro-apoptotic Bcl-2 relative Bim. *EMBO J*, **21**:6801-6810.

Cheng H C, Abdel-Ghany M, Elble R C and Pauli B U. **1998.** Lung endothelial dipeptidyl peptidase IV promotes adhesion and metastasis of rat breast cancer cells via tumor cell surface-associated fibronectin. *J Biol Chem*, **273**:24207-24215.

Cheng H C, Abdel-Ghany M and Pauli B U. **2003.** A novel consensus motif in fibronectin mediates dipeptidyl peptidase IV adhesion and metastasis. *J Biol Chem*, **278**:24600-24607.

Chiang C M and Roeder R G. **1995.** Cloning of an intrinsic human TFIID subunit that interacts with multiple transcriptional activators. *Science*, **267**:531-536.

Coffin J M. **1995.** HIV population dynamics in vivo: implications for genetic variation, pathogenesis, and therapy. *Science*, **267**:483-489.

Combettes M and Kargar C. **2007.** Newly approved and promising antidiabetic agents. *Therapie*, **62**:293-310.

Contreras X, Bennasser Y, Chazal N, Moreau M, Leclerc C, Tkaczuk J and Bahraoui E. **2005.** Human immunodeficiency virus type 1 Tat protein induces an intracellular calcium increase in human monocytes that requires DHP receptors: involvement in TNF-alpha production. *Virology*, **332**:316-328.

Corey S J and Anderson S M. **1999.** Src-related protein tyrosine kinases in hematopoiesis. *Blood*, **93**:1-14.

Couet J, Li S, Okamoto T, Ikezu T and Lisanti M P. **1997.** Identification of peptide and protein ligands for the caveolin-scaffolding domain. Implications for the interaction of caveolin with caveolae-associated proteins. *J Biol Chem*, **272**:6525-6533.

Covas M J, Pinto L A and Victorino R M. **1997.** Effects of substance P on human T cell function and the modulatory role of peptidase inhibitors. *Int J Clin Lab Res*, **27**:129-134.

Coyle-Rink J, Sweet T, Abraham S, Sawaya B, Batuman O, Khalili K and Amini S. **2002.** Interaction between TGFbeta signaling proteins and C/EBP controls basal and Tat-mediated transcription of HIV-1 LTR in astrocytes. *Virology*, **299**:240-247.

Crump M P, Gong J H, Loetscher P, Rajarathnam K, Amara A, Arenzana-Seisdedos F, Virelizier J L, Baggiolini M, Sykes B D and Clark-Lewis I. **1997.** Solution structure and

basis for functional activity of stromal cell-derived factor-1; dissociation of CXCR4 activation from binding and inhibition of HIV-1. *EMBO J*, **16**:6996-7007.

Cyster J G. **1999.** Chemokines and cell migration in secondary lymphoid organs. *Science*, **286**:2098-2102.

Cyster J G, Ngo V N, Ekland E H, Gunn M D, Sedgwick J D and Ansel K M. **1999.** Chemokines and B-cell homing to follicles. *Curr Top Microbiol Immunol*, **246**:87-92; discussion 93.

D'Oro U and Ashwell J D. **1999.** Cutting edge: the CD45 tyrosine phosphatase is an inhibitor of Lck activity in thymocytes. *J Immunol*, **162**:1879-1883.

Dal Monte P, Landini M P, Sinclair J, Virelizier J L and Michelson S. **1997.** TAR and Sp1-independent transactivation of HIV long terminal repeat by the Tat protein in the presence of human cytomegalovirus IE1/IE2. *AIDS*, **11**:297-303.

Dalgleish A G, Beverley P C, Clapham P R, Crawford D H, Greaves M F and Weiss R A. **1984.** The CD4 (T4) antigen is an essential component of the receptor for the AIDS retrovirus. *Nature*, **312**:763-767.

Dang N H, Torimoto Y, Schlossman S F and Morimoto C. **1990.** Human CD4 helper T cell activation: functional involvement of two distinct collagen receptors, 1F7 and VLA integrin family. *J Exp Med*, **172**:649-652.

Dano K, Andreasen P A, Grondahl-Hansen J, Kristensen P, Nielsen L S and Skriver L. **1985.** Plasminogen activators, tissue degradation, and cancer. *Adv Cancer Res*, **44**:139-266.

David F, Bernard A M, Pierres M and Marguet D. **1993.** Identification of serine 624, aspartic acid 702, and histidine 734 as the catalytic triad residues of mouse dipeptidyl-peptidase IV (CD26). A member of a novel family of nonclassical serine hydrolases. *J Biol Chem*, **268**:17247-17252.

Davidson D J and Castellino F J. **1993.** The influence of the nature of the asparagine 289-linked oligosaccharide on the activation by urokinase and lysine binding properties of natural and recombinant human plasminogens. *J Clin Invest*, **92**:249-254.

De Meester I, Korom S, Van Damme J and Scharpe S. **1999.** CD26, let it cut or cut it down. *Immunol Today*, **20**:367-375.

De Meester I, Vanham G, Kestens L, Vanhoof G, Bosmans E, Gigase P and Scharpe S. **1994.** Binding of adenosine deaminase to the lymphocyte surface via CD26. *Eur J Immunol*, **24**:566-570.

De Meester I A, Kestens L L, Vanham G L, Vanhoof G C, Vingerhoets J H, Gigase P L and Scharpe S L. **1995.** Costimulation of CD4+ and CD8+ T cells through CD26: the ADA-binding epitope is not essential for complete signaling. *J Leukoc Biol*, **58**:325-330.

de Roda Husman A M and Schuitemaker H. **1998.** Chemokine receptors and the clinical course of HIV-1 infection. *Trends Microbiol*, **6**:244-249.

Deacon C F, Hughes T E and Holst J J. **1998.** Dipeptidyl peptidase IV inhibition potentiates the insulinotropic effect of glucagon-like peptide 1 in the anesthetized pig. *Diabetes*, **47**:764-769.

DeClerck Y A and Laug W E. **1996.** Cooperation between matrix metalloproteinases and the plasminogen activator-plasmin system in tumor progression. *Enzyme Protein*, **49**:72-84.

Dietrich J, Menne C, Lauritsen J P, von Essen M, Rasmussen A B, Odum N and Geisler C. **2002.** Ligand-induced TCR down-regulation is not dependent on constitutive TCR cycling. *J Immunol*, **168**:5434-5440.

Dobers J, Grams S, Reutter W and Fan H. **2000.** Roles of cysteines in rat dipeptidyl peptidase IV/CD26 in processing and proteolytic activity. *Eur J Biochem*, **267**:5093-5100.

Dobers J, Zimmermann-Kordmann M, Leddermann M, Schewe T, Reutter W and Fan H. **2002.** Expression, purification, and characterization of human dipeptidyl peptidase IV/CD26 in Sf9 insect cells. *Protein Expr Purif*, **25**:527-532.

Dommett R M, Klein N and Turner M W. **2006.** Mannose-binding lectin in innate immunity: past, present and future. *Tissue Antigens*, **68**:193-209.

Dong R P, Kameoka J, Hegen M, Tanaka T, Xu Y, Schlossman S F and Morimoto C. **1996.** Characterization of adenosine deaminase binding to human CD26 on T cells and its biologic role in immune response. *J Immunol*, **156**:1349-1355.

Dong R P, Tachibana K, Hegen M, Munakata Y, Cho D, Schlossman S F and Morimoto C. **1997.** Determination of adenosine deaminase binding domain on CD26 and its immunoregulatory effect on T cell activation. *J Immunol*, **159**:6070-6076.

Doranz B J, Orsini M J, Turner J D, Hoffman T L, Berson J F, Hoxie J A, Peiper S C, Brass L F and Doms R W. **1999.** Identification of CXCR4 domains that support coreceptor and chemokine receptor functions. *J Virol*, **73**:2752-2761.

Drucker D J. **2003.** Glucagon-like peptide-1 and the islet beta-cell: augmentation of cell proliferation and inhibition of apoptosis. *Endocrinology*, **144**:5145-5148.

Drucker D J, Philippe J, Mojsov S, Chick W L and Habener J F. **1987.** Glucagon-like peptide I stimulates insulin gene expression and increases cyclic AMP levels in a rat islet cell line. *Proc Natl Acad Sci U S A*, **84**:3434-3438.

Duke-Cohan J S, Morimoto C, Rocker J A and Schlossman S F. **1995.** A novel form of dipeptidylpeptidase IV found in human serum. Isolation, characterization, and comparison with T lymphocyte membrane dipeptidylpeptidase IV (CD26). *J Biol Chem*, **270**:14107-14114.

Dunker A K, Garner E, Guilliot S, Romero P, Albrecht K, Hart J, Obradovic Z, Kissinger C and Villafranca J E. **1998.** Protein disorder and the evolution of molecular recognition: theory, predictions and observations. *Pac Symp Biocomput*:473-484.

Dunker A K, Lawson J D, Brown C J, Williams R M, Romero P, Oh J S, Oldfield C J, Campen A M, Ratliff C M, Hipps K W, Ausio J, Nissen M S, Reeves R, Kang C, Kissinger C R, Bailey R W, Griswold M D, Chiu W, Garner E C and Obradovic Z. **2001.** Intrinsically disordered protein. *J Mol Graph Model*, **19**:26-59.

Durinx C, Lambeir A M, Bosmans E, Falmagne J B, Berghmans R, Haemers A, Scharpe S and De Meester I. **2000.** Molecular characterization of dipeptidyl peptidase activity in serum: soluble CD26/dipeptidyl peptidase IV is responsible for the release of X-Pro dipeptides. *Eur J Biochem*, **267**:5608-5613.

Efendic S and Portwood N. **2004.** Overview of incretin hormones. *Horm Metab Res*, **36**:742-746.

Engel M, Hoffmann T, Wagner L, Wermann M, Heiser U, Kiefersauer R, Huber R, Bode W, Demuth H U and Brandstetter H. **2003.** The crystal structure of dipeptidyl peptidase IV (CD26) reveals its functional regulation and enzymatic mechanism. *Proc Natl Acad Sci U S A*, **100**:5063-5068.

Ensoli B, Buonaguro L, Barillari G, Fiorelli V, Gendelman R, Morgan R A, Wingfield P and Gallo R C. **1993.** Release, uptake, and effects of extracellular human immunodeficiency virus type 1 Tat protein on cell growth and viral transactivation. *J Virol*, **67**:277-287.

Estall J L and Drucker D J. **2006.** Glucagon and glucagon-like peptide receptors as drug targets. *Curr Pharm Des*, **12**:1731-1750.

Fan H, Meng W, Kilian C, Grams S and Reutter W. **1997.** Domain-specific N-glycosylation of the membrane glycoprotein dipeptidylpeptidase IV (CD26) influences its subcellular trafficking, biological stability, enzyme activity and protein folding. *Eur J Biochem*, **246**:243-251.

Feinberg M B, Baltimore D and Frankel A D. **1991.** The role of Tat in the human immunodeficiency virus life cycle indicates a primary effect on transcriptional elongation. *Proc Natl Acad Sci U S A*, **88**:4045-4049.

Feng Y, Broder C C, Kennedy P E and Berger E A. **1996.** HIV-1 entry cofactor: functional cDNA cloning of a seven-transmembrane, G protein-coupled receptor. *Science*, **272**:872-877.

Feron O and Kelly R A. **2001.** The caveolar paradox: suppressing, inducing, and terminating eNOS signaling. *Circ Res*, **88**:129-131.

Ferreira G N, Monteiro G A, Prazeres D M and Cabral J M. **2000.** Downstream processing of plasmid DNA for gene therapy and DNA vaccine applications. *Trends Biotechnol*, **18**:380-388.

Fleischer B. **1994.** CD26: a surface protease involved in T-cell activation. *Immunol Today*, **15**:180-184.

Flint A, Raben A, Astrup A and Holst J J. **1998.** Glucagon-like peptide 1 promotes satiety and suppresses energy intake in humans. *J Clin Invest*, **101**:515-520.

Fox D A, Hussey R E, Fitzgerald K A, Acuto O, Poole C, Palley L, Daley J F, Schlossman S F and Reinherz E L. **1984.** Ta1, a novel 105 KD human T cell activation antigen defined by a monoclonal antibody. *J Immunol*, **133**:1250-1256.

Franco R, Valenzuela A, Lluis C and Blanco J. **1998.** Enzymatic and extraenzymatic role of ecto-adenosine deaminase in lymphocytes. *Immunol Rev*, **161**:27-42.

Frank P G, Galbiati F, Volonte D, Razani B, Cohen D E, Marcel Y L and Lisanti M P. **2001.** Influence of caveolin-1 on cellular cholesterol efflux mediated by high-density lipoproteins. *Am J Physiol Cell Physiol*, **280**:C1204-1214.

Frank P G and Lisanti M P. **2004.** Caveolin-1 and caveolae in atherosclerosis: differential roles in fatty streak formation and neointimal hyperplasia. *Curr Opin Lipidol*, **15**:523-529.

Frankel A D, Chen L, Cotter R J and Pabo C O. **1988.** Dimerization of the tat protein from human immunodeficiency virus: a cysteine-rich peptide mimics the normal metal-linked dimer interface. *Proc Natl Acad Sci U S A*, **85**:6297-6300.

Frohman L A, Downs T R, Heimer E P and Felix A M. **1989.** Dipeptidylpeptidase IV and trypsin-like enzymatic degradation of human growth hormone-releasing hormone in plasma. *J Clin Invest*, **83**:1533-1540.

Fujiwara H, Maeda M, Imai K, Fukuoka M, Yasuda K, Takakura K and Mori T. **1992.** Human luteal cells express dipeptidyl peptidase IV on the cell surface. *J Clin Endocrinol Metab*, **75**:1352-1357.

Gaide O, Favier B, Legler D F, Bonnet D, Brissoni B, Valitutti S, Bron C, Tschopp J and Thome M. **2002.** CARMA1 is a critical lipid raft-associated regulator of TCR-induced NF-kappa B activation. *Nat Immunol*, **3**:836-843.

Gaide O, Martinon F, Micheau O, Bonnet D, Thome M and Tschopp J. **2001.** Carma1, a CARD-containing binding partner of Bcl10, induces Bcl10 phosphorylation and NF-kappaB activation. *FEBS Lett*, **496**:121-127.

Galbiati F, Volonte D, Liu J, Capozza F, Frank P G, Zhu L, Pestell R G and Lisanti M P. **2001.** Caveolin-1 expression negatively regulates cell cycle progression by inducing G(0)/G(1) arrest via a p53/p21(WAF1/Cip1)-dependent mechanism. *Mol Biol Cell*, **12**:2229-2244.

Gallwitz B, Ropeter T, Morys-Wortmann C, Mentlein R, Siegel E G and Schmidt W E. **2000.** GLP-1-analogues resistant to degradation by dipeptidyl-peptidase IV in vitro. *Regul Pept*, **86**:103-111.

Gatignol A and Jeang K T. **2000.** Tat as a transcriptional activator and a potential therapeutic target for HIV-1. *Adv Pharmacol*, **48**:209-227.

Gerli R, Muscat C, Bertotto A, Bistoni O, Agea E, Tognellini R, Fiorucci G, Cesarotti M and Bombardieri S. **1996.** CD26 surface molecule involvement in T cell activation and lymphokine synthesis in rheumatoid and other inflammatory synovitis. *Clin Immunol Immunopathol*, **80**:31-37.

Gerondakis S, Grumont R, Rourke I and Grossmann M. **1998.** The regulation and roles of Rel/NF-kappa B transcription factors during lymphocyte activation. *Curr Opin Immunol*, **10**:353-359.

Gervais F G and Veillette A. **1997.** Reconstitution of interactions between protein-tyrosine phosphatase CD45 and tyrosine-protein kinase p56(lck) in nonlymphoid cells. *J Biol Chem*, **272**:12754-12761.

Ghezzi S, Noonan D M, Aluigi M G, Vallanti G, Cota M, Benelli R, Morini M, Reeves J D, Vicenzi E, Poli G and Albini A. **2000.** Inhibition of CXCR4-dependent HIV-1 infection by extracellular HIV-1 Tat. *Biochem Biophys Res Commun*, **270**:992-996.

Gibellini D B A, Pierpaoli S, Bertolaso L, Milani D, Capitani S, La Placa M, Zauli G 1998 Extracellular HIV-1 Tat protein induces the rapid Ser133 phosphorylation and activation of CREB transcription factor in both Jurkat lymphoblastoid T cells and primary peripheral blood mononuclear cells. *J Immunol*, **160**:3891-3898

Girardi A C, Knauf F, Demuth H U and Aronson P S. **2004.** Role of dipeptidyl peptidase IV in regulating activity of Na+/H+ exchanger isoform NHE3 in proximal tubule cells. *Am J Physiol Cell Physiol*, **287**:C1238-1245.

Glenney J R, Jr. 1989. Tyrosine phosphorylation of a 22-kDa protein is correlated with transformation by Rous sarcoma virus. *J Biol Chem*, **264**:20163-20166.

Glenney J R, Jr. and Zokas L. **1989.** Novel tyrosine kinase substrates from Rous sarcoma virus-transformed cells are present in the membrane skeleton. *J Cell Biol*, **108**:2401-2408.

Gonzalez-Gronow M, Gawdi G and Pizzo S V. **1993.** Plasminogen activation stimulates an increase in intracellular calcium in human synovial fibroblasts. *J Biol Chem*, **268**:20791-20795.

Gonzalez-Gronow M, Gawdi G and Pizzo S V. **1994.** Characterization of the plasminogen receptors of normal and rheumatoid arthritis human synovial fibroblasts. *J Biol Chem*, **269**:4360-4366.

Gonzalez-Gronow M, Grenett H E, Weber M R, Gawdi G and Pizzo S V. **2001.** Interaction of plasminogen with dipeptidyl peptidase IV initiates a signal transduction mechanism which regulates expression of matrix metalloproteinase-9 by prostate cancer cells. *Biochem J*, **355**:397-407.

Gonzalez-Gronow M, Hershfield M S, Arredondo-Vega F X and Pizzo S V. **2004.** Cell surface adenosine deaminase binds and stimulates plasminogen activation on 1-LN human prostate cancer cells. *J Biol Chem*, **279**:20993-20998.

Gorrell M D. **2005.** Dipeptidyl peptidase IV and related enzymes in cell biology and liver disorders. *Clin Sci (Lond)*, **108**:277-292.

Gorrell M D, Gysbers V and McCaughan G W. **2001.** CD26: a multifunctional integral membrane and secreted protein of activated lymphocytes. *Scand J Immunol*, **54**:249-264.

Grande-Garcia A, Echarri A, de Rooij J, Alderson N B, Waterman-Storer C M, Valdivielso J M and del Pozo M A. **2007.** Caveolin-1 regulates cell polarization and directional migration through Src kinase and Rho GTPases. *J Cell Biol*, **177**:683-694.

Grandt D, Dahms P, Schimiczek M, Eysselein V E, Reeve J R, Jr. and Mentlein R. **1993.** [Proteolytic processing by dipeptidyl aminopeptidase IV generates receptor selectivity for peptide YY (PYY)]. *Med Klin (Munich)*, **88**:143-145.

Greene W C and Peterlin B M. **2002.** Charting HIV's remarkable voyage through the cell: Basic science as a passport to future therapy. *Nat Med*, **8**:673-680.

Gromada J, Holst J J and Rorsman P. **1998.** Cellular regulation of islet hormone secretion by the incretin hormone glucagon-like peptide 1. *Pflugers Arch*, **435**:583-594.

Grondin G, Hooper N M and LeBel D. **1999.** Specific localization of membrane dipeptidase and dipeptidyl peptidase IV in secretion granules of two different pancreatic islet cells. *J Histochem Cytochem*, **47**:489-498.

Grottesi A, Sette M, Palamara T, Rotilio G, Garaci E and Paci M. **1998.** The conformation of peptide thymosin alpha 1 in solution and in a membrane-like environment by circular dichroism and NMR spectroscopy. A possible model for its interaction with the lymphocyte membrane. *Peptides*, **19**:1731-1738.

Gruber M, Scholz W and Flad H D. **1988.** Influence of human T lymphocytes identified by antibodies to dipeptidyl peptidase IV on differentiation of human B lymphocytes stimulated with Staphylococcus aureus Cowan I and pokeweed mitogen. *Cell Immunol*, **113**:423-434.

Gutheil W G, Subramanyam M, Flentke G R, Sanford D G, Munoz E, Huber B T and Bachovchin W W. **1994.** Human immunodeficiency virus 1 Tat binds to dipeptidyl

aminopeptidase IV (CD26): a possible mechanism for Tat's immunosuppressive activity. *Proc Natl Acad Sci U S A*, **91**:6594-6598.

Hanski C, Huhle T, Gossrau R and Reutter W. **1988.** Direct evidence for the binding of rat liver DPP IV to collagen in vitro. *Exp cell Res*, **178**:64-72.

Hanski C, Huhle T and Reutter W. **1985.** Involvement of plasma membrane dipeptidyl peptidase IV in fibronectin-mediated adhesion of cells on collagen. *Biol Chem Hoppe Seyler*, **366**:1169-1176.

Hanski C, Zimmer T, Gossrau R and Reutter W. **1986.** Increased activity of dipeptidyl peptidase IV in serum of hepatoma-bearing rats coincides with the loss of the enzyme from the hepatoma plasma membrane. *Experientia*, **42**:826-828.

Hansotia T and Drucker D J. **2005.** GIP and GLP-1 as incretin hormones: lessons from single and double incretin receptor knockout mice. *Regul Pept*, **128**:125-134.

Hartel-Schenk S, Gossrau R and Reutter W. **1990.** Comparative immunohistochemistry and histochemistry of dipeptidyl peptidase IV in rat organs during development. *Histochem J*, **22**:567-578.

Hartel S, Hanski C, Neumeier R, Gossrau R and Reutter W. **1988.** Characterization of different forms of dipeptidyl peptidase IV from rat liver and hepatoma by monoclonal antibodies. *Adv Exp Med Biol*, **240**:207-214.

Hebert E. **2006.** Mannose-6-phosphate/insulin-like growth factor II receptor expression and tumor development. *Biosci Rep*, **26**:7-17.

Hegen M, Kameoka J, Dong R P, Schlossman S F and Morimoto C. **1997.** Cross-linking of CD26 by antibody induces tyrosine phosphorylation and activation of mitogen-activated protein kinase. *Immunology*, **90**:257-264.

Hegen M, Niedobitek G, Klein C E, Stein H and Fleischer B. **1990.** The T cell triggering molecule Tp103 is associated with dipeptidyl aminopeptidase IV activity. *J Immunol*, **144**:2908-2914.

Hemmings H C, Jr., Nairn A C, Aswad D W and Greengard P. **1984.** DARPP-32, a dopamine- and adenosine 3':5'-monophosphate-regulated phosphoprotein enriched in dopamine-innervated brain regions. II. Purification and characterization of the phosphoprotein from bovine caudate nucleus. *J Neurosci*, **4**:99-110.

Hermansen K and Mortensen L S. **2007.** Bodyweight changes associated with antihyperglycaemic agents in type 2 diabetes mellitus. *Drug Saf*, **30**:1127-1142.

Herrera C, Morimoto C, Blanco J, Mallol J, Arenzana F, Lluis C and Franco R. **2001.** Comodulation of CXCR4 and CD26 in human lymphocytes. *J Biol Chem*, **276**:19532-19539.

Hetzer C, Dormeyer W, Schnolzer M and Ott M. **2005.** Decoding Tat: the biology of HIV Tat posttranslational modifications. *Microbes Infect*, **7**:1364-1369.

Heukeshoven J and Dernick R. **1988.** Improved silver staining procedure for fast staining in PhastSystem Development Unit. I. Staining of sodium dodecyl sulfate gels. *Electrophoresis*, **9**:28-32.

Heymann E and Mentlein R. **1978.** Liver dipeptidyl aminopeptidase IV hydrolyzes substance P. *FEBS Lett*, **91**:360-364.

Hildebrandt M, Reutter W, Arck P, Rose M and Klapp B F. **2000.** A guardian angel: the involvement of dipeptidyl peptidase IV in psychoneuroendocrine function, nutrition and immune defence. *Clin Sci (Lond)*, **99**:93-104.

Hinke S A, Gelling R W, Pederson R A, Manhart S, Nian C, Demuth H U and McIntosh C H. **2002.** Dipeptidyl peptidase IV-resistant [D-Ala(2)]glucose-dependent insulinotropic polypeptide (GIP) improves glucose tolerance in normal and obese diabetic rats. *Diabetes*, **51**:652-661.

Hinke S A, Kuhn-Wache K, Hoffmann T, Pederson R A, McIntosh C H and Demuth H U. **2002.** Metformin effects on dipeptidylpeptidase IV degradation of glucagon-like peptide-1. *Biochem Biophys Res Commun*, **291**:1302-1308.

Hiramatsu H, Kyono K, Higashiyama Y, Fukushima C, Shima H, Sugiyama S, Inaka K, Yamamoto A and Shimizu R. **2003.** The structure and function of human dipeptidyl peptidase IV, possessing a unique eight-bladed beta-propeller fold. *Biochem Biophys Res Commun*, **302**:849-854.

Hoffmann J A, Kafatos F C, Janeway C A and Ezekowitz R A. **1999.** Phylogenetic perspectives in innate immunity. *Science*, **284**:1313-1318.

Hoffmann T, Faust J, Neubert K and Ansorge S. **1993.** Dipeptidyl peptidase IV (CD 26) and aminopeptidase N (CD 13) catalyzed hydrolysis of cytokines and peptides with N-terminal cytokine sequences. *FEBS Lett*, **336**:61-64.

Hong W J, Petell J K, Swank D, Sanford J, Hixson D C and Doyle D. **1989.** Expression of dipeptidyl peptidase IV in rat tissues is mainly regulated at the mRNA levels. *Exp cell Res*, **182**:256-266.

Hopsu-Havu V K and Glenner G G. **1966.** A new dipeptide naphthylamidase hydrolyzing glycyl-prolyl-beta-naphthylamide. *Histochemie*, **7**:197-201.

Howcroft T K, Strebel K, Martin M A and Singer D S. **1993.** Repression of MHC class I gene promoter activity by two-exon Tat of HIV. *Science*, **260**:1320-1322.

Huang L, Bosch I, Hofmann W, Sodroski J and Pardee A B. **1998.** Tat protein induces human immunodeficiency virus type 1 (HIV-1) coreceptors and promotes infection with both macrophage-tropic and T-lymphotropic HIV-1 strains. *J Virol*, **72**:8952-8960.

Huigen M C, Kamp W and Nottet H S. **2004.** Multiple effects of HIV-1 trans-activator protein on the pathogenesis of HIV-1 infection. *Eur J Clin Invest*, **34**:57-66.

Hwang I, Huang J F, Kishimoto H, Brunmark A, Peterson P A, Jackson M R, Surh C D, Cai Z and Sprent J. **2000.** T cells can use either T cell receptor or CD28 receptors to absorb and internalize cell surface molecules derived from antigen-presenting cells. *J Exp Med*, **191**:1137-1148.

Hwang I and Sprent J. **2001.** Role of the actin cytoskeleton in T cell absorption and internalization of ligands from APC. *J Immunol*, **166**:5099-5107.

Ikeda K, Sannoh T, Kawasaki N, Kawasaki T and Yamashina I. **1987.** Serum lectin with known structure activates complement through the classical pathway. *J Biol Chem*, **262**:7451-7454.

Ikezu T, Ueda H, Trapp B D, Nishiyama K, Sha J F, Volonte D, Galbiati F, Byrd A L, Bassell G, Serizawa H, Lane W S, Lisanti M P and Okamoto T. **1998.** Affinity-purification and characterization of caveolins from the brain: differential expression of caveolin-1, -2, and -3 in brain endothelial and astroglial cell types. *Brain Res*, **804**:177-192.

Ikushima H, Munakata Y, Ishii T, Iwata S, Terashima M, Tanaka H, Schlossman S F and Morimoto C. **2000.** Internalization of CD26 by mannose 6-phosphate/insulin-like growth factor II receptor contributes to T cell activation. *Proc Natl Acad Sci U S A*, **97**:8439-8444.

Ikushima H, Munakata Y, Iwata S, Ohnuma K, Kobayashi S, Dang N H and Morimoto C. **2002.** Soluble CD26/dipeptidyl peptidase IV enhances transendothelial migration via its interaction with mannose 6-phosphate/insulin-like growth factor II receptor. *Cell Immunol*, **215**:106-110.

Ishii T, Ohnuma K, Murakami A, Takasawa N, Kobayashi S, Dang N H, Schlossman S F and Morimoto C. **2001.** CD26-mediated signaling for T cell activation occurs in lipid rafts through its association with CD45RO. *Proc Natl Acad Sci U S A*, **98**:12138-12143.

Iwaki-Egawa S, Watanabe Y, Kikuya Y and Fujimoto Y. **1998.** Dipeptidyl peptidase IV from human serum: purification, characterization, and N-terminal amino acid sequence. *J Biochem*, **124**:428-433.

Jeang K T, Chang Y, Berkhout B, Hammarskjold M L and Rekosh D. **1991.** Regulation of HIV expression: mechanisms of action of Tat and Rev. *AIDS*, **5 Suppl 2**:S3-14.

Jost M M, Lamerz J, Tammen H, Menzel C, De Meester I, Lambeir A M, Augustyns K, Scharpe S, Zucht H D, Rose H, Jurgens M, Schulz-Knappe P and Budde P. **2009.** In vivo profiling of DPP4 inhibitors reveals alterations in collagen metabolism and accumulation of an amyloid peptide in rat plasma. *Biochem Pharmacol*, **77**:228-237.

Juarez J and Bendall L. **2004.** SDF-1 and CXCR4 in normal and malignant hematopoiesis. *Histol Histopathol*, **19**:299-309.

Jun J E and Goodnow C C. **2003.** Scaffolding of antigen receptors for immunogenic versus tolerogenic signaling. *Nat Immunol*, **4**:1057-1064.

Justement L B. **2001.** The role of the protein tyrosine phosphatase CD45 in regulation of B lymphocyte activation. *Int Rev Immunol*, **20**:713-738.

Kahn C R. **2003.** Knockout mice challenge our concepts of glucose homeostasis and the pathogenesis of diabetes. *Exp Diabesity Res*, **4**:169-182.

Kahne T, Kroning H, Thiel U, Ulmer A J, Flad H D and Ansorge S. **1996.** Alterations in structure and cellular localization of molecular forms of DP IV/CD26 during T cell activation. *Cell Immunol*, **170**:63-70.

Kahne T, Neubert K, Faust J and Ansorge S. **1998.** Early phosphorylation events induced by DPIV/CD26-specific inhibitors. *Cell Immunol*, **189**:60-66.

Kajiyama H, Kikkawa F, Khin E, Shibata K, Ino K and Mizutani S. **2003.** Dipeptidyl peptidase IV overexpression induces up-regulation of E-cadherin and tissue inhibitors of matrix metalloproteinases, resulting in decreased invasive potential in ovarian carcinoma cells. *Cancer Res*, **63**:2278-2283.

Kameoka J, Tanaka T, Nojima Y, Schlossman S F and Morimoto C. **1993.** Direct association of adenosine deaminase with a T cell activation antigen, CD26. *Science*, **261**:466-469.

Karn J. **1999.** Tackling Tat. *J Mol Biol*, **293**:235-254.

Kato H, Sumimoto H, Pognonec P, Chen C H, Rosen C A and Roeder R G. **1992.** HIV-1 Tat acts as a processivity factor in vitro in conjunction with cellular elongation factors. *Genes Dev*, **6**:655-666.

Kawasaki N, Lin C W, Inoue R, Khoo K H, Ma B Y, Oka S, Ishiguro M, Sawada T, Ishida H, Hashimoto T and Kawasaki T. **2009.** Highly fucosylated N-glycan ligands for mannan-binding protein expressed specifically on CD26 (DPPVI) isolated from a human colorectal carcinoma cell line, SW1116. *Glycobiology*, **19**:437-450.

Kawasaki T. **1999.** Structure and biology of mannan-binding protein, MBP, an important component of innate immunity. *Biochim Biophys Acta*, **1473**:186-195.

Kenny A J, Booth A G, Wood E J and Young A R. **1976.** Dipeptidyl peptidase IV, a kidney microvillus serine proteinase: evidence for its large subunit molecular weight and endopeptidase activity. *Biochem Soc Trans*, **4**:347-348.

Kiernan R E, Vanhulle C, Schiltz L, Adam E, Xiao H, Maudoux F, Calomme C, Burny A, Nakatani Y, Jeang K T, Benkirane M and Van Lint C. **1999.** HIV-1 tat transcriptional activity is regulated by acetylation. *EMBO J*, **18**:6106-6118.

Kim Y K, Bourgeois C F, Isel C, Churcher M J and Karn J. **2002.** Phosphorylation of the RNA polymerase II carboxyl-terminal domain by CDK9 is directly responsible for human immunodeficiency virus type 1 Tat-activated transcriptional elongation. *Mol Cell Biol*, **22**:4622-4637.

Korom S, De Meester I, Stadlbauer T H, Chandraker A, Schaub M, Sayegh M H, Belyaev A, Haemers A, Scharpe S and Kupiec-Weglinski J W. **1997.** Inhibition of CD26/dipeptidyl peptidase IV activity in vivo prolongs cardiac allograft survival in rat recipients. *Transplantation*, **63**:1495-1500.

Kreisel W, Heussner R, Volk B, Buchsel R, Reutter W and Gerok W. **1982.** Identification of the 110000 Mr glycoprotein isolated from rat liver plasma membrane as dipeptidylaminopeptidase IV. *FEBS Lett*, **147**:85-88.

Kreisel W, Hildebrandt H, Mossner W, Tauber R and Reutter W. **1993.** Oligosaccharide reprocessing and recycling of a cell surface glycoprotein in cultured rat hepatocytes. *Biol Chem Hoppe Seyler*, **374**:255-263.

Kubota T, Flentke G R, Bachovchin W W and Stollar B D. **1992.** Involvement of dipeptidyl peptidase IV in an in vivo immune response. *Clin Exp Immunol*, **89**:192-197.

Kucia M, Jankowski K, Reca R, Wysoczynski M, Bandura L, Allendorf D J, Zhang J, Ratajczak J and Ratajczak M Z. **2004.** CXCR4-SDF-1 signalling, locomotion, chemotaxis and adhesion. *J Mol Histol*, **35**:233-245.

Lambeir A M, Diaz Pereira J F, Chacon P, Vermeulen G, Heremans K, Devreese B, Van Beeumen J, De Meester I and Scharpe S. **1997.** A prediction of DPP IV/CD26 domain structure from a physico-chemical investigation of dipeptidyl peptidase IV (CD26) from human seminal plasma. *Biochim Biophys Acta*, **1340**:215-226.

Lambeir A M, Durinx C, Scharpe S and De Meester I. **2003.** Dipeptidyl-peptidase IV from bench to bedside: an update on structural properties, functions, and clinical aspects of the enzyme DPP IV. *Crit Rev Clin Lab Sci*, **40**:209-294.

Lambeir A M, Proost P, Durinx C, Bal G, Senten K, Augustyns K, Scharpe S, Van Damme J and De Meester I. **2001.** Kinetic investigation of chemokine truncation by CD26/dipeptidyl peptidase IV reveals a striking selectivity within the chemokine family. *J Biol Chem*, **276**:29839-29845.

Lambeir A M, Proost P, Scharpe S and De Meester I. **2002.** A kinetic study of glucagon-like peptide-1 and glucagon-like peptide-2 truncation by dipeptidyl peptidase IV, in vitro. *Biochem Pharmacol*, **64**:1753-1756.

Lapham C K, Ouyang J, Chandrasekhar B, Nguyen N Y, Dimitrov D S and Golding H. **1996.** Evidence for cell-surface association between fusin and the CD4-gp120 complex in human cell lines. *Science*, **274**:602-605.

Laspia M F, Rice A P and Mathews M B. **1989.** HIV-1 Tat protein increases transcriptional initiation and stabilizes elongation. *Cell*, **59**:283-292.

Lee K N, Jackson K W, Christiansen V J, Chung K H and McKee P A. **2004.** A novel plasma proteinase potentiates alpha2-antiplasmin inhibition of fibrin digestion. *Blood*, **103**:3783-3788.

Leiting B, Pryor K D, Wu J K, Marsilio F, Patel R A, Craik C S, Ellman J A, Cummings R T and Thornberry N A. **2003.** Catalytic properties and inhibition of proline-specific dipeptidyl peptidases II, IV and VII. *Biochem J*, **371**:525-532.

Li C J, Friedman D J, Wang C, Metelev V and Pardee A B. **1995.** Induction of apoptosis in uninfected lymphocytes by HIV-1 Tat protein. *Science*, **268**:429-431.

Liao Z, Graham D R and Hildreth J E. **2003.** Lipid rafts and HIV pathogenesis: virion-associated cholesterol is required for fusion and infection of susceptible cells. *AIDS Res Hum Retroviruses*, **19**:675-687.

Lopez M, Tetaert D, Juliant S, Gazon M, Cerutti M, Verbert A and Delannoy P. **1999.** O-glycosylation potential of lepidopteran insect cell lines. *Biochim Biophys Acta*, **1427**:49-61.

Loster K, Zeilinger K, Schuppan D and Reutter W. **1995.** The cysteine-rich region of dipeptidyl peptidase IV (CD 26) is the collagen-binding site. *Biochem Biophys Res Commun*, **217**:341-348.

Luster M I. **1998.** Inflammation, tumor necrosis factor, and toxicology. *Environ Health Perspect*, **106**:A418-419.

Ma Y, Uemura K, Oka S, Kozutsumi Y, Kawasaki N and Kawasaki T. **1999.** Antitumor activity of mannan-binding protein in vivo as revealed by a virus expression system: mannan-binding proteindependent cell-mediated cytotoxicity. *Proc Natl Acad Sci U S A*, **96**:371-375.

Magnuson N S and Perryman L E. **1986.** Metabolic defects in severe combined immunodeficiency in man and animals. *Comp Biochem Physiol B*, **83**:701-710.

Malhotra R, Lu J, Holmskov U and Sim R B. **1994.** Collectins, collectin receptors and the lectin pathway of complement activation. *Clin Exp Immunol*, **97 Suppl 2**:4-9.

Manes S, del Real G, Lacalle R A, Lucas P, Gomez-Mouton C, Sanchez-Palomino S, Delgado R, Alcami J, Mira E and Martinez A C. **2000.** Membrane raft microdomains mediate lateral assemblies required for HIV-1 infection. *EMBO Rep*, **1**:190-196.

Mantovani A, Gray P A, Van Damme J and Sozzani S. **2000.** Macrophage-derived chemokine (MDC). *J Leukoc Biol*, **68**:400-404.

Marguet D, Baggio L, Kobayashi T, Bernard A M, Pierres M, Nielsen P F, Ribel U, Watanabe T, Drucker D J and Wagtmann N. **2000.** Enhanced insulin secretion and improved glucose tolerance in mice lacking CD26. *Proc Natl Acad Sci U S A*, **97**:6874-6879.

Marguet D, Bernard A M, Vivier I, Darmoul D, Naquet P and Pierres M. **1992.** cDNA cloning for mouse thymocyte-activating molecule. A multifunctional ecto-dipeptidyl peptidase IV (CD26) included in a subgroup of serine proteases. *J Biol Chem*, **267**:2200-2208.

Markus G. **1965.** Protein substrate conformation and proteolysis. *Proc Natl Acad Sci U S A*, **54**:253-258.

Matveev S, van der Westhuyzen D R and Smart E J. **1999.** Co-expression of scavenger receptor-BI and caveolin-1 is associated with enhanced selective cholesteryl ester uptake in THP-1 macrophages. *J Lipid Res*, **40**:1647-1654.

Mazzieri R, Masiero L, Zanetta L, Monea S, Onisto M, Garbisa S and Mignatti P. **1997.** Control of type IV collagenase activity by components of the urokinase-plasmin system: a regulatory mechanism with cell-bound reactants. *EMBO J*, **16**:2319-2332.

McAllister-Lucas L M, Inohara N, Lucas P C, Ruland J, Benito A, Li Q, Chen S, Chen F F, Yamaoka S, Verma I M, Mak T W and Nunez G. **2001.** Bimp1, a MAGUK family member linking protein kinase C activation to Bcl10-mediated NF-kappaB induction. *J Biol Chem*, **276**:30589-30597.

Menegon A L C, Benfenati F, Valtorta F. **1997.** Tat protein from HIV-1 activates MAP kinase in granular neurons and glial cells from rat cerebellum. *Biochem Biophys Res Commun*, **238**:800-805

Menne C, Moller Sorensen T, Siersma V, von Essen M, Odum N and Geisler C. **2002.** Endo- and exocytic rate constants for spontaneous and protein kinase C-activated T cell receptor cycling. *Eur J Immunol*, **32**:616-626.

Mentlein R. **1999.** Dipeptidyl-peptidase IV (CD26)--role in the inactivation of regulatory peptides. *Regul Pept*, **85**:9-24.

Mentlein R, Dahms P, Grandt D and Kruger R. **1993.** Proteolytic processing of neuropeptide Y and peptide YY by dipeptidyl peptidase IV. *Regul Pept*, **49**:133-144.

Mentlein R, Gallwitz B and Schmidt W E. **1993.** Dipeptidyl-peptidase IV hydrolyses gastric inhibitory polypeptide, glucagon-like peptide-1(7-36)amide, peptide histidine methionine and is responsible for their degradation in human serum. *Eur J Biochem*, **214**:829-835.

Mentlein R, Rix H, Feller A C and Heymann E. **1986.** Characterization of dipeptidyl peptidase IV from lymphocytes of chronic lymphocytic leukemia of T-type. *Biomed Biochim Acta*, **45**:567-574.

Michel M C, Beck-Sickinger A, Cox H, Doods H N, Herzog H, Larhammar D, Quirion R, Schwartz T and Westfall T. **1998.** XVI. International Union of Pharmacology recommendations for the nomenclature of neuropeptide Y, peptide YY, and pancreatic polypeptide receptors. *Pharmacol Rev*, **50**:143-150.

Micouin A and Bauvois B. **1997.** Expression of dipeptidylpeptidase IV (DPP IV/CD26) activity on human myeloid and B lineage cells, and cell growth suppression by the inhibition of DPP IV activity. *Adv Exp Med Biol*, **421**:201-205.

Misumi Y, Hayashi Y, Arakawa F and Ikehara Y. **1992.** Molecular cloning and sequence analysis of human dipeptidyl peptidase IV, a serine proteinase on the cell surface. *Biochim Biophys Acta*, **1131**:333-336.

Monier S, Parton R G, Vogel F, Behlke J, Henske A and Kurzchalia T V. **1995.** VIP21-caveolin, a membrane protein constituent of the caveolar coat, oligomerizes in vivo and in vitro. *Mol Biol Cell*, **6**:911-927.

Montori V M, Gandhi G Y and Guyatt G H. **2007.** Patient-important outcomes in diabetes--time for consensus. *Lancet*, **370**:1104-1106.

Mori K, Dwek R A, Downing A K, Opdenakker G and Rudd P M. **1995.** The activation of type 1 and type 2 plasminogen by type I and type II tissue plasminogen activator. *J Biol Chem*, **270**:3261-3267.

Morimoto C and Schlossman S F. **1998.** The structure and function of CD26 in the T-cell immune response. *Immunol Rev*, **161**:55-70.

Morris L, Cilliers T, Bredell H, Phoswa M and Martin D J. **2001.** CCR5 is the major coreceptor used by HIV-1 subtype C isolates from patients with active tuberculosis. *AIDS Res Hum Retroviruses*, **17**:697-701.

Muchmore S W, Sattler M, Liang H, Meadows R P, Harlan J E, Yoon H S, Nettesheim D, Chang B S, Thompson C B, Wong S L, Ng S L and Fesik S W. **1996.** X-ray and NMR structure of human Bcl-xL, an inhibitor of programmed cell death. *Nature*, **381**:335-341.

Muller W A, Faloona G R, Aguilar-Parada E and Unger R H. **1970.** Abnormal alpha-cell function in diabetes. Response to carbohydrate and protein ingestion. *N Engl J Med*, **283**:109-115.

Mullis K B and Faloona F A. **1987.** Specific synthesis of DNA in vitro via a polymerase-catalyzed chain reaction. *Methods Enzymol*, **155**:335-350.

Mustelin T, Coggeshall K M and Altman A. **1989.** Rapid activation of the T-cell tyrosine protein kinase pp56lck by the CD45 phosphotyrosine phosphatase. *Proc Natl Acad Sci U S A*, **86**:6302-6306.

Muto S, Takada T and Matsumoto K. **2001.** Biological activities of human mannose-binding lectin bound to two different ligand sugar structures, Lewis A and Lewis B antigens and high-mannose type oligosaccharides. *Biochim Biophys Acta*, **1527**:39-46.

Nagasawa T, Hirota S, Tachibana K, Takakura N, Nishikawa S, Kitamura Y, Yoshida N, Kikutani H and Kishimoto T. **1996.** Defects of B-cell lymphopoiesis and bone-marrow myelopoiesis in mice lacking the CXC chemokine PBSF/SDF-1. *Nature*, **382**:635-638.

Nagase H, Suzuki K, Itoh Y, Kan C C, Gehring M R, Huang W and Brew K. **1996.** Involvement of tissue inhibitors of metalloproteinases (TIMPS) during matrix metalloproteinase activation. *Adv Exp Med Biol*, **389**:23-31.

Naim H Y, Joberty G, Alfalah M and Jacob R. **1999.** Temporal association of the N- and O-linked glycosylation events and their implication in the polarized sorting of intestinal brush border sucrase-isomaltase, aminopeptidase N, and dipeptidyl peptidase IV. *J Biol Chem*, **274**:17961-17967.

Nauck M A, Heimesaat M M, Orskov C, Holst J J, Ebert R and Creutzfeldt W. **1993.** Preserved incretin activity of glucagon-like peptide 1 [7-36 amide] but not of synthetic human gastric inhibitory polypeptide in patients with type-2 diabetes mellitus. *J Clin Invest*, **91**:301-307.

Nausch I, Mentlein R and Heymann E. **1990.** The degradation of bioactive peptides and proteins by dipeptidyl peptidase IV from human placenta. *Biol Chem Hoppe Seyler*, **371**:1113-1118.

Nemoto E, Sugawara S, Takada H, Shoji S and Horiuch H. **1999.** Increase of CD26/dipeptidyl peptidase IV expression on human gingival fibroblasts upon stimulation with cytokines and bacterial components. *Infect Immun*, **67**:6225-6233.

Nguyen D H and Hildreth J E. **2000.** Evidence for budding of human immunodeficiency virus type 1 selectively from glycolipid-enriched membrane lipid rafts. *J Virol*, **74**:3264-3272.

Nikolaidis L A, Elahi D, Hentosz T, Doverspike A, Huerbin R, Zourelias L, Stolarski C, Shen Y T and Shannon R P. **2004.** Recombinant glucagon-like peptide-1 increases myocardial glucose uptake and improves left ventricular performance in conscious dogs with pacing-induced dilated cardiomyopathy. *Circulation*, **110**:955-961.

Nuck R, Zimmermann M, Sauvageot D, Josi D and Reutter W. **1990.** Optimized deglycosylation of glycoproteins by peptide-N4-(N-acetyl-beta-glucosaminyl)-asparagine amidase from Flavobacterium meningosepticum. *Glycoconj J*, **7**:279-286.

Ogata S, Misumi Y and Ikehara Y. **1989.** Primary structure of rat liver dipeptidyl peptidase IV deduced from its cDNA and identification of the NH2-terminal signal sequence as the membrane-anchoring domain. *J Biol Chem*, **264**:3596-3601.

Ogata S, Misumi Y, Tsuji E, Takami N, Oda K and Ikehara Y. **1992.** Identification of the active site residues in dipeptidyl peptidase IV by affinity labeling and site-directed mutagenesis. *Biochemistry*, **31**:2582-2587.

Ohnuma K, Ishii T, Iwata S, Hosono O, Kawasaki H, Uchiyama M, Tanaka H, Yamochi T, Dang N H and Morimoto C. **2002.** G1/S cell cycle arrest provoked in human T cells by antibody to CD26. *Immunology*, **107**:325-333.

Ohnuma K, Uchiyama M, Yamochi T, Nishibashi K, Hosono O, Takahashi N, Kina S, Tanaka H, Lin X, Dang N H and Morimoto C. **2007.** Caveolin-1 triggers T-cell activation via CD26 in association with CARMA1. *J Biol Chem*, **282**:10117-10131.

Ohnuma K, Yamochi T, Uchiyama M, Nishibashi K, Yoshikawa N, Shimizu N, Iwata S, Tanaka H, Dang N H and Morimoto C. **2004.** CD26 up-regulates expression of CD86 on antigen-presenting cells by means of caveolin-1. *Proc Natl Acad Sci U S A*, **101**:14186-14191.

Ohtsuki T, Tsuda H and Morimoto C. **2000.** Good or evil: CD26 and HIV infection. *J Dermatol Sci*, **22**:152-160.

Olsen C and Wagtmann N. **2002.** Identification and characterization of human DPP9, a novel homologue of dipeptidyl peptidase IV. *Gene*, **299**:185-193.

Oravecz T, Pall M, Roderiquez G, Gorrell M D, Ditto M, Nguyen N Y, Boykins R, Unsworth E and Norcross M A. **1997.** Regulation of the receptor specificity and function of the chemokine RANTES (regulated on activation, normal T cell expressed and secreted) by dipeptidyl peptidase IV (CD26)-mediated cleavage. *J Exp Med*, **186**:1865-1872.

Orsini M J, Parent J L, Mundell S J, Marchese A and Benovic J L. **2000.** Trafficking of the HIV coreceptor CXCR4: role of arrestins and identification of residues in the C-terminal tail that mediate receptor internalization. *J Biol Chem*, **275**:25876.

Ostergaard H L, Shackelford D A, Hurley T R, Johnson P, Hyman R, Sefton B M and Trowbridge I S. **1989.** Expression of CD45 alters phosphorylation of the lck-encoded tyrosine protein kinase in murine lymphoma T-cell lines. *Proc Natl Acad Sci U S A*, **86**:8959-8963.

Ostrowski M A, Chun T W, Justement S J, Motola I, Spinelli M A, Adelsberger J, Ehler L A, Mizell S B, Hallahan C W and Fauci A S. **1999.** Both memory and CD45RA+/CD62L+ naive CD4(+) T cells are infected in human immunodeficiency virus type 1-infected individuals. *J Virol*, **73**:6430-6435.

Paillard M. **1997.** Na+/H+ exchanger subtypes in the renal tubule: function and regulation in physiology and disease. *Exp Nephrol*, **5**:277-284.

Pang T, Wakabayashi S and Shigekawa M. **2002.** Expression of calcineurin B homologous protein 2 protects serum deprivation-induced cell death by serum-independent activation of Na+/H+ exchanger. *J Biol Chem*, **277**:43771-43777.

Pangalos M N, Neefs J M, Somers M, Verhasselt P, Bekkers M, van der Helm L, Fraiponts E, Ashton D and Gordon R D. **1999.** Isolation and expression of novel human glutamate carboxypeptidases with N-acetylated alpha-linked acidic dipeptidase and dipeptidyl peptidase IV activity. *J Biol Chem*, **274**:8470-8483.

Peloponese J M, Jr., Gregoire C, Opi S, Esquieu D, Sturgis J, Lebrun E, Meurs E, Collette Y, Olive D, Aubertin A M, Witvrow M, Pannecouque C, De Clercq E, Bailly C, Lebreton J and Loret E P. **2000.** 1H-13C nuclear magnetic resonance assignment and structural characterization of HIV-1 Tat protein. *C R Acad Sci III*, **323**:883-894.

Perkins D N, Pappin D J, Creasy D M and Cottrell J S. **1999.** Probability-based protein identification by searching sequence databases using mass spectrometry data. *Electrophoresis*, **20**:3551-3567.

Petell J K, Diamond M, Hong W J, Bujanover Y, Amarri S, Pittschieler K and Doyle D. **1987.** Isolation and characterization of a Mr = 110,000 glycoprotein localized to the hepatocyte bile canaliculus. *J Biol Chem*, **262**:14753-14759.

Pethiyagoda C L, Welch D R and Fleming T P. **2000.** Dipeptidyl peptidase IV (DPPIV) inhibits cellular invasion of melanoma cells. *Clin Exp Metastasis*, **18**:391-400.

Petsch D and Anspach F B. **2000.** Endotoxin removal from protein solutions. *J Biotechnol*, **76**:97-119.

Piazza G A, Callanan H M, Mowery J and Hixson D C. **1989.** Evidence for a role of dipeptidyl peptidase IV in fibronectin-mediated interactions of hepatocytes with extracellular matrix. *Biochem J*, **262**:327-334.

Pirie-Shepherd S R, Jett E A, Andon N L and Pizzo S V. **1995.** Sialic acid content of plasminogen 2 glycoforms as a regulator of fibrinolytic activity. Isolation, carbohydrate analysis, and kinetic characterization of six glycoforms of plasminogen. *J Biol Chem*, **270**:5877-5881.

Pospisilik J A, Ehses J A, Doty T, McIntosh C H, Demuth H U and Pederson R A. **2003.** Dipeptidyl peptidase IV inhibition in animal models of diabetes. *Adv Exp Med Biol*, **524**:281-291.

Proost P, Menten P, Struyf S, Schutyser E, De Meester I and Van Damme J. **2000.** Cleavage by CD26/dipeptidyl peptidase IV converts the chemokine LD78beta into a most efficient monocyte attractant and CCR1 agonist. *Blood*, **96**:1674-1680.

Proost P, Struyf S, Schols D, Durinx C, Wuyts A, Lenaerts J P, De Clercq E, De Meester I and Van Damme J. **1998.** Processing by CD26/dipeptidyl-peptidase IV reduces the chemotactic and anti-HIV-1 activity of stromal-cell-derived factor-1alpha. *FEBS Lett*, **432**:73-76.

Proost P, Struyf S, Schols D, Opdenakker G, Sozzani S, Allavena P, Mantovani A, Augustyns K, Bal G, Haemers A, Lambeir A M, Scharpe S, Van Damme J and De Meester I. **1999.** Truncation of macrophage-derived chemokine by CD26/ dipeptidyl-peptidase IV beyond its predicted cleavage site affects chemotactic activity and CC chemokine receptor 4 interaction. *J Biol Chem*, **274**:3988-3993.

Puschel G, Mentlein R and Heymann E. **1982.** Isolation and characterization of dipeptidyl peptidase IV from human placenta. *Eur J Biochem*, **126**:359-365.

Radel C and Rizzo V. **2005.** Integrin mechanotransduction stimulates caveolin-1 phosphorylation and recruitment of Csk to mediate actin reorganization. *Am J Physiol Heart Circ Physiol*, **288**:H936-945.

Ramos-DeSimone N, Hahn-Dantona E, Sipley J, Nagase H, French D L and Quigley J P. **1999.** Activation of matrix metalloproteinase-9 (MMP-9) via a converging plasmin/stromelysin-1 cascade enhances tumor cell invasion. *J Biol Chem*, **274**:13066-13076.

Rana T M and Jeang K T. **1999.** Biochemical and functional interactions between HIV-1 Tat protein and TAR RNA. *Arch Biochem Biophys*, **365**:175-185.

Rasmussen H B, Branner S, Wiberg F C and Wagtmann N. **2003.** Crystal structure of human dipeptidyl peptidase IV/CD26 in complex with a substrate analog. *Nat Struct Biol*, **10**:19-25.

Razani B and Lisanti M P. **2001.** Caveolins and caveolae: molecular and functional relationships. *Exp cell Res*, **271**:36-44.

Reaven G M, Chen Y D, Golay A, Swislocki A L and Jaspan J B. **1987.** Documentation of hyperglucagonemia throughout the day in nonobese and obese patients with noninsulin-dependent diabetes mellitus. *J Clin Endocrinol Metab*, **64**:106-110.

Reinhold D, Bank U, Buhling F, Neubert K, Mattern T, Ulmer A J, Flad H D and Ansorge S. **1993.** Dipeptidyl peptidase IV (CD26) on human lymphocytes. Synthetic inhibitors of and antibodies against dipeptidyl peptidase IV suppress the proliferation of pokeweed mitogen-stimulated peripheral blood mononuclear cells, and IL-2 and IL-6 production. *Immunobiology*, **188**:403-414.

Reinhold D, Bank U, Buhling F, Tager M, Born I, Faust J, Neubert K and Ansorge S. **1997.** Inhibitors of dipeptidyl peptidase IV (DP IV, CD26) induces secretion of transforming growth factor-beta 1 (TGF-beta 1) in stimulated mouse splenocytes and thymocytes. *Immunol Lett*, **58**:29-35.

Richter B, Bandeira-Echtler E, Bergerhoff K and Lerch C. **2008.** Emerging role of dipeptidyl peptidase-4 inhibitors in the management of type 2 diabetes. *Vasc Health Risk Manag*, **4**:753-768.

Rifkin D B, Gleizes P E, Harpel J, Nunes I, Munger J, Mazzieri R and Noguera I. **1997.** Plasminogen/plasminogen activator and growth factor activation. *Ciba Found Symp*, **212**:105-115; discussion 116-108.

Rifkin D B, Mazzieri R, Munger J S, Noguera I and Sung J. **1999.** Proteolytic control of growth factor availability. *APMIS*, **107**:80-85.

Roach T, Slater S, Koval M, White L, Cahir McFarland E D, Okumura M, Thomas M and Brown E. **1997.** CD45 regulates Src family member kinase activity associated with macrophage integrin-mediated adhesion. *Curr Biol*, **7**:408-417.

Rothberg K G, Heuser J E, Donzell W C, Ying Y S, Glenney J R and Anderson R G. **1992.** Caveolin, a protein component of caveolae membrane coats. *Cell*, **68**:673-682.

Rothwarf D M and Karin M. **1999.** The NF-kappa B activation pathway: a paradigm in information transfer from membrane to nucleus. *Sci STKE*, **1999**:RE1.

Ruiz P, Zacharievich N, Hao L, Viciana A L and Shenkin M. **1998.** Human thymocyte dipeptidyl peptidase IV (CD26) activity is altered with stage of ontogeny. *Clin Immunol Immunopathol*, **88**:156-168.

Ruoslahti E and Pierschbacher M D. **1987.** New perspectives in cell adhesion: RGD and integrins. *Science*, **238**:491-497.

Santisteban I, Arredondo-Vega F X, Kelly S, Loubser M, Meydan N, Roifman C, Howell P L, Bowen T, Weinberg K I, Schroeder M L and et al. 1995. Three new adenosine deaminase mutations that define a splicing enhancer and cause severe and partial phenotypes: implications for evolution of a CpG hotspot and expression of a transduced ADA cDNA. *Hum Mol Genet*, **4**:2081-2087.

Sargiacomo M, Scherer P E, Tang Z, Kubler E, Song K S, Sanders M C and Lisanti M P. **1995.** Oligomeric structure of caveolin: implications for caveolae membrane organization. *Proc Natl Acad Sci U S A*, **92**:9407-9411.

Sato K, Aytac U, Yamochi T, Ohnuma K, McKee K S, Morimoto C and Dang N H. **2003.** CD26/dipeptidyl peptidase IV enhances expression of topoisomerase II alpha and sensitivity to apoptosis induced by topoisomerase II inhibitors. *Br J Cancer*, **89**:1366-1374.

Sattentau Q J. **1998.** HIV gp120: double lock strategy foils host defences. *Structure*, **6**:945-949.

Scanlan M J, Raj B K, Calvo B, Garin-Chesa P, Sanz-Moncasi M P, Healey J H, Old L J and Rettig W J. **1994.** Molecular cloning of fibroblast activation protein alpha, a member of the serine protease family selectively expressed in stromal fibroblasts of epithelial cancers. *Proc Natl Acad Sci U S A*, **91**:5657-5661.

Scarlatti G, Tresoldi E, Bjorndal A, Fredriksson R, Colognesi C, Deng H K, Malnati M S, Plebani A, Siccardi A G, Littman D R, Fenyo E M and Lusso P. **1997.** In vivo evolution of HIV-1 co-receptor usage and sensitivity to chemokine-mediated suppression. *Nat Med*, **3**:1259-1265.

Scherer P E, Lewis R Y, Volonte D, Engelman J A, Galbiati F, Couet J, Kohtz D S, van Donselaar E, Peters P and Lisanti M P. **1997.** Cell-type and tissue-specific expression of caveolin-2. Caveolins 1 and 2 co-localize and form a stable hetero-oligomeric complex in vivo. *J Biol Chem*, **272**:29337-29346.

Schon E, Eichmann E, Grunow R, Jahn S, Kiessig S T, Volk H D and Ansorge S. **1986.** Dipeptidyl peptidase IV in human T lymphocytes. An approach to the role of a membrane peptidase in the immune system. *Biomed Biochim Acta*, **45**:1523-1528.

Schultheis P J, Clarke L L, Meneton P, Miller M L, Soleimani M, Gawenis L R, Riddle T M, Duffy J J, Doetschman T, Wang T, Giebisch G, Aronson P S, Lorenz J N and Shull G E. **1998.** Renal and intestinal absorptive defects in mice lacking the NHE3 Na+/H+ exchanger. *Nat Genet*, **19**:282-285.

Scott C D and Firth S M. **2004.** The role of the M6P/IGF-II receptor in cancer: tumor suppression or garbage disposal? *Horm Metab Res*, **36**:261-271.

Seavitt J R, White L S, Murphy K M, Loh D Y, Perlmutter R M and Thomas M L. **1999.** Expression of the p56(Lck) Y505F mutation in CD45-deficient mice rescues thymocyte development. *Mol Cell Biol*, **19**:4200-4208.

Secchiero P, Zella D, Capitani S, Gallo R C and Zauli G. **1999.** Extracellular HIV-1 tat protein up-regulates the expression of surface CXC-chemokine receptor 4 in resting CD4+ T cells. *J Immunol*, **162**:2427-2431.

Shane R, Wilk S and Bodnar R J. **1999.** Modulation of endomorphin-2-induced analgesia by dipeptidyl peptidase IV. *Brain Res*, **815**:278-286.

Shaul P W and Anderson R G. **1998.** Role of plasmalemmal caveolae in signal transduction. *Am J Physiol*, **275**:L843-851.

Shenoi H, Seavitt J, Zheleznyak A, Thomas M L and Brown E J. **1999.** Regulation of integrin-mediated T cell adhesion by the transmembrane protein tyrosine phosphatase CD45. *J Immunol*, **162**:7120-7127.

Shioda T, Kato H, Ohnishi Y, Tashiro K, Ikegawa M, Nakayama E E, Hu H, Kato A, Sakai Y, Liu H, Honjo T, Nomoto A, Iwamoto A, Morimoto C and Nagai Y. **1998.** Anti-HIV-1 and chemotactic activities of human stromal cell-derived factor 1alpha (SDF-1alpha) and SDF-1beta are abolished by CD26/dipeptidyl peptidase IV-mediated cleavage. *Proc Natl Acad Sci U S A*, **95**:6331-6336.

Shiraki K, Kudou M, Fujiwara S, Imanaka T and Takagi M. **2002.** Biophysical effect of amino acids on the prevention of protein aggregation. *J Biochem*, **132**:591-595.

Shojania S and O'Neil J D. **2006.** HIV-1 Tat is a natively unfolded protein: the solution conformation and dynamics of reduced HIV-1 Tat-(1-72) by NMR spectroscopy. *J Biol Chem*, **281**:8347-8356.

Siddappa N B, Venkatramanan M, Venkatesh P, Janki M V, Jayasuryan N, Desai A, Ravi V and Ranga U. **2006.** Transactivation and signaling functions of Tat are not correlated: biological and immunological characterization of HIV-1 subtype-C Tat protein. *Retrovirology*, **3**:53.

Singer S J and Nicolson G L. **1972.** The fluid mosaic model of the structure of cell membranes. *Science*, **175**:720-731.

Sloth B, Holst J J, Flint A, Gregersen N T and Astrup A. **2007.** Effects of PYY1-36 and PYY3-36 on appetite, energy intake, energy expenditure, glucose and fat metabolism in obese and lean subjects. *Am J Physiol Endocrinol Metab*, **292**:E1062-1068.

Smart E J, Graf G A, McNiven M A, Sessa W C, Engelman J A, Scherer P E, Okamoto T and Lisanti M P. **1999.** Caveolins, liquid-ordered domains, and signal transduction. *Mol Cell Biol*, **19**:7289-7304.

Smith R E, Talhouk J W, Brown E E and Edgar S E. **1998.** The significance of hypersialylation of dipeptidyl peptidase IV (CD26) in the inhibition of its activity by Tat and other cationic peptides. CD26: a subverted adhesion molecule for HIV peptide binding. *AIDS Res Hum Retroviruses*, **14**:851-868.

Sodroski J, Wyatt R, Olshevsky U, Olshevsky V and Moore J. **1996.** Conformation of the HIV-1 gp 120 envelope glycoprotein. *Antibiot Chemother*, **48**:184-187.

Song K S, Tang Z, Li S and Lisanti M P. **1997.** Mutational analysis of the properties of caveolin-1. A novel role for the C-terminal domain in mediating homo-typic caveolin-caveolin interactions. *J Biol Chem*, **272**:4398-4403.

Stahlhut M and van Deurs B. **2000.** Identification of filamin as a novel ligand for caveolin-1: evidence for the organization of caveolin-1-associated membrane domains by the actin cytoskeleton. *Mol Biol Cell*, **11**:325-337.

Struyf S, Proost P, Schols D, De Clercq E, Opdenakker G, Lenaerts J P, Detheux M, Parmentier M, De Meester I, Scharpe S and Van Damme J. **1999.** CD26/dipeptidyl-peptidase IV down-regulates the eosinophil chemotactic potency, but not the anti-HIV activity of human eotaxin by affecting its interaction with CC chemokine receptor 3. *J Immunol*, **162**:4903-4909.

Struyf S, Proost P, Sozzani S, Mantovani A, Wuyts A, De Clercq E, Schols D and Van Damme J. **1998.** Enhanced anti-HIV-1 activity and altered chemotactic potency of NH2-terminally processed macrophage-derived chemokine (MDC) imply an additional MDC receptor. *J Immunol*, **161**:2672-2675.

Subramanyam M, Gutheil W G, Bachovchin W W and Huber B T. **1993.** Mechanism of HIV-1 Tat induced inhibition of antigen-specific T cell responsiveness. *J Immunol*, **150**:2544-2553.

Super M, Thiel S, Lu J, Levinsky R J and Turner M W. **1989.** Association of low levels of mannan-binding protein with a common defect of opsonisation. *Lancet*, **2**:1236-1239.

Szondy Z. **1994.** Adenosine stimulates DNA fragmentation in human thymocytes by Ca(2+)-mediated mechanisms. *Biochem J*, **304 (Pt 3)**:877-885.

Tahirov T H, Babayeva N D, Varzavand K, Cooper J J, Sedore S C and Price D H. **2010.** Crystal structure of HIV-1 Tat complexed with human P-TEFb. *Nature*, **465**:747-751.

Tanaka S, Murakami T, Horikawa H, Sugiura M, Kawashima K and Sugita T. **1997.** Suppression of arthritis by the inhibitors of dipeptidyl peptidase IV. *Int J Immunopharmacol*, **19**:15-24.

Tanaka T, Camerini D, Seed B, Torimoto Y, Dang N H, Kameoka J, Dahlberg H N, Schlossman S F and Morimoto C. **1992.** Cloning and functional expression of the T cell activation antigen CD26. *J Immunol*, **149**:481-486.

Tanner M J, Hanel W, Gaffen S L and Lin X. **2007.** CARMA1 coiled-coil domain is involved in the oligomerization and subcellular localization of CARMA1 and is required for T cell receptor-induced NF-kappaB activation. *J Biol Chem*, **282**:17141-17147.

Tarasova N I, Stauber R H and Michejda C J. **1998.** Spontaneous and ligand-induced trafficking of CXC-chemokine receptor 4. *J Biol Chem*, **273**:15883-15886.

Tarentino A L, Gomez C M and Plummer T H, Jr. 1985. Deglycosylation of asparagine-linked glycans by peptide:N-glycosidase F. *Biochemistry*, **24**:4665-4671.

Taylor J P, Cupp C, Diaz A, Chowdhury M, Khalili K, Jimenez S A and Amini S. **1992.** Activation of expression of genes coding for extracellular matrix proteins in Tat-producing glioblastoma cells. *Proc Natl Acad Sci U S A*, **89**:9617-9621.

Taylor M E and Drickamer K. **2007.** Paradigms for glycan-binding receptors in cell adhesion. *Curr Opin Cell Biol*, **19**:572-577.

Teillet F, Dublet B, Andrieu J P, Gaboriaud C, Arlaud G J and Thielens N M. **2005.** The two major oligomeric forms of human mannan-binding lectin: chemical characterization, carbohydrate-binding properties, and interaction with MBL-associated serine proteases. *J Immunol*, **174**:2870-2877.

Terada M, Khoo K H, Inoue R, Chen C I, Yamada K, Sakaguchi H, Kadowaki N, Ma B Y, Oka S, Kawasaki T and Kawasaki N. **2005.** Characterization of oligosaccharide ligands expressed on SW1116 cells recognized by mannan-binding protein. A highly fucosylated polylactosamine type N-glycan. *J Biol Chem*, **280**:10897-10913.

Thielitz A, Reinhold D, Vetter R, Bank U, Helmuth M, Hartig R, Wrenger S, Wiswedel I, Lendeckel U, Kahne T, Neubert K, Faust J, Zouboulis C C, Ansorge S and Gollnick H. **2007.** Inhibitors of dipeptidyl peptidase IV and aminopeptidase N target major pathogenetic steps in acne initiation. *J Invest Dermatol*, **127**:1042-1051.

Thompson M A, Ohnuma K, Abe M, Morimoto C and Dang N H. **2007.** CD26/dipeptidyl peptidase IV as a novel therapeutic target for cancer and immune disorders. *Mini Rev Med Chem*, **7**:253-273.

Toft-Nielsen M B, Madsbad S and Holst J J. **2001.** Determinants of the effectiveness of glucagon-like peptide-1 in type 2 diabetes. *J Clin Endocrinol Metab*, **86**:3853-3860.

Torimoto Y, Dang N H, Vivier E, Tanaka T, Schlossman S F and Morimoto C. **1991.** Coassociation of CD26 (dipeptidyl peptidase IV) with CD45 on the surface of human T lymphocytes. *J Immunol*, **147**:2514-2517.

Trowbridge I S and Thomas M L. **1994.** CD45: an emerging role as a protein tyrosine phosphatase required for lymphocyte activation and development. *Annu Rev Immunol*, **12**:85-116.

Turner M W. **1996.** Mannose-binding lectin: the pluripotent molecule of the innate immune system. *Immunol Today*, **17**:532-540.

Tyagi M, Rusnati M, Presta M and Giacca M. **2001.** Internalization of HIV-1 tat requires cell surface heparan sulfate proteoglycans. *J Biol Chem*, **276**:3254-3261.

Utzschneider K M, Tong J, Montgomery B, Udayasankar J, Gerchman F, Marcovina S M, Watson C E, Ligueros-Saylan M A, Foley J E, Holst J J, Deacon C F and Kahn S E.

2008. The dipeptidyl peptidase-4 inhibitor vildagliptin improves beta-cell function and insulin sensitivity in subjects with impaired fasting glucose. *Diabetes Care*, **31**:108-113.

Uversky V N. **2002.** Natively unfolded proteins: a point where biology waits for physics. *Protein Sci*, **11**:739-756.

Uversky V N. **2010.** The mysterious unfoldome: structureless, underappreciated, yet vital part of any given proteome. *J Biomed Biotechnol*, **2010**:568068.

van den Hoek A M, Heijboer A C, Voshol P J, Havekes L M, Romijn J A, Corssmit E P and Pijl H. **2007.** Chronic PYY3-36 treatment promotes fat oxidation and ameliorates insulin resistance in C57BL6 mice. *Am J Physiol Endocrinol Metab*, **292**:E238-245.

van Die I, van Tetering A, Bakker H, van den Eijnden D H and Joziasse D H. **1996.** Glycosylation in lepidopteran insect cells: identification of a beta 1-->4-N-acetylgalactosaminyltransferase involved in the synthesis of complex-type oligosaccharide chains. *Glycobiology*, **6**:157-164.

Van Duyne R, Easley R, Wu W, Berro R, Pedati C, Klase Z, Kehn-Hall K, Flynn E K, Symer D E and Kashanchi F. **2008.** Lysine methylation of HIV-1 Tat regulates transcriptional activity of the viral LTR. *Retrovirology*, **5**:40.

van West D, Monteleone P, Di Lieto A, De Meester I, Durinx C, Scharpe S, Lin A, Maj M and Maes M. **2000.** Lowered serum dipeptidyl peptidase IV activity in patients with anorexia and bulimia nervosa. *Eur Arch Psychiatry Clin Neurosci*, **250**:86-92.

Vanham G, Kestens L, De Meester I, Vingerhoets J, Penne G, Vanhoof G, Scharpe S, Heyligen H, Bosmans E, Ceuppens J L and et al. 1993. Decreased expression of the memory marker CD26 on both CD4+ and CD8+ T lymphocytes of HIV-infected subjects. *J Acquir Immune Defic Syndr*, **6**:749-757.

Vanhoof G, Goossens F, De Meester I, Hendriks D and Scharpe S. **1995.** Proline motifs in peptides and their biological processing. *FASEB J*, **9**:736-744.

Varki A. **1993.** Biological roles of oligosaccharides: all of the theories are correct. *Glycobiology*, **3**:97-130.

Vendeville A, Rayne F, Bonhoure A, Bettache N, Montcourrier P and Beaumelle B. **2004.** HIV-1 Tat enters T cells using coated pits before translocating from acidified endosomes and eliciting biological responses. *Mol Biol Cell*, **15**:2347-2360.

Verhoef K, Bauer M, Meyerhans A and Berkhout B. **1998.** On the role of the second coding exon of the HIV-1 Tat protein in virus replication and MHC class I downregulation. *AIDS Res Hum Retroviruses*, **14**:1553-1559.

Vetter R, Reinhold D, Buhling F, Lendeckel U, Born I, Faust J, Neubert K, Ansorge S and Gollnick H. **2000.** DNA synthesis in cultured human keratinocytes and HaCaT keratinocytes is reduced by specific inhibition of dipeptidyl peptidase IV (CD26) enzymatic activity. *Adv Exp Med Biol*, **477**:167-171.

von Bonin A, Huhn J and Fleischer B. **1998.** Dipeptidyl-peptidase IV/CD26 on T cells: analysis of an alternative T-cell activation pathway. *Immunol Rev*, **161**:43-53.

Wakabayashi S, Ikeda T, Noel J, Schmitt B, Orlowski J, Pouyssegur J and Shigekawa M. **1995.** Cytoplasmic domain of the ubiquitous Na+/H+ exchanger NHE1 can confer Ca2+ responsiveness to the apical isoform NHE3. *J Biol Chem*, **270**:26460-26465.

Walborg E F, Jr., Tsuchida S, Weeden D S, Thomas M W, Barrick A, McEntire K D, Allison J P and Hixson D C. **1985.** Identification of dipeptidyl peptidase IV as a protein shared by the plasma membrane of hepatocytes and liver biomatrix. *Exp cell Res*, **158**:509-518.

Wang T, Yang C L, Abbiati T, Schultheis P J, Shull G E, Giebisch G and Aronson P S. **1999.** Mechanism of proximal tubule bicarbonate absorption in NHE3 null mice. *Am J Physiol*, **277**:F298-302.

Wary K K, Mariotti A, Zurzolo C and Giancotti F G. **1998.** A requirement for caveolin-1 and associated kinase Fyn in integrin signaling and anchorage-dependent cell growth. *Cell*, **94**:625-634.

Wei Y, Yang X, Liu Q, Wilkins J A and Chapman H A. **1999.** A role for caveolin and the urokinase receptor in integrin-mediated adhesion and signaling. *J Cell Biol*, **144**:1285-1294.

Weihofen W A, Liu J, Reutter W, Saenger W and Fan H. **2004.** Crystal structure of CD26/dipeptidyl-peptidase IV in complex with adenosine deaminase reveals a highly amphiphilic interface. *J Biol Chem*, **279**:43330-43335.

Weihofen W A, Liu J, Reutter W, Saenger W and Fan H. **2005.** Crystal structures of HIV-1 Tat-derived nonapeptides Tat-(1-9) and Trp2-Tat-(1-9) bound to the active site of dipeptidyl-peptidase IV (CD26). *J Biol Chem*, **280**:14911-14917.

Weil R and Veillette A. **1996.** Signal transduction by the lymphocyte-specific tyrosine protein kinase p56lck. *Curr Top Microbiol Immunol*, **205**:63-87.

Weinman E J, Minkoff C and Shenolikar S. **2000.** Signal complex regulation of renal transport proteins: NHERF and regulation of NHE3 by PKA. *Am J Physiol Renal Physiol*, **279**:F393-399.

Weinman E J, Steplock D, Donowitz M and Shenolikar S. **2000.** NHERF associations with sodium-hydrogen exchanger isoform 3 (NHE3) and ezrin are essential for cAMP-mediated phosphorylation and inhibition of NHE3. *Biochemistry*, **39**:6123-6129.

Weinreb P H, Zhen W, Poon A W, Conway K A and Lansbury P T, Jr. 1996. NACP, a protein implicated in Alzheimer's disease and learning, is natively unfolded. *Biochemistry*, **35**:13709-13715.

Wesley U V, Albino A P, Tiwari S and Houghton A N. **1999.** A role for dipeptidyl peptidase IV in suppressing the malignant phenotype of melanocytic cells. *J Exp Med*, **190**:311-322.

Westendorp M O, Li-Weber M, Frank R W and Krammer P H. **1994.** Human immunodeficiency virus type 1 Tat upregulates interleukin-2 secretion in activated T cells. *J Virol*, **68**:4177-4185.

Willheim M, Ebner C, Baier K, Kern W, Schrattbauer K, Thien R, Kraft D, Breiteneder H, Reinisch W and Scheiner O. **1997.** Cell surface characterization of T lymphocytes and allergen-specific T cell clones: correlation of CD26 expression with T(H1) subsets. *J Allergy Clin Immunol*, **100**:348-355.

Willms B, Werner J, Holst J J, Orskov C, Creutzfeldt W and Nauck M A. **1996.** Gastric emptying, glucose responses, and insulin secretion after a liquid test meal: effects of exogenous glucagon-like peptide-1 (GLP-1)-(7-36) amide in type 2 (noninsulin-dependent) diabetic patients. *J Clin Endocrinol Metab*, **81**:327-332.

Wilson M J, Ruhland A R, Pryor J L, Ercole C, Sinha A A, Hensleigh H, Kaye K W, Dawkins H J, Wasserman N F, Reddy P and Ahmed K. **1998.** Prostate specific origin of dipeptidylpeptidase IV (CD-26) in human seminal plasma. *J Urol*, **160**:1905-1909.

Worbs M, Huber R and Wahl M C. **2000.** Crystal structure of ribosomal protein L4 shows RNA-binding sites for ribosome incorporation and feedback control of the S10 operon. *EMBO J*, **19**:807-818.

Wrenger S, Faust J, Mrestani-Klaus C, Fengler A, Stockel-Maschek A, Lorey S, Kahne T, Brandt W, Neubert K, Ansorge S and Reinhold D. **2000.** Down-regulation of T cell activation following inhibition of dipeptidyl peptidase IV/CD26 by the N-terminal part of the thromboxane A2 receptor. *J Biol Chem*, **275**:22180-22186.

Wrenger S, Hoffmann T, Faust J, Mrestani-Klaus C, Brandt W, Neubert K, Kraft M, Olek S, Frank R, Ansorge S and Reinhold D. **1997.** The N-terminal structure of HIV-1 Tat is required for suppression of CD26-dependent T cell growth. *J Biol Chem*, **272**:30283-30288.

Wrenger S, Reinhold D, Hoffmann T, Kraft M, Frank R, Faust J, Neubert K and Ansorge S. **1996.** The N-terminal X-X-Pro sequence of the HIV-1 Tat protein is important for the inhibition of dipeptidyl peptidase IV (DP IV/CD26) and the suppression of mitogen-induced proliferation of human T cells. *FEBS Lett*, **383**:145-149.

Xiao H, Neuveut C, Tiffany H L, Benkirane M, Rich E A, Murphy P M and Jeang K T. **2000.** Selective CXCR4 antagonism by Tat: implications for in vivo expansion of coreceptor use by HIV-1. *Proc Natl Acad Sci U S A*, **97**:11466-11471.

Yaron A and Naider F. **1993.** Proline-dependent structural and biological properties of peptides and proteins. *Crit Rev Biochem Mol Biol*, **28**:31-81.

Yun C C, Chen Y and Lang F. **2002.** Glucocorticoid activation of Na(+)/H(+) exchanger isoform 3 revisited. The roles of SGK1 and NHERF2. *J Biol Chem*, **277**:7676-7683.

11 Supplementary Data

11.1 Abbreviations

AP	Alkaline Phosphatase
APS	Ammonium persulphate
BCA	Biccin-chonin acid
bp	Base pair
BSA	Bovine Serum albumin
CD	Cluster of Differentiation
CHAPS	3-[(3-chloamidopropyl) dimethylammonio]-1-propan sulfonate
CHAPSO	3-[(3- Cholamidopropyl)dimethylammonio]-2-hydroxy-1- propanesulfonate
CHO	Chinese hamster ovary
CHS	Cholesteryl Hemi-succinate
CIAP	Calf intestinal alkaline Phosphatase
CTD	C-terminal domain
CTL	Cytotoxic T-Lymphocytes
Cys	Cysteine
DDM	n-dodecyl-β-D-maltoside
DHB	Dihydroxy-Benzoic acid
DMSO	Dimethylsulfoxide
DNA	Deoxyribonucleic Acid
dNTP	Dideoxynucleotide
DSP	Dithiobis succinimidyl propionate
DSS	Disuccinimidyl suberate
DTT	Dithiothreitol
E. coli	Escherichia coli
ECL	Enhanced Chemiluminescence
ECM	Extracellular Matrix
EDTA	Ethylen diamintetraaceticacid
EGF	Epidermal Growth Factor
EGTA	Ethylenglycol-bis(2-aminoethyl)tetraacetic acid
ELISA	Enzyme-Linked Immunosorbent-Assay
ER	Endoplasmic reticulum
et al	*et alii* (and others)
FACS	Fluorescence-Activated Cell Sorting
FCS	Fetal calf serum
FITC	Fluorescein isothiocyanate
GFP	Green-Fluorescent Protein

GLP1	Glucagon-Like-Peptide 1
GST	Glutathione-S-Transferase
GTP	Guanosine triphosphate
HBS	Hepes-buffered saline
HEK	Human embryonic kidney
Hepes	N-[2-Hydroxyethyl]piperazin-N'-[2-ethansulforic acid]
His	Histidine
HPLC	High Performance Liquid Chromatography
HRP	Horse Radish Peroxidase
IF	Indirect Immunofluorescence
Ig	Immune globulin
IP	Immunoprecipitation
IPTG	Isopropyl-β-D-Thiogalactoside
KD	Kilo dalton
LB	Lurea-Bertani
M	Molar
mAb	monoclonal Antibody
MALDI-TOF	Matrix-assisted laser desorption/ionisation-time of flight
MBP	Mannan binding protein or Mannan binding lectin
MCS	Multiple cloning site
MES	N-Morpholino ethane sulphuric acid
mM	milli Molar
MOI	Multiplicity of infection
mRNA	messenger Ribonucleic Acid
MS	mass spectrometry
MW	Molecular Weight
NBT	Nitroblue tetrazolium chloride
NCBI	National Center for Biotechnology Information
NEM	N-Ethylmaleimid
OD	Optical Density
pAb	polyclonal Antibody
PBS	Phosphate buffered saline
PBS-T	PBS-Tween
PCR	Polymerase chain reaction
PEG	Polyethylenglycol
pfu	Plaque forming units
PI	Propidium iodide
PKC	Protein kinase C
PMA	Phorbol 12-myristate 13-acetate

PMF	Peptide mass fingerprinting
PMSF	Phenyl-methyl-sulfonyl fluoride
PNGase F	peptide-N4-(N-acetyl-beta-glucosaminyl) asparagine amidase or N-linked glycopeptide-(N-acetyl-beta-D-glucosaminyl)-L-asparagine amidohydrolase
POD	Peroxidase
PVDF	Polyvinyl difluoride
RNA	Ribonucleic Acid
rpm	rotations per minute
SDS	Sodium dodecyl sulfate
SDS PAGE	SDS-poly acrylamide gel-electrophoresis
Sf	*Spodoptera frugiperda*
SPR	Surface Plasmon Resonance
TAE	Tris Acetate EDTA-buffer
TBS	Tris-buffered Saline
TBS-T	TBS- Tween 20
TCA	Trichloro acetic acid
TCEP-HCl	Tris (2-carboxyethyl) phosphine-HCl
TE	Tris-EDTA
TEMED	N,N,N',N'-Tetramethylendiamine
TFA	Trifluoro acetic acid
Tris	Tris (hydromethyl) aminomethane
U	Units
wt	Wild type
X-Gal	5-Bromo-4-chloro-3-indoyl-β-D-galactoside

11.2 cDNA sequences

11.2.1 CXCR4

The cDNA of the human CXCR4-Variant 2 that was amplified by PCR is given below. The bases in blue constitute the primers used in PCR. Underlined are the recognition sites for the restriction endonucleases used in cloning. The start codon of the CXCR4 ORF is highlighted in red. The bases in green indicate additional bases which lie before the ORF of the CXCR4 gene.

ACTATAGGGC GGCCGCGAAT TCGGCACGAG GGCCGAGGGC CTGAGTGCTC
CAGTAGCCAC CGCATCTGGA GAACCAGCGG TTACCATGGA GGGGATCAGT
ATATACACTT CAGATAACTA CACCGAGGAA ATGGGCTCAG GGGACTATGA
CTCCATGAAG GAACCCTGTT TCCGTGAAGA AAATGCTAAT TTCAATAAAA
TCTTCCTGCC CACCATCTAC TCCATCATCT TCTTAACTGG CATTGTGGGC
AATGGATTGG TCATCCTGGT CATGGGTTAC CAGAAGAAAC TGAGAAGCAT
GACGGACAAG TACAGGCTGC ACCTGTCAGT GGCCGACCTC CTCTTTGTCA
TCACGCTTCC CTTCTGGGCA GTTGATGCCG TGGCAAACTG GTACTTTGGG
AACTTCCTAT GCAAGGCAGT CCATGTCATC TACACAGTCA ACCTCTACAG
CAGTGTCCTC ATCCTGGCCT TCATCAGTCT GGACCGCTAC CTGGCCATCG
TCCACGCCAC CAACAGTCAG AGGCCAAGGA AGCTGTTGGC TGAAAAGGTG
GTCTATGTTG GCGTCTGGAT CCCTGCCCTC CTGCTGACTA TTCCCGACTT
CATCTTTGCC AACGTCAGTG AGGCAGATGA CAGATATATC TGTGACCGCT
TCTACCCCAA TGACTTGTGG GTGGTTGTGT TCCAGTTTCA GCACATCATG
GTTGGCCTTA TCCTGCCTGG TATTGTCATC CTGTCCTGCT ATTGCATTAT
CATCTCCAAG CTGTCACACT CCAAGGGCCA CCAGAAGCGC AAGGCCCTCA
AGACCACAGT CATCCTCATC CTGGCTTTCT TCGCCTGTTG GCTGCCTTAC
TACATTGGGA TCAGCATCGA CTCCTTCATC CTCCTGGAAA TCATCAAGCA
AGGGTGTGAG TTTGAGAACA CTGTGCACAA GTGGATTTCC ATCACCGAGG
CCCTAGCTTT CTTCCACTGT TGTCTGAACC CCATCCTCTA TGCTTTCCTT
GGAGCCAAAT TTAAAACCTC TGCCCAGCAC GCACTCACCT CTGTGAGCAG
AGGGTCCAGC CTCAAGATCC TCTCCAAAGG AAAGCGAGGT GGACATTCAT
CTGTTTCCAC TGAGTCTGAG TCTTCAAGTT TTCACTCCAG TCTAGATGC

11.2.2 Caveolin-1

The cDNA of the human-Caveolin-1 that was amplified by PCR is given below. The bases in blue constitute the primers used in PCR. Underlined are the recognition sites for the restriction endonucleases used in cloning. The start codon of the Caveolin-1 ORF is highlighted in bold.

GAATTC**ATG**T CTGGGGGCAA ATACGTAGAC TCGGAGGGAC ATCTCTACAC
CGTTCCCATC CGGGAACAGG GCAACATCTA CAAGCCCAAC AACAAGGCCA
TGGCAGACGA GCTGAGCGAG AAGCAAGTGT ACGACGCGCA CACCAAGGAG
ATCGACCTGG TCAACCGCGA CCCTAAACAC CTCAACGATG ACGTGGTCAA
GATTGACTTT GAAGATGTGA TTGCAGAACC AGAAGGGACA CACAGTTTTG
ACGGCATTTG GAAGGCCAGC TTCACCACCT TCACTGTGAC GAAATACTGG
TTTTACCGCT TGCTGTCTGC CCTCTTTGGC ATCCCGATGG CACTCATCTG
GGGCATTTAC TTCGCCATTC TCTCTTTCCT GCACATCTGG GCAGTTGTAC
CATGCATTAA GAGCTTCCTG ATTGAGATTC AGTGCATCAG CCGTGTCTAT
TCCATCTACG TCCACACCGT CTGTGACCCA CTCTTTGAAG CTGTTGGGAA
AATATTCAGC AATGTCCGCA TCAACTTGCA GAAAGAAATA CTGCAG

11.3 MALDI-TOF peptide-mass-fingerprints of analysed purified protein

The recombinant HIV1-TAT, human-DPPIV and human-Caveolin-1 protein were purified and analysed by MALDI-TOF peptide-mass-fingerprinting as indicated under results. The identified peptides of the various proteins are given below.

11.3.1 Recombinant proteins expressed in *E. coli*

Peptide masses of the GST-TAT-His double band

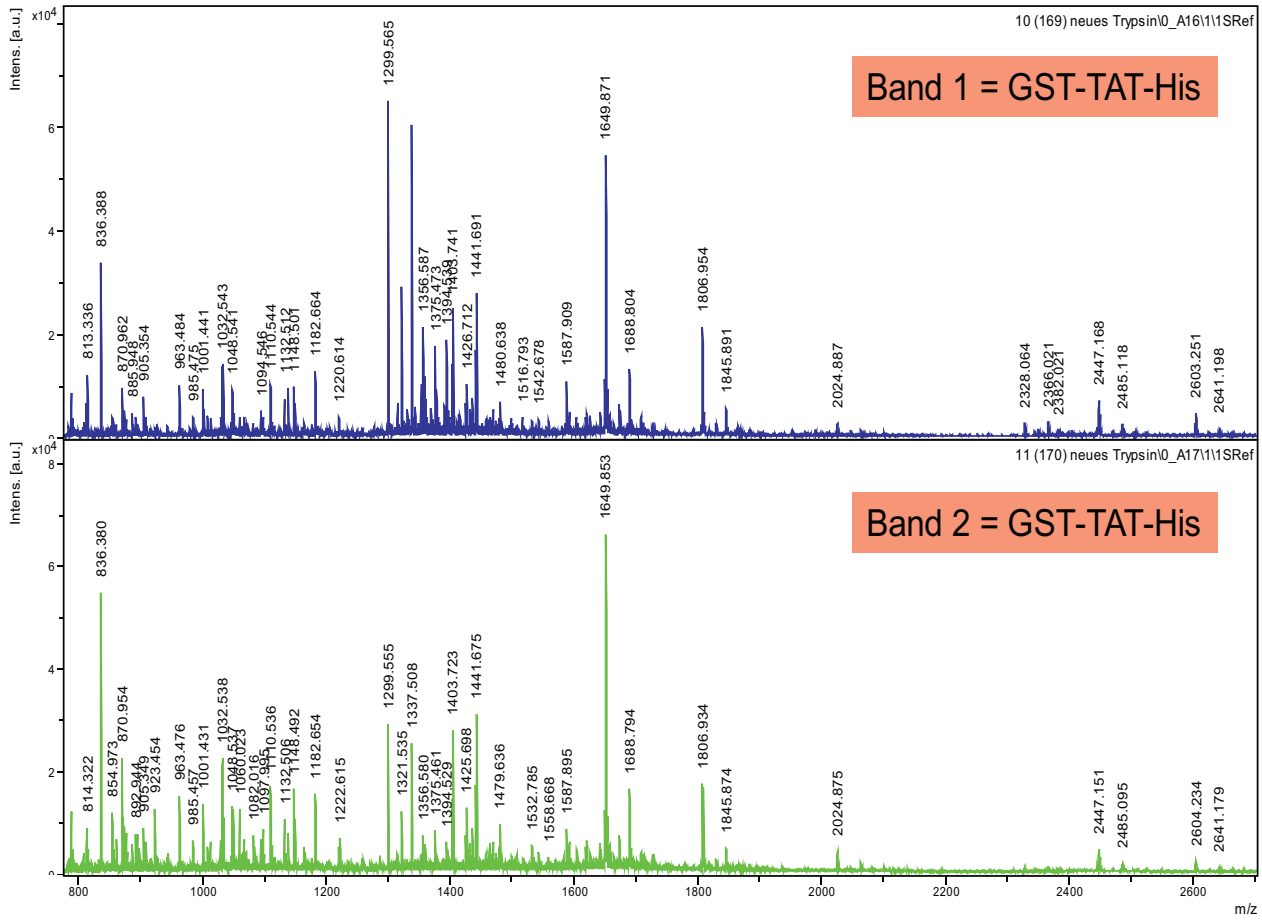

GST-TAT-His

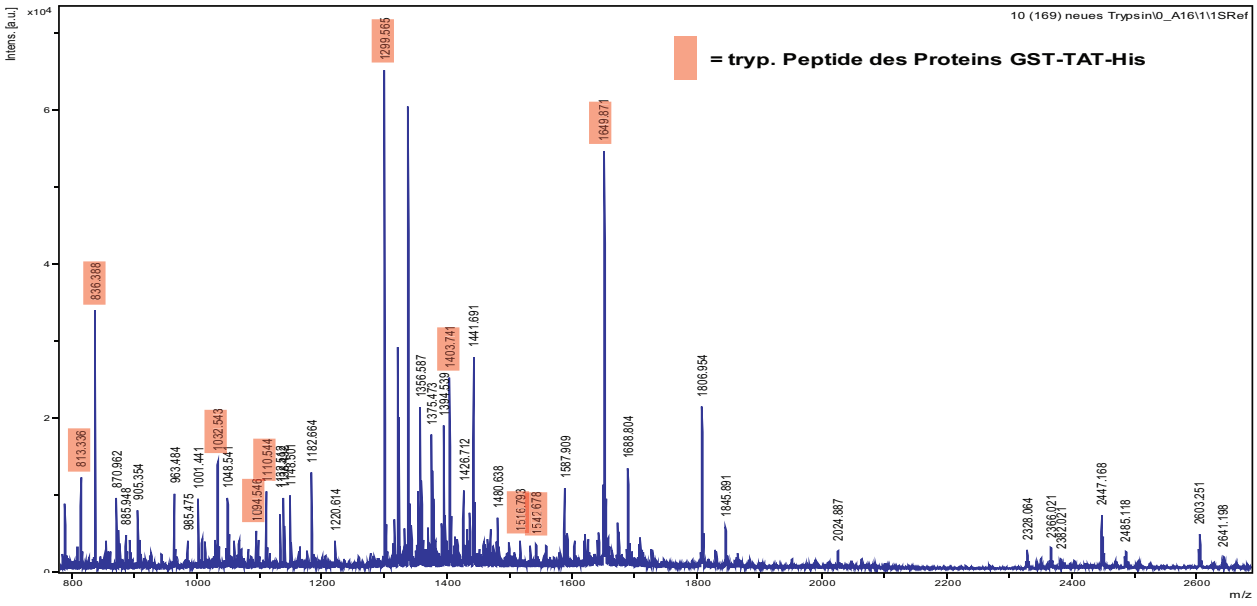
10 (169) neues Trypsin\0_A16\1\1SRef
= tryp. Peptide des Proteins GST-TAT-His
Intens. [a.u.]
x10⁴
m/z

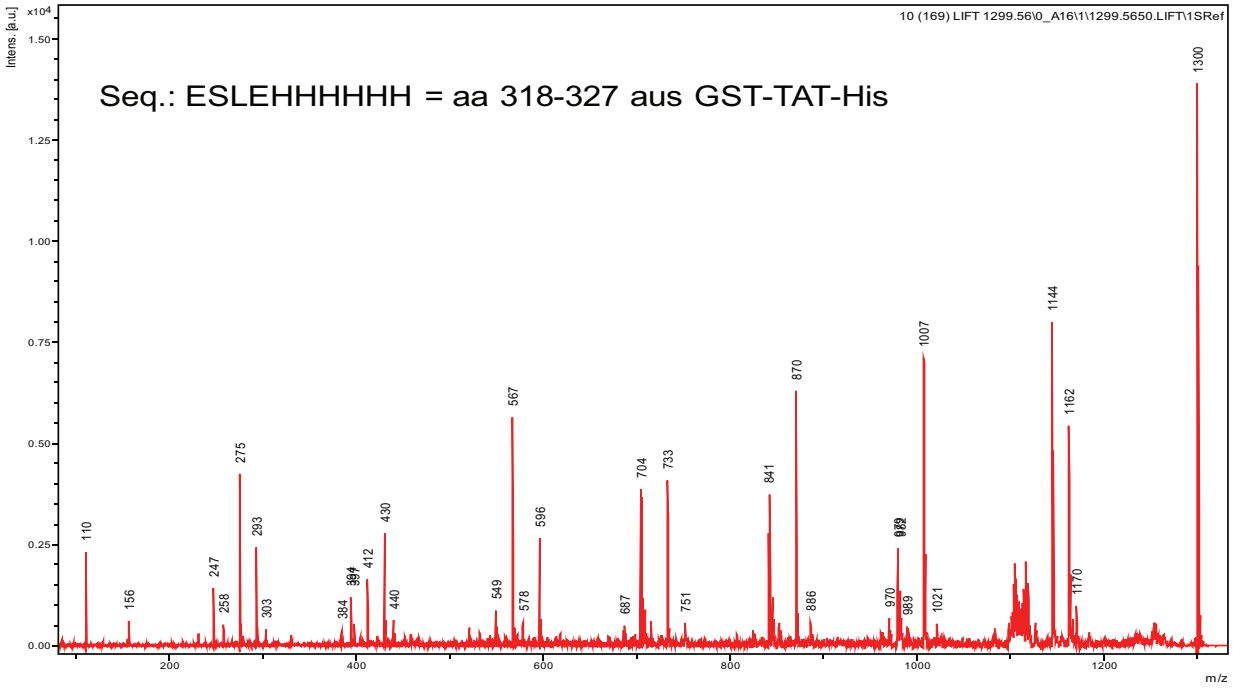
10 (169) LIFT 1299.56\0_A16\1\1299.5650.LIFT\1SRef
Seq.: ESLEHHHHHH = aa 318-327 aus GST-TAT-His
Intens. [a.u.]
x10⁴
m/z

TAT-1-86 (blue), and TATHis (red) from *E. coli*

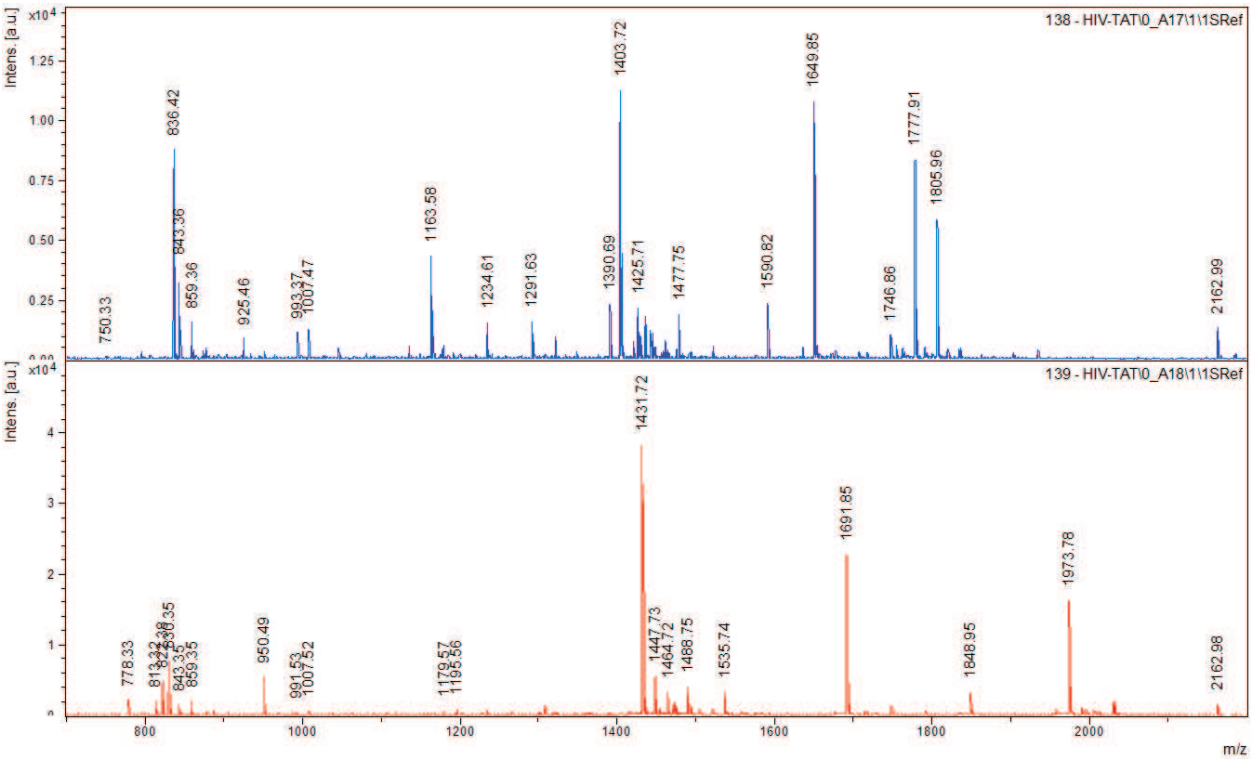

N-terminal analysis TAT and TATHis *(E. coli)*

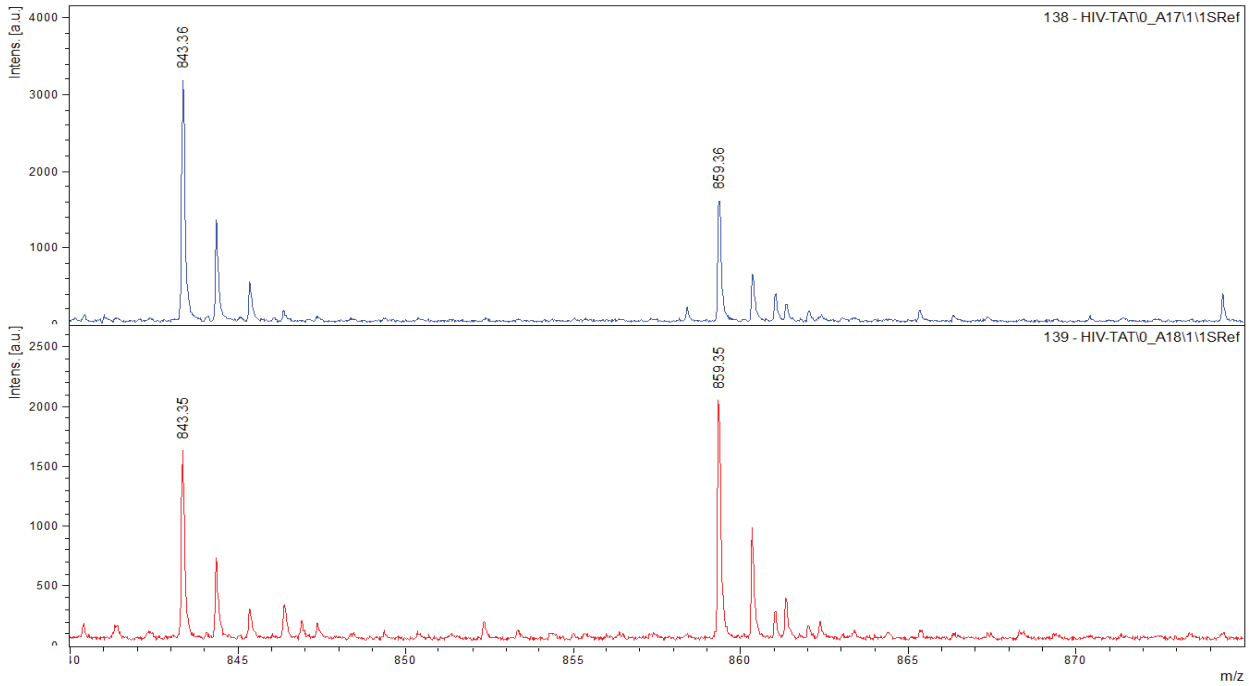

GST Caveolin-1

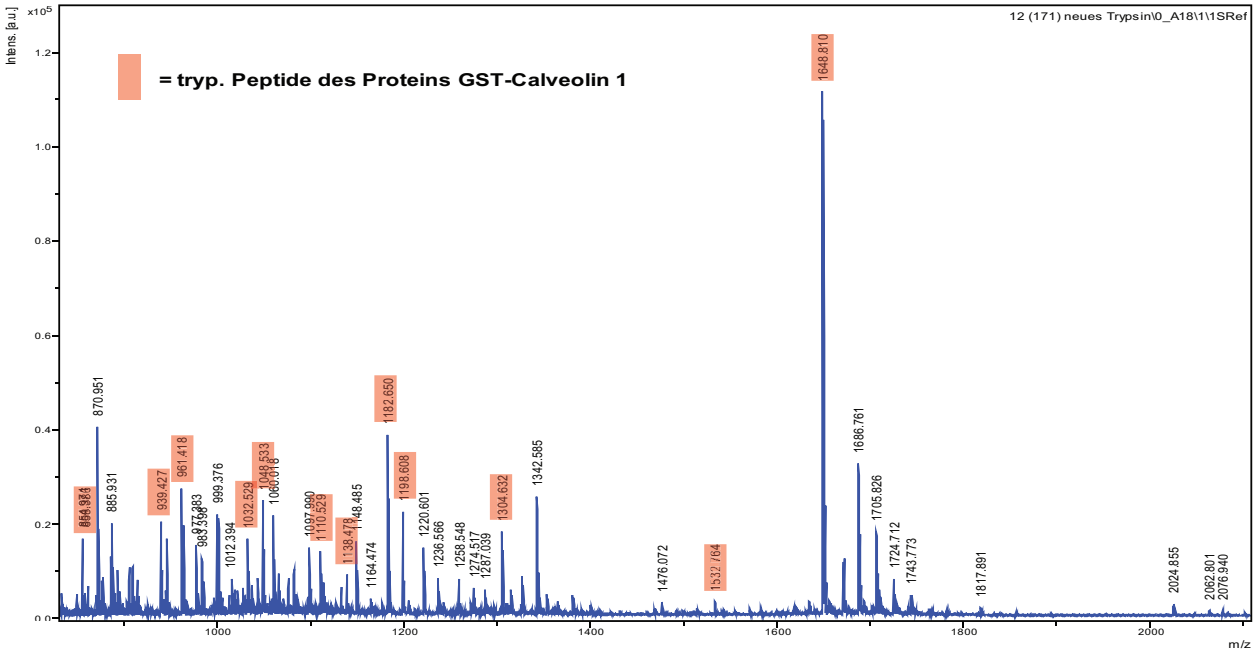

11.3.2 Recombinant proteins expressed in *Sf9 cells*

Human-DPPIV from *Sf9* cells. The identified peptides are highlighted in red.

```
1 MKTPWKVLLG LLGAAALVTI ITVPVVLLNK GTDDATADSR KTYTLTDYLK
51 NTYRLKLYSL RWISDHEYLY KQENNILVFN AEYGNSSVFL ENSTFDEFGH
101 SINDYSISPD GQFILLEYNY VKQWRHSYTA SYDIYDLNKR QLITEERIPN
151 NTQWVTWSPV GHKLAYVWNN DIYVKIEPNL PSYRITWTGK EDIIYNGITD
201 WVYEEEVFSA YSALWWSPNG TFLAYAQFND TEVPLIEYSF YSDESLQYPK
251 TVRVPYPKAG AVNPTVKFFV VNTDSLSSVT NATSIQITAP ASMLIGDHYL
301 CDVTWATQER ISLQWLRRIQ NYSVMDICDY DESSGRWNCL VARQHIEMST
351 TGWVGRFRPS EPHFTLDGNS FYKIISNEEG YRHICYFQID KKDCTFITKG
401 TWEVIGIEAL TSDYLYYISN EYKGMPGGRN LYKIQLSDYT KVTCLSCELN
451 PERCQYYSVS FSKEAKYYQL RCSGPGLPLY TLHSSVNDKG LRVLEDNSAL
501 DKMLQNVQMP SKKLDFIILN ETKFWYQMIL PPHFDKSKKY PLLLDVYAGP
551 CSQKADTVFR LNWATYLAST ENIIVASFDG RGSGYQGDKI MHAINRRLGT
601 FEVEDQIEAA RQFSKMGFVD NKRIAIWGWS YGGYVTSMVL GSGSGVFKCG
651 IAVAPVSRWE YYDSVYTERY MGLPTPEDNL DHYRNSTVMS RAENFKQVEY
701 LLIHGTADDN VHFQQSAQIS KALVDVGVDF QAMWYTDEDH GIASSTAHQH
751 IYTHMSHFIK QCFSLP
```

HIV1-TAT co-purified with human-DPPIV from *Sf9* cells. The identified peptides are highlighted in red.

```
          10         20         30         40         50         60
MEPVDPRLEP WKHPGSQPKT ACTTCYCKKC CFHCQVCFTT KALGISYGRK KRRQRRRPPQ

          70         80
GSQTHQVSLS KQPTSQPRGD PTGPKES
```

11.4 Maps of cloning vectors used

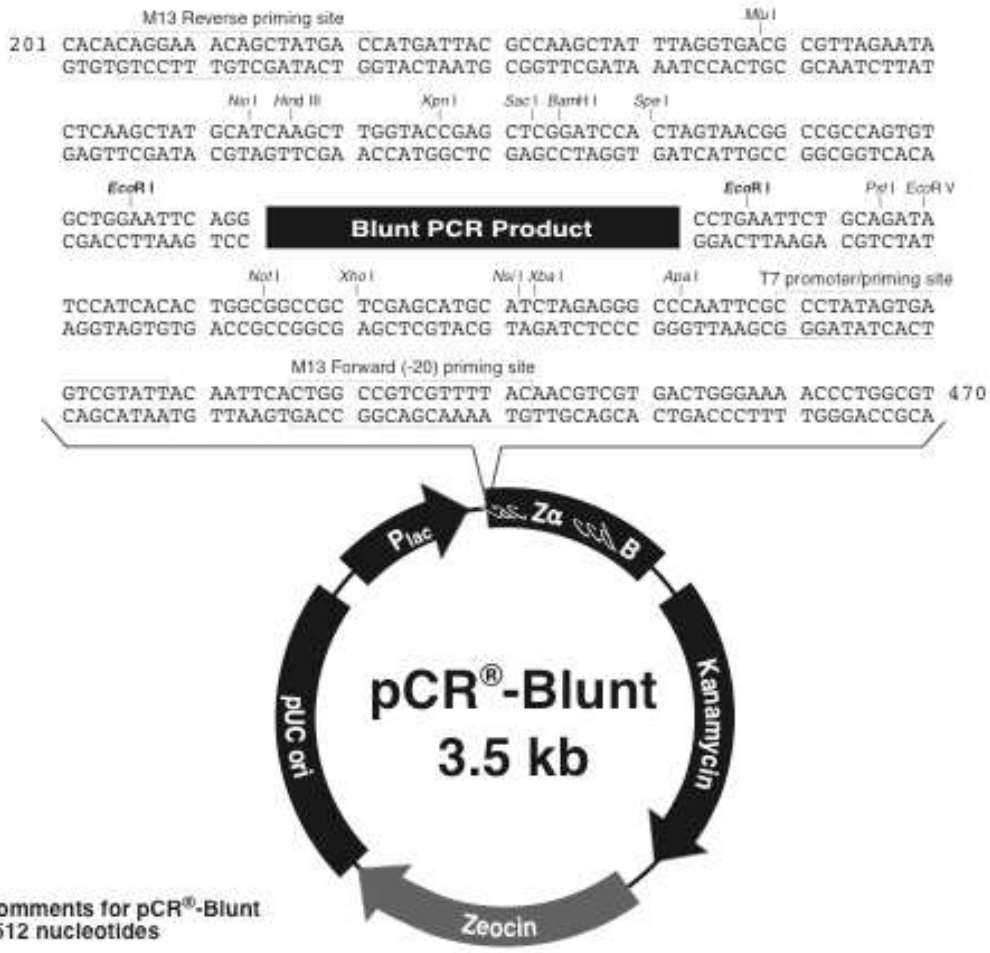

Comments for pCR®-Blunt
3512 nucleotides

Lac promoter/operator region: bases 95-216
M13 Reverse priming site: bases 205-221
*Lac*Z-alpha ORF: bases 217-570
T7 promoter priming site: bases 400-419
M13 Forward (-20) priming site: bases 427-442
Fusion joint: bases 571-579
*ccd*B lethal gene ORF: bases 580-882
Kanamycin resistance ORF: bases 1231-2025
Zeocin resistance ORF: bases 2231-2605
pUC origin: bases 2673-3386

Invitrogen™
life technologies

pQE-60 Vector (QIAGEN)

pQE-60 Vector

Positions of elements in bases

Vector size (bp)	3431
Start of numbering at *Xho*I (CTCGAG)	1–6
T5 promoter/lac operator element	7–87
T5 transcription start	61
6xHis-tag coding sequence	133–150
Multiple cloning site	113–132
Lambda t_0 transcriptional termination region	173–267
rrnB T1 transcriptional termination region	1033–1131
ColE1 origin of replication	1608
β-lactamase coding sequence	3226–2366

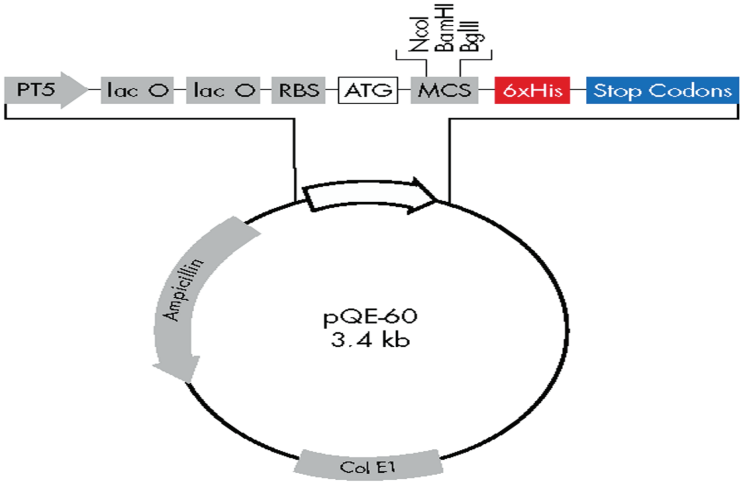

pQE-60

Eco RI/RBS Nco I Bam HI Bgl II 6xHis Hind III t_0

CCATGGGAGGATCCAGATCT TAAGCTTAATTAGCTGAG

Map of pRSET A, B, and C

pRSET A, B, and C The map below shows the features of pRSET A, B, and C. The complete sequence of the vector is available for downloading from our website at www.invitrogen.com or from Technical Support (see page 18).

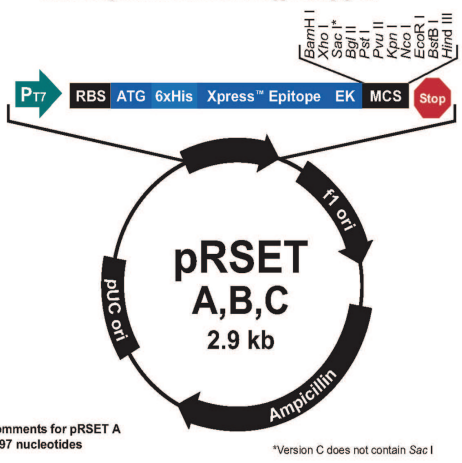

Comments for pRSET A
2897 nucleotides

*Version C does not contain *Sac* I

Multiple Cloning Site of pRSET B Below is the multiple cloning site for pRSET B. Restriction sites are labeled to indicate the actual cleavage site. The boxed nucleotides indicate the variable region. Sequencing and functional testing have confirmed the multiple cloning site. The complete sequence of pRSET B is available for downloading at www.invitrogen.com or from Technical Support (see page 18). For a map and description of the features of pRSET B, please refer to pages 14–15.

```
                                                                T7 promoter                                                                RBS
21   AATACGACTC ACTATAGGGA GACCACAACG GTTTCCCTCT AGAAATAATT TTGTTTAACT TTAAGAAGGA

                                                  Polyhistidine (6xHis) region
91   GATATACAT ATG CGG GGT TCT CAT CAT CAT CAT CAT CAT GGT ATG GCT AGC ATG ACT
          Met Arg Gly Ser His His His His His His Gly Met Ala Ser Met Thr

          T7 gene 10 leader                                  Xpress™ Epitope                    BamH I          Xho I Sac I
148  GGT GGA CAG CAA ATG GGT CGG GAT CTG TAC GAC GAT GAC GAT AAG GAT CCG AGC TCG
     Gly Gly Gln Gln Met Gly Arg Asp Leu Tyr Asp Asp Asp Asp Lys Asp Pro Ser Ser
                                                  EK recognition site   EK cleavage site
     Bgl II     Pst I  Pvu II  Kpn I Nco I  EcoR I  BstB I Hind III
205  AGA TCT GCA GCT GGT ACC ATG GAA TTC GAA GCT TGA TCCGGCTGCT AACAAAGCCC
     Arg Ser Ala Ala Gly Thr Met Glu Phe Glu Ala ***

                                                  T7 reverse priming site
261  GAAAGGAAGC TGAGTTGGCT GCTGCCACCG CTGAGCAATA ACTAGCATAA
```

pEGFP-N1 Vector (CLONTECH)

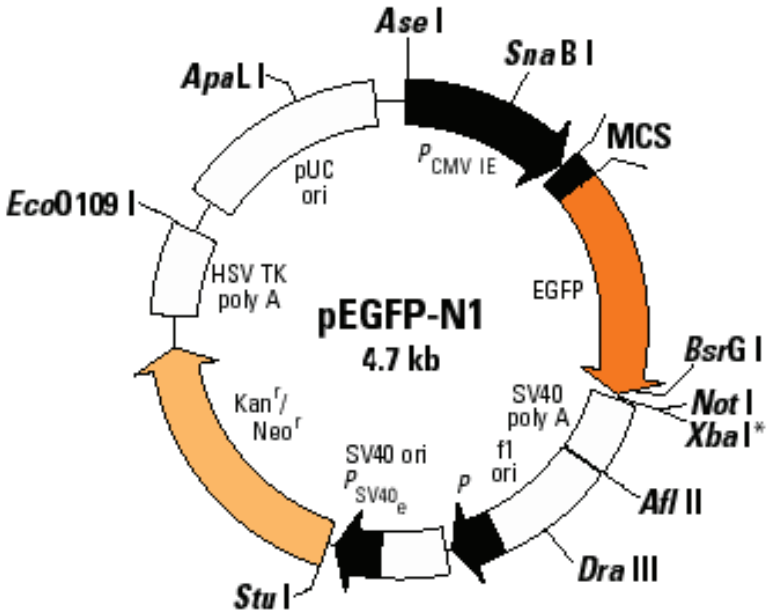

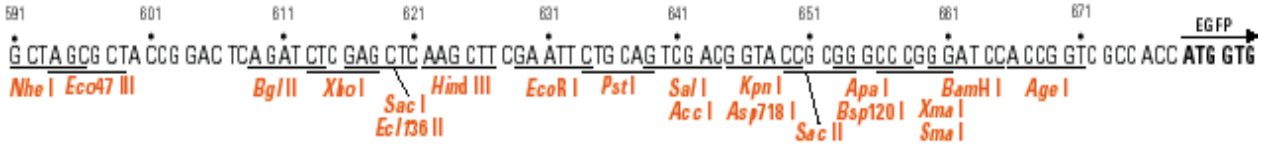

pGEX4T vector (from Amersham)

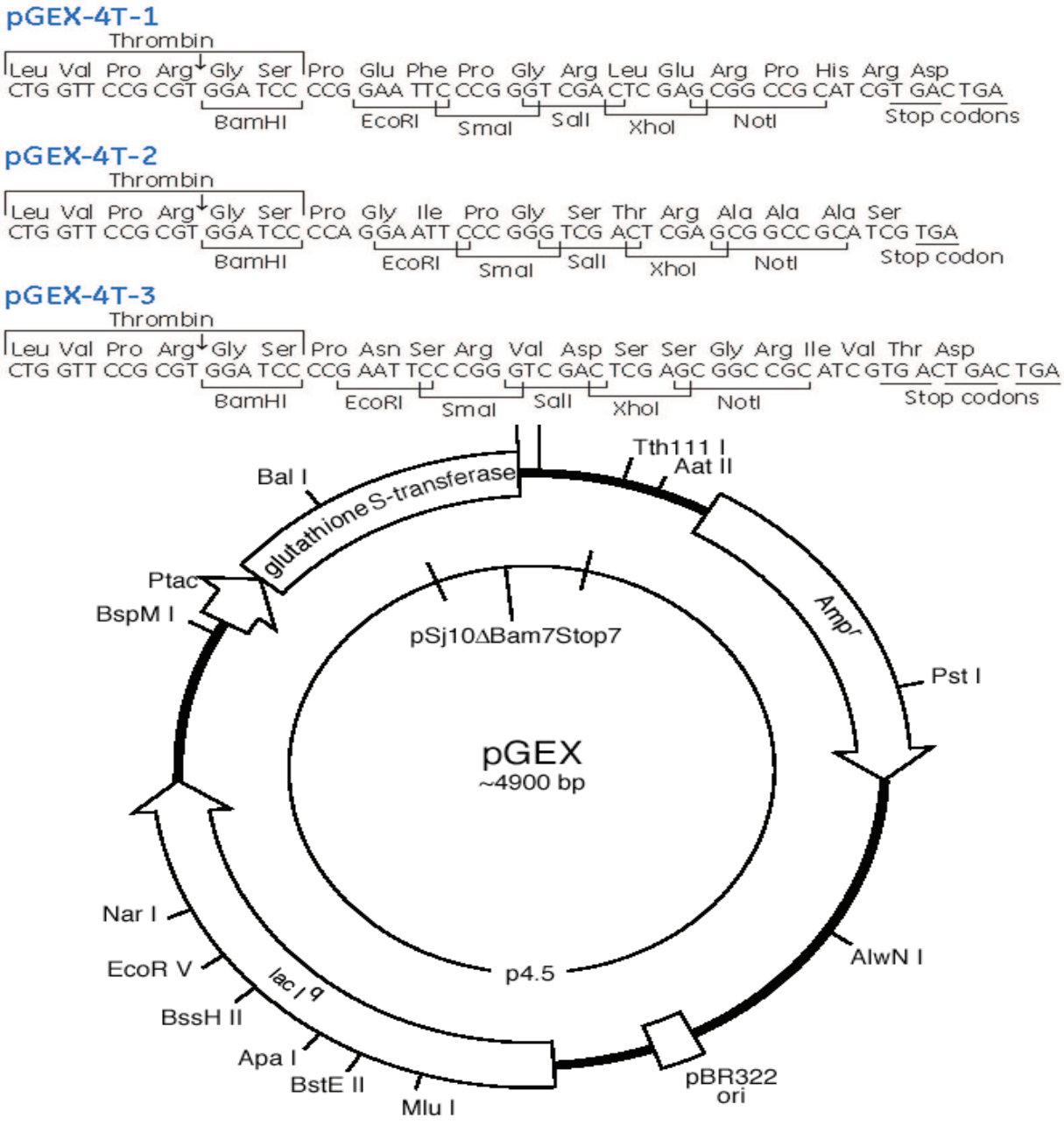

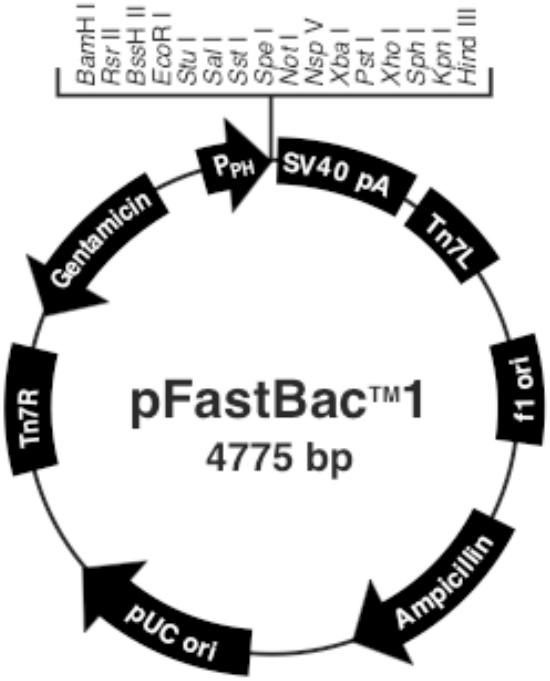

Comments for pFastBac™1
4775 nucleotides

f1 origin: bases 2-457
Ampicillin resistance gene: bases 589-1449
pUC origin: bases 1594-2267
Tn7R: bases 2511-2735
Gentamicin resistance gene: bases 2802-3335 (complementary strand)
Polyhedrin promoter (P_{PH}): bases 3904-4032
Multiple cloning site: bases 4037-4142
SV40 polyadenylation signal: bases 4160-4400
Tn7L: bases 4429-4594

Invitrogen™
life technologies

11.5 Publications and manuscripts under preparation

- **Felista L. Tansi**, Véronique Blanchard, Markus Berger, Rudolf Tauber, Werner Reutter and Hua Fan (2010): **Interaction of human dipeptidyl peptidase IV and human immunodeficiency virus type-1 transcription transactivator in *Sf9* cells. *Virology J 7, 267***

- **Felista L. Tansi**, Véronique Blanchard, Markus Berger, Rudolf Tauber, Werner Reutter and Hua Fan: **Co-expression and co-purification of human dipeptidyl peptidase IV and human immunodeficiency virus type 1 transcription transactivator. *under preparation***

- **Felista L. Tansi**, Werner Reutter and Hua Fan: **Human dipeptidyl peptidase IV- dependent induction of apoptosis in CHO cells by the human immunodeficiency virus type-1 transcription transactivator. *under preparation***

11.6 Selected posters and abstracts

- Felista Tansi, Markus Berger, Werner Reutter and Stephan Hinderlich: **Potential interaction between *N*-acetylglucosamine kinase and different proteins using a yeast two-hybrid screen.** Glykane – neuartige Basisstrukturen in Therapie und Diagnose; Innovationsforum 02- 03.12.2004 in Berlin.

- Tansi, F., Reutter, W., Fan, H.: **Inhibition of the Activity of Dipeptidyl Peptidase IV by HIV-1 TAT Protein.** 9th International Dahlem Symposium on „Cellular Signal Recognition and Transduction". Oct. 13-15, 2005, Berlin, Germany, p22.

- H. Fan, W. Weihofen, F. Tansi, J. Peng, M. Leddermann, S. Stehling, W. Reutter and W. Saenger: **Structure and molecular basis of DPPIV/CD26 in immune regulation and HIV-disease.** International symposium "Understanding Structure-Function Relationships in Membrane Proteins" Berlin, October 5-7, 2006.

- Felista L. Tansi, Véronique Blanchard, Markus Berger, Hua Fan. **Monitoring the effects of HIV TAT protein on DPPIV/CD26 degradation of GLP1 by MALDI TOF analysis.** 3rd International Conference on Dipeptidyl Peptidase and Related Proteins Antwerp, Belgium, April 23–25, 2008.

11.7 Curriculum Vitae

For reasons of data protection,

the curriculum vitae is not included in the online version

11.8 Acknowledgements

This work was supported by a grant from the *Deutsche Forschungsgemeinschaft* Bonn (Sonderforschungsbereich 366 and 449) and the *Sonnenfeld Stiftung,* Berlin.

I would like to express my sincere gratitude to Prof. Dr. Werner Reutter for providing me an opportunity to fulfil my goals in conducting the dissertation in this institute. I very much appreciate his motivating words and the personal moral support without which this work would not have been conducted to completion.

I am very grateful to Priv. Doz. Dr. Hua Fan for supervising this work and her advice in scientific work. I also thank her for sharing some of her past experiences in the science field with me, and for her readiness to critically review this work.

I immensely appreciate Prof. Dr. Rupert Mutzel for readily accepting to review this work.

I am very grateful to Prof. Dr. Stephan Hinderlich for his constant support in the past years and for always being there to give advice and critically review some parts of my work.

I am grateful to Priv. Doz. Dr. Kerstin Danker, Dr. Markus Berger, Dr. Mathias Kaup and Dr. Veronique Blanchard from Charite-Mitte for constant assistance and also for providing reagents whenever I was in need.

I especially thank Dr. Maria Kontou for the time devoted to answer my at times (not so) silly questions and for her constant assistance in scientific and private issues and also for critically reviewing some sections of my work.

Without the assistance of Melanie Ledderman at the beginning of my work the controversy surrounding the topic of this dissertation might have caused me to give up. I greatly appreciate her for enlightening me on her past experience with the topic and for strongly believing that I would see to the end of this dissertation successfully. Thanks a lot for the motivation!

I want to thank Dr. Faustin Kamena and Dr. Bernd Lepenies from the group of Prof. Seeberger for assistance with confocal microscopy and FACS analysis and also for their willingness to assist me whenever I was in need.

I also appreciate the assistance of Dr. Kira Gromova from the group of Prof. Haucke, for assistance with confocal microscopy. I'm also very grateful to Yijian and Arndt Pechstein both of the group of Prof. Haucke for assisting me with the SPR analysis and also their advice on technical questions.

I am very grateful to Dr. Eva Tauberger and Jacobo Martinez from the group of Prof. Sanger for assisting me in some practical work, for the purification of one of the proteins used in this work and also for conducting the crystallography.

My special thanks go to Priv Doz. Dr. Böttcher from FU-Berlin for electron microscopy.

I also thank Dr. Christoph Kannicht (Octapharma) for permitting me to do some of my experiments in his group and to Ivona Cubic and Dr. Birte Fuchs also from the same group for assisting me in conducting 2D PAGE and my thesis respectively.

I would like to thank Susanne Thamm for her assistance whenever I was in need, for the harmonious atmosphere she brought with her to our work group and also for giving me the feeling that I can always share my troubles with her and let her help where she could.

Mrs Katrin Büttner from the group of Prof. Wittig analysed the sequences of all the DNAs used in this work. I thank her very much for that and also for her readiness to help and general concern about my work.

My special thanks also to Jing Hu for being part of my life both in the lab and out of the lab, for sharing whatever joy and troubles we could with each other and for keeping up to the constant struggle we encountered in the complex topics of our dissertations. Thanks for being there and for giving me the feeling that I'm not in the struggle alone and that none of us has to give-up. Hope you finish soon so that we make a huge "Afro-Chinese" parrrrrrty!

My profound gratitude to my colleagues Duc Nguyen and Yujing Yao who brought more life and joy to our group and for the harmonious working atmosphere and assistance they provided.

Prof. Dr. Rudiger Horstkorte, Dr. Darius Ghaderi, Dr. Stefan Reinke, Dr. Kaya Bork, Dr. Rolf Nuck, Mrs Christiane Kilian and Verena Diehm contributed enormously to the realisation of this work. I am very grateful to them for their constant moral and scientific support. Mrs Felicitas Kern, Mr. Zeynel Gün, Mr. Pypno, Mrs Sabine Nöhring, Mr. Werner Hoffmann and all the other colleagues from the AG Reutter whose names I have not mentioned here were all very helpful to me during the preparation of this dissertation and I appreciate this very much.

Last but not the least, I will like to thank my family "at large" for absolutely being there (200%) for me no matter what it took. I am very grateful for the constant motivation and prayers. I didn't plan to mention names but Bobbo and my daughter Vanessa accompanied me 24 h a day during the struggle to realize this work. Thanks for your patience and the "readiness to bring a blanket to the lab when I seemed to need one" and thanks Bobbo for unconsciously (through your seriousness) giving me the impression that the formula "meh tur ya natural fee" does not hold in all stages of education but rather "hard work". Thanks to (Baby) Vanessa for bearing the hardship all these years due to the long time it took to realize this work. I thank you for your patience and for being as strong and independent as you are.

My special thanks to Father Johannes Willeit and Dr. Christian Bongmba for their financial support which laid a solid foundation for my entire studies.

Thank you almighty God for guiding me through these years to make sure I complete this work with this sentence!